

# Holotype sequencing of *Silvatares holzenthali* Rázuri-Gonzales, Ngera & Pauls, 2022 (Trichoptera, Pisuliidae)

Jacqueline Heckenhauer<sup>1,2\*</sup>, Ernesto Razuri-Gonzales<sup>1\*</sup>,  
Francois Ngera Mwangi<sup>3</sup>, Julio Schneider<sup>1</sup>, Steffen U. Pauls<sup>1,2,4</sup>

**1** Senckenberg Research Institute and Natural History Museum Frankfurt, Frankfurt, Germany **2** LOEWE Centre for Translational Biodiversity Genomics (LOEWE-TBG), Frankfurt, Germany **3** Centre de Recherche en Sciences Naturelles, Lwiro, Bukavu, Democratic Republic of the Congo **4** Institute for Insect Biotechnology, Justus-Liebig-University, Gießen, Germany

Corresponding author: Jacqueline Heckenhauer ([jacqueline.heckenhauer@senckenberg.de](mailto:jacqueline.heckenhauer@senckenberg.de))

Academic editor: Ana Previšić | Received 7 December 2022 | Accepted 6 March 2023 | Published 24 April 2023

<https://zoobank.org/19EF70AC-4C66-437C-B77F-890CAB3ED25C>

**Citation:** Heckenhauer J, Razuri-Gonzales E, Mwangi FN, Schneider J, Pauls SU (2023) Holotype sequencing of *Silvatares holzenthali* Rázuri-Gonzales, Ngera & Pauls, 2022 (Trichoptera, Pisuliidae). ZooKeys 1159: 1–15. <https://doi.org/10.3897/zookeys.1159.98439>

## Abstract

While DNA barcodes are increasingly provided in descriptions of new species, the whole mitochondrial and nuclear genomes are still rarely included. This is unfortunate because whole genome sequencing of holotypes allows perpetual genetic characterization of the most representative specimen for a given species. Thus, *de novo* genomes are invaluable additional diagnostic characters in species descriptions, provided the structural integrity of the holotype specimens remains intact. Here, we used a minimally invasive method to extract DNA of the type specimen of the recently described caddisfly species *Silvatares holzenthali* Rázuri-Gonzales, Ngera & Pauls, 2022 (Trichoptera: Pisuliidae) from the Democratic Republic of the Congo. A low-cost next generation sequencing strategy was used to generate the complete mitochondrial and draft nuclear genome of the holotype. The data in its current form is an important extension to the morphological species description and valuable for phylogenomic studies.

## Keywords

Caddisflies, extended specimen, holotype genomics, taxonomy

\* Contributed equally as the first authors.

## Introduction

In zoology, especially when considering invertebrates, new species are often not recognized as such in the field due to the minute size of the structures used to differentiate them from already described species. Intensive treatment (e.g., preparation and preservation) and careful examination of the collected specimens are required to determine if they are indeed undescribed. In addition, many new species are discovered in regions of the world where the scientific infrastructure is insufficient to guarantee high-quality, unfragmented DNA in collected specimens. Such was also the case for the holotype of *Silvatares holzenthali* Rázuri-Gonzales, Ngera & Pauls, 2022 (Trichoptera: Pisuliidae) (Rázuri-Gonzales et al. 2022). This species belongs to the African endemic family Pisuliidae. Currently, there are 12 valid species in the genus. The taxonomic history and distribution of *Silvatares* were described by Stoltze (1989), discussed in detail by Prather and Holzenthal (2002), and most recently summarized by Rázuri-Gonzales et al. (2022).

The holotype specimen (SMFTRI00018633) was collected by FNM in the eastern D.R. Congo in 2017 and preserved in locally produced 80% ethanol. By the time the specimen was identified as representing a new species, it had been transferred into new ethanol, analyzed multiple times under the stereoscope, and shipped between countries. Without the possibility of cooling the preservative or the specimen in the D.R. Congo, it was clear that the DNA of this specimen would be substandard to what might be extractable from a freshly caught caddisfly specimen preserved in high-quality ethanol and with uninterrupted cooling. However, the described scenario for the holotype of *S. holzenthali* is the norm rather than the exception. In this paper, we want to showcase that it is possible and very valuable to generate a genomic resource from holotypes, even if the quality of the starting DNA is far from ideal.

Many initiatives are currently trying to harness recent technological developments to sequence and produce reference genomes for all species on Earth (Lewin et al. 2018; Rhie et al. 2021; Blaxter et al. 2022; Formenti et al. 2022). A reference genome is a highly contiguous, accurate, and annotated genome assembly, which represents the structure and organization of the genome of a species at a particular point in time (Formenti et al. 2022). These endeavors are crucial for documenting the Earth's biodiversity at its most fundamental organization level (i.e., genomic diversity). Understandably, these initiatives focus first on those species that are relatively easy to sequence (i.e., often larger species where tissue is available without destroying the entire specimen and where targeted sampling of freshly collected tissues, cells, or specimens is possible). Attempts to sequence the genome of even the tiniest individuals with minimal input DNA are becoming possible (Schneider et al. 2021), but they still cannot reach the quality standards required for reference genome assemblies. The same is true for specimens and holotypes collected in scenarios similar to the one described above for *S. holzenthali*.

Another limitation of many genome sequencing initiatives is that they generally do not focus on the holotype of a species. However, in the currently accepted type-based taxonomy, the holotype (or, if necessary, the designated lectotype and neotype) serves as a species' reference. For many species, sequencing a reference genome from the holotype is not a viable option. Many type specimens are old, and naturally, all

type specimens are rare and of singular value, requiring special care, and non-invasive DNA extraction methods for genome sequencing. Thus, reference genome sequencing initiatives that require ample amounts of high-quality DNA for long-read sequencing technologies are logically and correctly focused on less valuable specimens, at best, from the *locus typicus* or from a paratype. Nevertheless, sequencing the holotype of a species allows for the genetic characterization of the most representative specimen for a given species as an eternal digital reference. Here we show that using a minimally invasive method to extract DNA from poorly preserved specimens allows taxonomists to capture and present the genetic characterization of the holotype while maintaining most of its morphological and structural integrity.

## Materials and methods

### DNA extraction, library preparation, whole genome sequencing, and sequence read processing

Genomic DNA was extracted from two legs as described in Rázuri-Gonzales et al. (2022). A total of 110 ng gDNA was sheared to a mean fragment size of about 420 bp using a Bioruptor Pico (Diagenode, Seraing, Belgium). Genomic libraries were prepared using the NEBNext Ultra II DNA Library Preparation Kit for Illumina (New England Biolabs, Ipswich, MA, USA) according to the manufacturer's manual. Adapters were diluted 1:10 as recommended for low input libraries, and size selection was conducted based on the insert size using SPRIselect beads (Beckman, Indianapolis, USA). A dual indexing PCR was run for eight cycles on a Mastercycler (Eppendorf, Germany). After cleanup, the library was eluted in 0.1X TE and shipped for 150 bp paired-end sequencing (ordering 20 Gb output) on a partial lane of an Illumina NovaSeq 6000 platform (San Diego, CA) at Novogene (Cambridge, UK). Raw reads are deposited at the NCBI SRA archive under the accession number SRR22404850. The quality of the raw reads was evaluated using FastQC v.0.11.9 (Andrews 2019). FastQC reports were summarized with MultiQC v.0.10 (Ewels et al. 2016, Fig. 1). Raw reads were trimmed for low-quality regions, adapter sequences, and over-represented *k-mers* using autotrim.pl v.0.6.1 (Waldvogel et al. 2018) and Trimmomatic v.0.39 (Bolger et al. 2014) using the adapter\_all.fa of Trimmomatic and the following settings ILLUMINACLIP:2:30:10:8:true, SLIDINGWINDOW:4:20, MINLEN:50, and TOPHRED33 (Fig. 1). Unpaired reads were discarded. Contaminated reads were filtered using Kraken v.2.0.9 (Wood and Salzberg 2014). The quality of trimmed, contamination-free reads was evaluated with FastQC as described above.

### Genome size estimation and genomic characterization

We used two different approaches to estimate the genome size. First, we used a *k-mer* distribution-based method. For this, *k-mers* were counted with JELLYFISH v.2.3.0 (Marçais and Kingsford 2011) using jellyfish count -C -s 1000000000 -F 2 and a

*k*-mer length of 21 based on the raw sequence reads. A histogram of *k*-mer frequencies was created with jellyfish histo and used for analysis with the online web tool GenomeScope v.2.0 (Ranallo-Benavidez et al. 2020) using the following parameters: *k*-mer length = 21, ploidy = 2, max *k*-mer coverage = 10000. In addition, we estimated genome size with a re-mapping-based approach using backmap.pl (Schell et al. 2017; Pfenninger et al. 2022). This wrapper script uses the following dependencies samtools (Li et al. 2009), bwa mem (Li 2013), qualimap (Okonechnikov et al. 2015), MultiQC (Ewels et al. 2016), bedtools (Quinlan and Hall 2010), and RScript (R Core Team 2021) to automatically map the trimmed, contamination-free reads to the assembly (see *de novo* nuclear genome assembly) with bwa mem. Then, it executes qualimap bamqc and finally estimates genome size by dividing the mapped nucleotides by the mode of the coverage distribution (>0).

### Mitogenome assembly

The mitochondrial genome was first assembled with the raw reads using NOVO-plasty v.4.2 (Dierckxsens et al. 2016) using the following parameters: type = mito, genome range = 12000–22000, *k*-mer = 33, max memory = 100, read length = 150, insert size = 300, platform = illumina, paired = PE, insert size auto = yes. The partial sequence of the *cytochrome c oxidase subunit I (COXI)* gene of *Silvatares ensifera* Barnard, 1934, KX291165, was used as seed input. All other parameters were kept as default. The circularized mitogenome was aligned to the complete mitochondrial sequence of *Phryganea cinerea* Walker, 1852, MG980616, with MAFFT in Geneious Prime v.2022.1.1 with default settings to set the correct start position. Annotation of tRNAs, rRNAs, and protein-coding genes was done with MitoZ v.2.3 (Meng et al. 2019) using the module “annotate with genetic\_code 5” and clade Arthropoda. Positions of *trnL*, *trnT*, and *trnS* were manually curated based on the alignment to *P. cinerea*. The mitochondrial genome assembly was deposited in GenBank under the accession OP921089.

### *De novo* nuclear genome assembly

Nuclear genome assembly was conducted in Spades v.3.14.1 (Bankevich et al. 2012) with the default settings. After scaffolds smaller than 500 bp and those matching the mitochondrial genome assembly were filtered out, assembly statistics were calculated with Quast v.5.0.2 (Gurevich et al. 2013), and quality was assessed in several ways. First, completeness was accessed via screening for single-copy orthologs with BUSCO v.4.1.4 (Simão et al. 2015) using the endopterygota\_odb10 dataset. Second, the backmapping rate of the trimmed reads to the assembly was calculated with backmap.pl 0.3 as described above (see “Genome size estimation and genomic characterization”). Third, the final genome assemblies were screened for potential contaminations with taxon-annotated GC-coverage (TAGC) plots using BlobTools v.1.1.1 (Laetsch and Blaxter 2017). For this purpose, the bam file resulting from the backmapping analysis was converted

to a blobtools readable cov file with blobtools map2cov. Taxonomic assignment for BlobTools was done with blastn 2.10.0+ (Camacho et al. 2009) using -task megablast and -e-value 1e-25. The blobDB was created and plotted from the cov file and blast hits. The nuclear draft genome assembly was deposited in GenBank under the accession JAPMAF000000000. All commands used in this study are given in Suppl. material 1.

## Results

### Whole genome sequencing and genome characterization

Illumina sequencing resulted in 160 534 832 raw short reads with a data amount of 24.1 Gb. 3.3% of reads were identified as contaminated (2.7% *Homo sapiens*, 0.6% bacteria, 0.1% viruses, 0.03% other). Over-represented *k-mers* were successfully removed using autotrim.pl v.0.6.1 (Fig. 1). After trimming and contamination filtering, 149 928 720 reads (~21.8 Gb) were kept.

*K-mer* analysis based on raw read data estimated the genome size to be 531.15 Mb, with a heterozygosity of 37.7% (Fig. 2), while backmap.pl revealed a genome size of 643.02 Mb (Fig. 3).

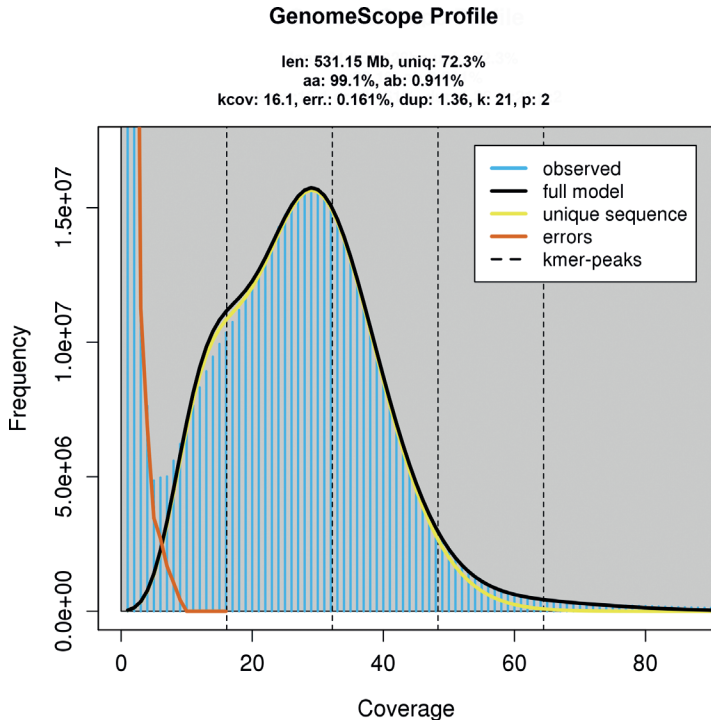
### Mitochondrial genome

The NOVOplasty assembly resulted in a 17 205 bp-long and circularized contig (Fig. 4). Its annotation revealed all expected 13 protein-coding genes and both rRNAs and 23 tRNAs. The d-loop was manually curated based on a comparison with the complete mitochondrial sequence of *Limnephilus decipiens* Kolenati, 1848, AB971912.



**Figure 1.** FastQC status checks of raw and trimmed reads (\*autotrim), green: good, yellow: ok, red: failed.

**A**



**B**

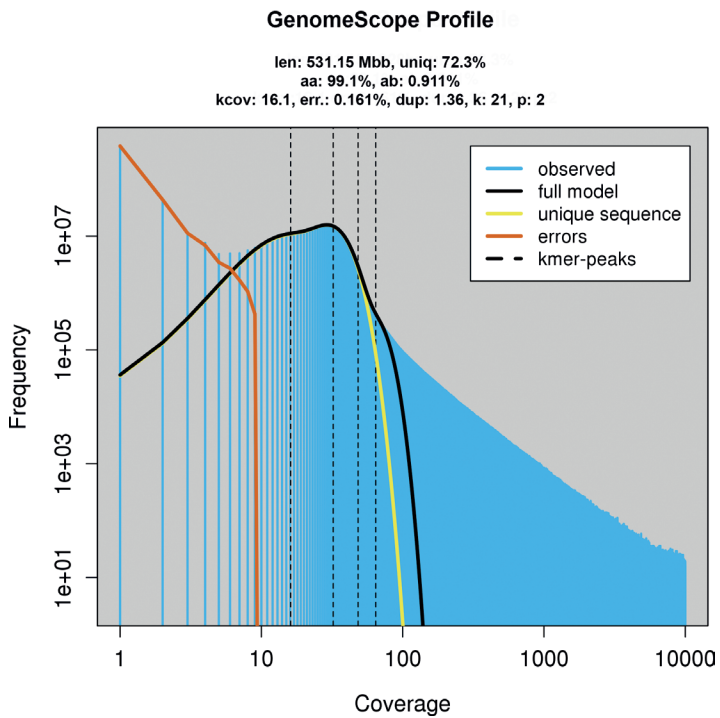


**Figure 2.** Genomescope2 profiles **A** linear plot **B** log plot; len: inferred total genome length, uniq: percent of the genome that is unique (not repetitive), kcov: mean *k*-mer coverage for heterozygous bases, err: error rate of the reads, dup: average rate of read duplications.

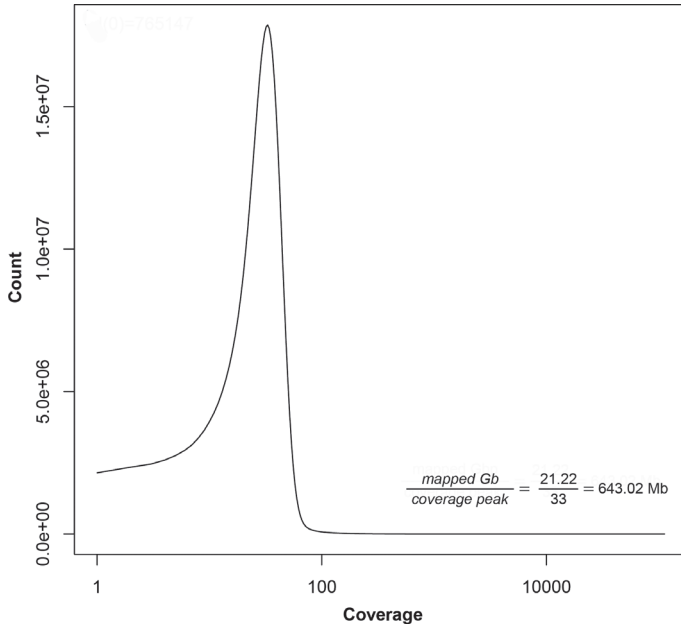


**Figure 3.** Coverage distribution per position. The x-axis is given in log-scale. Mapped nucleotides: 21.22 Gb. The peak coverage is 33. This results in genome size estimation of 643.02 Mb.

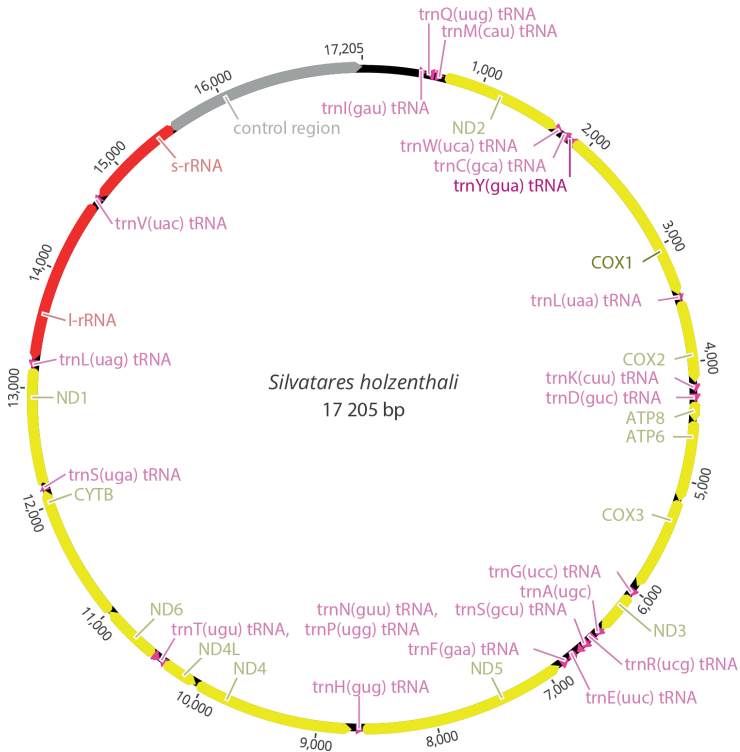


**Figure 4.** Circular mitochondrial genome of the holotype of *Silvatares holzenthali*.

aDC150301.blobDB.json.bestsum.phylum.p8.span.100.blobplot.cov0

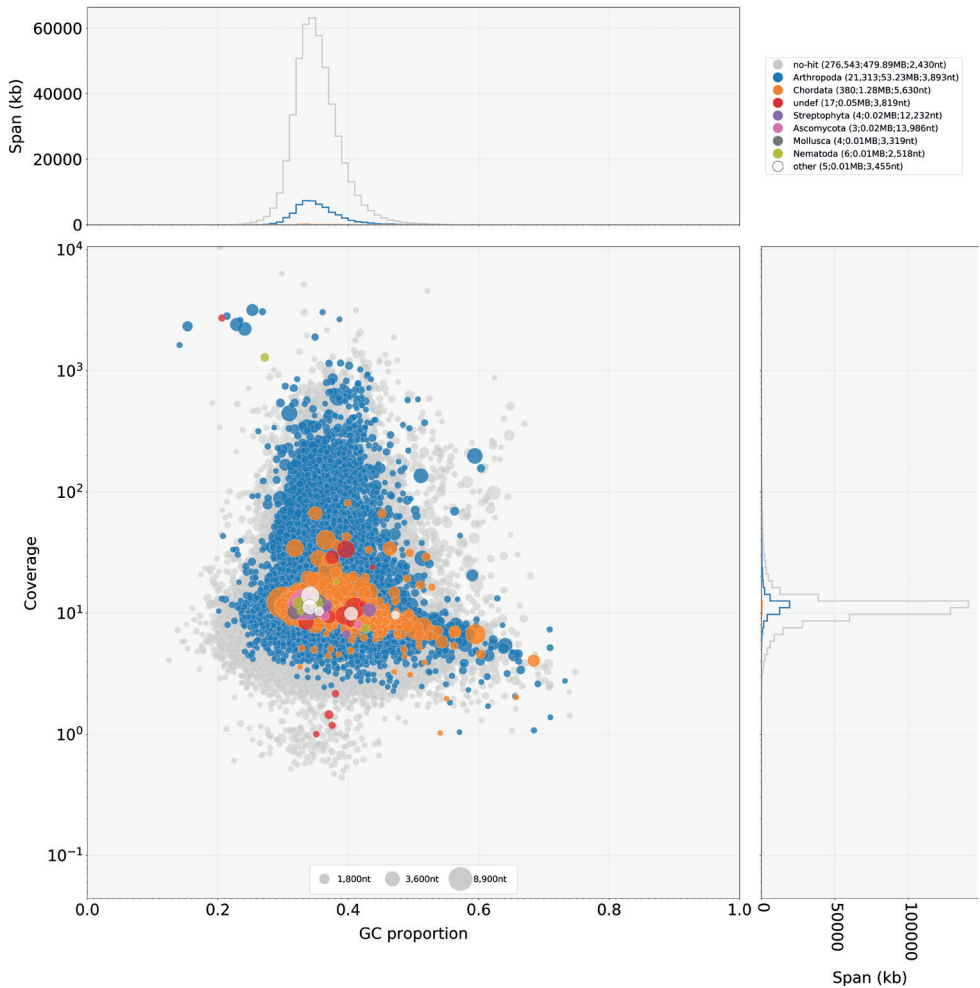


**Figure 5.** Taxon-annotated GC-coverage (TAGC) plots for the nuclear genome assembly. Scaffolds are represented with circles. Colors indicate the best match to the corresponding taxonomic annotation (grey= no hits, blue= Arthropoda, for other colors see legend in the figure, upper right box). The distribution of the total span (kb) of contigs for a given GC proportion or coverage is given in the upper- and right panels, respectively.

Standard abbreviations are given for protein-coding (yellow), transfer (pink), and ribosomal RNA (red) genes. The control region is shown in gray. Orientation of genes is indicated by direction of arrows.

### Nuclear genome

The nuclear genome assembly contains 298 265 scaffolds with a total length of 534.50 Mb, an N50 of 2 549, and a GC of 35.27%. 99.07% of reads were mapped

back to the assembly. The BUSCO search with 2 124 Endopterygota orthologs resulted in 74.7% BUSCOs; of these, 44.7% were complete (44.3% single, 0.4% duplicated), and 31% were fragmented. Blobtools detected no contaminations based on GC content and coverage distribution (Fig. 5). While uploading the genome to NCBI, NCBI's contamination screening detected and filtered a 29 bp-long contamination (vector, etc.) at the beginning of one scaffold.

## Discussion

While the morphology of the genus *Silvatares* has been described extensively, less than a handful of partial genes have been published or uploaded to NCBI GenBank. For example, *cadherin*, *cytochrome oxidase subunit 1 (COX1)*, and the 28S large subunit and 18S small subunit ribosomal RNA are available for *S. ensifera* (MN364796, KX291165, KX106901, AF436522, AF436172, AF436293, MN296628, AF436410); *carbamoylphosphate synthase domain protein*, *isocitrate dehydrogenase*, *RNA polymerase II*, and *COX1* for *Silvatares* sp. (KC559510, KC559654, KC559734, KC559575); *COX1* for *S. collyrififer* Barnard, 1934, (KX291056); and *COX1* for *S. thrymmifer* Barnard, 1934 (MN344469; MN344493) (Malm et al. 2013; Zhou et al. 2016; Thomas et al. 2020).

Here, we present the mitogenome and a draft nuclear genome assembly through our  $\sim 45\times$  sequencing coverage of short-read data. This genome assembly is admittedly far away from the quality standards of a reference genome; however, we argue that this genomic resource is still an invaluable addition to the characterization of the holotype of *Silvatares holzenthali*. The genome assembly reported in this study includes all the partial genes that had been hitherto sequenced for other *Silvatares* species, as well as 74.7% of the 2 442 benchmarking universal single-copy orthologs in Endopterygota. Additionally, this assembly provides the complete mitogenome, including the barcode markers. This highlights that for a few hundred dollars we can produce much more genomic information on type specimens than the “DNA barcode,” which has already become an important addition to many morphological species descriptions (e.g., Hebert and Gregory 2005; Padial and De la Riva 2007; Pohl et al. 2012; Egan et al. 2017). Sequencing the genome of the holotype permanently links the genetic characterization to the name-bearing specimen of a given species. This information is very valuable for studying the systematics and evolution of the species in question. Especially in variable taxa or clades with high levels of cryptic diversity, anchoring species delimitation analyses, taxonomic work or evolutionary studies on the genetic make-up of the name-bearing specimens can be extremely helpful. Genome wide data have been used to help delimit closely related species in Trichoptera (e.g., Deng et al. 2021); however, since the holotypes of the species in question were not among the analyzed specimens, the nomenclature and taxonomy of each species could not be fully resolved. This case highlights the value of sequencing the genome of the primary type. Since the genome of *S. holzenthali* is the first holotype genome in caddisflies there are no examples of species delimitation based on the name-bearing type specimen yet.

In other taxa, holotype genomes have already been published. In a pioneering study, Pohl et al. (2012) provided a complete short-read-based genome in the description of a new Strepsiptera species using specimens from the type series. Since then, *de novo* genomes are increasingly included in new species descriptions across the animal kingdom, such as in *Caenorhabditis* Osche, 1952 (Kanzaki et al. 2018), mud snakes and frogs (Köhler et al. 2021a, b, c), gall wasps (Brandão-Dias et al. 2022), fungi (Emanuel et al. 2022) and fishes (Sullivan et al. 2022).

The draft genome assembly generated in this study can be applied in population genetic studies, for example, to assess the heterozygosity of the type specimen as a proxy for population genetic variation at the time of sampling (Köhler et al. 2021a). Furthermore, the data is valuable in a phylogenomic context (Brandão-Dias et al. 2022). For other downstream genomic analyses, the provided data from the holotype can always be mapped to a higher-quality reference genome generated from specimens of lesser value and better DNA quality. Notably, the approach we present here also lends itself to museum specimens, which are usually of older age. Being able to tap into these immense and often irreplaceable resources for genomic study opens a wealth of scientific opportunity and has developed in the growing genomic field of museomics (Raxworthy and Smith 2021) which propagates generating genomic data from historical specimens using a variety of methods. This includes shotgun genome sequencing as presented here, but also hybrid capture approaches for degraded DNA once appropriate bait sets have been developed (Bi et al. 2013; Raxworthy and Smith 2021; Castañeda-Rico et al. 2022).

While we think a *de novo* genome or a genomic resource of any kind is an invaluable added resource and important additional diagnostic character in species descriptions, priority should be given to preserving specimen integrity of the type specimens. Most methods for extracting DNA ultimately cause at least minimal structural damage to the holotype. In our case, this damage (removing and clearing the abdomen; DNA extraction from two legs) was necessary to recognize and identify the holotype as a new species. No additional damage was done to extract DNA for generating the genome. However, in other situations, the methods used to preserve and store insects may not always allow for generating a *de novo* genome from holotypes without causing significant additional damage to the type. In this case we maintain that priority should be given to safekeeping the structural integrity of the holotype specimen, and genomic information possibly obtained from a paratype or a duplicated structure on the holotype.

## Acknowledgements

Field work and taxonomy were funded by German Science Foundation Grant (DFG PA1617/4-1) to SUP. The genome sequencing is a result of the LOEWE Centre for Translational Biodiversity Genomics funded by the Hessen State Ministry of Higher Education, Research and the Arts (HMWK). JH was supported by the LOEWE Centre for Translational Biodiversity Genomics. Tilman Schell (LOEWE-TBG, Frankfurt) is acknowledged for his advice on bioinformatic methods.

## References

- Andrews S (2019) FastQC: a quality control tool for high throughput sequence data. <http://www.bioinformatics.babraham.ac.uk/projects/fastqc/>
- Bankevich A, Nurk S, Antipov D, Gurevich AA, Dvorkin M, Kulikov AS, Lesin VM, Nikolenko SI, Pham S, Pribelski AD, Pyshkin AV, Sirotkin AV, Vyahhi N, Tesler G, Alekseyev MA, Pevzner PA (2012) SPAdes: a new genome assembly algorithm and its applications to single-cell sequencing. *Journal of Computational Biology* 19(5): 455–477. <https://doi.org/10.1089/cmb.2012.0021>
- Bi K, Linderoth T, Vanderpool D, Good JM, Nielsen R, Moritz C (2013) Unlocking the vault: Next-generation museum population genomics. *Molecular Ecology* 22(24): 6018–6032. <https://doi.org/10.1111/mec.12516>
- Blaxter M, Mieszkowska N, Di Palma F, Holland P, Durbin R, Richards T, Berriman M, Kelsey P, Hollingsworth P, Wilson W, Twyford A, Gaya E, Lawniczak M, Lewis O, Broad G, Howe K, Hart M, Flicek P, Barnes I (2022) Sequence locally, think globally: The Darwin Tree of Life Project. *Proceedings of the National Academy of Sciences of the United States of America* 119(4): e2115642118. <https://doi.org/10.1073/pnas.2115642118>
- Bolger AM, Lohse M, Usadel B (2014) Trimmomatic: A flexible trimmer for Illumina sequence data. *Bioinformatics* 30(15): 2114–2120. <https://doi.org/10.1093/bioinformatics/btu170>
- Brandão-Dias PFP, Zhang YM, Pirro S, Vinson CC, Weinersmith KL, Ward AKG, Forbes AA, Egan SP (2022) Describing biodiversity in the genomics era: A new species of Nearctic Cynipidae gall wasp and its genome. *Systematic Entomology* 47(1): 94–112. <https://doi.org/10.1111/syen.12521>
- Camacho C, Coulouris G, Avagyan V, Ma N, Papadopoulos J, Bealer K, Madden TL (2009) BLAST+: Architecture and applications. *BMC Bioinformatics* 10(1): e421. <https://doi.org/10.1186/1471-2105-10-421>
- Castañeda-Rico S, Edwards CW, Hawkins MTR, Maldonado JE (2022) Museomics and the holotype of a critically endangered cricetid rodent provide key evidence of an undescribed genus. *Frontiers in Ecology and Evolution* 10: e930356. <https://doi.org/10.3389/fevo.2022.930356>
- Deng XL, Favre A, Lemmon EM, Lemmon AR, Pauls SU (2021) Gene flow and diversification in *Himalopsyche martynovi* species complex (Trichoptera: Rhyacophilidae) in the Hengduan Mountains. *Biology* 10(8): e816. <https://doi.org/10.3390/biology10080816>
- Dierckxsens N, Mardulyn P, Smits G (2016) NOVOPlasty: *De novo* assembly of organelle genomes from whole genome data. *Nucleic Acids Research* 45(4): e18. <https://doi.org/10.1093/nar/gkw955>
- Egan SP, Weinersmith KL, Liu S, Ridenbaugh RD, Zhang YM, Forbes AA (2017) Description of a new species of *Euderus* Haliday from the southeastern United States (Hymenoptera, Chalcidoidea, Eulophidae): The crypt-keeper wasp. *ZooKeys* 645: 37–49. <https://doi.org/10.3897/zookeys.645.11117>
- Emanuel IB, Konkel ZM, Scott KL, Valero David GE, Slot JC, Hand FP (2022) Whole-Genome sequence data for the holotype strain of *diaporthe ilicicola*, a fungus associated with latent fruit rot in deciduous holly. *Microbiology Resource Announcements* 11(9): e00631-22. <https://doi.org/10.1128/mra.00631-22>

- Ewels P, Magnusson M, Lundin S, Käller M (2016) MultiQC: Summarize analysis results for multiple tools and samples in a single report. *Bioinformatics* 32(19): 3047–3048. <https://doi.org/10.1093/bioinformatics/btw354>
- Formenti G, Theissinger K, Fernandes C, Bista I, Bombarely A, Bleidorn C, Ciofi C, Crottini A, Godoy JA, Höglund J, Malukiewicz J, Mouton A, Oomen RA, Paez S, Palsbøll PJ, Pampoulie C, Ruiz-López MJ, Svardal H, Theofanopoulou C, De Vries J, Waldvogel A-M, Zhang G, Mazzoni CJ, Jarvis ED, Bálint M, Formenti G, Theissinger K, Fernandes C, Bista I, Bombarely A, Bleidorn C, Čiampor F, Ciofi C, Crottini A, Godoy JA, Högglund J, Malukiewicz J, Mouton A, Oomen RA, Paez S, Palsbøll P, Pampoulie C, Ruiz-López MJ, Svardal H, Theofanopoulou C, De Vries J, Waldvogel A-M, Zhang G, Mazzoni CJ, Jarvis E, Bálint M, Aghayan SA, Alioto TS, Almudi I, Alvarez N, Alves PC, Amorim IR, Antunes A, Arribas P, Baldrian P, Berg PR, Bertorelle G, Böhne A, Bonisoli-Alquati A, Boštjančić LL, Boussau B, Breton CM, Buzan E, Campos PF, Carreras C, Castro LF, Chueca LJ, Conti E, Cook-Deegan R, Croll D, Cunha MV, Delsuc F, Dennis AB, Dimitrov D, Faria R, Favre A, Fedrigo OD, Fernández R, Ficetola GF, Flot J-F, Gabaldón T, Galea Agius DR, Gallo GR, Giani AM, Gilbert MTP, Grebenc T, Guschanski K, Guyot R, Hausdorf B, Hawlitschek O, Heintzman PD, Heinze B, Hiller M, Husemann M, Iannucci A, Irisarri I, Jakobsen KS, Jentoft S, Klinga P, Kloch A, Kratochwil CF, Kusche H, Layton KKS, Leonard JA, Lerat E, Liti G, Manousaki T, Marques-Bonet T, Matos-Maraví P, Matschiner M, Maumus F, Mc Cartney AM, Meiri S, Melo-Ferreira J, Mengual X, Monaghan MT, Montagna M, Mysłajek RW, Neiber MT, Nicolas V, Novo M, Ozretić P, Palero F, Pârvolescu L, Pascual M, Paulo OS, Pavlek M, Pegueroles C, Pellissier L, Pesole G, Primmer CR, Riesgo A, Rüber L, Rubolini D, Salvi D, Seehausen O, Seidel M, Secomandi S, Studer B, Theodoridis S, Thines M, Urban L, Vasemägi A, Vella A, Vella N, Vernes SC, Vernesi C, Vieites DR, Waterhouse RM, Wheat CW, Wörheide G, Wurm Y, Zammit G (2022) The era of reference genomes in conservation genomics. *Trends in Ecology & Evolution* 37(3): 197–202. <https://doi.org/10.1016/j.tree.2021.11.008>
- Gurevich A, Saveliev V, Vyahhi N, Tesler G (2013) QUASt: Quality assessment tool for genome assemblies. *Bioinformatics* 29(8): 1072–1075. <https://doi.org/10.1093/bioinformatics/btt086>
- Hebert PD, Gregory TR (2005) The promise of DNA barcoding for taxonomy. *Systematic Biology* 54(5): 852–859. <https://doi.org/10.1080/10635150500354886>
- Kanzaki N, Tsai IJ, Tanaka R, Hunt VL, Liu D, Tsuyama K, Maeda Y, Namai S, Kumagai R, Tracey A, Holroyd N, Doyle SR, Woodruff GC, Murase K, Kitazume H, Chai C, Akagi A, Panda O, Ke H-M, Schroeder FC, Wang J, Berriman M, Sternberg PW, Sugimoto A, Kikuchi T (2018) Biology and genome of a newly discovered sibling species of *Caenorhabditis elegans*. *Nature Communications* 9(1): e3216. <https://doi.org/10.1038/s41467-018-05712-5>
- Köhler G, Khaing KPP, Than NL, Baranski D, Schell T, Greve C, Janke A, Pauls SU (2021a) A new genus and species of mud snake from Myanmar (Reptilia, Squamata, Homalopsidae). *Zootaxa* 4915(3): 301–325. <https://doi.org/10.11646/zootaxa.4915.3.1>
- Köhler G, Vargas J, Than NL, Schell T, Janke A, Pauls SU, Thammachoti P (2021b) A taxonomic revision of the genus *Phrynoglossus* in Indochina with the description of a new species and comments on the classification within Occidozyginae (Amphibia, Anura, Dicroglossidae). *Vertebrate Zoology* 71: 1–26. <https://doi.org/10.3897/vz.71.e60312>
- Köhler G, Zwitwers B, Than NL, Gupta DK, Janke A, Pauls SU, Thammachoti P (2021c) Bioacoustics Reveal Hidden Diversity in Frogs: Two New Species of the Genus *Limnonectes*

- from Myanmar (Amphibia, Anura, Dicroglossidae). *Diversity* 13(9): e399. <https://doi.org/10.3390/d13090399>
- Laetsch DR, Blaxter ML (2017) BlobTools: Interrogation of genome assemblies. *F1000 Research* 6: e1287. <https://doi.org/10.12688/f1000research.12232.1>
- Lewin HA, Robinson GE, Kress WJ, Baker WJ, Coddington J, Crandall KA, Durbin R, Edwards SV, Forest F, Gilbert MTP, Goldstein MM, Grigoriev IV, Hackett KJ, Haussler D, Jarvis ED, Johnson WE, Patrinos A, Richards S, Castilla-Rubio JC, Van Sluys M-A, Soltis PS, Xu X, Yang H, Zhang G (2018) Earth biogenome project: sequencing life for the future of life. *Proceedings of the National Academy of Sciences of the United States of America* 115(17): 4325–4333. <https://doi.org/10.1073/pnas.1720115115>
- Li H (2013) Aligning sequence reads, clone sequences and assembly contigs with BWA-MEM. arXiv: 1303.3997.
- Li H, Handsaker B, Wysoker A, Fennell T, Ruan J, Homer N, Marth G, Abecasis G, Durbin R, Subgroup GPD (2009) The sequence alignment/map format and SAMtools. *Bioinformatics* 25(16): 2078–2079. <https://doi.org/10.1093/bioinformatics/btp352>
- Malm T, Johanson KA, Wahlberg N (2013) The evolutionary history of Trichoptera (Insecta): A case of successful adaptation to life in freshwater. *Systematic Entomology* 38(3): 459–473. <https://doi.org/10.1111/syen.12016>
- Marçais G, Kingsford C (2011) A fast, lock-free approach for efficient parallel counting of occurrences of k-mers. *Bioinformatics* 27(6): 764–770. <https://doi.org/10.1093/bioinformatics/btr011>
- Meng G, Li Y, Yang C, Liu S (2019) MitoZ: A toolkit for animal mitochondrial genome assembly, annotation and visualization. *Nucleic Acids Research* 47(11): e63–e63. <https://doi.org/10.1093/nar/gkz173>
- Okonechnikov K, Conesa A, García-Alcalde F (2015) Qualimap 2: Advanced multi-sample quality control for high-throughput sequencing data. *Bioinformatics* 32(2): 292–294. <https://doi.org/10.1093/bioinformatics/btv566>
- Padial JM, De la Riva I (2007) Integrative taxonomists should use and produce DNA barcodes. *Zootaxa* 1586(1): 67–68. <https://doi.org/10.11646/zootaxa.1586.1.7>
- Pfenninger M, Schönnenbeck P, Schell T (2022) ModEst: Accurate estimation of genome size from next generation sequencing data. *Molecular Ecology Resources* 22(4): 1454–1464. <https://doi.org/10.1111/1755-0998.13570>
- Pohl H, Niehuis O, Gloyna K, Misof B, Beutel R (2012) A new species of *Mengenilla* (Insecta, Strepsiptera) from Tunisia. *ZooKeys* 198: 79–102. <https://doi.org/10.3897/zookeys.198.2334>
- Prather AL, Holzenthal RW (2002) The identity of *Silvatares excelsus* Navás, 1931. *Nova Supplementa Entomologica* (Proceedings of the 10<sup>th</sup> International Symposium on Trichoptera) 15: 231–234.
- Quinlan AR, Hall IM (2010) BEDTools: A flexible suite of utilities for comparing genomic features. *Bioinformatics* 26(6): 841–842. <https://doi.org/10.1093/bioinformatics/btq033>
- R Core Team (2021) R: A language and Environment for Statistical Computing. Vienna.
- Ranallo-Benavidez TR, Jaron KS, Schatz MC (2020) GenomeScope 2.0 and Smudgeplot for reference-free profiling of polyploid genomes. *Nature Communications* 11(1): e1432. <https://doi.org/10.1038/s41467-020-14998-3>

- Raxworthy CJ, Smith BT (2021) Mining museums for historical DNA: Advances and challenges in museomics. *Trends in Ecology & Evolution* 36(11): 1049–1060. <https://doi.org/10.1016/j.tree.2021.07.009>
- Rázuri-Gonzales E, Ngera MF, Pauls SU (2022) A new species of *Silvatares* (Trichoptera, Pisuliidae) from the Democratic Republic of the Congo. *ZooKeys* 1111: 371–380. <https://doi.org/10.3897/zookeys.1111.85307>
- Rhie A, McCarthy SA, Fedrigo O, Damas J, Formenti G, Koren S, Uliano-Silva M, Chow W, Functammasan A, Kim J, Lee C, Ko BJ, Chaisson M, Gedman GL, Cantin LJ, Thibaud-Nissen F, Haggerty L, Bista I, Smith M, Haase B, Mountcastle J, Winkler S, Paez S, Howard J, Vernes SC, Lama TM, Grutzner F, Warren WC, Balakrishnan CN, Burt D, George JM, Biegler MT, Iorns D, Digby A, Eason D, Robertson B, Edwards T, Wilkinson M, Turner G, Meyer A, Kautt AF, Franchini P, Detrich III HW, Svardal H, Wagner M, Naylor GJP, Pippel M, Malinsky M, Mooney M, Simbirsky M, Hannigan BT, Pesout T, Houck M, Misuraca A, Kingan SB, Hall R, Kronenberg Z, Sović I, Dunn C, Ning Z, Hastie A, Lee J, Selvaraj S, Green RE, Putnam NH, Gut I, Ghurye J, Garrison E, Sims Y, Collins J, Pelan S, Torrance J, Tracey A, Wood J, Dagnew RE, Guan D, London SE, Clayton DF, Mello CV, Friedrich SR, Lovell PV, Osipova E, Al-Ajli FO, Secomandi S, Kim H, Theofanopoulou C, Hiller M, Zhou Y, Harris RS, Makova KD, Medvedev P, Hoffman J, Masterson P, Clark K, Martin F, Howe K, Flicek P, Walenz BP, Kwak W, Clawson H, Diekhans M, Nassar L, Paten B, Kraus RHS, Crawford AJ, Gilbert MTP, Zhang G, Venkatesh B, Murphy RW, Koepfli K-P, Shapiro B, Johnson WE, Di Palma F, Marques-Bonet T, Teeling EC, Warnow T, Graves JM, Ryder OA, Haussler D, O'Brien SJ, Korlach J, Lewin HA, Howe K, Myers EW, Durbin R, Phillippy AM, Jarvis ED (2021) Towards complete and error-free genome assemblies of all vertebrate species. *Nature* 592(7856): 737–746. <https://doi.org/10.1038/s41586-021-03451-0>
- Schell T, Feldmeyer B, Schmidt H, Greshake B, Tills O, Truebano M, Rundle SD, Paule J, Ebersberger I, Pfenninger M (2017) An annotated draft genome for *Radix auricularia* (Gastropoda, Mollusca). *Genome Biology and Evolution* 9(3): 585–592. <https://doi.org/10.1093/gbe/evx032>
- Schneider C, Woehle C, Greve C, D'Haese CA, Wolf M, Hiller M, Janke A, Bálint M, Huettel B (2021) Two high-quality *de novo* genomes from single ethanol-preserved specimens of tiny metazoans (Collembola). *GigaScience* 10: giab035. <https://doi.org/10.1093/gigascience/giab035>
- Simão FA, Waterhouse RM, Ioannidis P, Kriventseva EV, Zdobnov EM (2015) BUSCO: Assessing genome assembly and annotation completeness with single-copy orthologs. *Bioinformatics* 31(19): 3210–3212. <https://doi.org/10.1093/bioinformatics/btv351>
- Stoltze M (1989) The afrotropical caddisfly family Pisuliidae. Systematics, zoogeography, and biology (Trichoptera: Pisuliidae). *Steenstrupia* 15: 1–50.
- Sullivan JP, Hopkins CD, Pirro S, Peterson R, Chakona A, Mutizwa TI, Mukweze Mulelenu C, Alqahtani FH, Vreven E, Dillman CB (2022) Mitogenome recovered from a 19<sup>th</sup> Century holotype by shotgun sequencing supplies a generic name for an orphaned clade of African weakly electric fishes (Osteoglossomorpha, Mormyridae). *ZooKeys* 1129: 163–196. <https://doi.org/10.3897/zookeys.1129.90287>
- Thomas JA, Frandsen PB, Prendini E, Zhou X, Holzenthal RW (2020) A multigene phylogeny and timeline for Trichoptera (Insecta). *Systematic Entomology* 45(3): 670–686. <https://doi.org/10.1111/syen.12422>

- Waldvogel AM, Wieser A, Schell T, Patel S, Schmidt H, Hankeln T, Feldmeyer B, Pfenninger M (2018) The genomic footprint of climate adaptation in *Chironomus riparius*. *Molecular Ecology* 27(6): 1439–1456. <https://doi.org/10.1111/mec.14543>
- Wood DE, Salzberg SL (2014) Kraken: Ultrafast metagenomic sequence classification using exact alignments. *Genome Biology* 15(3): R46. <https://doi.org/10.1186/gb-2014-15-3-r46>
- Zhou X, Frandsen PB, Holzenthal RW, Beet CR, Bennett KR, Blahnik RJ, Bonada N, Cartwright D, Chuluunbat S, Cocks GV, Collins GE, deWaard J, Dean J, Flint Jr OS, Hausmann A, Hendrich L, Hess M, Hogg ID, Kondratieff BC, Malicky H, Milton MA, Morinière J, Morse JC, Mwangi FN, Pauls SU, Gonzalez MR, Rinne A, Robinson JL, Salokannel J, Shackleton M, Smith B, Stamatakis A, StClair R, Thomas JA, Zamora-Muñoz C, Ziesmann T, Kjer KM (2016) The Trichoptera barcode initiative: A strategy for generating a species-level Tree of Life. *Philosophical Transactions of the Royal Society of London, Series B, Biological Sciences* 371(1702): e20160025. <https://doi.org/10.1098/rstb.2016.0025>

## Supplementary material 1

### **Commands used in the study Heckenhauer, J., Rázuri-Gonzales, E., Mwangi, F.N., Schneider, J., Pauls, S. U. (2022) Holotype sequencing of *Silvatares holzenthali* (Trichoptera: Pisuliidae)**

Authors: Jacqueline Heckenhauer, Ernesto Razuri-Gonzales, Francois Ngera Mwangi, Julio Schneider, Steffen U. Pauls

Data type: Bioinformatic commands

Copyright notice: This dataset is made available under the Open Database License (<http://opendatacommons.org/licenses/odbl/1.0/>). The Open Database License (ODbL) is a license agreement intended to allow users to freely share, modify, and use this Dataset while maintaining this same freedom for others, provided that the original source and author(s) are credited.

Link: <https://doi.org/10.3897/zookeys.1159.98439.suppl1>

## Supplementary material 2

### **Genomic DNA degradation assessment on a TapeStation 2200**

Authors: Jacqueline Heckenhauer, Ernesto Razuri-Gonzales, Francois Ngera Mwangi, Julio Schneider, Steffen U. Pauls

Data type: DNA Extraction quality control

Copyright notice: This dataset is made available under the Open Database License (<http://opendatacommons.org/licenses/odbl/1.0/>). The Open Database License (ODbL) is a license agreement intended to allow users to freely share, modify, and use this Dataset while maintaining this same freedom for others, provided that the original source and author(s) are credited.

Link: <https://doi.org/10.3897/zookeys.1159.98439.suppl2>



# Diversity of flesh flies (Sarcophagidae, Sarcophaginae) of pond habitats in rural areas in the Croatian part of Baranja

Stjepan Krčmar<sup>1</sup>

<sup>1</sup> Department of Biology, Josip Juraj Strossmayer University of Osijek, Cara Hadrijana 8/A, HR-31000 Osijek, Croatia

Corresponding author: Stjepan Krčmar ([stjepan@biologija.unios.hr](mailto:stjepan@biologija.unios.hr))

---

Academic editor: Marc De Meyer | Received 21 January 2023 | Accepted 7 April 2023 | Published 24 April 2023

---

<https://zoobank.org/CB922F29-F5C6-4AB0-928D-5C69B15F3B0F>

---

**Citation:** Krčmar S (2023) Diversity of flesh flies (Sarcophagidae, Sarcophaginae) of pond habitats in rural areas in the Croatian part of Baranja. ZooKeys 1159: 17–36. <https://doi.org/10.3897/zookeys.1159.100878>

---

## Abstract

The diversity of grey flesh flies (Sarcophagidae: Sarcophaginae) from the Croatian part of Baranja was studied during 2019 to 2021, resulting in 37 species, of which the following are new for the area: *Ravinia pernix* (Harris, 1780); *Sarcophaga* (*Het.*) *depressifrons* Zetterstedt, 1845; *S.* (*Het.*) *filia* Rondani, 1860; *S.* (*Het.*) *haemorrhoides* Böttcher, 1913; *S.* (*Het.*) *pumila* Meigen, 1826; *S.* (*Het.*) *vagans* Meigen, 1826; *S.* (*Lis.*) *dux* Thomson, 1869; *S.* (*Lis.*) *tuberosa* Pandellé, 1896; *S.* (*Meh.*) *sexpunctata* (Fabricius, 1805); *S.* (*Pan.*) *protuberans* Pandellé, 1896; *S.* (*Sar.*) *carnaria* (Linnaeus, 1758); *S.* (*Sar.*) *variegata* (Scopoli, 1763), and *S.* (*Pse.*) *spinosa* Villeneuve, 1912. New locality records are provided for 25 species. *Sarcophaga* (*Sar.*) *croatica* Baranov, 1941 was the most abundant with 37%, followed by *S.* (*Sar.*) *lehmanni* Müller, 1922 (21%), and *S.* (*Pas.*) *albiceps* Meigen, 1826 (5%), making up 63% of all collected specimens. Most species (35) were collected in locality of Zmajevac, while the fewest (3) were collected in Bilje locality. During this study, *S.* (*Pse.*) *spinosa* was recorded in Croatia for the first time. Combined with previous records, 42 species of flesh flies have been recorded from Croatian Baranja, which comprise 27% of the flesh flies known to occur in Croatia. The total number of species of the family Sarcophagidae currently known in Croatia has increased to 156.

## Keywords

Baranja, Croatia, Diptera, flesh flies, Sarcophagidae, Sarcophaginae

## Introduction

The European fauna of flesh flies (Sarcophagidae) comprises 310 species (Pape et al. 2015; Whitmore et al. 2020), of which approximately 150 species occur in Central Europe (Povolný and Verves 1997) and 155 species have been recorded from Croatia (Krčmar et al. 2019; Verves and Barták 2021). Verves and Barták (2021) erroneously listed *Paragusia multipunctata* (Rondani, 1859) as new for Croatia, but this species was already listed by Krčmar et al. (2019) under the name *Taxigramma multipunctata* (Rondani, 1859). Also, under a broad concept of *Sarcophaga*, the species name *Heteronychia* (s.str.) *rohdendorfi* (Povolný & Slamečková, 1959) represents a junior secondary homonym of *Sarcophaga rohdendorfi* Salem, 1936, *Parasarcophaga rohdendorfi* Baranov, 1938, and *Sarcophaga rohdendorfi* Baranov, 1941 (Whitmore 2011), and the valid name for this species is *Sarcophaga* (*Heteronychia*) *lederbergi* (Lehrer, 1995). Of the Croatian Sarcophagidae, most species (108) belong to subfamily Sarcophaginae, followed by Miltogramminae (38) and Paramacronychiinae (9) (Krčmar et al. 2019; Verves and Barták 2021). By reviewing the published data of Langhoffer (1920), Baranov (1928, 1929, 1938, 1941, 1942, 1943), Strukan (1964, 1967, 1970), Sisojević et al. (1989), Rucner (1994), as well as the recently published data of Whitmore (2010, 2011), Whitmore et al. (2013), and Krčmar et al. (2019), 90 species of flesh flies have been recorded in the Pannonian–Peripannonian biogeographic region of Croatia (Sarcophaginae: 68; Miltogramminae: 19; Paramacronychiinae: 3). Most of the studies were done and most species were recorded in the northern part of this region. In the recent study of Krčmar et al. (2019), 29 species of flesh flies were collected from only two localities in the Croatian part of Baranja, which is far from the total number of species considering the great landscape diversity of this area. The principal aims of this study are to give the first overview of the flesh fly fauna from subfamily Sarcophaginae in rural settlements in the Croatian part of Baranja and to emphasize the importance of these habitats for flesh fly diversity.

## Materials and methods

### Study area

Baranja is a Pannonian Plain region of Hungary (its northern portion) and Croatia (its southern portion). It is situated in the eastern part of Croatia and forms part of Osijek-Baranja County. Triangular in shape, it covers an area of 1147 km<sup>2</sup> between the Drava, the Danube, and the state border with Hungary (Bognar et al. 1975). The Croatian part of Baranja is a predominantly lowland area (elevation ≤ 259 m). Bansko brdo (Bansko Hill) is the most prominent part of Baranja in terms of relief and extends NE-SW for 21 km, whereas its width is much smaller (Bognar et al. 1975). The steppe, the natural vegetation that covers Bansko Hill, has completely disappeared. The belt along the Danube and Drava is a flooded area (– 63% of the territory) with many secondary tributaries

and wetlands (Kopački rit) (Bognar et al. 1975). The Kopački rit Nature Park is one of the largest fluvial-marshy plains in Europe (Schneider-Jacoby 1994), and the basic ecological features relate to the river dynamics (Schneider-Jacoby 1994; Mihaljević et al. 1999). Forests cover ~ 20% of the Croatian part of Baranja. The climate is moderately continental with significant temperature fluctuations. The average January temperature is ~ -1.3 °C, and the July temperature is ~ 22 °C; the average annual rainfall is ~ 650 mm (Bognar et al. 1975). The Croatian part of Baranja contains 54 settlements, some of which contain pond habitats, which increasingly serve as places for recreation of people and their pets. All seven sampling sites are situated at the periphery of the settlements (Fig. 1). Geographical coordinates of these seven sampling sites are given in Table 1. Pond habitats in settlements of Kotlina, Suza, and Zmajevac are surrounded by species of willow (*Salix*) and poplar (*Populus*). Sampling sites in the settlements of Petlovac and Popovac are overgrown mainly with reeds (*Phragmites australis*), sedges (*Carex* ssp.), and rush (*Typha* ssp.) without forest vegetation at its edges. A similar type of vegetation is present at the pond in Darda, with the addition of water lilies (*Nymphaea alba*) and nenuphar (*Nuphar luteum*), while pond habitats in Bilje settlement are overgrown with different species of low grasses exposed to the open sun throughout the day.

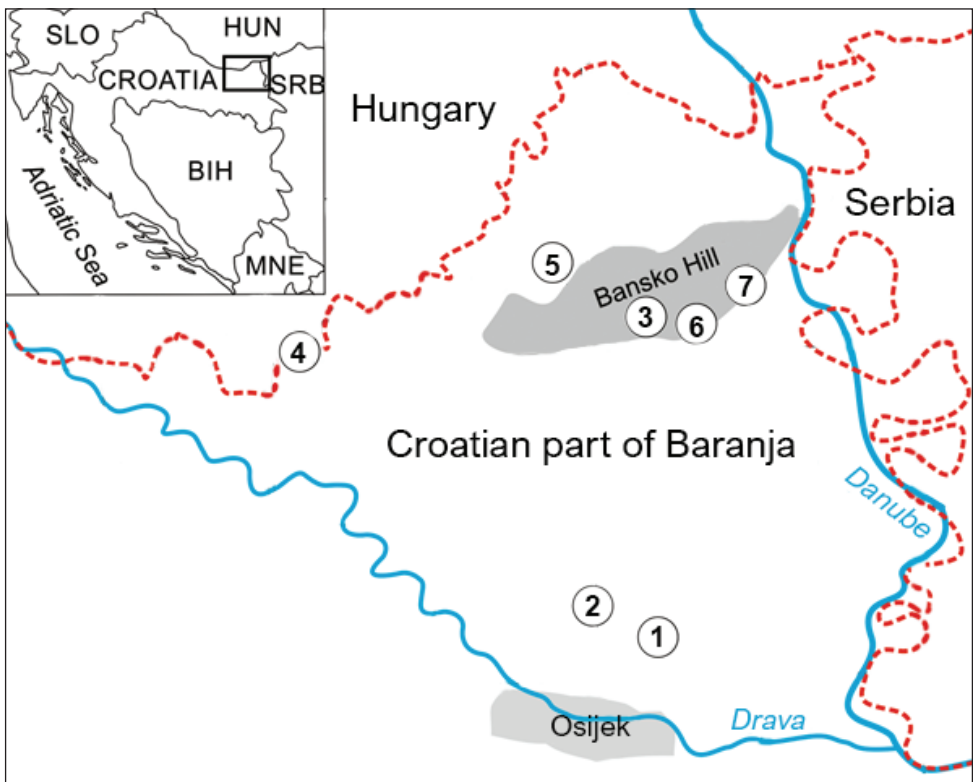


**Figure 1.** Sampling sites for flesh flies (Sarcophagidae: Sarcophaginae) in the Croatian part of Baranja. Legend: 1. Bilje; 2. Darda; 3. Kotlina; 4. Petlovac; 5. Popovac; 6. Suza; 7. Zmajevac.

**Table 1.** List of sampling sites around pond habitats in Croatian part of Baranja.

No. of locality	Locality	Geographical coordinates
1	Bilje	45°36'16"N, 18°44'39"E
2	Darda	45°37'30"N, 18°41'21"E
3	Kotlina	45°47'17"N, 18°44'16"E
4	Petlovac	45°45'31"N, 18°31'41"E
5	Popovac	45°48'22"N, 18°39'34"E
6	Suza	45°46'55"N, 18°46'32"E
7	Zmajevac	45°48'03"N, 18°48'29"E

## Sampling and identification

Collections of sarcophagids from pond habitats were made frequently over a period of seven months (April–October) from 2019 to 2021. During 2019 and 2020, from April to October, sampling at the pond habitat in Zmajevac was done 1–5 times a month. Samplings in 2021 were carried out once per month from May to August. Flesh flies were sampled from 1 pm to 5 pm using a standard insect sweep net to selectively collect flies resting on soil and vegetation, or attracted to animal faeces and the remains of discarded food. The collected specimens were preserved in 96% ethanol. Male terminalia were prepared for species identification following the method of Richet et. al (2011). After two days in ethanol, male abdomens were dissected and soaked in a 10% KOH solution for 72 h. They were then immersed in 10% acetic acid for 1 min and rinsed with water for 1 min. They were then dehydrated in beech-wood creosote for 4 h. The phallus, pregonites and postgonites, sternite 5, cerci, and surstyli were separated from the rest of abdomen and placed into a plastic vial (volume of 2 ml) with 96% of ethanol solution. Identifications were carried out using keys for Sarcophagidae (Pape 1987; Povolný and Verves 1997; Richet et al. 2011) and descriptions and illustrations in Whitmore (2009, 2010, 2011) and Whitmore et al. (2013). Nomenclature and classification follow the Fauna Europaea database (Pape 2004). For all samples, the following information is provided: locality and date of collection, collector(s), number and sex of specimens, and depository. Also, 33 unidentified specimens from May 2018 are now identified and their data have been included in this study. One species newly recorded for the Croatian fauna is marked with a black triangle (▲). Specimens examined for this study are deposited in the collections of the Department of Biology, Josip Juraj Strossmayer University of Osijek, Osijek, Croatia (DBUO) and the Staatliches Museum für Naturkunde, Stuttgart, Germany (SMNS).

## Terminology

Subgeneric names are abbreviated as follows:

**Bel.** *Bellieriomima*  
**Ber.** *Bercaea*  
**Hel.** *Helicophagella*  
**Het.** *Heteronychia*

**Kra.** *Krameromyia*  
**Lip.** *Liopygia*  
**Lis.** *Liosarcophaga*  
**Meh.** *Mehria*

<b>Myo.</b>	<i>Myorhina</i>	<b>Ros.</b>	<i>Rosellea</i>
<b>Pan.</b>	<i>Pandelleana</i>	<b>Sar.</b>	<i>Sarcophaga</i>
<b>Pas.</b>	<i>Parasarcophaga</i>	<b>Sac.</b>	<i>Sarcotachinella</i>
<b>Pad.</b>	<i>Pandelleisca</i>	<b>Ser.</b>	<i>Servaisia</i>
<b>Pse.</b>	<i>Pseudothyrsocnema</i>	<b>Thy.</b>	<i>Thyrsocnema</i>
<b>Rob.</b>	<i>Robineauella</i>		

## Results

A total of 1293 flesh flies belonging to 37 species was collected (Table 2). *Sarcophaga* (*Sar.*) *croatica* Baranov, 1941 was the most abundant with 37%, followed by *S. (Sar.) lehmanni* Müller, 1922 (21%), *S. (Pas.) albiceps* Meigen, 1826 (5%), *S. (Sar.) baranoffi* Rohdendorf, 1937 (5%), *S. (Thy.) incisilobata* Pandellé, 1896 (5%), *S. (Lis.) emdeni* (Rohdendorf, 1969) (3%), *S. (Lis.) aegyptica* Salem, 1935 (3%), *S. (Hel.) melanura* Meigen, 1826 (3%), *S. (Het.) filia* Rondani, 1860 (3%), *S. (Ros.) aratrix* Pandellé, 1896 (2%), *S. (Hel.) noverca* Rondani, 1860 (2%), *S. (Bel.) subulata* Pandellé, 1896 (1%), *S. (Pad.) similis* Meade, 1876 (1%), and *Ravinia pernix* (Harris, 1780) (1%). These fourteen species comprised 92% of the samples; the remaining 23 species represented 8% (Table 2). Most species (35) and specimens (75%) were collected in Zmajevac (Table 2). The lowest number of species was collected in Bilje (3), whereas in other localities the number of collected species was between 8 and 11. The largest number of specimens and species was collected during 2019 (Table 3). New records for Baranja are provided for 25 species, with the record of *S. (Pse.) spinosa* representing a first record for Croatia.

## List of recorded species

### Subfamily Sarcophaginae Macquart, 1834

#### 1. *Ravinia pernix* (Harris, 1780)

**New records for Croatian Baranja.** Zmajevac, 5.IX.2019, S. Krčmar leg. (1♂) (SMNS); same locality, 28.VI.2020, S. Krčmar leg. (2♂) (DBUO); same locality, 13.IX.2020, S. Krčmar leg. (2♂) (DBUO); same locality, 20.VI.2021, S. Krčmar leg. (1♂) (DBUO); Kotlina, 18.V.2021, S. Krčmar leg. (1♂) (DBUO); same locality, 18.VI.2021, S. Krčmar leg. (1♂) (DBUO); Popovac, 11.VI.2021, S. Krčmar leg. (1♂) (DBUO); same locality, 10.VII.2021, S. Krčmar leg. (5♂) (DBUO); Darda, 17.VI.2021, S. Krčmar leg. (1♂) (DBUO).

#### 2. *Sarcophaga (Bellieriomima) subulata* Pandellé, 1896

**Records.** Zmajevac, 9.V.2018, S. Krčmar leg. (4♂) (DBUO); same locality, 22.IV.2019, S. Krčmar leg. (1♂) (DBUO); same locality, 29.VII.2019, S. Krčmar leg. (8♂) (DBUO); same locality, 8.V.2020, S. Krčmar leg. (1♂) (DBUO); same locality,

12.VI.2020, S. Krčmar leg. (1♂) (DBUO); same locality, 12.VIII.2020, S. Krčmar leg. (2♂) (DBUO); same locality, 11.V.2021, S. Krčmar leg. (1♂) (DBUO).

### 3. *Sarcophaga (Bercaea) africa* (Wiedemann, 1824)

**Records.** Zmajevac, 16.V.2019, S. Krčmar leg. (1♂) (DBUO); same locality, 24.VIII.2019, S. Krčmar leg. (1♂) (DBUO).

### 4. *Sarcophaga (Helicophagella) crassimargo* Pandellé, 1896

**Records.** Zmajevac, 17.VI.2019, S. Krčmar leg. (1♂) (SMNS); same locality, 24.VIII.2019, S. Krčmar leg. (1♂) (SMNS); same locality, 28.VI.2020, S. Krčmar leg. (3♂) (DBUO); same locality, 28.VII.2020, S. Krčmar leg. (1♂) (DBUO).

### 5. *Sarcophaga (Helicophagella) hirticrus* Pandellé, 1896

**Records.** Zmajevac, 5.IX.2019, S. Krčmar leg. (1♂) (SMNS); same locality, 8.V.2020, S. Krčmar leg. (1♂) (DBUO).

### 6. *Sarcophaga (Helicophagella) melanura* Meigen, 1826

**Records.** Zmajevac, 9.V.2018, S. Krčmar leg. (2♂) (DBUO); same locality, 19.VIII.2019, S. Krčmar leg. (1♂) (DBUO); same locality, 22.VIII.2019, S. Krčmar leg. (3♂) (DBUO); same locality, 24.VIII.2019, S. Krčmar leg. (1♂) (DBUO); same locality, 5.IX.2019, S. Krčmar leg. (3♂) (DBUO); same locality, 6.IX.2019, S. Krčmar leg. (9♂) (DBUO, SMNS); same locality, 17.IX.2019, S. Krčmar leg. (1♂) (DBUO); same locality, 30.IX.2019, S. Krčmar leg. (2♂) (DBUO); same locality, 28.VI.2020, S. Krčmar leg. (1♂) (DBUO); same locality, 28.VII.2020, S. Krčmar leg. (1♂) (DBUO); same locality, 20.VI.2021, S. Krčmar leg. (9♂) (DBUO).

**New records for Croatian Baranja.** Popovac, 11.VI.2021, S. Krčmar leg. (1♂) (DBUO); same locality, 10.VII.2021, S. Krčmar leg. (2♂) (DBUO); Petlovac, 18.VI.2021, S. Krčmar leg. (1♂) (DBUO); Darda, 19.VIII.2021, S. Krčmar leg. (1♂) (DBUO).

### 7. *Sarcophaga (Helicophagella) noverca* Rondani, 1860

**Records.** Zmajevac, 9.V.2018, S. Krčmar leg. (6♂) (DBUO); same locality, 16.V.2019, S. Krčmar leg. (2♂) (DBUO); same locality, 22.V.2019, S. Krčmar leg. (12♂) (DBUO); same locality, 22.VIII.2019, S. Krčmar leg. (2♂) (DBUO); same locality, 5.IX.2019, S. Krčmar leg. (1♂) (DBUO); same locality, 6.IX.2019, S. Krčmar leg. (1♂) (DBUO); same locality, 13.IX.2019, S. Krčmar leg. (1♂) (SMNS); same locality, 8.V.2020, S. Krčmar leg. (1♂) (DBUO); same locality, 12.VIII.2020, S. Krčmar leg. (2♂) (DBUO); same locality, 13.IX.2020, S. Krčmar leg. (1♂) (DBUO).

**8. *Sarcophaga (Heteronychia) depressifrons* Zetterstedt, 1845**

**New records for Croatian Baranja.** Zmajevac, 12.VIII.2020, S. Krčmar leg. (1♂) (DBUO).

**9. *Sarcophaga (Heteronychia) filia* Rondani, 1860**

**New records for Croatian Baranja.** Zmajevac, 6.IX.2019, S. Krčmar leg. (1♂) (SMNS); same locality, 12.VI.2020, S. Krčmar leg. (6♂) (DBUO); same locality, 19.VI.2020, S. Krčmar leg. (1♂) (DBUO); same locality, 28.VI.2020, S. Krčmar leg. (17♂) (DBUO); same locality, 28.VII.2020, S. Krčmar leg. (6♂) (DBUO); same locality, 12.VIII.2020, S. Krčmar leg. (1♂) (DBUO); Petlovac, 18.V.2021, S. Krčmar leg. (1♂) (DBUO); same locality, 18.VI.2021, S. Krčmar leg. (2♂) (DBUO); Suza, 18.V.2021, S. Krčmar leg. (2♂) (DBUO).

**10. *Sarcophaga (Heteronychia) haemorrhoea* Meigen, 1826**

**Records.** Zmajevac, 9.V.2018, S. Krčmar leg. (1♂) (SMNS); same locality, 16.V.2019, S. Krčmar leg. (1♂) (SMNS); same locality, 29.VI.2019, S. Krčmar leg. (1♂) (DBUO); same locality, 5.IX.2019, S. Krčmar leg. (1♂) (SMNS); same locality, 12.VI.2020, S. Krčmar leg. (1♂) (DBUO); same locality, 28.VI.2020, S. Krčmar leg. (3♂) (DBUO); same locality, 28.VII.2020, S. Krčmar leg. (1♂) (DBUO); same locality, 12.VIII.2020, S. Krčmar leg. (1♂) (DBUO).

**11. *Sarcophaga (Heteronychia) haemorrhoides* Böttcher, 1913**

**New records for Croatian Baranja.** Zmajevac, 28.VI.2020, S. Krčmar leg. (1♂) (DBUO); same locality, 12.VIII.2020, S. Krčmar leg. (1♂) (DBUO).

**12. *Sarcophaga (Heteronychia) proxima* Rondani, 1860**

**Records.** Zmajevac, 22.V.2019, S. Krčmar leg. (1♂) (SMNS); same locality, 24.VIII.2019, S. Krčmar leg. (1♂) (SMNS); same locality, 30.VIII.2019, S. Krčmar leg. (1♂) (SMNS).

**13. *Sarcophaga (Heteronychia) pseudobenaci* (Baranov, 1942)**

**Records.** Zmajevac, 29.VI.2019, S. Krčmar leg. (1♂) (DBUO); same locality, 8.V.2020, S. Krčmar leg. (1♂) (DBUO); same locality, 13.IX.2020, S. Krčmar leg. (2♂) (DBUO).

**New records for Croatian Baranja.** Petlovac, 29.VIII.2021, S. Krčmar leg. (2♂) (DBUO).

**14. *Sarcophaga (Heteronychia) pumila* Meigen, 1826**

**New records for Croatian Baranja.** Popovac, 11.VI.2021, S. Krčmar leg. (1♂) (DBUO); Zmajevac, 30.VII.2021, S. Krčmar leg. (1♂) (DBUO).

**15. *Sarcophaga (Heteronychia) schineri* Bezzi, 1891**

**Records.** Zmajevac, 9.V. 2018, S. Krčmar leg. (1♂) (SMNS); same locality, 22.V.2019, S. Krčmar leg. (1♂) (SMNS); same locality, 12.VI.2020, S. Krčmar leg. (1♂) (DBUO); same locality, 28.VI.2020, S. Krčmar leg. (1♂) (DBUO); same locality, 12.VIII.2020, S. Krčmar leg. (1♂) (DBUO).

**16. *Sarcophaga (Heteronychia) vagans* Meigen, 1826**

**New records for Croatian Baranja.** Zmajevac, 19.VIII.2019, S. Krčmar leg. (1♂) (SMNS); same locality, 19.VI.2020, S. Krčmar leg. (1♂) (DBUO); same locality, 28.VI.2020, S. Krčmar leg. (1♂) (DBUO).

**17. *Sarcophaga (Liopygia) argyrostoma* (Robineau-Desvoidy, 1830)**

**Records.** Zmajevac, 29.VII.2019, S. Krčmar leg. (1♂) (DBUO); same locality, 22.VIII.2019, S. Krčmar leg. (1♂) (SMNS); same locality, 6.IX.2019, S. Krčmar leg. (1♂) (SMNS).

**New records for Croatian Baranja.** Popovac, 13.VIII.2021, S. Krčmar leg. (1♂) (DBUO).

**18. *Sarcophaga (Liopygia) crassipalpis* Macquart, 1839**

**New records for Croatian Baranja.** Popovac, 10.VII.2021, S. Krčmar leg. (1♂) (DBUO).

**19. *Sarcophaga (Liosarcophaga) aegyptica* Salem, 1935**

**Records.** Zmajevac, 22.VIII.2019, S. Krčmar leg. (1♂) (DBUO); same locality, 24.VIII.2019, S. Krčmar leg. (2♂) (DBUO); same locality, 30.VIII.2019, S. Krčmar leg. (2♂) (SMNS); same locality, 5.IX.2019, S. Krčmar leg. (5♂) (DBUO); same locality, 6.IX.2019, S. Krčmar leg. (2♂) (SMNS); same locality, 13.IX.2019, S. Krčmar leg. (1♂) (DBUO); same locality, 17.IX.2019, S. Krčmar leg. (1♂) (DBUO); same locality, 30.IX.2019, S. Krčmar leg. (9♂) (DBUO); same locality, 12.VI.2020, S. Krčmar leg. (1♂) (DBUO); same locality, 28.VI.2020, S. Krčmar leg. (1♂) (DBUO); same locality, 13.IX.2020, S. Krčmar leg. (2♂) (DBUO); same locality, 20.VI.2021, S. Krčmar leg. (2♂) (DBUO).

**New records for Croatian Baranja.** Kotlina, 18.V.2021, S. Krčmar leg. (1♂) (DBUO); Darda, 17.VI.2021, S. Krčmar leg. (1♂) (DBUO); Petlovac, 18.VI.2021, S.

Krčmar leg. (5♂) (DBUO); same locality, 20.VII.2021, S. Krčmar leg. (1♂) (DBUO); Suza, 25.VI.2021, S. Krčmar leg. (1♂) (DBUO); Popovac, 10.VII.2021, S. Krčmar leg. (2♂) (DBUO); same locality, 13.VIII.2021, S. Krčmar leg. (1♂) (DBUO).

## 20. *Sarcophaga (Liosarcophaga) dux* Thomson, 1869

**New records for Croatian Baranja.** Darda, 17.VI. 2021, S. Krčmar leg. (1♂) (DBUO).

## 21. *Sarcophaga (Liosarcophaga) emdeni* (Rohdendorf, 1969)

**Records.** Zmajevac, 9.V.2018, S. Krčmar leg. (1♂) (DBUO); same locality, 16.V.2019, S. Krčmar leg. (4♂) (DBUO); same locality, 22.V.2019, S. Krčmar leg. (3♂) (DBUO); same locality, 17.VI.2019, S. Krčmar leg. (2♂) (DBUO); same locality, 6.VII.2019, S. Krčmar leg. (4♂) (DBUO); same locality, 29.VII.2019, S. Krčmar leg. (2♂) (DBUO); same locality, 22.VIII.2019, S. Krčmar leg. (1♂) (DBUO); same locality, 24.VIII.2019, S. Krčmar leg. (2♂) (DBUO); same locality, 30.VIII.2019, S. Krčmar leg. (2♂) (DBUO); same locality, 5.IX.2019, S. Krčmar leg. (1♂) (DBUO); same locality, 13.IX.2019, S. Krčmar leg. (1♂) (DBUO); same locality, 8.V.2020, S. Krčmar leg. (1♂) (DBUO); same locality, 12.VI.2020, S. Krčmar leg. (1♂) (DBUO); same locality, 19.VI.2020, S. Krčmar leg. (1♂) (DBUO); same locality, 28.VI.2020, S. Krčmar leg. (4♂) (DBUO); same locality, 13.IX.2020, S. Krčmar leg. (1♂) (DBUO); same locality, 11.V.2021, S. Krčmar leg. (2♂) (DBUO).

**New records for Croatian Baranja.** Suza, 18.V.2021, S. Krčmar leg. (1♂) (DBUO); same locality, 11.VII.2021, S. Krčmar leg. (7♂) (DBUO); same locality, 12.VIII.2021, S. Krčmar leg. (2♂) (DBUO).

## 22. *Sarcophaga (Liosarcophaga) tuberosa* Pandellé, 1896

**New records for Croatian Baranja.** Zmajevac, 17.VI.2019, S. Krčmar leg. (1♂) (DBUO); Suza, 18.V.2021, S. Krčmar leg. (1♂) (DBUO).

## 23. *Sarcophaga (Mebria) sexpunctata* (Fabricius, 1805)

**New records for Croatian Baranja.** Zmajevac, 12.VI.2020, S. Krčmar leg. (1♂) (DBUO).

## 24. *Sarcophaga (Myorhina) nigriventris* Meigen, 1826

**Records.** Zmajevac, 16.V.2019, S. Krčmar leg. (1♂) (SMNS); same locality, 22.V.2019, S. Krčmar leg. (1♂) (DBUO); same locality, 30.IX.2019, S. Krčmar leg. (1♂) (SMNS); same locality, 28.VI.2020, S. Krčmar leg. (2♂) (DBUO); same locality, 28.VII.2020, S. Krčmar leg. (1♂) (DBUO); same locality, 20.X.2020, S. Krčmar leg. (1♂) (DBUO).

### 25. *Sarcophaga (Myorhina) soror Rondani, 1860*

**Records.** Zmajevac, 9.V.2018, S. Krčmar leg. (1♂) (DBUO); same locality, 16.V.2019, S. Krčmar leg. (3♂) (SMNS); same locality, 22.V.2019, S. Krčmar leg. (3♂) (DBUO); same locality, 29.VII.2019, S. Krčmar leg. (2♂) (DBUO); same locality, 19.VI.2020, S. Krčmar leg. (3♂) (DBUO).

### 26. *Sarcophaga (Pandelleana) protuberans Pandellé, 1896*

**New records for Croatian Baranja.** Zmajevac, 28.VI.2020, S. Krčmar leg. (1♂) (DBUO).

### 27. *Sarcophaga (Pandelleisca) similis Meade, 1876*

**Records.** Zmajevac, 16.V.2019, S. Krčmar leg. (1♂) (DBUO); same locality, 22.V.2019, S. Krčmar leg. (3♂) (DBUO); same locality, 24.VIII.2019, S. Krčmar leg. (1♂) (DBUO); same locality, 30.VIII.2019, S. Krčmar leg. (2♂) (SMNS); same locality, 5.IX.2019, S. Krčmar leg. (1♂) (DBUO); same locality, 6.IX.2019, S. Krčmar leg. (2♂) (DBUO); same locality, 13.IX.2019, S. Krčmar leg. (1♂) (DBUO); same locality, 30.IX.2019, S. Krčmar leg. (1♂) (DBUO); same locality, 28.VI.2020, S. Krčmar leg. (1♂) (DBUO).

**New records for Croatian Baranja.** Popovac, 11.VI.2021, S. Krčmar leg. (1♂) (DBUO); Petlovac, 18.VI.2021, S. Krčmar leg. (1♂) (DBUO); same locality, 20.VII.2021, S. Krčmar leg. (1♂) (DBUO); Darda, 19.VIII.2021, S. Krčmar leg. (1♂) (DBUO).

### 28. *Sarcophaga (Parasarcophaga) albiceps Meigen, 1826*

**Records.** Zmajevac, 16.V.2019, S. Krčmar leg. (1♂) (DBUO); same locality, 22.V.2019, S. Krčmar leg. (3♂) (DBUO); same locality, 29.VII.2019, S. Krčmar leg. (5♂) (DBUO); same locality, 19.VIII.2019, S. Krčmar leg. (1♂) (DBUO); same locality, 22.VIII.2019, S. Krčmar leg. (5♂) (DBUO); same locality, 24.VIII.2019, S. Krčmar leg. (4♂) (DBUO); same locality, 5.IX.2019, S. Krčmar leg. (5♂) (DBUO); same locality, 6.IX.2019, S. Krčmar leg. (16♂) (DBUO, SMNS); same locality, 8.V.2020, S. Krčmar leg. (1♂) (DBUO); same locality, 19.VI.2020, S. Krčmar leg. (2♂) (DBUO); same locality, 28.VI.2020, S. Krčmar leg. (7♂) (DBUO); same locality, 28.VII.2020, S. Krčmar leg. (2♂) (DBUO); same locality, 20.VI.2021, S. Krčmar leg. (7♂) (DBUO).

**New records for Croatian Baranja.** Bilje, 24.VII.2021, S. Krčmar leg. (6♂) (DBUO); Kotlina, 12.VIII.2021, S. Krčmar leg. (1♂) (DBUO).

### 29. *Sarcophaga (Robineauella) caerulea Zetterstedt, 1838*

**Records.** Zmajevac, 22.V.2019, S. Krčmar leg. (1♂) (SMNS); same locality, 17.VI.2019, S. Krčmar leg. (1♂) (DBUO); same locality, 8.V.2020, S. Krčmar leg. (1♂) (DBUO); same locality, 28.VII.2020, S. Krčmar leg. (1♂) (DBUO).

**30. *Sarcophaga (Rosellea) aratrix* Pandellé, 1896**

**Records.** Zmajevac, 9.V.2018, S. Krčmar leg. (1♂) (DBUO); same locality, 22.IV.2019, S. Krčmar leg. (1♂) (SMNS); same locality, 16.V.2019, S. Krčmar leg. (2♂) (DBUO); same locality, 22.V.2019, S. Krčmar leg. (2♂) (SMNS); same locality, 17.VI.2019, S. Krčmar leg. (1♂) (DBUO); same locality, 24.VIII.2019, S. Krčmar leg. (1♂) (DBUO); same locality, 30.VIII.2019, S. Krčmar leg. (5♂) (DBUO); same locality, 5.IX.2019, S. Krčmar leg. (2♂) (DBUO); same locality, 8.V.2020, S. Krčmar leg. (3♂) (DBUO); same locality, 12.VI.2020, S. Krčmar leg. (1♂) (DBUO); same locality, 13.IX.2020, S. Krčmar leg. (2♂) (DBUO); same locality, 20.VI.2021, S. Krčmar leg. (2♂) (DBUO); same locality, 30.VII.2021, S. Krčmar leg. (1♂) (DBUO); same locality, 12.VIII.2021, S. Krčmar leg. (1♂) (DBUO).

**New records for Croatian Baranja.** Suza, 18.V.2021, S. Krčmar leg. (3♂) (DBUO); same locality, 11.VII.2021, S. Krčmar leg. (1♂) (DBUO); Petlovac, 20.VII.2021, S. Krčmar leg. (1♂) (DBUO); Darda, 24.VII.2021, S. Krčmar leg. (1♂) (DBUO); Popovac, 13.VIII.2021, S. Krčmar leg. (1♂) (DBUO).

**31. *Sarcophaga (Sarcophaga) baranoffi* Rohdendorf, 1937**

**Records.** Zmajevac, 9.V.2018, S. Krčmar leg. (2♂) (DBUO); same locality, 16.V.2019, S. Krčmar leg. (8♂) (DBUO, SMNS); same locality, 22.V.2019, S. Krčmar leg. (4♂) (DBUO); same locality, 29.VII.2019, S. Krčmar leg. (7♂) (DBUO); same locality, 22.VIII.2019, S. Krčmar leg. (1♂) (DBUO); same locality, 24.VIII.2019, S. Krčmar leg. (2♂) (DBUO); same locality, 30.VIII.2019, S. Krčmar leg. (4♂) (DBUO); same locality, 5.IX.2019, S. Krčmar leg. (1♂) (DBUO); same locality, 6.IX.2019, S. Krčmar leg. (6♂) (DBUO); same locality, 30.IX.2019, S. Krčmar leg. (1♂) (DBUO); same locality, 19.VI.2020, S. Krčmar leg. (1♂) (DBUO); same locality, 28.VI.2020, S. Krčmar leg. (2♂) (DBUO); same locality, 12.VIII.2020, S. Krčmar leg. (1♂) (DBUO); same locality, 13.IX.2020, S. Krčmar leg. (1♂) (DBUO); same locality, 11.V.2021, S. Krčmar leg. (1♂) (DBUO); same locality, 20.VI.2021, S. Krčmar leg. (1♂) (DBUO); same locality, 30.VII.2021, S. Krčmar leg. (6♂) (DBUO); same locality, 12.VIII.2021, S. Krčmar leg. (3♂) (DBUO).

**New records for Croatian Baranja.** Kotlina, 18.V.2021, S. Krčmar leg. (2♂) (DBUO); Suza, 25.VI.2021, S. Krčmar leg. (2♂) (DBUO); same locality, 12.VIII.2021, S. Krčmar leg. (2♂) (DBUO); Darda, 24.VII.2021, S. Krčmar leg. (2♂) (DBUO); Petlovac, 29.VIII.2021, S. Krčmar leg. (2♂) (DBUO).

**32. *Sarcophaga (Sarcophaga) carnaria* (Linnaeus, 1758)**

**New records for Croatian Baranja.** Zmajevac, 13.IX.2019, S. Krčmar leg. (1♂) (DBUO); same locality, 20.VI.2021, S. Krčmar leg. (1♂) (DBUO); Kotlina, 18.V.2021, S. Krčmar leg. (3♂) (DBUO).

### 33. *Sarcophaga (Sarcophaga) croatica* Baranov, 1941

**Records.** Zmajevac, 9.V.2018, S. Krčmar leg. (14♂) (DBUO); same locality, 22.IV.2019, S. Krčmar leg. (17♂) (DBUO, SMNS); same locality, 16.V.2019, S. Krčmar leg. (20♂) (DBUO); same locality, 22.V.2019, S. Krčmar leg. (15♂) (DBUO); same locality, 17.VI.2019, S. Krčmar leg. (10♂) (DBUO); same locality, 6.VII.2019, S. Krčmar leg. (1♂) (DBUO); same locality, 29.VII.2019, S. Krčmar leg. (5♂) (DBUO); same locality, 19.VIII.2019, S. Krčmar leg. (19♂) (DBUO); same locality, 22.VIII.2019, S. Krčmar leg. (19♂) (DBUO); same locality, 24.VIII.2019, S. Krčmar leg. (29♂) (DBUO); same locality, 30.VIII.2019, S. Krčmar leg. (34♂) (DBUO); same locality, 5.IX.2019, S. Krčmar leg. (9♂) (DBUO); same locality, 13.IX.2019, S. Krčmar leg. (8♂) (DBUO); same locality, 17.IX.2019, S. Krčmar leg. (1♂) (DBUO); same locality, 30.IX.2019, S. Krčmar leg. (3♂) (DBUO); same locality, 8.V.2020, S. Krčmar leg. (12♂) (DBUO); same locality, 12.VI.2020, S. Krčmar leg. (8♂) (DBUO); same locality, 19.VI.2020, S. Krčmar leg. (29♂) (DBUO); same locality, 28.VI.2020, S. Krčmar leg. (8♂) (DBUO); same locality, 28.VII.2020, S. Krčmar leg. (2♂) (DBUO); same locality, 12.VIII.2020, S. Krčmar leg. (3♂) (DBUO); same locality, 13.IX.2020, S. Krčmar leg. (22♂) (DBUO); same locality, 11.X.2020, S. Krčmar leg. (1♂) (DBUO); same locality, 20.X.2020, S. Krčmar leg. (5♂) (DBUO); same locality, 11.V.2021, S. Krčmar leg. (8♂) (DBUO); same locality, 20.VI.2021, S. Krčmar leg. (17♂) (DBUO); same locality, 30.VII.2021, S. Krčmar leg. (4♂) (DBUO); same locality, 12.VIII.2021, S. Krčmar leg. (5♂) (DBUO).

**New records for Croatian Baranja.** Kotlina, 18.V.2021, S. Krčmar leg. (8♂) (DBUO); same locality, 18.VI.2021, S. Krčmar leg. (9♂) (DBUO); Petlovac, 18.V.2021, S. Krčmar leg. (9♂) (DBUO); same locality, 18.VI.2021, S. Krčmar leg. (22♂) (DBUO); same locality, 20.VII.2021, S. Krčmar leg. (10♂) (DBUO); Suza, 18.V.2021, S. Krčmar leg. (6♂) (DBUO); same locality, 25.VI.2021, S. Krčmar leg. (17♂) (DBUO); same locality, 11.VII.2021, S. Krčmar leg. (5♂) (DBUO); same locality, 12.VIII.2021, S. Krčmar leg. (5♂) (DBUO); Popovac, 11.VI.2021, S. Krčmar leg. (1♂) (DBUO); Bilje, 17.VI.2021, S. Krčmar leg. (17♂) (DBUO); same locality, 19.VIII.2021, S. Krčmar leg. (3♂) (DBUO); Darda, 17.VI.2021, S. Krčmar leg. (2♂) (DBUO); same locality, 24.VII.2021, S. Krčmar leg. (16♂) (DBUO); same locality, 19.VIII.2021, S. Krčmar leg. (14♂) (DBUO).

### 34. *Sarcophaga (Sarcophaga) lehmanni* Müller, 1922

**Records.** Zmajevac, 22.IV.2019, S. Krčmar leg. (4♂) (DBUO, SMNS); same locality, 16.V.2019, S. Krčmar leg. (10♂) (DBUO); same locality, 22.V.2019, S. Krčmar leg. (19♂) (DBUO); same locality, 17.VI.2019, S. Krčmar leg. (6♂) (DBUO); same locality, 6.VII.2019, S. Krčmar leg. (5♂) (DBUO); same locality, 29.VII.2019, S. Krčmar leg. (3♂) (DBUO); same locality, 22.VIII.2019, S. Krčmar leg. (1♂) (DBUO); same locality, 24.VIII.2019, S. Krčmar leg. (3♂) (DBUO); same locality, 30.VIII.2019, S. Krčmar leg. (4♂) (DBUO); same locality, 5.IX.2019, S. Krčmar leg. (3♂) (DBUO); same locality, 6.IX.2019, S. Krčmar leg. (10♂) (DBUO); same locality, 13.IX.2019, S. Krčmar leg. (7♂) (DBUO); same locality, 17.IX.2019, S. Krčmar leg. (2♂) (DBUO);

same locality, 30.IX.2019, S. Krčmar leg. (13♂) (DBUO); same locality, 29.VI.2019, S. Krčmar leg. (1♂) (DBUO); same locality, 8.V.2020, S. Krčmar leg. (17♂) (DBUO); same locality, 12.VI.2020, S. Krčmar leg. (18♂) (DBUO); same locality, 19.VI.2020, S. Krčmar leg. (12♂) (DBUO); same locality, 28.VI.2020, S. Krčmar leg. (16♂) (DBUO); same locality, 28.VII.2020, S. Krčmar leg. (6♂) (DBUO); same locality, 13.IX.2020, S. Krčmar leg. (6♂) (DBUO); same locality, 11.X.2020, S. Krčmar leg. (2♂) (DBUO); same locality, 20.X.2020, S. Krčmar leg. (4♂) (DBUO); same locality, 11.V.2021, S. Krčmar leg. (13♂) (DBUO); same locality, 20.VI.2021, S. Krčmar leg. (4♂) (DBUO); same locality, 12.VIII.2021, S. Krčmar leg. (2♂) (DBUO).

**New records for Croatian Baranja.** Kotlina, 18.V.2021, S. Krčmar leg. (9♂) (DBUO); same locality, 18.VI.2021, S. Krčmar leg. (10♂) (DBUO); same locality, 12.VIII.2021, S. Krčmar leg. (1♂) (DBUO); Petlovac, 18.V.2021, S. Krčmar leg. (3♂) (DBUO); same locality, 18.VI.2021, S. Krčmar leg. (3♂) (DBUO); same locality, 20.VII.2021, S. Krčmar leg. (2♂) (DBUO); Suza, 18.V.2021, S. Krčmar leg. (4♂) (DBUO); same locality, 25.VI.2021, S. Krčmar leg. (2♂) (DBUO); same locality, 11.VII.2021, S. Krčmar leg. (29♂) (DBUO); same locality, 12.VIII.2021, S. Krčmar leg. (7♂) (DBUO); Popovac, 11.VI.2021, S. Krčmar leg. (9♂) (DBUO); same locality, 13.VIII.2021, S. Krčmar leg. (2♂) (DBUO); Bilje, 17.VI.2021, S. Krčmar leg. (4♂) (DBUO).

### 35. *Sarcophaga (Sarcophaga) variegata* (Scopoli, 1763)

**New records for Croatian Baranja.** Zmajevac, 30.VIII.2019, S. Krčmar leg. (2♂) (SMNS); same locality, 11.V.2021, S. Krčmar leg. (1♂) (DBUO); Petlovac, 18.VI.2021, S. Krčmar leg. (4♂) (DBUO).

### 36. *Sarcophaga (Thyrsocnema) incisilobata* Pandellé, 1896

**Records.** Zmajevac, 16.V.2019, S. Krčmar leg. (2♂) (DBUO, SMNS); same locality, 17.VI.2019, S. Krčmar leg. (3♂) (DBUO); 22.VIII.2019, S. Krčmar leg. (1♂) (DBUO); same locality, 24.VIII.2019, S. Krčmar leg. (3♂) (DBUO); same locality, 5.IX.2019, S. Krčmar leg. (4♂) (DBUO); same locality, 6.IX.2019, S. Krčmar leg. (10♂) (DBUO); same locality, 8.V.2020, S. Krčmar leg. (2♂) (DBUO); same locality, 12.VI.2020, S. Krčmar leg. (1♂) (DBUO); same locality, 19.VI.2020, S. Krčmar leg. (2♂) (DBUO); same locality, 28.VI.2020, S. Krčmar leg. (3♂) (DBUO); same locality, 12.VIII.2020, S. Krčmar leg. (3♂) (DBUO); same locality, 11.X.2020, S. Krčmar leg. (1♂) (DBUO); same locality, 20.X.2020, S. Krčmar leg. (4♂) (DBUO); same locality, 20.VI.2021, S. Krčmar leg. (4♂) (DBUO); same locality, 12.VIII.2021, S. Krčmar leg. (1♂) (DBUO).

**New records for Croatian Baranja.** Petlovac, 18.V.2021, S. Krčmar leg. (3♂) (DBUO); same locality, 18.VI.2021, S. Krčmar leg. (1♂) (DBUO); same locality, 20.VII.2021, S. Krčmar leg. (1♂) (DBUO); Suza, 18.V.2021, S. Krčmar leg. (1♂) (DBUO); same locality, 25.VI.2021, S. Krčmar leg. (1♂) (DBUO); same locality, 11.VII.2021, S. Krčmar leg. (1♂) (DBUO); Darda, 17.VI.2021, S. Krčmar leg.

(1♂) (DBUO); Kotlina, 18.VI.2021, S. Krčmar leg. (1♂) (DBUO); same locality, 20.VII.2021, S. Krčmar leg. (1♂) (DBUO); same locality, 12.VIII.2021, S. Krčmar leg. (3♂) (DBUO); Popovac, 13.VIII.2021, S. Krčmar leg. (1♂) (DBUO).

### 37. *Sarcophaga (Pseudothyrsoctema) spinosa* Villeneuve, 1912 ▲

**New records for Croatian Baranja.** Zmajevac, 12.VIII.2020, S. Krčmar leg. (1♂) (SMNS). New for Croatia.

**Table 2.** Number of species and specimens of flesh flies from subfamily Sarcophaginae collected at seven localities in Croatian part of Baranja from 2018 to 2021.

Species / Locality	1 Bilje	2 Darda	3 Kotlina	4 Petlovac	5 Popovac	6 Suza	7 Zmajevac	Σ
<i>Sarcophaga (Sar.) croatica</i>	20	32	17	41	1	33	328	472
<i>S. (Sar.) lehmanni</i>	4	-	20	8	11	42	191	276
<i>S. (Pas.) albiceps</i>	6	-	1	-	-	-	59	66
<i>S. (Sar.) baranoffi</i>	-	2	2	2	-	4	52	62
<i>S. (Thy.) incisilobata</i>	-	1	5	5	1	3	44	59
<i>S. (Lis.) emdeni</i>	-	-	-	-	-	10	33	43
<i>S. (Lis.) aegyptica</i>	-	1	1	6	3	1	29	41
<i>S. (Hel.) melanura</i>	-	1	-	1	3	-	33	38
<i>S. (Het.) filia</i>	-	-	-	3	-	2	32	37
<i>S. (Ros.) aratrix</i>	-	1	-	-	1	5	25	32
<i>S. (Hel.) noverca</i>	-	-	-	-	-	-	29	29
<i>S. (Bel.) subulata</i>	-	-	-	-	-	-	18	18
<i>S. (Pad.) similis</i>	-	1	-	2	1	-	13	17
<i>Ravinia pernix</i>	-	1	2	-	6	-	6	15
<i>S. (Myo.) soror</i>	-	-	-	-	-	-	12	12
<i>S. (Het.) haemorrhoba</i>	-	-	-	-	-	-	10	10
<i>S. (Myo.) nigriventris</i>	-	-	-	-	-	-	7	7
<i>S. (Sar.) variegata</i>	-	-	-	4	-	-	3	7
<i>S. (Hel.) crassimargo</i>	-	-	-	-	-	-	6	6
<i>S. (Het.) pseudobenaci</i>	-	-	-	2	-	-	4	6
<i>S. (Het.) schineri</i>	-	-	-	-	-	-	5	5
<i>S. (Sar.) carnaria</i>	-	-	3	-	-	-	2	5
<i>S. (Lip.) argyrostoma</i>	-	-	-	-	1	-	3	4
<i>S. (Rob.) caeruleascens</i>	-	-	-	-	-	-	4	4
<i>S. (Het.) proxima</i>	-	-	-	-	-	-	3	3
<i>S. (Het.) vagans</i>	-	-	-	-	-	-	3	3
<i>S. (Ber.) africa</i>	-	-	-	-	-	-	2	2
<i>S. (Hel.) hirticus</i>	-	-	-	-	-	-	2	2
<i>S. (Het.) haemorrhoides</i>	-	-	-	-	-	-	2	2
<i>S. (Het.) pumila</i>	-	-	-	-	1	-	1	2
<i>S. (Lis.) tuberosa</i>	-	-	-	-	-	1	1	2
<i>S. (Het.) depressifrons</i>	-	-	-	-	-	-	1	1
<i>S. (Lip.) crassipalpis</i>	-	-	-	-	1	-	-	1
<i>S. (Lis.) dux</i>	-	1	-	-	-	-	-	1
<i>S. (Meh.) sexpunctata</i>	-	-	-	-	-	-	1	1
<i>S. (Pan.) protuberans</i>	-	-	-	-	-	-	1	1
<i>S. (Pse.) spinosa</i>	-	-	-	-	-	-	1	1
Σ = 37	30	41	51	74	30	101	966	1293

**Table 3.** Number of collected flesh flies from subfamily Sarcophaginae according to sampling years in the Croatian part of Baranja.

Species / Year	2018	2019	2020	2021	Σ
<i>Sarcophaga (Sar.) croatica</i>	14	190	90	178	472
<i>S. (Sar.) lehmanni</i>	-	91	81	104	276
<i>S. (Pas.) albiceps</i>	-	40	12	14	66
<i>S. (Sar.) baranoffi</i>	2	34	5	21	62
<i>S. (Thy.) incisilobata</i>	-	23	16	20	59
<i>S. (Lis.) emdeni</i>	1	22	8	12	43
<i>S. (Lis.) aegyptica</i>	-	23	4	14	41
<i>S. (Hel.) melanura</i>	2	20	2	14	38
<i>S. (Het.) filia</i>	-	1	31	5	37
<i>S. (Ros.) aratrix</i>	1	14	6	11	32
<i>S. (Hel.) noverca</i>	6	19	4	-	29
<i>S. (Bel.) subulata</i>	4	9	4	1	18
<i>S. (Pad.) similis</i>	-	12	1	4	17
<i>Ravinia pernix</i>	-	1	4	10	15
<i>S. (Myo.) soror</i>	1	8	3	-	12
<i>S. (Het.) haemorrhoea</i>	1	3	6	-	10
<i>S. (Myo.) nigriventris</i>	-	3	4	-	7
<i>S. (Sar.) variegata</i>	-	2	-	5	7
<i>S. (Hel.) crassimargo</i>	-	2	4	-	6
<i>S. (Het.) pseudobenaci</i>	-	1	3	2	6
<i>S. (Het.) schineri</i>	1	1	3	-	5
<i>S. (Sar.) carnaria</i>	-	1	-	4	5
<i>S. (Lip.) argyrostoma</i>	-	3	-	1	4
<i>S. (Rob.) caerulea</i>	-	2	2	-	4
<i>S. (Het.) proxima</i>	-	3	-	-	3
<i>S. (Het.) vagans</i>	-	1	2	-	3
<i>S. (Ber.) africa</i>	-	2	-	-	2
<i>S. (Hel.) hirticus</i>	-	1	1	-	2
<i>S. (Het.) haemorrhoides</i>	-	-	2	-	2
<i>S. (Het.) pumila</i>	-	-	-	2	2
<i>S. (Lis.) tuberosa</i>	-	1	-	1	2
<i>S. (Het.) depressifrons</i>	-	-	1	-	1
<i>S. (Lip.) crassipalpis</i>	-	-	-	1	1
<i>S. (Lis.) dux</i>	-	-	-	1	1
<i>S. (Meh.) sexpunctata</i>	-	-	1	-	1
<i>S. (Pan.) protuberans</i>	-	-	1	-	1
<i>S. (Pse.) spinosa</i>	-	-	1	-	1
Σ = 37	33	533	302	425	1293

## Discussion

The first samples of flesh flies from Croatian Baranja were collected from 2014 to 2017 in the localities Zmajevac and Kamenac, at which time 29 species were recorded (Krčmar et al. 2019). Of those 29, the following five species were not confirmed in the present study: *Blaesoxipha (Ser.) rossica* Villeneuve, 1912; *S. (Het.) benaci* Böttcher, 1913;

*S. (Kra.) anaces* Walker, 1849; *S. (Lis.) portschinskyi* (Rohdendorf, 1937), and *S. (Sac.) sinuata* Meigen, 1826. Meanwhile, 13 species were newly recorded for the area in this study. Of all the 42 species recorded from Croatian Baranja, 41 are widely distributed in Central Europe (Povolný and Verves 1997), whereas one, *S. (Het.) pseudobenaci*, is restricted to southeastern Europe (Pape 2004). *Sarcophaga (Pse.) spinosa* represents a new record for Croatia, which is not surprising as this species is recorded from neighbouring Hungary and Serbia, and has also been recorded from Albania, French mainland, Italian mainland, North Macedonia, Romania, and Ukraine (Pape 2004). Most species were found in natural and semi-natural habitats, although some of the species recorded in this study, i.e., *S. (Ber.) africa*, *S. (Hel.) hirticrus*, *S. (Het.) depressifrons*, *S. (Lip.) argyrostoma*, *S. (Ros.) aratrix*, and *S. (Sar.) carnaria* are known to be found also in urban habitats (Hwang and Turner 2005). Some species of significance for forensic entomology were collected on several localities around pond habitats in rural settlements, in particular *S. (Lip.) argyrostoma* and *S. (Lis.) dux*, both of which colonize decomposing human remains (Draber-Moňko et al. 2009; Sukontason et al. 2014), whereas *S. (Lis.) dux* has a medical importance as an agent of myiasis (Sukontason et al. 2014). Also, an important role of *S. (Lip.) argyrostoma* in accidental intestinal myiasis was recently confirmed (Najjari et al. 2020). Moreover, *S. (Ber.) africa*, *S. (Lip.) argyrostoma*, *S. (Pad.) similis*, and *S. (Rob.) caerulescens* have been found on corpses in indoor cases in Switzerland and Finland (Cherix et al. 2012; Ren et al. 2018), while *S. (Lip.) crassipalpis* was found on corpses at the earliest stage of decomposition in Australia (Ren et al. 2018). All these five species were recorded in this study (Table 2). *Sarcophaga (Pad.) similis* was recorded in four localities (Darda, Petlovac, Popovac, Zmajevac). *Sarcophaga (Lip.) argyrostoma* was recorded on two localities (Popovac, Zmajevac), *S. (Ber.) africa*, and *S. (Rob.) caerulescens* were only recorded in Zmajevac, while *S. (Lip.) crassipalpis* was recorded only in Popovac (Table 2). In this study, a large number of flesh fly specimens were collected on or nearby pet animal faeces and on discarded leftover food. This is not surprising since it is known that *S. (Pas.) albiceps*, *S. (Thy.) incisilobata*, and *Ravinia pernix* visit excrements from humans and (other) animals (Papp 1992a, 1992b). Several species of flesh flies are also known to visit different animal carcasses (Szpila et al. 2015). Among them, the following species were recorded during this study: *R. pernix*, *S. (Hel.) melanura*, *S. (Lip.) argyrostoma*, *S. (Pad.) similis*, *S. (Pas.) albiceps*, *S. (Rob.) caerulescens*, *S. (Ros.) aratrix*, *S. (Sar.) carnaria*, *S. (Sar.) lehmanni*, *S. (Sar.) variegata*, and *S. (Thy.) incisilobata*. During this study not a single specimen of flesh flies was collected from carcasses. In Yozgat province of Turkey, 21 flesh flies species were recorded visiting small carrion (Pekbey 2019) from which *S. (Ber.) africa*, *S. (Hel.) hirticrus*, *S. (Hel.) melanura*, *S. (Lip.) argyrostoma*, *S. (Lip.) crassipalpis*, *S. (Lis.) aegyptica*, *S. (Lis.) emdeni*, *S. (Lis.) tuberosa*, *S. (Myo.) nigriventris*, *S. (Sar.) lehmanni* and *S. (Thy.) incisilobata* were also collected in this study. Eighty years ago, Baranov (1940) confirmed the presence of five flesh fly species in a laystall in the village of Metajna on the Island of Pag, four of which were also recorded in this study. In a similar study from the Polish Baltic coast, a number of species were recorded from a marshy habitat (15) and a sandy habitat (24) (Kaczorowska 2009), while in this study 37 species were recorded from pond habitats. Regardless of the distance and different climatic conditions, 11 species are present in all three types of habitats: *S. (Ber.) africa*,

*S. (Hel.) crassimargo*, *S. (Hel.) melanura*, *S. (Het.) haemorrhoea*, *S. (Het.) vagans*, *S. (Myo.) nigriventris*, *S. (Rob.) caerulea*, *S. (Ros.) aratrix*, *S. (Sar.) carnaria*, *S. (Sac.) sinuata*, and *S. (Thy.) incisilobata*. In marshy and sandy habitats the most numerous species was *S. (Sar.) carnaria* (Kaczorowska 2009), while *S. (Sar.) croatica* was the most abundant around pond habitats in rural settlements. Martínez-Sánchez et al. (2000) recorded 12 species from a holm-oak pasture agroecosystem in Salamanca province (Spain), from which four species *S. (Ber.) africa*, *S. (Hel.) melanura*, *S. (Lip.) crassipalpis*, and *S. (Sar.) lehmanni* were also collected in this study. The large differences in the number of recorded species between Zmajevac and other localities may be explained by the much higher number of samples. This is clearly shown by the fact that in 2021 only 15 species were collected at the Zmajevac locality compared to the total number of 35 species that were sampled during all three years (2019–2021) at this locality. The lower number of recorded species at the Bilje locality was influenced by environmental factors such as open sun throughout the day (with afternoon temperatures  $\geq 32$  °C) and a lack of animal faeces and remains for food, which reduced the number of recorded species. The seven localities around pond habitats are polluted by different organic contaminations caused by various human activities, which can attract certain species for feeding and breeding.

## Conclusions

The species *S. (Sar.) croatica* and *S. (Sar.) lehmanni* were recorded from almost all sampling sites around pond habitats in the Croatian part of Baranja. They belong to the most widespread and abundant flesh flies in Croatia and have been recorded in all three biogeographic regions: Alpine, Mediterranean, and Pannonian–Peripannonian. By merging data from earlier studies (2014–2017) and this study, altogether 42 species of flesh flies were recorded in the Croatian part of Baranja. The species *S. (Pse.) spinosa* is recorded as new for the Croatian fauna, thus increasing the total number of recorded species of flesh flies in Croatia to 156.

## Acknowledgements

I am very grateful to Daniel Whitmore (Naturkunde Museum, Stuttgart, Germany) for the identification of newly recorded species of flesh flies for the Croatian fauna, as well as to Thomas Pape (Natural History Museum of Denmark) for help with literature. I am also grateful to reviewers for all improvements in this paper and to Stephen M. Smith, University of Waterloo, Waterloo, Canada for his linguistic corrections and improvements. This study was funded by the Department of Biology, Josip Juraj Strossmayer University of Osijek under the project OZB-ZP2021 (Sarcophagidae- 31053) “Diversity of flesh flies fauna from subfamily Sarcophaginae (Diptera: Sarcophagidae) in pond habitats in rural settlements in Croatian part of Baranja” and the Foundation of the Croatian Academy of Sciences and Arts from the project “Comparison of repellent activity of different essential oils and plant extracts against hard ticks (Acari: Ixodidae)“.

## References

- Baranov N (1928) Tachinidensammlung des zoologischen Museums in Zagreb. Glasnik Hrvatskoga Prirodoslovnoga Društva 39/40: 196–200.
- Baranov N (1929) Beitrag zur Kenntnis der Gattung *Sarcophaga* (Mg.) Böttcher (Dipt., Tach.). Neue Beiträge zur Systematische Insektenkunde 4: 142–153.
- Baranov N (1938) Raupenfliegen (Tachinidae s.l.) welche auf der Adria-Insel Pag bei trinken von Meerwasser gefangen wurden. Encyclopédie entomologique Série B II (Diptera) 9: 103–107.
- Baranov N (1940) Die Düngerstätten im Dorfe Metajna als Brutplätze der Hausfliegen. Veterinarski Arhiv 10: 193–213. [In Croatian with German abstract]
- Baranov N (1941) Zweiter Beitrag zur Kenntnis der Gattung *Sarcophaga* s.l. Veterinarski Arhiv 11: 361–404. [In Croatian with German abstract]
- Baranov N (1942) Sarcophagen im Unabhängigen Staate Kroatien. Veterinarski Arhiv 12: 497–659. [In Croatian with German abstract]
- Baranov N (1943) *Wohlfahrtia magnifica* Schin., als Erreger der Schweine-Myiasis in Kroatien. Veterinarski Arhiv 13: 447–456. [In Croatian with German abstract]
- Bognar A, Crkvenčić I, Pepeonik Z, Ridanović J, Roglić J, Sić M, Šegota T, Vresk M (1975) Geography of SR Croatia. Eastern Croatia. Školska knjiga, Zagreb, 256 pp. [In Croatian with English abstract]
- Cherix D, Wyss C, Pape T (2012) Occurrences of flesh flies (Diptera: Sarcophagidae) on human cadavers in Switzerland, and their importance as forensic indicators. Forensic Science International 220(1–3): 158–163. <https://doi.org/10.1016/j.forsciint.2012.02.016>
- Draber-Mońko A, Malewski T, Pomorski J, Łoś M, Ślipiński P (2009) On the morphology and mitochondrial DNA barcoding of the flesh fly *Sarcophaga (Liopygia) argyrostoma* (Robineau-Desvoidy, 1830) (Diptera: Sarcophagidae) – an important species in forensic entomology. Annales Zoologici 59(4): 465–493. <https://doi.org/10.3161/000345409X484865>
- Hwang C, Turner BD (2005) Spatial and temporal variability of necrophagous Diptera from urban to rural areas. Medical and Veterinary Entomology 19(4): 379–391. <https://doi.org/10.1111/j.1365-2915.2005.00583.x>
- Kaczorowska E (2009) Flesh flies (Diptera: Sarcophagidae) of sandy and marshy habitats of the Polish Baltic coast. Entomologica Fennica 20(1): 61–64. <https://doi.org/10.33338/ef.84461>
- Krčmar S, Whitmore D, Pape T, Buenaventura E (2019) Checklist of the Sarcophagidae (Diptera) of Croatia, with new records from Croatia and other Mediterranean countries. ZooKeys 831: 95–155. <https://doi.org/10.3897/zookeys.831.30795>
- Langhoffer A (1920) Beiträge zur Dipterenfauna Kroatiens. Glasnik hrvatskoga prirodoslovnoga društva 32: 57–63. <https://www.biodiversitylibrary.org/page/11380253>
- Martínez-Sánchez A, Rojo S, Marcos-García MA (2000) Necrophagous and coprophagous flesh flies associated with a holm-oak pasture agroecosystem (Diptera: Sarcophagidae). Boletín de la Asociación Española de Entomología 24: 171–185. [In Spanish with English abstract]
- Mihaljević M, Getz D, Tadić Z, Živanović B, Gucunski D, Topić J, Kalinović I, Mikuska J (1999) Kopački rit research survey and bibliography. Hrvatska akademija znanosti i

- umjetnosti, Zavod za znanstveni rad Osijek, Zagreb-Osijek, 188 pp. [In Croatian with English, German and Hungarian abstract]
- Najjari M, Dik B, Pekbey G (2020) Gastrointestinal Myiasis Due to *Sarcophaga argyrostoma* (Diptera: Sarcophagidae) in Mashhad, Iran: a Case Report. *Journal of Arthropod-Borne Diseases* 14: 317–324. <https://doi.org/10.18502/jad.v14i3.4565>
- Pape T (1987) The Sarcophagidae (Diptera) of Fennoscandia and Denmark. *Fauna Entomologica Scandinavica*, 19. E. J. Brill/Scandinavian Science Press Ltd., Leiden-Copenhagen, 203 pp. <https://doi.org/10.1163/9789004273436>
- Pape T (2004) Fauna Europaea: Diptera, Sarcophagidae. Fauna Europaea version 2.4. <http://www.faunaeur.org> [Accessed 28 December 2017]
- Pape T, Beuk P, Pont A, Shatalkin A, Ozerov A, Woźnica A, Merz B, Bystrowski C, Raper C, Bergström C, Kehlmaier C, Clements D, Greathead D, Kameneva E, Nartshuk E, Petersen F, Weber G, Bächli G, Geller-Grimm F, Van de Weyer G, Tschorsnig H, de Jong H, van Zuijlen J, Vaňhara J, Roháček J, Ziegler J, Majer J, Hurka K, Holston K, Rognes K, Greve-Jensen L, Munari L, de Meyer M, Pollet M, Speight M, Ebejer M, Martinez M, Carles-Tolrá M, Földvári M, Chvála M, Barták M, Evenhuis N, Chandler P, Cerretti P, Meier R, Rozkosny R, Prescher S, Gaimari S, Zatwarnicki T, Zeegers T, Dikow T, Korneyev V, Richter V, Michelsen V, Tanasijtshuk V, Mathis W, Hubenov Z, de Jong Y (2015) Fauna Europaea: Diptera-Brachycera. *Biodiversity Data Journal* 3: e4187. <https://doi.org/10.3897/BDJ.3.e4187>
- Papp L (1992a) Flies (Diptera) visiting human faeces in mountain creek valleys in Hungary. *Parasitologia Hungarica* 25: 85–96. <https://www.publication.nhmus.hu/pdf/parasitologia/bannaes.php>
- Papp L (1992b) Fly communities in pasture dung: some results and problems (Diptera). *Acta Zoologica Hungarica* 38: 75–88. <http://real-j.mtak.hu/id/eprint/4317>
- Pekbey G (2019) A preliminary study on determination of small carrion visitor Sarcophagidae (Diptera) species from Yozgat (Turkey), with two new records. *Turkish Journal of Agricultural and Natural Sciences* 6: 354–362. <https://doi.org/10.30910/turkjans.595085>
- Povolný D, Verves YuG (1997) The Flesh-Flies of Central Europe (Insecta, Diptera, Sarcophagidae). *Spixiana* (Suppl. 24): 1–264. <https://www.zobodat.at/pdf/SpixSupp0240001-0260.pdf>
- Ren L, Shang Y, Chen W, Meng F, Cai J, Zhu G, Chen L, Wang Y, Deng J, Guo Y (2018) A brief review of forensically important flesh flies (Diptera: Sarcophagidae). *Forensic Sciences Research* 3(1): 16–26. <https://doi.org/10.1080/20961790.2018.1432099>
- Richet R, Blackith RM, Pape T (2011) *Sarcophaga* of France (Diptera: Sarcophagidae). Pensoft Publishers, Sofia-Moscow, 327 pp.
- Rucner Z (1994) Beitrag zur Entomofauna einiger waldassoziationen Kroatiens. *Natura Croatica* 3: 1–22. <https://www.hrcak.srce.hr/file/16607>
- Schneider-Jacoby M (1994) Sava and Drava ecological value and future of the two main rivers in Croatia. *Periodicum Biologorum* 96: 348–356.
- Sisojević P, Čepelak J, Slamečkova M (1989) Contribution to the fauna of Sarcophagidae (Diptera) of Yugoslavia. *Biosistematika* 15: 71–79. [In Croatian with English abstract]
- Strukan D (1964) Contribution to the knowledge of Sarcophaginae species and types in Yugoslavia. PhD dissertation, University of Zagreb, Zagreb, Croatia [In Croatian with English abstract]

- Strukan D (1967) Remarques sur deux Sarcophaginae peu connus de Yougoslavie (Diptera Sarcophagidae). Cahiers des Naturalistes, Bulletin NP, n.s. 23: 45–47.
- Strukan D (1970) Les Parasarcophaginae de Yougoslavie (Sarcophagidae – Diptera). Matica Srpska Zbornik za Prirodne Nauke 38: 90–114. [In Serbian with French abstract]
- Sukontason KI, Sanit S, Klong-Klaew T, Tomberlin JK, Sukontason K (2014) *Sarcophaga (Liosarcophaga) dux* (Diptera: Sarcophagidae): A flesh fly species of medical importance. Biological Research 47(1): 14. <https://doi.org/10.1186/0717-6287-47-14>
- Szpila K, Mađra A, Jarmusz M, Matuszewski S (2015) Flesh flies (Diptera: Sarcophagidae) colonising large carcasses in Central Europe. Parasitology Research 114(6): 2341–2348. <https://doi.org/10.1007/s00436-015-4431-1>
- Verves Yu G, Barták M (2021) New faunistic data on Sarcophagidae (Diptera) from Croatia. The Kharkov Entomological Society Gazette 29(1): 71–76. <https://doi.org/10.36016/KhESG-2021-29-1-6>
- Whitmore D (2009) A review of the *Sarcophaga (Heteronychia)* (Diptera: Sarcophagidae) of Sardinia. In: Cerretti P, Mason F, Minelli A, Nardi G, Whitmore D (Eds) Research on the Terrestrial Arthropods of Sardinia. Zootaxa 2318: 566–588. <https://doi.org/10.11646/zootaxa.2318.1.24>
- Whitmore D (2010) Systematics and phylogeny of *Sarcophaga (Heteronychia)* (Diptera, Sarcophagidae). PhD dissertation. Università degli Studi di Roma “La Sapienza”, Dipartimento di Biologia Animale e dell’Uomo, Rome, Italy, [v +] 257 pp.
- Whitmore D (2011) New taxonomic and nomenclatural data on *Sarcophaga (Heteronychia)* (Diptera: Sarcophagidae), with description of six new species. Zootaxa 2778(1): 1–57. <https://doi.org/10.11646/zootaxa.2778.1.1>
- Whitmore D, Pape T, Cerretti P (2013) Phylogeny of *Heteronychia*: the largest lineage of *Sarcophaga* (Diptera: Sarcophagidae). Zoological Journal of the Linnean Society 169(3): 604–639. <https://doi.org/10.1111/zoj.12070>
- Whitmore D, Plummer S, Clemons L (2020) First records of *Sarcophaga (Heteronychia) bulgarica* (Enderlein) (Diptera, Sarcophagidae) from Great Britain. Dipterists Digest 27: 223–229.

# Caribbean Amphipoda (Crustacea) of Panama. Part I: parvorder Oedicerotidira

Elizabeth L. Durham<sup>1</sup>, Kristine N. White<sup>1</sup>

<sup>1</sup> Georgia College & State University, Department of Biological and Environmental Sciences, Milledgeville, GA 31061, USA

Corresponding author: Kristine N. White ([kristine.white@gcsu.edu](mailto:kristine.white@gcsu.edu))

---

Academic editor: Alan Myers | Received 15 February 2023 | Accepted 5 April 2023 | Published 24 April 2023

<https://zoobank.org/8FEFD7CD-4AC1-484F-ACB8-42A440ADB866>

---

**Citation:** Durham EL, White KN (2023) Caribbean Amphipoda (Crustacea) of Panama. Part I: parvorder Oedicerotidira. ZooKeys 1159: 37–50. <https://doi.org/10.3897/zookeys.1159.102034>

---

## Abstract

Amphipods in the parvorder Oedicerotidira are burrowers, furrowers, or surface skimmers. Members of the parvorder share a well-developed posteroventral lobe on coxa 4, an equilobate coxa 5, an immensely elongate pereopod 7 that differs in structure from pereopod 6, and an entire telson. Within the parvorder, only the family Oedicerotidae has been documented from Bocas del Toro, Panama, represented by two species. This research documents a range extension for *Hartmanodes nyei* (Shoemaker, 1933) and describes a new species of *Synchelidium* Sars, 1892. An identification key to the species of Caribbean Oedicerotidae of Panama is provided.

## Keywords

Bocas del Toro, Caribbean, *Hartmanodes nyei*, identification key, new species, Oedicerotidae, Panama, *Synchelidium purpurivitellum* sp. nov.

## Introduction

Parvorder Oedicerotidira Lilljeborg, 1865 (Lilljeborg 1865b) is comprised of 302 species, with representative species documented around the world. Members of Oedicerotidira share a well-developed posteroventral lobe on coxa 4, an equilobate coxa 5, an immensely elongate pereopod 7 that differs in structure from pereopod

6, and an entire telson (Lowry and Myers 2017). The parvorder contains three families of burrowing, furrowing, or surface skimming amphipods: Exoedicerotidae Barnard & Drummond, 1982 (20 spp.), Oedicerotidae Lilljeborg, 1865 (262 spp.), and Paracalliopiidae Barnard & Karaman, 1982 (20 spp.). Only one of these families, the Oedicerotidae, is known to occur in the Caribbean Sea and, to date, only six species within that family have been reported from the Caribbean: *Aceroides (Patoides) synparis* (Barnard, 1964); *Americhelidium americanum* (Bousfield, 1973); *Hartmanodes nyei* (Shoemaker, 1933); *Kroyera carinata* Bate, 1857 (as *Monoculodes* cf. *carinatus*); *Periocolodes cerasinus* Thomas & Barnard, 1985; *Westwoodilla longimana* Shoemaker, 1934 (LeCroy et. al. 2009; Martín et. al. 2013). Of these Caribbean species, only *A. synparis* has been documented from Panamanian waters, occurring at a depth of 850 m (Barnard 1964).

Defining characteristics of amphipods in the family Oedicerotidae include having a well-developed antenna 2, reaching at least half the length of antenna 1; a strong down-curved rostrum; well-developed dorsolateral eyes; coxae 1–3 well-developed, each longer than the previous coxa; a subchelate gnathopod 1; article 3 of gnathopod 2 less than  $2 \times$  as long as wide; and a distally attenuate pereopod 7 that is longer and more slender than pereopod 6. Amphipods in the family Oedicerotidae differ from those in the families Exoedicerotidae and Paracalliopiidae in having separate urosomite segments and lacking the oblique setal row on the maxilla 2 inner plate (Lowry and Myers 2017). Most species of the parvorder burrow into sediment, but little else is known about their ecology.

Two species of oedicerotid amphipods were collected from Bocas del Toro, Panama, one of which is new to science. Both species are diagnosed and the new species is described herein, and an identification key is provided to distinguish between the three species known from the Caribbean waters of Panama.

## Materials and methods

Amphipods were collected by hand using a Ziploc bag to scoop up fine sand from Crawl Cay, Bocas del Toro, Panama at depths of 1.5–5.0 m. The sand was elutriated with freshwater to remove amphipods. Live specimens were sorted to morphospecies, placed in clove oil for imaging, and preserved in 99.5% EtOH for later examination. Preserved specimens were transferred to glycerol, measured from the tip of the rostrum to the base of the telson, and dissected under a stereomicroscope. Specimens were illustrated using a Meiji MT5900L phase contrast microscope with an Olympus U-DA drawing tube attached. Illustrations were digitally inked following Coleman (2003) in Adobe Illustrator 2020 using a Wacom Intuos Pro Pen Tablet. Specimens are deposited in the Smithsonian Institution, U.S. National Museum of Natural History (USNM).

## Results

### Descriptions

**Parvorder Oedicerotidira Lilljeborg, 1865 (Lilljeborg, 1865b)**

**Superfamily Oedicerotoidea Lilljeborg, 1865 (Lilljeborg, 1865a)**

**Family Oedicerotidae Lilljeborg, 1865 (Lilljeborg, 1865b)**

### **Genus *Hartmanodes* Bousfield & Chevrier, 1996**

**Generic diagnosis.** Antenna 1 shorter than antenna 2; male antenna 2 much longer than that of female; head, rostrum large, apex deflexed. Gnathopods 1 and 2 not sexually dimorphic; gnathopod 1 carpus broad, propodus long, ovate; Gnathopod 2 subchelate, carpus narrow, propodus elongate, narrowing distally. Pereopod 5 coxa large, deep, equilobate. Pereopod 7 basis with small posterodistal lobe. Telson short, apex truncate or emarginate.

### ***Hartmanodes nyei* (Shoemaker, 1933)**

Figs 1, 2, 6A

*Monoculodes nyei* Shoemaker, 1933: 9, fig. 5.

*Hartmanodes nyei*: Bousfield and Chevrier 1996: 92; LeCroy 2000: 169, fig. 205.

**Material examined.** PANAMA • 1 ♀, 4.0 mm; Bocas del Toro, Crawl Cay; 9.2475°N, 82.1290°W; depth 5 m, in sand; 12 Aug 2021; K.N. White leg; USNM 1522425 • 1 ♂, 3.5 mm; same station data as for preceding; USNM 1522426 • 4 ♀; same station data as for preceding; USNM 1522427 • 1 ♀, 1 ♂, 2 juvenile; Bocas del Toro, Crawl Caye; 9.2376°N, 82.1438°W; depth 2 m, in sand, 11 Aug 2021; K.N. White leg.; USNM 1522428.

**Diagnosis.** Antenna 1 of female subequal to peduncle of antenna 2; antenna 2 of male much longer than that of female; head, anterodorsal angle broadly subquadrate. Pereopods 3 and 4 propodus subrectangular, dactylus elongate, slender; pereopods 5 and 6 dactylus elongate, subequal to propodus in length; pereopod 7 basis posterior margin with several short setae, carpus and propodus, posterior margin with several spine groups, dactylus elongate, slender.

**Distribution.** U.S.A.: Gulf of Mexico (Rakocinski et al. 1993), South Florida (Shoemaker 1933; Thomas 1993), Pacific California (Barnard 1962; Bousfield and Chevrier 1996); South America: Brazil (Shoemaker 1933); Central America: Belize (Thomas 1993), Panama (present study).

**Ecology.** These amphipods burrow into sand in shallow subtidal habitats.



**Figure 1.** *Hartmanodes nyei*, female, 4.0 mm, pereopod 3, pereopod 3 dactyl with setae removed, pereopod 6 and 7, antennae 1 and 2; male, 3.5 mm, antenna 1 and antenna 2 (broken). Scale bars: 0.1 mm.

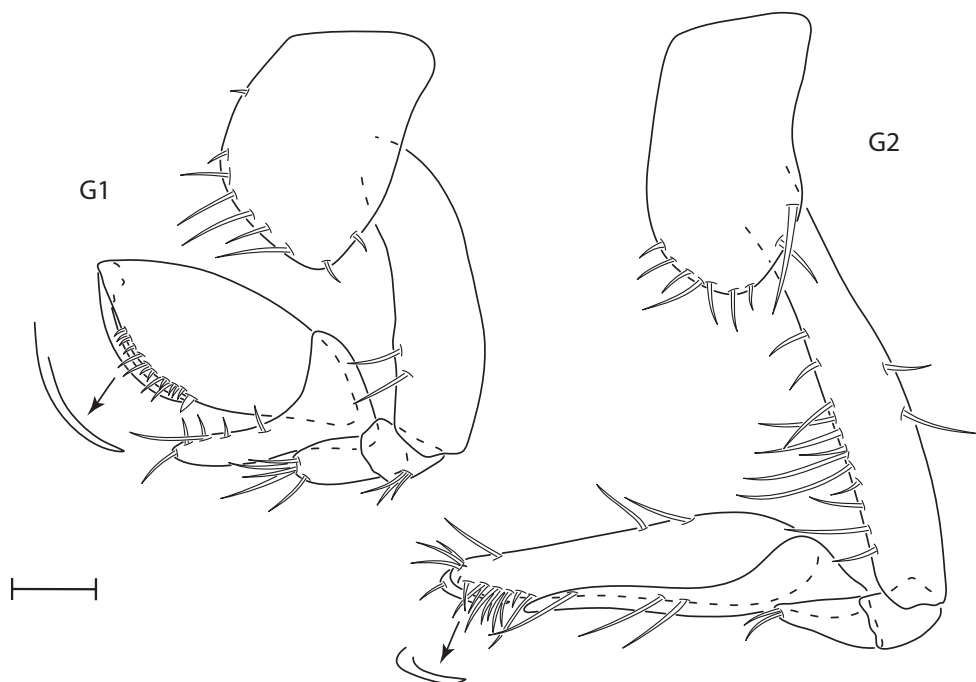


**Figure 2.** *Hartmanodes nyei*, female, 4.0 mm, gnathopods 1 and 2 lateral. Scale bar 0.1 mm.

### Genus *Synchelidium* Sars, 1892

**Generic diagnosis.** Antenna 1 shorter than antenna 2; male antenna 2 much longer than that of female; head, rostrum strong, distally deflexed. Gnathopods 1 and 2 not sexually dimorphic; gnathopod 1 carpus elongate, slender, propodus broad; Gnathopod 2 chelate, carpal lobe slender, propodus elongate. Pereopod 5 coxa medium, deep, equilobate. Pereopod 7 basis lacking or with weak posterior lobe. Telson short, apex emarginate or rounded.

#### *Synchelidium purpurivitellum* sp. nov.

<https://zoobank.org/117F5F75-7DE0-403D-8C9E-34DCB11C8EC1>

Figs 3–5, 6B

**Type locality.** Bocas del Toro, Panama: Crawl Cay, 9.2475°N, 82.1290°W, depth 5 m, in sand.

**Material examined. Holotype:** PANAMA • 1 ♀, 2.3 mm; Bocas del Toro, Crawl Cay; 9.2475°N, 82.1290°W; depth 5 m, in sand; 12 Aug 2021; K.N. White leg; USNM 1522429.

**Paratypes:** PANAMA • 1 ♂, 2.0 mm; same station data as for preceding; USNM 1522430 • 1 ♀, 2.0 mm; same station data as for preceding; USNM 1522431.

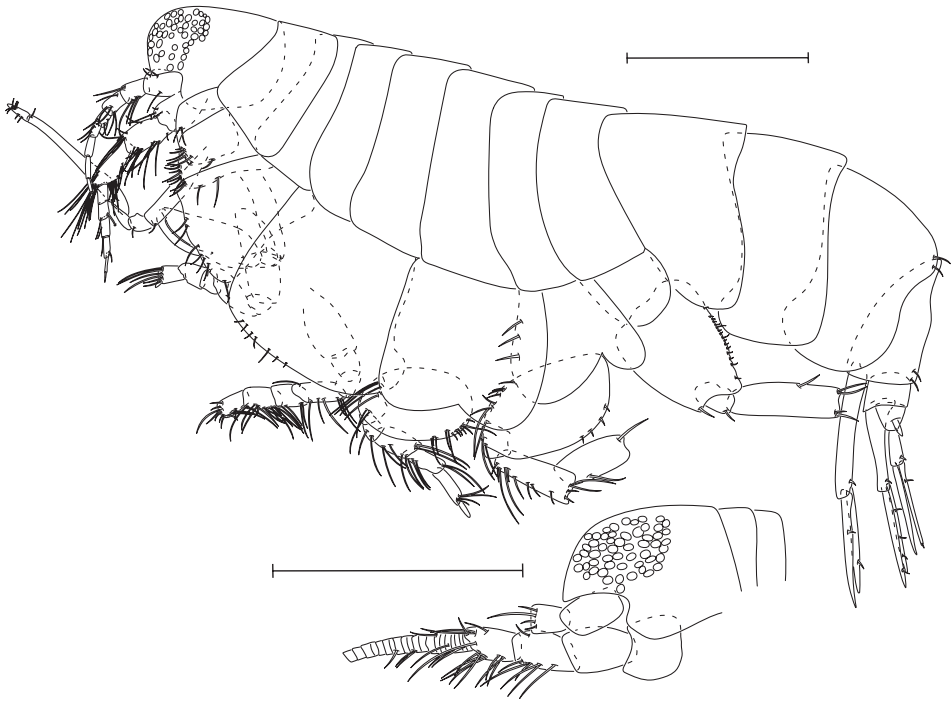


**Figure 3.** *Synchelidium purpurivitellum* sp. nov. holotype female, 2.3 mm, habitus; paratype male, 2.0 mm: head, antennae broken. Scale bars: 0.5 mm.

**Other material:** PANAMA • 2 ♀, 1 ♂, 3 juvenile, same station data as for preceding; USNM 1522432.

**Diagnosis.** Gnathopod 1 propodus, palm regularly toothed. Gnathopod 2 propodus slender,  $6 \times$  length of dactyl. Pereopod 3 propodus with anteroproximal margin longer than anterodistal margin, dactylus short, stubby. Coxa 4 posteroventral angle slightly produced. Coxa 6 posteroventral angle narrowly rounded. Pereopod 7 merus with spines on posterior margin slightly shorter than width of article. Epimeron 3 anteroventral margin narrowly produced. Telson thickened dorsoventrally, narrowing distally, apex subtruncate with two medium setae dorsolaterally, two short setae medially.

**Description. Female** (holotype, 2.3 mm). **Head.** Rostrum deflexed, reaching ventral margin of head, not surpassing article 1 of antenna 1. Eyes large, covering entire anterior portion of head. Antenna 1 length surpassing peduncle of antenna 2, moderately setose, peduncle segments subequal; flagellum 5-articulate. Antenna 2 is  $1.2 \times$  length of antenna 1, flagellum 5-articulate. Maxilliped, inner plate with four apical setae, outer plate with four or five distomedial, marginal setae. Lower lip, inner lobes rounded, outer lobes with large gape, apically setose. Maxilla 1 outer lobe with five apical plumose setae; palp bi-articulate, with three apical setae. Maxilla 2 inner plate with two apical setae, outer plate with three apical setae. Mandibles similar, incisors dentate; left mandible lacinia mobilis 6-dentate, right mandible lacinia mobilis 4-dentate; four

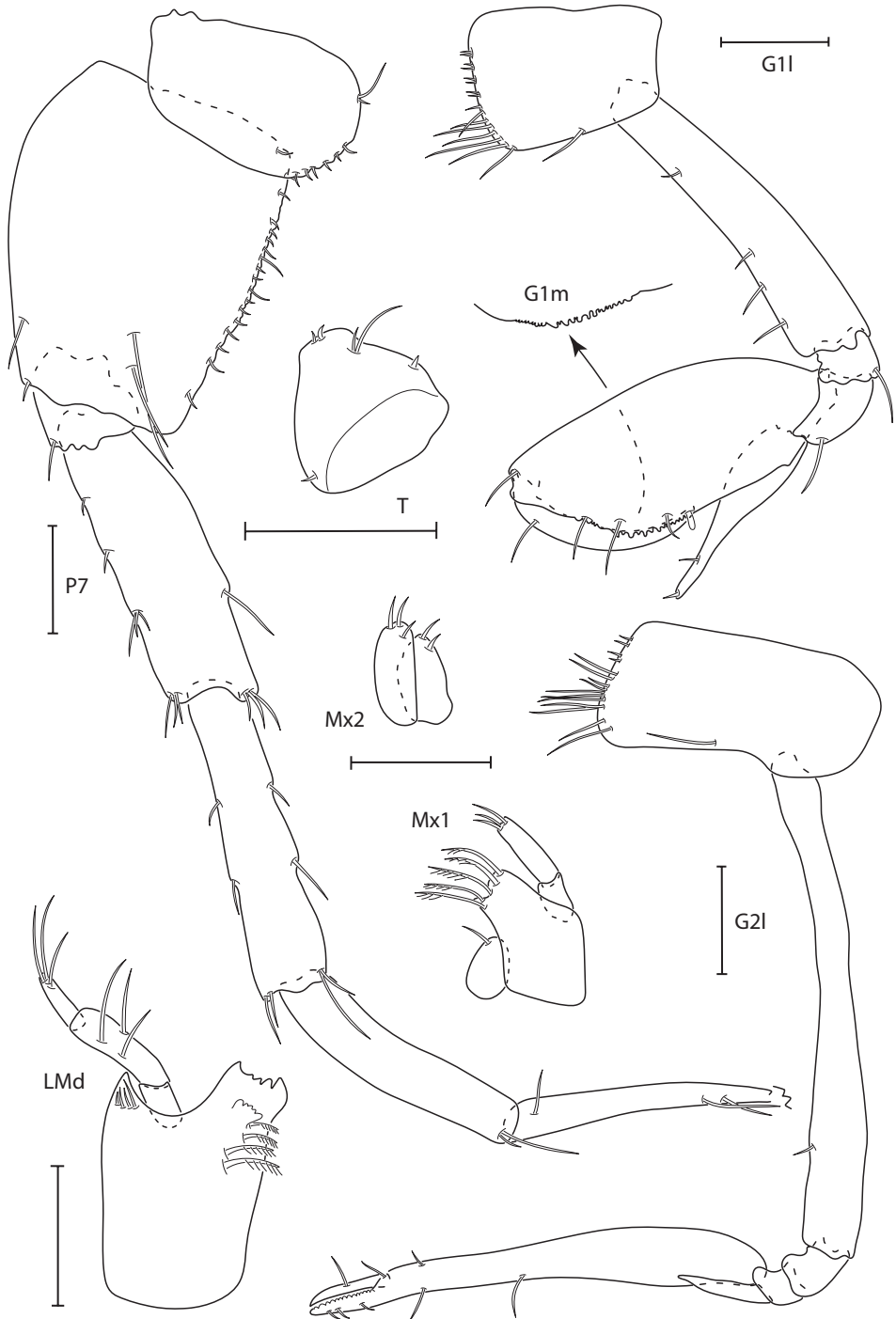


**Figure 4.** *Synchelidium purpurivitellum* sp. nov. holotype female, 2.3 mm, gnathopods 1 and 2 lateral, G1 medial palm, left mandible, maxilla 1 and 2; paratype male, 2.0 mm: pereopod 7 (dactyl broken), telson. Scale bars: 0.1 mm.

accessory spines; molar process small; palp tri-articulate, article 2 with three setae, article 3 subequal in length with article 1, with two or three setae. Upper lip asymmetrical, apically setose.

**Pereon.** Coxae weakly setose on distal margin; coxae 1–3 subrectangular; coxa 4 subquadrate, slightly produced posterodistally. Gnathopod 1 subchelate; basis with few short setae on anterior margin; merus not expanded; carpal lobe reaching palmar angle, with two distal setae; propodus ovate, palm oblique, regularly toothed, defined by blunt tipped spine; dactylus reaching palmar angle. Gnathopod 2 chelate; basis slender, with one short seta on anterodistal margin; propodus minutely toothed on cutting edge of fixed finger, sparsely setose; total length of dactylus one-sixth of propodus, smooth. Pereopods 3 and 4 bases slender, with long plumose setae on anterodistal and posterodistal margins; propodus with anteroproximal margin longer than anterodistal margin; dactylus short, stout, one-fourth length of propodus. Pereopod 5 basis anterior margin with distally located plumose setae and a single row of medial plumose setae along the midline; propodus subequal to carpus. Pereopod 6 moderately setose; propodus subequal to carpus. Pereopod 7 basis subrectangular, lacking posterodistal lobe, posterior margin lined with short setae; dactylus styliform, at least as long as propodus (broken).

**Pleon.** Epimera 1–3 margins smooth, bare; epimeron 3, posteroventral margin evenly rounded. Uropod 1, peduncle  $1.2 \times$  length of outer ramus, inner and outer rami subequal in length, inner ramus with one robust marginal seta, outer ramus with four robust setae, inner and outer rami lined with fine setae. Uropod 2 peduncle subequal in length to outer ramus, inner ramus broken, inner ramus with one robust marginal seta, outer ramus with three robust setae, inner and outer rami lined with fine setae. Uropod 3 peduncle  $0.3 \times$  length of outer ramus, inner ramus  $1.2 \times$  length of outer ramus, each ramus with one robust seta, lined with fine setae. Telson thickened dorsoventrally, narrowing distally, apex subtruncate with two medium setae dorsolaterally, two short setae medially.

**Male** (paratype, 2.0 mm). Similar in all aspects to the female with the exception of the following: Eye slightly larger; antenna 2 flagellum elongate, at least  $0.5 \times$  body length (broken); gnathopods 1 and 2 bases slightly wider than in female.

**Etymology.** After the Latin *purpur*, meaning purple and *vitellum*, meaning yolk and referring to the striking purple color of the eggs in the brood pouch of females of this species.

**Distribution.** Panama: Bocas del Toro (present study).

**Ecology.** These amphipods burrow into sand in shallow subtidal habitats.

**Remarks.** *Synchelidium purpurivitellum* sp. nov. is similar to the geographically close species *Americhelidium americanum* in many aspects, but differs in having a strongly toothed gnathopod 1 propodal palm (smooth in *A. americanum*), a broadly rounded posteroventral corner of epimeron 2 (produced in *A. americanum*), and lacking the posterodistal lobe found on the basis of pereopod 7 in *A. americanum*.

Within the genus, *Synchelidium purpurivitellum* sp. nov. is most similar to *Synchelidium maculatum* Stebbing, 1906, sharing the long gnathopod 1 carpus and toothed

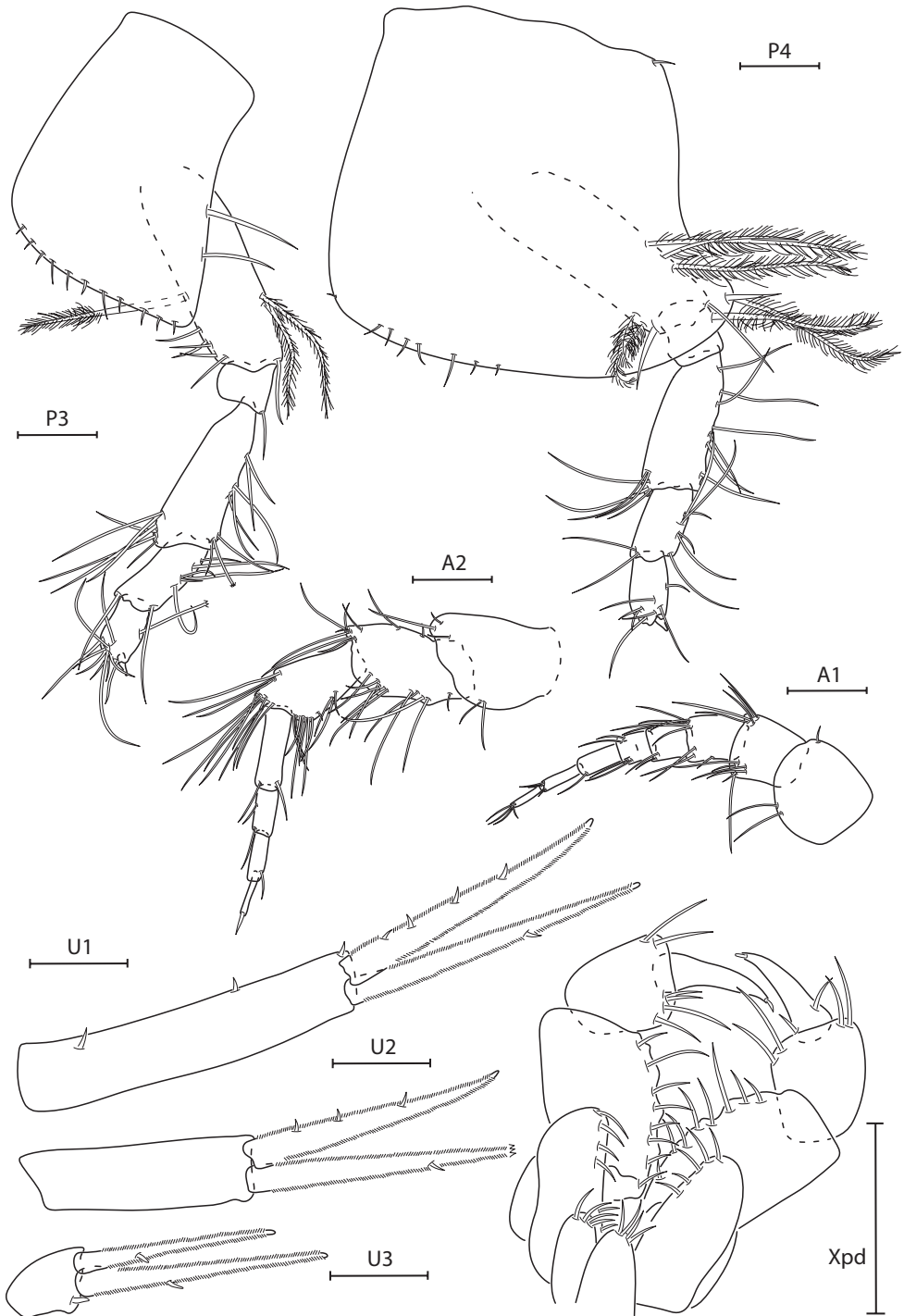


**Figure 5.** *Synchelidium purpurivitellum* sp. nov. holotype female, 2.3 mm, antennae 1 and 2, pereopods 3 and 4, uropods 1–3; paratype male, 2.0 mm: maxilliped. Scale bars: 0.1 mm.



**Figure 6.** Photographs of live specimens **A** *Hartmanodes nyei*, male **B** *Synchelidium purpurivitellum* sp. nov. female. Scale bar: 1.0 mm.

propodus palm, minute pereopod 3 and 4 dactyls, and rounded posteroventral corner of epimeron 2. It differs from *S. maculatum* in having shorter antenna 1 flagellum, subrectangular gnathopod 1 propodus (ovate in *S. maculatum*), and subtruncate telson (rounded in *S. maculatum*). The subtruncate telson distinguishes *S. purpurivitellum* sp. nov. from all other *Synchelidium* species, but this character most resembles *Synchelidium intermedium* Sars, 1892, which has a truncate telson.

### Identification Key to the Caribbean Oedicerotae of Panama

- 1 Gnathopod 1, carpal lobe slender; gnathopod 2 chelate; pereopods 3 and 4, dactylus short..... ***Synchelidium purpurivitellum* sp. nov**
- Gnathopod 1, carpal lobe broad; gnathopod 2 subchelate; pereopods 3 and 4, dactylus long..... **2**
- 2 Eye well-developed; pereopods 3 and 4, carpus subquadrate, not produced, subequal in width to propodus; pereopod 7, basis without facial setae; telson apically truncate..... ***Hartmanodes nyei***
- Eye absent; pereopods 3 and 4, carpus posteroventrally produced, 3 × as wide as propodus; pereopod 7, basis with facial setae; telson apically convex.....  
..... ***Aceroides (Patoides) synparis***

### Discussion

The results of this study increase the number of Caribbean oedicerotid amphipods known from Panama to three, with the documentation of a new species and a range extension to include Panama for *H. nyei*. *Hartmanodes nyei* has previously been reported from the western Atlantic Ocean, including the Caribbean Sea (Shoemaker 1933; Rakocinski et al. 1993; Thomas 1993; LeCroy 2000), with two questionable records in the Pacific Gulf of California (Barnard 1962; Bousfield and Chevrier 1996).

The genus *Synchelidium* now contains eight species worldwide, with *Synchelidium purpurivitellum* sp. nov. being the first Caribbean species of the genus. *Americhelidium americanum* was reported from the Caribbean as *Synchelidium americanum* before the closely related genus *Americhelidium* Bousfield & Chevrier, 1996 was erected (Thomas 1993). Bousfield and Chevrier (1996) designated *Americhelidium* as a North Pacific coastal marine genus, including *A. americanum*, and *Synchelidium* as a European Atlantic genus. Despite this designation, *Synchelidium purpurivitellum* sp. nov. is placed in the genus based on the strongly toothed gnathopod 1 propodus, broadly rounded epimeron 2, and the lack of a posterodistal lobe on the basis of pereopod 7, all of which are the diagnostic characters selected by Bousfield and Chevrier (1996) to distinguish this genus from *Americhelidium*. It is likely that the genera have a wider distribution, but have yet to be documented properly, given the similarities among the species, which would explain its presence in Caribbean Panama. Future investigation

of additional material, including type material will aid in understanding the relationships between species of the *Americhelidium* and *Synchelidium*. Documenting these sand burrowing species from Bocas del Toro may allow their inclusion in future applied studies, including studies on trophic interactions, habitat-use, and population or community analyses.

## Funding

Funding for this study was provided by a National Science Foundation grant: Collaborative Research: ARTS: Understanding Tropical Invertebrate Diversity Through Integrative Revisionary Systematics and Training (1856421). Publication costs were provided by the Georgia College & State University GC Journeys Program.

## Acknowledgements

Logistical support and facilities were provided by Georgia College & State University Department of Biological and Environmental Sciences and the Smithsonian Tropical Research Institute (STRI). Special thanks to Carolina Cesar for assistance with diving and collecting in Bocas del Toro. Comments and suggestions from Sara LeCroy and Azman Abdul Rahim greatly improved the manuscript.

## References

- Barnard JL (1962) Benthic marine Amphipoda of southern California: Family Oedicerotidae. *Pacific Naturalist* 3(12): 349–371. <http://hdl.handle.net/1834/27427>
- Barnard JL (1964) Deep-sea Amphipoda (Crustacea) collected by R.V. “Vema” in the eastern Pacific Ocean and the Caribbean and Mediterranean Seas. *Bulletin of the American Museum of Natural History* 127(1): 3–46. <http://hdl.handle.net/2246/1119>
- Barnard JL, Drummond MM (1982) Redescription of *Exoediceros fossor* (Stimpson, 1856), an Australian marine fossorial Amphipod, the type-genus of the new family Exoedicerotidae. *Proceedings of the Biological Society of Washington* 95(3): 610–620. <http://www.biodiversitylibrary.org/page/1694499>
- Barnard JL, Karaman GS (1982) Classificatory revisions in gammaridean Amphipoda (Crustacea), Part 2. *Proceedings of the Biological Society of Washington* 95(1): 167–187. <https://doi.org/10.5479/si.00810282.360>
- Bate CS (1857) A synopsis of the British edriophthalmous Crustacea Part I. Amphipoda. *The Annals and Magazine of Natural History*, series 2 19(110): 135–152. <https://doi.org/10.1080/00222935708697715>
- Bousfield EL (1973) *Shallow-water Gammaridean Amphipoda of New England*. Cornell University Press, New York, 312 pp.

- Bousfield EL, Chevrier A (1996) The Amphipod Family Oedicerotidae on the Pacific Coast of North America. 1. The *Monoculodes* & *Synchelidium* Generic Complexes. Systematics and Distributional Ecology: Amphipacifica 2(2): 75–148.
- Coleman CO (2003) “Digital inking”: How to make perfect line drawings on computers. Organisms, Diversity & Evolution 3(14): 1–14. <https://doi.org/10.1078/1439-6092-00081>
- LeCroy SE (2000) An Illustrated Identification Guide to The Nearshore Marine and Estuarine Gammaridean Amphipoda of Florida: Families Gammaridae, Hadziidae, Isaeidae, Melitidae and Oedicerotidae. Florida Department of Environmental Protection Annual Report Contract No. WM724 1: 1–195.
- LeCroy SE, Gasca R, Winfield I, Ortiz M, Escobar-Briones E (2009) Amphipoda (Crustacea) of the Gulf of Mexico. In: Felder DL, Camp DK (Eds) Gulf of Mexico: Origin, Waters, and Biota. Texas A&M University Press, Texas, 941–972.
- Lilljeborg W (1865a) Bidrag till kannedomen om underfamiljen Lysianassina inom underordningen Amphipoda bland kraftdjuren. Nova Acta Regiae Societatis Scientiarum Upsaliensis 3: 1–25.
- Lilljeborg W (1865b) On the *Lysianassa magellanica* H. Milne Edwards, and on the Crustacea of the suborder Amphipoda and the subfamily Lysianassina found on the coast of Sweden and Norway. Nova Acta Regiae Societatis Scientiarum Upsaliensis 6(1): 1–38. <https://doi.org/10.5962/bhl.title.6806>
- Lowry JK, Myers AA (2017) A Phylogeny and Classification of the Amphipoda with the establishment of the new order Ingolfiellida (Crustacea: Peracarida). Zootaxa 4265(1): 1–89. <https://doi.org/10.11646/zootaxa.4265.1.1>
- Martín A, Díaz Y, Miloslavich P, Escobar-Briones E, Guerra-García JM, Ortiz M, Valencia B, Giraldo A, Klein E (2013) Regional diversity of Amphipoda in the Caribbean Sea. Revista de Biología Tropical 61(4): 1681–1720. <https://doi.org/10.15517/rbt.v61i4.12816>
- Rakocinski CF, Heard RW, LeCroy SE, McLelland JA, Simons T (1993) Seaward change and zonation of the sandy shore macrofauna at Perdido Key, Florida, U.S.A. Estuarine, Coastal and Shelf Science 36(1): 81–104. <https://doi.org/10.1006/ecss.1993.1007>
- Sars GO (1892) Amphipoda. Part XIV. Oediceridae (continued). An account of the Crustacea of Norway, with short descriptions and figures of all the species 1: 297–320[ pls 105–112]. <https://doi.org/10.5962/bhl.title.1164>
- Shoemaker CR (1933) Amphipoda from Florida and the West Indies. American Museum Novitates 598: 1–24.
- Shoemaker CR (1934) Three new amphipods. Reports on the collections obtained by the first Johnson-Smithsonian deep-sea expedition to the Puerto Rican Deep. Smithsonian Miscellaneous Collections 91(12): 1–6.
- Stebbing TRR (1906) Amphipoda I. Gammaridea. Das Tierreich 21: 1–806. <https://doi.org/10.5962/bhl.title.1224>
- Thomas JD (1993) Identification manual for marine Amphipoda (Gammaridea): I. Common coral reef and rocky bottom amphipods of South Florida. Florida Department of Environmental Protection Final Report Contract No. SP290: 1–83.
- Thomas JD, Barnard JL (1985) *Periculodes cerasimus*, n. sp., the first record of the genus from the Caribbean Sea (Amphipoda: Oedicerotidae). Proceedings of the Biological Society of Washington 98(1): 98–106.

## Supplementary material I

### Collection data for Caribbean Oedicerotidira of Panama

Authors: Elizabeth L. Durham, Kristine N. White

Data type: COL (.xlsx file)

Copyright notice: This dataset is made available under the Open Database License (<http://opendatacommons.org/licenses/odbl/1.0/>). The Open Database License (ODbL) is a license agreement intended to allow users to freely share, modify, and use this Dataset while maintaining this same freedom for others, provided that the original source and author(s) are credited.

Link: <https://doi.org/10.3897/zookeys.1159.102034.suppl1>

# *Yunguirius* gen. nov., a new genus of Coelotinae (Araneae, Agelenidae) spiders from southwest China

Bing Li<sup>1</sup>, Zhe Zhao<sup>2</sup>, Ken-ichi Okumura<sup>3</sup>, Kaibayier Meng<sup>2</sup>,  
Shuqiang Li<sup>2</sup>, Haifeng Chen<sup>1</sup>

**1** College of Life Sciences, Langfang Normal University, Langfang, Hebei 065000, China **2** Institute of Zoology, Chinese Academy of Sciences, Beijing 100101, China **3** Department of Zoology, National Museum of Nature and Science, 4-1-1 Amakubo, Tsukuba, Ibaraki 305-0005, Japan

Corresponding authors: Zhe Zhao ([zhaozhe@ioz.ac.cn](mailto:zhaozhe@ioz.ac.cn)); Haifeng Chen ([chenhaifeng@lfnu.edu.cn](mailto:chenhaifeng@lfnu.edu.cn))

Academic editor: Dimitar Dimitrov | Received 19 January 2023 | Accepted 29 March 2023 | Published 25 April 2023

<https://zoobank.org/C2BD6C63-A9D2-4C3E-8189-3F9E3001AC64>

**Citation:** Li B, Zhao Z, Okumura K-i, Meng K, Li S, Chen H (2023) *Yunguirius* gen. nov., a new genus of Coelotinae (Araneae, Agelenidae) spiders from southwest China. ZooKeys 1159: 51–67. <https://doi.org/10.3897/zookeys.1159.100786>

## Abstract

A new genus of the subfamily Coelotinae F. O. Pickard-Cambridge, 1893, *Yunguirius* gen. nov. is described, comprising two new species and three species previously described in *Draconarius* Ovtchinnikov, 1999, all from southwest China: *Y. duoge* sp. nov. (♀), *Y. xiangding* sp. nov. (♀), *Y. ornatus* (Wang, Yin, Peng & Xie, 1990) comb. nov. (♂♀) (the type species of *Yunguirius* gen. nov.), *Y. subterebratus* (Zhang, Zhu & Wang, 2017) comb. nov. (♀), and *Y. terebratus* (Peng & Wang, 1997) comb. nov. (♂♀). Molecular analyses support *Yunguirius* gen. nov. as a monophyletic group, with the *Sinodraconarius* clade as its sister group: *Yunguirius* gen. nov. + (*Hengconarius* + (*Nuconarius* + *Sinodraconarius*)).

## Keywords

Asia, *Draconarius*, funnel weaver spider, new combination, new species, phylogeny

## Introduction

The subfamily Coelotinae F. O. Pickard-Cambridge 1893 (Araneae: Agelenidae) is distributed worldwide (i.e., throughout Asia, Europe and North America) and is represented by 798 species in 37 genera (WSC 2023). Over the past decade, with the concerted efforts of arachnologists, this subfamily has achieved a basic and relatively stable

framework, both in morphology and molecular phylogeny amongst the known genera (Chen et al. 2015, 2016; Zhao and Li 2016, 2017; Okumura 2017, 2020; Zhu et al. 2017; Li et al. 2018a–c, 2019b, c; Okumura and Zhao 2022). Herein, we focus on the taxonomy of the paraphyletic *Draconarius*-clades defined by Zhao and Li (2017).

*Draconarius* Ovtchinnikov, 1999 is exceptionally species rich (i.e., currently comprising 274 valid species) and morphologically diverse, but some studies have shown that it is not monophyletic (Zhao and Li 2017; Li et al. 2018b; Zhao et al. 2020), and that the genus is in the need of a thorough revision. Species currently considered in this genus are mainly distributed from the Pamir Mountains to the Himalayas (Li et al. 2018b). Considering that the type species (*D. venustus* Ovtchinnikov, 1999) is from Tajikistan, the known *Draconarius* species distributed in the Yunnan-Guizhou Plateau to the east need further taxonomic study (Yin et al. 2012; Zhu et al. 2017). Twenty five species have recently been transferred to seven other genera, for example, *Nuconarius* Zhao & Li, 2018: *N. capitulates* (Wang, 2003) and *N. pseudocapitulatus* (Wang, 2003); *Hengconarius* Zhao & Li, 2018: *H. exilis* (Zhang, Zhu & Wang, 2005), *H. falcatus* (Xu & Li, 2006), *H. incertus* (Wang, 2003), *H. latusincertus* (Wang, Griswold & Miller, 2010) and *H. pseudobrunneus* (Wang, 2003); *Sinodraconarius* Zhao & Li, 2018: *S. patellabifidus* (Wang, 2003), and *Troglocoelotes* Zhao & Li, 2019: *T. proximus* (Chen, Zhu & Kim, 2008), *T. tortus* (Chen, Zhu & Kim, 2008) and *T. yosiiianus* (Nishikawa, 1999), etc.

Recently, when examining specimens collected from southwest China and comparing them with known species in the literature, we realized that they represent two undescribed species, and suspected that they may belong to a new genus. The two species are closely related to *D. ornatus* (Wang, Yin, Peng & Xie, 1990), *D. terebratus* (Peng & Wang, 1997), and *D. subterebratus* Zhang, Zhu & Wang, 2017. Therefore, morphological and phylogenetic studies were carried out on these closely related species to elucidate their taxonomy.

## Materials and methods

### Sampling and morphological examination

All specimens studied in this paper were collected from southwest China. Fresh specimens were preserved in 95% ethanol with storage at -20 °C for DNA extraction and 75% ethanol for morphological study. Specimens were examined with a LEICA M205 C stereomicroscope. Photos were taken with an Olympus C7070 wide zoom digital camera (7.1 megapixels) mounted either on an Olympus SZX12 dissecting microscope or on an Olympus BX51 compound microscope. Images from multiple focal ranges were combined using Helicon Focus v. 6.80 photo stacking software program. The epigyne and male palp were dissected from the body for examination. The epigyne was treated in a warm 10% potassium hydroxide (KOH) solution. Images of the left male palp are presented. Measurements were obtained with a LEICA M205 C stereomicroscope and are given in millimetres. Eye diameters were measured as the maximum distance in

either dorsal or frontal views. Leg measurements are given as follows: total length (coxa, trochanter, femur, patella, tibia, metatarsus, tarsus). Terminology follows Wang et al. (1990), Peng and Wang (1997) and Zhu et al. (2017). Abbreviations are as follows:

### Eye area

<b>ALE</b>	anterior lateral eye;
<b>ALE–PLE</b>	distance between ALE and PLE;
<b>AME</b>	anterior median eye;
<b>AME–ALE</b>	distance between AME and ALE;
<b>AME–AME</b>	distance between AME and AME;
<b>AME–PME</b>	distance between AME and PME;
<b>PLE</b>	posterior lateral eye;
<b>PME</b>	posterior median eye;
<b>PME–PLE</b>	distance between PME and PLE;
<b>PME–PME</b>	distance between PME and PME.

### Depositories of the specimens

<b>HNNU</b>	Hunan Normal University;
<b>IZCAS</b>	Institute of Zoology, Chinese Academy of Sciences;
<b>MHBU</b>	Museum of Hebei University.

### Laboratory protocols and phylogenetic analyses

DNA barcodes were obtained for delimiting the species. A partial fragment of the mitochondrial cytochrome oxidase subunit I (*COI*) gene was amplified and sequenced for the new and type species using primers LCO1490-oono (5'-CWACAAAYCATAR-RGATATTTGG-3') and HCO2198-zz (5'-TAAACTTCCAGGTGACCAAAAAAT-CA-3'), following Zhao and Li (2017) and Zhao et al. (2020). GenBank accession numbers of *COI* are listed separately in Table 1.

To perform phylogenetic analyses, part of the molecular data of coelotine spiders from Zhao and Li (2017), Zhao et al. (2020), and Okumura and Zhao (2022) were collected. The new molecular dataset consists of eight genes: *COI*, NADH dehydrogenase subunit I (*ND1*) gene, histone 3 (*H3*) gene, *wingless* gene and the ribosomal RNA genes *12S*, *16S*, *18S*, and *28S*. They were assembled from 72 species, 67 known species (with 26 type species from different genera) in 32 known genera of Coelotinae as the ingroup, and three species of Ageleninae and one species of Amaurobiidae as the outgroup, alongside three new sequences. GenBank accession numbers for all the above genes are shown in Suppl. material 1.

Phylogenetic relationships were inferred using both maximum likelihood (ML) and Bayesian inference (BI). First, the best-fit partitioning schemes and models were selected for the RAxML and MrBayes analyses using PartitionFinder v.2.1.1 (Lanfear

**Table 1.** Voucher specimen information.

Species	Voucher code	GenBank accession number	Sequence length	Collection localities
<i>Y. ornatus</i> comb. nov.	IZCAS-Ar44406 (YX055)	OQ243292	771bp	Kunming, Yunnan, China
<i>Y. ornatus</i> comb. nov.	IZCAS-Ar44407 (YX366)	OQ243293	798bp	Yuxi, Yunnan, China
<i>Y. duoge</i> sp. nov.	IZCAS-Ar44401 (YX066)	OQ243294	780bp	Kunming, Yunnan, China
<i>Y. xiangding</i> sp. nov.	IZCAS-Ar44408 (CL048)	KY778892	1194bp	Luzhou, Sichuan, China

et al. 2012). ML analysis was conducted in RAxML v.8.0.0 (Stamatakis 2006) using the GTRCAT substitution model for all partitions (partitioned by gene). A rapid bootstrap of 1,000 replicate ML inferences was performed to determine the best-scoring ML tree and nodal support values. BI analyses were performed in MrBayes v.3.2.2 (Ronquist and Huelsenbeck 2003) with posterior distributions estimated by Markov chain Monte Carlo (MCMC) sampling. The appropriate model was selected for each partition (gene): the GTR + I + G model was favored for each partition, except that different models were selected for *H3* (HKY + I + G), *wingless* (SYM + I + G) and *18S* (K80 + I + G). Two simultaneous runs with four MCMC chains were performed for 10 million generations to ensure that the average standard deviation of the split frequency was below 0.01 and to obtain a well-supported consensus tree. Additional ML analysis was performed in IQ-TREE (Nguyen et al. 2015) using the ModelFinder function (-m MFP + MERGE) to select the best-fit model for each partition, and the option '-bb 1,000' to estimate nodal support values.

## Results and discussion

By examining specimens collected from southwest China, we found that two species with particular external genital morphology could not be placed into existing genera. They are morphologically similar to three *Draconarius* species, *D. ornatus*, *D. terebratus*, and *D. subterebratus* (Wang 2003; Zhu et al. 2017). The epigynes of these five species all lack epigynal teeth but have a large central atrium. In the vulva, the copulatory ducts are broad, anteriorly extended and curved, and the spermathecal stalks are elongated. Males also show similar homologous characteristics, such as a thick embolus beginning at a 7 o'clock position, and a short cymbial furrow less than half the length of cymbium, although only two males out of five species have been described so far. All species are closely related to each other by the comprehensive characteristics mentioned above and differ from the type species *D. venustus* Ovtchinnikov, 1999 and the *venustus* group of *Draconarius* which share a pair of triangular epigynal teeth commonly (Wang 2003; Li et al. 2019a). Therefore, we establish a new genus, *Yunguirius* gen. nov., and herein transfer the three *Draconarius* species to it.

Our different phylogenetic analyses infer similar tree topologies (Fig. 1) and strongly support *Yunguirius* gen. nov. as a monophyletic group (ML rapid bootstrap = 100 and 95; BI posterior probability = 1.00). Although the relationships within the

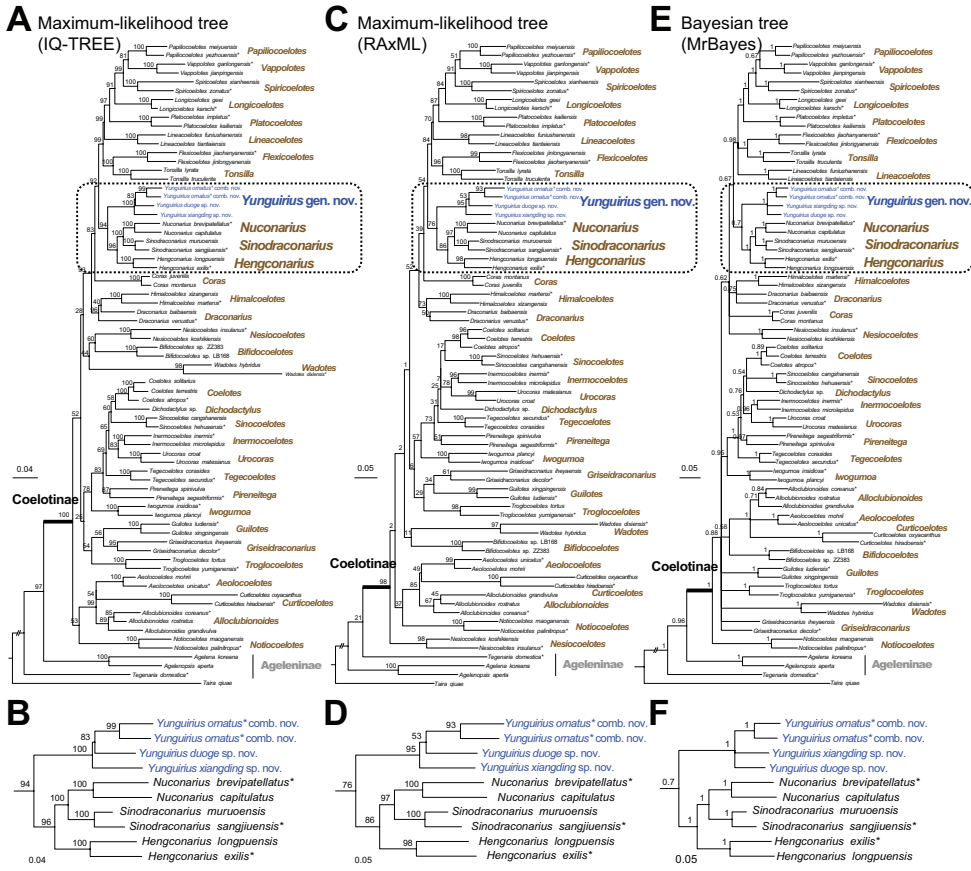


**Figure 1.** Phylogenetic trees **A, B** maximum likelihood (ML) trees obtained by using IQ-TREE **C, D** ML trees obtained by using RAxML **E, F** bayesian trees obtained by using MrBayes. Support values for major nodes are shown. Scale bar corresponds to the expected number of substitutions per site. Asterisks express the type species of each genus.

genus are unclear (two species lack molecular data), the other three species are indeed genetically closely related. The genus is sister to the *Sinodraconarius* clade (*Hengconarius* + (*Nuconarius* + *Sinodraconarius*)) and genetically distant from the genus *Draconarius*. The close relationship between *Yunguirius* gen. nov. and the *Sinodraconarius* clade can also be confirmed by having common morphological features such as bifurcated conductors and absent epigynal teeth, which obviously differ from *Draconarius*. Geographically, species of *Yunguirius* gen. nov. are restricted to southwest China (Fig. 5). Zoogeographic studies suggest that the genus-level distribution of coelotine spiders is regional, and the divergence and formation of these monophyletic genera are closely related to geological and climatic events in Eurasia (Zhao and Li 2017; Zhao et al. 2022). From the above results, including morphological differences between the *Sinodraconarius* clade and *Draconarius*, we consider that the establishment of *Yunguirius* gen. nov. is justified.

## Taxonomy

Family Agelenidae C.L. Koch, 1837

Subfamily Coelotinae F.O. Pickard-Cambridge, 1893

Genus *Yunguirius* B. Li, Zhao & S. Li, gen. nov.

<https://zoobank.org/95909E7E-61FF-4CCC-9747-900F0304B3BF>

**Type species.** *Coelotes ornatus* Wang, Yin, Peng & Xie, 1990, from Kunming, Yunnan, China (designated herein).

**Etymology.** The generic name is derived from the pinyin word “Yungui”, referring to Yunnan-Guizhou Plateau where the genus is distributed, and “-rius” refers to the genus as part of its sister groups of genera: *Nuconarius*, *Hengconarius*, and *Sinodraconarius*. The gender is masculine.

**Diagnosis.** Morphological characteristics of *Yunguirius* gen. nov. resemble those of *Nuconarius*, *Hengconarius*, and *Sinodraconarius*, which are distributed in southeastern China, by cymbial furrow short, with a length less than half of cymbium (fig. 3 in Zhang 1993; fig. 31 in Peng and Wang 1997), embolus thick, conductor with two branches (figs 1–3 in Zhang 1993; figs 30, 31 in Peng and Wang 1997), and epigyne with posterior sclerite, epigynal teeth absent, atrium with sclerotic margin (Figs 2A, 3A, 4A). However, it can be distinguished from these genera by habitus, and detailed structures of male palp and epigyne as follows: 1) carapace tonneau-shaped, first half wide, and abdomen beloid (Figs 2C, 3C, 4C); 2) male palp with bifurcate conductor, the upper branch large and wide with groove, while the lower one is more elongated (fig. 2 in Zhang 1993; fig. 252D in Zhu et al. 2017); 3) epigynal atrium very large, in the centre of epigyne and occupying c. 1/2 the size of epigyne (Figs 2A, 3A, 4A); 4) epigyne dark and sclerotic, with lateral folds that are located between the lateral margin of the atrium and the epigynal hood (Figs 2A, 3A, 4A); 5) copulatory duct and spermathecal head concomitant, along the contour of the atrium (Figs 2B, 3B, 4B); and 6) spermatheca located posteriorly, spermathecal head very long and continuous with the copulatory duct (Figs 2B, 3B, 4B).

**Description.** Small to very large spiders, body length 6.00 to 21.80. Carapace brown to black, tonneau-shaped, longer than or as long as abdomen, with longitudinal fovea and dark radial grooves; chelicerae black, with three promarginal and two retromarginal teeth; endites and labium brown to dark brown, anterior white with black hairs; sternum brownish to brown, longer than wide. Abdomen yellowish-brown, nearly oval, posterior widest, with four to six darker chevrons or speckles, or without any pattern. Leg formula  $4 > 1 > 2 > 3$  or  $1 > 4 > 2 > 3$ . Male palp: patellar apophysis finger-shaped, retrolateral tibial apophysis large, lateral tibial apophysis small, median apophysis spoon-shaped; conductor large, with two branches; embolus thick, beginning at a 7 o'clock position, embolic base swollen; cymbial furrow short, with the length less than half of cymbium. Epigyne: posterior epigynal sclerite varying in shape; atrium very large, wide to narrow, with osteosclerotic lateral

margin, inside white osteon, outside with brownish or brown markings and brown or darker folds; copulatory duct membranous, arising posteriorly, extending to anterior, opening anteriorly; spermatheca brown, spermathecal base swollen, spermathecal head long and line-shaped, extending anteriorly, opposite end swollen, lamellar or connected with a stalk.

**Distribution.** Guizhou, Hunan, Sichuan and Yunnan, China (Fig. 5).

***Yunguirius duoge* B. Li, Zhao & S. Li, sp. nov.**

<https://zoobank.org/81FED4C8-2649-48C5-B19E-8F717873A382>

Figs 2, 5

**Type material.** *Holotype* ♀ (IZCAS-Ar44401): CHINA: Yunnan Province: Kunming City: Panlong District, Duoge Village, Laohuanglong Cave, 25.4254°N, 102.9259°E, elevation: 2731 m, 4.XII.2014, Y. Li and Z. Chen leg. *Paratypes*: 4♀♀ (IZCAS-Ar44402–Ar44405): CHINA: Yunnan Province: Kunming City: Panlong District, Duoge Village, Huanglong Cave, 25.4285°N, 102.9244°E, elevation: 2337 m, 8.XII.2019, Z. Chen leg.

**Etymology.** The new species is named after the type locality (Duoge Village); noun in apposition.

**Diagnosis.** *Yunguirius duoge* sp. nov. resembles *Y. terebratus* by having rectangular posterior epigynal sclerite, subrounded atrium and dumbbell-shaped spermatheca at its first half. However, it can be distinguished from *Y. terebratus* as follows: 1) posterior margin of the epigyne narrow and pointed in the middle (Fig. 2A) in *Y. duoge* sp. nov., but flat (fig. 28 in Peng and Wang 1997) in *Y. terebratus*; 2) epigynal folds banded (Fig. 2A) in *Y. duoge* sp. nov., but dentiform (fig. 28 in Peng and Wang 1997) in *Y. terebratus*; 3) anterior copulatory duct close to each other (Fig. 2B) in *Y. duoge* sp. nov., but lapped (fig. 29 in Peng and Wang 1997) in *Y. terebratus*; and 4) stalk of spermatheca extending laterally (Fig. 2B) in *Y. duoge* sp. nov., but extending anteriorly (fig. 29 in Peng and Wang 1997) in *Y. terebratus*.

**Description. Female** (holotype) (Fig. 2). Body length 13.27. Carapace 6.04 long, 3.66 wide. Abdomen 7.23 long, 4.86 wide. Eye sizes and interdistances: AME: 0.13, ALE: 0.17, PME: 0.15, PLE: 0.15; AME–AME: 0.09; AME–ALE: 0.13; AME–PME: 0.04; ALE–PLE: 0.03; PME–PME: 0.07; PME–PLE: 0.18. Leg measurements: I: 16.43 (1.86, 0.82, 4.08, 1.62, 3.30, 2.73, 2.02); II: 14.90 (1.73, 0.77, 3.55, 1.56, 2.82, 2.48, 1.99); III: 11.43 (1.39, 0.79, 3.04, 1.08, 1.98, 1.54, 1.61); IV: 16.86 (1.79, 0.81, 4.06, 1.92, 3.72, 2.84, 1.72). Leg formula 4 > 1 > 2 > 3. Carapace brown, anterior and lateral black; fovea and radial grooves dark; chelicerae black, with three promarginal and two retromarginal teeth; endites and labium dark brown, anterior white with thin hairs; sternum brownish, lateral brown, c. 1.4 times longer than wide. Abdomen yellowish-brown, nearly oval, with five dark chevrons and dark speckles. Epigyne (Fig. 2A, B): posterior epigynal sclerite rectangular, atrium large, anterior widest, with wide lateral margins, inside with osteon cordiform, outside with brown

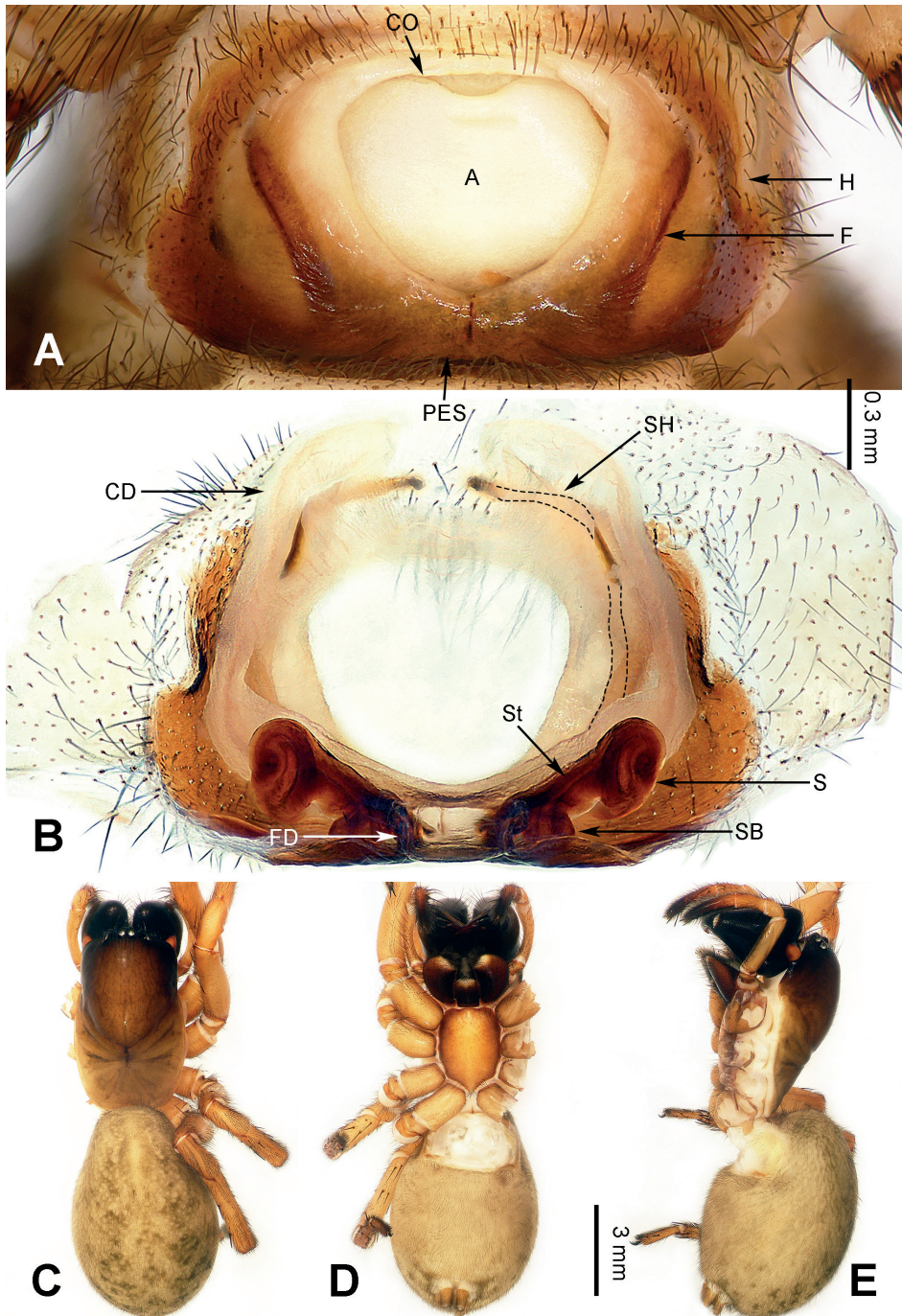


**Figure 2.** Epigyne and female habitus of *Yunguirius duoge* sp. nov. **A** epigyne, ventral **B** vulva, dorsal **C** female habitus, dorsal **D** same, ventral **E** same, lateral. Scale bar equal for **C–E**. Abbreviations: A = atrium; CD = copulatory duct; CO = copulatory opening; F = fold; FD = fertilization duct; H = hood; PES = posterior epigynal sclerite; S = spermatheca; SB = spermathecal base; SH = spermathecal head; St = stalk.

markings, fold slender and banded, c. 6 times longer than wide; copulatory opening located anteriorly; copulatory duct symmetric, posterior widest; spermatheca dumb-bell-shaped at first half, its head continuous through the copulatory duct; fertilization duct long, c. 5 times longer than wide, with a bent end.

**Male.** Unknown.

**Distribution.** Yunnan Province, China (Fig. 5).

***Yunguirius ornatus* (Wang, Yin, Peng & Xie, 1990), comb. nov.**

Figs 3, 5

*Coelotes ornatus* Wang, Yin, Peng & Xie, 1990: in Wang et al. 1990: 199, figs 53, 54; Zhang 1993: 47, figs 1–3; Song et al. 1999: 377, fig. 221O, P.

*Draconarius ornatus* (Wang, Yin, Peng & Xie, 1990): in Wang 2003: 541, figs 46A–C, 96C; Wang and Jäger 2008: 2285, fig. 22; Wang et al. 2010: 77, figs 316–321; Zhu et al. 2017: 329, fig. 200A–E.

**Type material (not examined).** *Holotype* ♀ (HNNU): CHINA, Yunnan Province, Kunming City, Xishan District, Xishan Mountain, 25.X.1987, J. Wang leg. **Paratypes:** 15♀♀ (HNNU): same data as the holotype.

**Other material (not examined).** 2♂♂ (HNNU): CHINA, Yunnan Province, Kunming City, Xishan District, Xishan Mountain, 8.VIII.1991; 1♀ (MHBU): CHINA, Yunnan Province, Kunming City, Xishan District, Xishan Mountain, 28.IV.2004, Z. Zhang leg.

**Material examined.** 1♀ (IZCAS-Ar44406): CHINA, Yunnan Province, Kunming City, Xishan District, Xishan Mountain, National Forest Park, Longmen, 24.9511°N, 102.6385°E, elevation: 2437 m, 5.XII.2014, Y. Li and Z. Chen leg.; 1♀ (IZCAS-Ar44407), China, Yunnan Province, Yuxi City, Xiping County, Mopanshan Mountain, National Forest Park, 23.9448°N, 101.9660°E, elevation: 2269 m, 19.III.2019, Z. Chen leg.

**Diagnosis.** *Yunguirius ornatus* can be distinguished from other species of this genus as follows: 1) atrium inverted trapezoid (Fig. 3A; fig. 53 in Wang et al. 1990) in *Y. ornatus*, but cordiform (fig. 245A in Zhu et al. 2017) in *Y. subterebratus* and *Y. xiangding* sp. nov. (Fig. 4A), or subrounded (Fig. 2A) in *Y. duoge* sp. nov. and (fig. 28 in Peng and Wang 1997) *Y. terebratus*; 2) median septum present (Fig. 3A; fig. 53 in Wang et al. 1990) in *Y. ornatus*; 3) copulatory opening away from each other and the midline (Fig. 3A; fig. 53 in Wang et al. 1990) in *Y. ornatus*, but close to each other and the midline (fig. 245A in Zhu et al. 2017) in *Y. subterebratus* and (Fig. 4A) *Y. xiangding* sp. nov.; 4) patellar apophysis long, extending beyond the patella to the middle of the tibia (fig. 3 in Zhang 1993) in *Y. ornatus*, but extending to the quarter of the tibia (fig. 31 in Peng and Wang 1997) in *Y. terebratus*; and 5) lateral tibial apophysis short, c. 1/4 the length of retrolateral tibial apophysis (fig. 3 in Zhang 1993) in *Y. ornatus*, but c. 1/3 (fig. 31 in Peng and Wang 1997) in *Y. terebratus*.

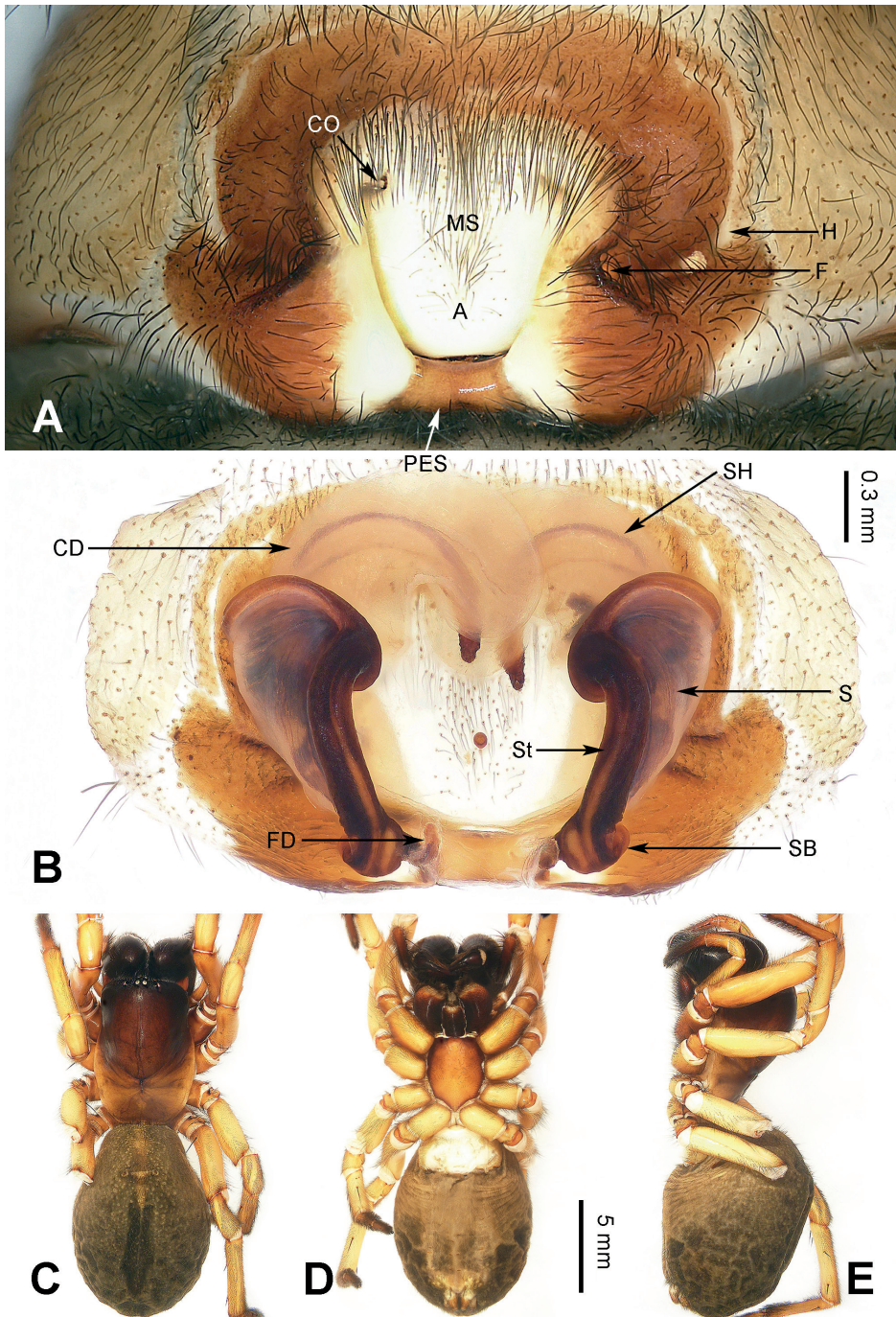


**Figure 3.** Epigyne and female habitus of *Yunguirius ornatus* comb. nov. **A** epigyne, ventral **B** vulva, dorsal **C** female habitus, dorsal **D** same, ventral **E** same, lateral. Scale bar equal for **C–E**. Abbreviations: A = atrium; CD = copulatory duct; CO = copulatory opening; F = fold; FD = fertilization duct; H = hood; MS = median septum; PES = posterior epigynal sclerite; S = spermatheca; SB = spermathecal base; SH = spermathecal head; St = stalk.

**Description. Male.** See Zhang (1993, figs 1–3) for complete description of male habitus, Wang (2003 fig. 46A–C) and Zhu et al. (2017, fig. 200C–E) for complete description of male palp.

**Female** (IZCAS-Ar44406) (Fig. 3). Body length 21.44. Carapace 10.54 long, 5.32 wide. Abdomen 10.90 long, 7.35 wide. Eye sizes and interdistances: AME: 0.15, ALE: 0.16, PME: 0.16, PLE: 0.17; AME–AME: 0.09; AME–ALE: 0.17; AME–PME: 0.08; ALE–PLE: 0.06; PME–PME: 0.09; PME–PLE: 0.28. Leg measurements: I: 25.71 (2.84, 1.14, 6.60, 2.62, 5.39, 4.17, 2.95); II: 21.70 (2.56, 1.05, 5.69, 2.21, 3.91, 3.49, 2.79); III: 17.08 (1.99, 1.01, 4.69, 2.14, 2.69, 2.69, 1.87); IV: 22.19 (2.34, 1.19, 6.06, 2.63, 4.39, 3.28, 2.30). Leg formula 1 > 4 > 2 > 3. Sternum c. 1.5 times longer than wide. Epigyne (Fig. 3A, B): posterior epigynal sclerite rectangular, atrium with white margins, outside with brownish markings, fold bell-jar-shaped, c. 2 times larger than hood; copulatory opening located anteriorly, away from each other, close to the lateral margin of the atrium; copulatory duct semiluculent; spermatheca lamellar at first half, its head longer than the length of the copulatory duct; fertilization duct long and bent, c. 4 times longer than wide. For further details, see Wang et al. (1990).

**Distribution.** Yunnan Province, China (Fig. 5).

***Yunguirius subterebratus* (Zhang, Zhu & Wang, 2017), comb. nov.**

*Draconarius subterebratus* Zhang, Zhu & Wang, 2017 in Zhu et al. 2017: 379, fig. 245A, B.

**Type material (not examined).** *Holotype* ♀ (MHBUS): CHINA: Guizhou Province: Zunyi City: Daozhen County, Dashahegou Nature Reserve, Xieshiyan Cave to Dashahe River, 18.VIII.2004, Z. Zhang leg. *Paratypes*: 3 ♀♀ (MHBUS): same data as the holotype.

**Diagnosis.** *Yunguirius subterebratus* can be distinguished from other species of this genus as follows: 1) atrium cordiform (fig. 245A in Zhu et al. 2017) in *Y. subterebratus*, but inverted trapezoid (Fig. 3A; fig. 53 in Wang et al. 1990) in *Y. ornatus*, or subrounded (Fig. 2A) in *Y. duoge* sp. nov. and (fig. 28 in Peng and Wang 1997) *Y. terebratus*; and 2) posterior epigynal sclerite longer than wide, waist-drum-shaped (fig. 245A in Zhu et al. 2017) in *Y. subterebratus*, but vase-shaped (Fig. 4A) in *Y. xiangding* sp. nov., or rectangular (Figs 2A, 3A; fig. 53 in Wang et al. 1990; fig. 28 in Peng and Wang 1997) in others.

**Description. Female:** See Zhu et al. (2017) for complete description (fig. 245A, B).

**Male.** Unknown.

**Distribution.** Guizhou Province, China (Fig. 5).

***Yunguirius terebratus* (Peng & Wang, 1997), comb. nov.**

*Coelotes terebratus* Peng & Wang, 1997 in Peng and Wang 1997: 330, figs 27–31; Song et al. 1999: 378, figs 225M, N, 227E, 228H.

*Draconarius terebratus* (Peng & Wang, 1997) in Wang 2003: 551, figs 63A–E, 96G, H; Yin et al. 2012: 1015, fig. 525a–f; Zhu et al. 2017: 387, fig. 252A–E; Jiang, Chen and Zhang 2018: 77, figs 12A, B, 26K.

**Type material (not examined).** *Holotype* ♀ (HNNU): CHINA: Hunan Province: Zhangjiajie City: Sangzhi County, Tianpingshan Mountain, 16.X.1986, J. Wang leg. *Paratype*: 1♂ (HNNU): same data as the holotype.

**Diagnosis.** *Yunguirius terebratus* can be distinguished from other species of this genus as follows: 1) atrium subrounded (fig. 28 in Peng and Wang 1997; fig. 252A in Zhu et al. 2017) in *Y. terebratus*, but inverted trapezoid (Fig. 3A; fig. 53 in Wang et al. 1990) in *Y. ornatus*, or cordiform (fig. 245A in Zhu et al. 2017) in *Y. subterebratus* and *Y. xiangding* sp. nov. (Fig. 4A); 2) posterior epigynal sclerite rectangular (fig. 28 in Peng and Wang 1997; fig. 252A in Zhu et al. 2017), but waist-drum-shaped (fig. 245A in Zhu et al. 2017) in *Y. subterebratus*, or vase-shaped (Fig. 4A) in *Y. xiangding* sp. nov.; 3) embolic base with a round apophysis (fig. 31 in Peng and Wang 1997; fig. 252E in Zhu et al. 2017), while subapically with a dentiform apophysis (fig. 30 in Peng and Wang 1997; fig. 252C in Zhu et al. 2017) in *Y. terebratus*, but absent in *Y. ornatus*; and 4) lower branch of conductor falcate and bent ventrally, longer than the length of the upper one (fig. 252D in Zhu et al. 2017) in *Y. terebratus*, but lamellar, fluted, and pointed, shorter than the length of the upper one (fig. 2 in Zhang 1993; fig. 200D in Zhu et al. 2017) in *Y. ornatus*.

**Description. Male.** See Peng and Wang (1997 figs 30, 31) and Zhu et al. (2017 fig. 252C, D) for complete description.

**Female:** (fig. 27 in Peng and Wang 1997). Carapace gourd-shaped, longer than abdomen. Abdomen oblong. Epigyne (figs 28, 29 in Peng and Wang 1997; fig. 252A, B in Zhu et al. 2017): epigynal teeth absent, posterior epigynal sclerite rectangular, fold triangular, hood large, c. 2 times larger than the size of its fold; spermathecal head long, twisted and sigmoid in the middle. For further details, see Peng and Wang (1997) and Zhu et al. (2017).

**Distribution.** Hunan Province, China (Fig. 5).

***Yunguirius xiangding* B. Li, Zhao & S. Li, sp. nov.**

<https://zoobank.org/6AD39BEA-5092-45C4-8159-A62F88866643>

Figs 4, 5

**Type material.** *Holotype* ♀ (IZCAS-Ar44408): CHINA: Sichuan Province: Luzhou City: Gulin County, Shiping Township, Xiangding Village, Huaer Cave, 28.0294°N, 106.0073°E, elevation: 641 m, 22.IV.2014, Y. Lin, H. Zhao, Y. Li, J. Wu and F. Li leg.

**Etymology.** The new species is named after the type locality (Xiangding Village); noun in apposition.

**Diagnosis.** *Yunguirius xiangding* sp. nov. resembles *Y. subterebratus* by having a cordiform atrium, asymmetric copulatory ducts, arch-shaped spermathecal stalks, fists on both sides, and the unilateral end of spermathecal head exposed. However, it can be

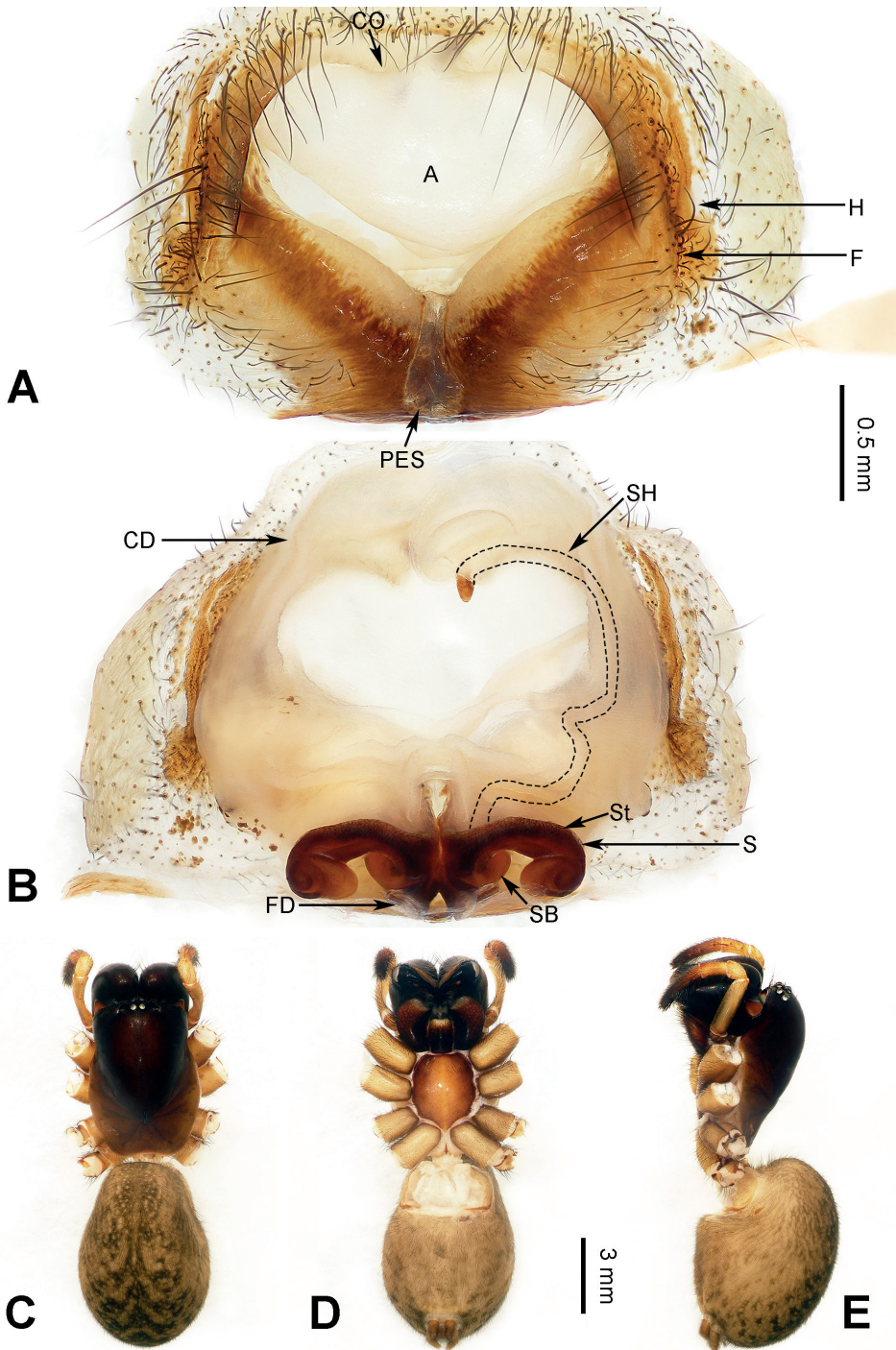


**Figure 4.** Epigyne and female habitus of *Yunguirius xiangding* sp. nov. **A** epigyne, ventral **B** vulva, dorsal **C** female habitus, dorsal **D** same, ventral **E** same, lateral. Scale bar equal for **C–E**. Abbreviations: A = atrium; CD = copulatory duct; CO = copulatory opening; F = fold; FD = fertilization duct; H = hood; PES = posterior epigynal sclerite; S = spermatheca; SB = spermathecal base; SH = spermathecal head; St = stalk.

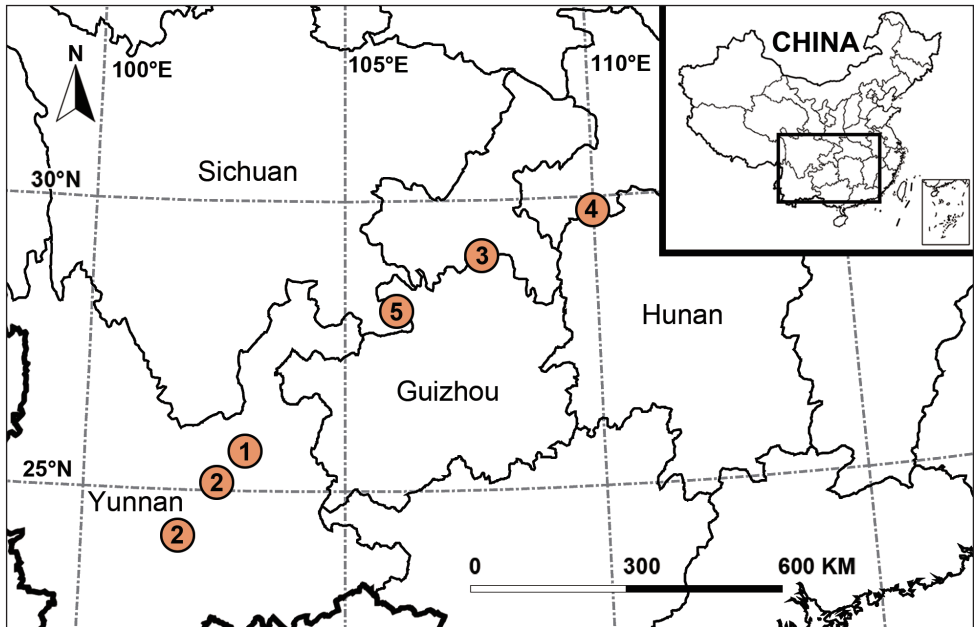


**Figure 5.** Distribution records of species of *Yunguiurus* gen. nov. in China 1 *Y. duoge* sp. nov. 2 *Y. ornatus* 3 *Y. subterebratus* 4 *Y. terebratus* 5 *Y. xiangding* sp. nov.

distinguished from *Y. subterebratus* as follows: 1) crevice breaking at lateral margin of the atrium, below its hoods (Fig. 4A) in *Y. xiangding* sp. nov., but at anterior margin of the atrium, above its hoods (fig. 245A in Zhu et al. 2017) in *Y. subterebratus*; 2) the mid part of anterior margin of the atrium raised (Fig. 4A) in *Y. xiangding* sp. nov., but concave (fig. 245A in Zhu et al. 2017) in *Y. subterebratus*; 3) posterior epigynal sclerite vase-shaped (Fig. 4A) in *Y. xiangding* sp. nov., but waist-drum-shaped (fig. 245A in Zhu et al. 2017) in *Y. subterebratus*; and 4) spermathecal stalks extending laterally (Fig. 4B) in *Y. xiangding* sp. nov., but extending anteriorly (fig. 245B in Zhu et al. 2017) in *Y. subterebratus*.

**Description. Female** (holotype) (Fig. 4). Body length 13.29. Carapace 6.21 long, 4.22 wide. Abdomen 7.08 long, 5.02 wide. Eye sizes and interdistances: AME: 0.14, ALE: 0.17, PME: 0.15, PLE: 0.16; AME–AME: 0.08; AME–ALE: 0.12; AME–PME: 0.06; ALE–PLE: 0.05; PME–PME: 0.07; PME–PLE: 0.22. All legs were used for prophase work of DNA extractions. Carapace dark brown, anterior black; fovea and radial grooves dark; chelicerae black, with three promarginal and two retromarginal teeth; endites and labium dark brown to black, anterior white with several hairs; sternum brownish, lateral brown, c. 1.2 times longer than wide. Abdomen yellowish-brown, nearly oval, posterior widest, with four dark chevrons and dark brown speckles. Epigyne (Fig. 4A, B): posterior epigynal sclerite vase-shaped, atrium cordiform, anterior widest, with sclerotic lateral margin, inside with inverted triangle osteon, outside with brownish markings, fold brown, ridge-shaped, close to the deep hood; copulatory opening small, located anteriorly, near the midline, and symmetric; copulatory duct beloid, and then swollen; first half of spermatheca dumbbell-shaped, long spermathecal head

wrapped in copulatory duct, with unilateral end exposed; fertilization duct c. 3.5 times longer than wide, pointed laterally.

**Male.** Unknown.

**Distribution.** Sichuan Province, China (Fig. 5).

## Acknowledgements

The manuscript benefited greatly from comments by Dimitar Dimitrov and Alireza Zamani. Danni Sherwood checked English. Xiaoqing Zhang helped lab work and illustrations. This study was supported by the National Natural Sciences Foundation of China (NSFC–32170447; NSFC–31970396) and the program of Youth Innovation Promotion Association of Chinese Academy of Sciences (No. 2019087).

## References

- Chen H, Zhu M, Kim JP (2008) Three new eyeless *Draconarius* spiders (Araneae, Amaurobiidae) from limestone caves in Guizhou, southwestern China. *Korean Arachnology* 24: 85–95.
- Chen L, Li S, Zhao Z (2015) A new genus of Coelotinae (Araneae, Agelenidae) from southern China. *ZooKeys* 541: 41–56. <https://doi.org/10.3897/zookeys.541.6678>
- Chen L, Zhao Z, Li S (2016) *Sinocoelotes* gen. n., a new genus of the subfamily Coelotinae (Araneae, Agelenidae) from Southeast Asia. *ZooKeys* 614: 51–86. <https://doi.org/10.3897/zookeys.614.8663>
- Jiang X, Chen H, Zhang Z (2018) Spiders' diversity in Fanjing Mountain Nature Reserve, Guizhou, China, IV: Coelotine spiders (Araneae, Agelenidae). *Acta Arachnologica Sinica* 27(2): 65–95. <https://doi.org/10.3969/j.issn.1005-9628.2018.02.001>
- Koch CL (1837) Übersicht des Arachnidensystems. Nürnberg, Heft 1, 39 pp. <https://doi.org/10.5962/bhl.title.39561>
- Langford R, Calcott B, Ho SYW, Guindon S (2012) Partition-Finder: Combined selection of partitioning schemes and substitution models for phylogenetic analyses. *Molecular Biology and Evolution* 29(6): 1695–1701. <https://doi.org/10.1093/molbev/mss020>
- Li B, Zhao Z, Chen H, Wu Z, Zhang C, Li S (2018a) *Guilotes*, a new genus of Coelotinae spiders from Guangxi Zhuang Autonomous Region, China (Araneae, Agelenidae). *ZooKeys* 802: 1–17. <https://doi.org/10.3897/zookeys.802.29913>
- Li B, Zhao Z, Zhang C, Li S (2018b) *Nuconarius* gen. n. and *Hengconarius* gen. n., two new genera of Coelotinae (Araneae, Agelenidae) spiders from southwest China. *Zootaxa* 4457(2): 237–262. <https://doi.org/10.11646/zootaxa.4457.2.2>
- Li B, Zhao Z, Zhang C, Li S (2018c) *Sinodraconarius* gen. n., a new genus of Coelotinae spiders from southwest China (Araneae, Agelenidae). *ZooKeys* 770: 117–135. <https://doi.org/10.3897/zookeys.770.22470>
- Li B, Zhao Z, Chen H, Wu Z, Li S (2019a) Four new species of the genus *Draconarius* Ovtchinnikov, 1999 (Araneae, Agelenidae) from the Tibetan Plateau, China. *Zootaxa* 4648(1): 141–154. <https://doi.org/10.11646/zootaxa.4648.1.7>

- Li B, Zhao Z, Chen Y, Chen H, Wu Z, Li S (2019b) *Vappolotes*, a new genus of coelotine spiders (Araneae, Agelenidae) from Guizhou, China. *Zootaxa* 4701(5): 434–442. <https://doi.org/10.11646/zootaxa.4701.5.3>
- Li B, Zhao Z, Zhang C, Li S (2019c) *Troglocoelotes* gen. n., a new genus of Coelotinae spiders (Araneae, Agelenidae) from caves in South China. *Zootaxa* 4554(1): 219–238. <https://doi.org/10.11646/zootaxa.4554.1.7>
- Nguyen LT, Schmidt HA, von Haeseler A, Minh BQ (2015) IQ-TREE: A fast and effective stochastic algorithm for estimating maximum likelihood phylogenies. *Molecular Biology and Evolution* 32(1): 268–274. <https://doi.org/10.1093/molbev/msu300>
- Nishikawa Y (1999) A new eyeless agelenid spider from a limestone cave in Guangxi, south China. *Journal of the Speleological Society of Japan* 24: 23–26.
- Okumura K (2017) *Dichodactylus* gen. nov. (Araneae: Agelenidae: Coelotinae) from Japan. *Species Diversity : An International Journal for Taxonomy, Systematics, Speciation, Biogeography, and Life History Research of Animals* 22(1): 29–36. [https://doi.org/10.12782/sd.22\\_29](https://doi.org/10.12782/sd.22_29)
- Okumura K (2020) Three new genera with taxonomic revisions of the subfamily Coelotinae (Araneae: Agelenidae) from Japan. *Acta Arachnologica* 69(2): 77–94. <https://doi.org/10.2476/asjaa.69.77>
- Okumura K, Zhao Z (2022) Taxonomic revision of six species of the subfamily Coelotinae (Araneae: Agelenidae) from Japan accompanied with the description of *Nesiocoelotes* gen. n. *Acta Arachnologica* 71(2): 93–103. <https://doi.org/10.2476/asjaa.71.93>
- Ovtchinnikov SV (1999) On the supraspecific systematics of the subfamily Coelotinae (Araneae, Amaurobiidae) in the former USSR fauna. *Tethys Entomological Research* 1: 63–80.
- Peng X, Wang J (1997) Seven new species of the genus *Coelotes* (Araneae: Agelenidae) from China. *Bulletin – British Arachnological Society* 10: 327–333.
- Pickard-Cambridge FO (1893) Handbook to the study of British spiders (Drassidae and Agelenidae). *British Naturalist* 3: 117–170.
- Ronquist F, Huelsenbeck JP (2003) MrByes 3: Bayesian phylogenetic inference under mixed models. *Bioinformatics* 19(12): 1572–1574. <https://doi.org/10.1093/bioinformatics/btg180>
- Song D, Zhu M, Chen J (1999) *The Spiders of China*. Hebei Science and Technology Publishing House Press, Shijiazhuang, 640 pp.
- Stamatakis A (2006) RAxML-VI-HPC: Maximum likelihood-based phylogenetic analyses with thousands of taxa and mixed models. *Bioinformatics* 22(21): 2688–2690. <https://doi.org/10.1093/bioinformatics/btl446>
- Wang X (2003) Species revision of the coelotine spider genera *Bifidocoelotes*, *Coronilla*, *Dracognarius*, *Femoracoelotes*, *Leptocoelotes*, *Longicoelotes*, *Platocoelotes*, *Spiricoelotes*, *Tegeocoelotes*, and *Tonsilla* (Araneae: Amaurobiidae). *Proceedings of the California Academy of Sciences* 54: 499–662.
- Wang X, Jäger P (2008) First record of the subfamily Coelotinae in Laos, with review of Coelotinae embolus morphology and description of seven new species from Laos and Vietnam (Araneae, Amaurobiidae). *Journal of Natural History* 42(35, 36): 2277–2304. <https://doi.org/10.1080/00222930802209783>
- Wang J, Yin C, Peng X, Xie L (1990) New species of the spiders of the genus *Coelotes* from China (Araneae: Agelenidae). *Spiders in China: One Hundred New and Newly Recorded Species of the Families Araneidae and Agelenidae*. Hunan Normal University Press, 172–253.

- Wang X, Griswold CE, Miller JA (2010) Revision of the genus *Draconarius* Ovtchinnikov 1999 (Agelenidae: Coelotinae) in Yunnan, China, with an analysis of the Coelotinae diversity in the Gaoligongshan Mountains. *Zootaxa* 2593(1): 1–127. <https://doi.org/10.11646/zootaxa.2593.1.1>
- WSC (2023) World Spider Catalog, version 23.5. Natural History Museum Bern. <http://wsc.nmbe.ch> [Accessed on 8<sup>th</sup> January 2023]
- Xu X, Li S (2006) Coelotine spiders of the *Draconarius incertus* group (Araneae: Amaurobiidae) from southwestern China. *Revue Suisse de Zoologie* 113: 777–787. <https://doi.org/10.5962/bhl.part.80374>
- Yin C, Peng X, Yan H, Bao Y, Xu X, Tang G, Zhou Q, Liu P (2012) Fauna Hunan: Araneae in Hunan, China. Hunan Science and Technology Press, Changsha, 1590 pp.
- Zhang Z (1993) Description of the male spider *Coelotes ornatus* Wang et al. (Araneae: Agelenidae). *Journal of Yunnan Normal University* 13(2): 47–49.
- Zhang Z, Zhu M, Wang X (2005) *Draconarius exilis*, a new species of coelotine spider from China (Araneae, Amaurobiidae). *Zootaxa* 1057(1): 45–50. <https://doi.org/10.11646/zootaxa.1057.1.2>
- Zhao Z, Li S (2016) *Papiliocoelotes* gen. n., a new genus of Coelotinae (Araneae, Agelenidae) spiders from the Wuling Mountains, China. *ZooKeys* 585: 33–50. <https://doi.org/10.3897/zookeys.585.8007>
- Zhao Z, Li S (2017) Extinction vs. rapid radiation: The juxtaposed evolutionary histories of coelotine spiders support the Eocene–Oligocene orogenesis of the Tibetan Plateau. *Systematic Biology* 66(6): 988–1006. <https://doi.org/10.1093/sysbio/syx042>
- Zhao Z, Shao L, Li F, Zhang X, Li S (2020) Tectonic evolution of the region created the Eurasian extratropical biodiversity hotspots: Tracing *Pireneitega* spiders' diversification history. *Ecography* 43(9): 1400–1411. <https://doi.org/10.1111/ecog.05044>
- Zhao Z, Hou Z, Li S (2022) Cenozoic Tethyan changes dominated Eurasian animal evolution and diversity patterns. *Zoological Research* 43(1): 3–13. <https://doi.org/10.24272/j.issn.2095-8137.2021.322>
- Zhu M, Wang X, Zhang Z (2017) Fauna Sinica: Invertebrata (Vol. 59) Arachnida: Araneae: Agelenidae and Amaurobiidae. Science Press, Beijing, 727 pp.

## Supplementary material I

### The species names, DNA sequences and GenBank accession numbers of all Coelotinae samples and outgroups.

Authors: Bing Li, Zhe Zhao, Ken-ichi Okumura, Kaibayier Meng, Shuqiang Li, Haifeng Chen

Data type: phylogenetic data

Copyright notice: This dataset is made available under the Open Database License (<http://opendatacommons.org/licenses/odbl/1.0/>). The Open Database License (ODbL) is a license agreement intended to allow users to freely share, modify, and use this Dataset while maintaining this same freedom for others, provided that the original source and author(s) are credited.

Link: <https://doi.org/10.3897/zookeys.1159.100786.suppl1>



# DNA barcoding and morphology reveal European and western Asian *Arctia villica* (Linnaeus, 1758) as a complex of species (Lepidoptera, Erebidae, Arctiinae)

Antonio S. Ortiz<sup>1</sup>, Rosa M. Rubio<sup>1</sup>, Josef J. de Freina<sup>2</sup>,  
Juan J. Guerrero<sup>1</sup>, Manuel Garre<sup>1</sup>, José Luis Yela<sup>3</sup>

**1** Department of Zoology and Physical Anthropology, University of Murcia, Campus de Espinardo, 30100 Murcia, Spain **2** Eduard Schmid-Str. 10, D-81541, München, Germany **3** Grupo DITEG, Área de Zoología, Facultad de Ciencias Ambientales, Universidad de Castilla-La Mancha, Avda. Carlos III, s.n., Campus Real Fábrica de Armas, E-45071, Toledo, Spain

Corresponding author: Antonio S. Ortiz ([aortiz@um.es](mailto:aortiz@um.es))

---

Academic editor: Reza Zahiri | Received 22 September 2022 | Accepted 23 February 2023 | Published 25 April 2023

---

<https://zoobank.org/F1FB6D98-C86D-4C4A-92A4-C82287CF11D8>

---

**Citation:** Ortiz AS, Rubio RM, de Freina JJ, Guerrero JJ, Garre M, Yela JL (2023) DNA barcoding and morphology reveal European and western Asian *Arctia villica* (Linnaeus, 1758) as a complex of species (Lepidoptera, Erebidae, Arctiinae). ZooKeys 1159: 69–86. <https://doi.org/10.3897/zookeys.1159.95225>

---

## Abstract

Currently, the genus *Arctia* Schrank, 1802 includes approximately 16 species in the Palaearctic region, depending on the taxonomic interpretation. Here, populations of the *Arctia villica* (Linnaeus, 1758) morphospecies complex were studied from Europe to the Middle East (Turkey, northern Iran) by molecular methods. Morphological treatment has traditionally revealed the presence of five nominal taxa: *A. villica* (Linnaeus, 1758), *A. angelica* (Boisduval, 1829), *A. konewkaii* (Freyer, 1831), *A. marchandi* de Freina, 1983, and *A. confluens* Romanoff, 1884. The molecular approach tests whether they represent well-delimited species. Subsequently, this study corroborates the suitability of the mitochondrial cytochrome c oxidase subunit 1 (COI) marker sequence for species delimitation. In total, 55 barcodes of the *Arctia villica* complex were compared, and two molecular species delimitation algorithms were applied to reveal the potential Molecular Operational Taxonomic Units (MOTUs), namely the distance-based Barcode Index Number (BIN) System, and the hierarchical clustering algorithm based on a pairwise genetic distances approach using the Assemble Species by Automatic Partitioning (ASAP). The applied ASAP distance-based species delimitation method for the analysed dataset revealed an interspecific threshold of 2.0–3.5% K2P

distance as suitable for species identification purposes of the Iberian *A. angelica* and the Sicilian *A. konewkaii* and less than 2% for the three taxa of the *A. villica* clade: *A. villica*, *A. confluens*, and *A. marchandi*. This study contributes to a better understanding of the taxonomy of the genus *Arctia* and challenges future revision of this genus in Turkey, the Caucasus, Transcaucasia as well as northern Iran using standard molecular markers.

### Keywords

*Arctia*, COI, DNA barcoding, Europe, species delimitation, western Asia

## Introduction

The European fauna of Arctiinae moths (Erebidae) is particularly well-known comprising 113 species (Witt and Ronkay 2011), although some genera still require revision in terms of their composition and the taxonomic status of some species (e.g., *Setina* Schrank, 1802, *Eilema* Hübner, [1819], *Ocnogyna* Lederer, 1853, etc). Traditionally, the genus *Arctia* Schrank, 1802 was considered to include six or seven species in the West Palearctic region and ten species in the East Palearctic region divided into different species groups (*Arctia* Schrank, 1802, *Epicallia* Hübner, [1820], *Eucharia* Hübner [1820], and *Pericallia* Hübner, [1820]), depending on the taxonomic interpretation of the status for a number of taxa (de Freina and Witt 1987; Murzin 2003; Witt et al. 2011).

More recently, the use of eight molecular markers coupled with proper analytical algorithms (Maximum Likelihood and Bayesian Inference) has postulated a much more comprehensive view of the genus *Arctia* and closely related genera, including *Acerbia* Sotavalta, 1863, *Ammobiota* Wallengren, 1885, *Atlantarctia* Dubatolov, 1990, *Borearctia* Dubatolov, 1884, *Epicallia*, *Eucharia*, *Hyphoraia* Hübner, [1820], *Pararctia* Sotavalta, 1965, *Parasemia* Hübner, [1820], and *Pericallia* as synonyms or potential subgenera (Rönkä et al. 2016). Thus, the total number of species within the genus has significantly increased. Some of these *Arctia* species, such as *Arctia caja* (Linnaeus, 1758), *A. festiva* (Hufnagel, 1766), *A. flavia* (Fuessly, 1779), and *A. villica* have a broad distribution from Europe to the Siberian mountains and steppes with several geographical subspecies and forms.

Following the current view, *Arctia villica* is an extremely variable species in body size, coloration, wing pattern, and size of spots including the so far considered subspecies *A. v. villica* s.str., *A. v. angelica* (Boisduval, 1829), *A. v. konewkaii* (Freyer, 1831), *A. v. confluens* Romanoff, 1884 and *A. v. marchandi* de Freina, 1983 (Murzin 2003; Witt and Ronkay 2011). Murzin (2003) and Witt and Ronkay (2011) considered *A. villica* as having a West Palearctic distribution, occurring in the central and southern parts of Europe, from NW Africa and the Iberian Peninsula to Asia Minor, the Caucasus range and Transcaucasia, northern Iran and along the steppe belt to SW Siberia.

In the revisions of the *Arctia villica* complex, de Freina and Nardelli (2007) and de Freina (2011) studied the nomenclature and systematics based on a large number of specimens from across their distribution range and concluded that all of its subspecies

should be considered as species. *Arctia villica* s. str. has a wide distribution from central and southern Europe to the Caucasus and west Siberia, *A. angelica* is restricted in the Iberian Peninsula and North Africa, *A. konevkaii* is endemic to Sicily, and *A. marchandi* and *A. confluens* are distributed from Transcaucasia and adjacent areas such as eastern Turkey, northern Syria, Iraq, and northern Iran to Central Asia. In the mentioned works, taxonomy and systematics based on external appearance and genital structures were reviewed, including eleven COI sequences from Caucasian and trans-Caucasian specimens of *A. villica*. Subsequently, Kizildağ et al. (2019) examined the taxonomic status of *A. marchandi* in southeastern Turkey. Their note, dealing with some barcodes of *A. villica* and *A. marchandi*, suggested subspecific status for *A. marchandi*, although the sequences were not published in GenBank or BOLD for their evaluation in later studies, which precludes any further comments.

The study of the morphological features and genitalia structures provides valuable criteria for species recognition according to de Freina and Nardelli (2007), de Freina (2011), and others. The recent integration of morphological and DNA-based approaches has proven to be a most effective way to advance species discovery and delineation (e.g., Lumley and Sperling 2010; Padial and De La Riva 2010; Schlick-Steiner et al. 2010), as well as to assist in detecting previously cryptic species (e.g., Hebert et al. 2004; Huemer and Hausmann 2009; Hausmann and Huemer 2011; Mutanen et al. 2012). Integration of molecular methods with morphological analyses may accelerate biodiversity inventories and corroborate the status of doubtful taxa (Smith et al. 2009).

In this paper, we present new insights from DNA barcodes of material collected along the geographical distribution of the different taxa of *Arctia villica* complex to be added to the previous morphological studies in order to substantiate their taxonomic range.

## Materials and methods

### Abbreviations of specimen repositories

<b>MWM</b>	Museum WITT, München (in ZSM);
<b>RCBA-UMU</b>	Research Collection of Biología Animal, Universidad de Murcia;
<b>ZSM</b>	Zoologische Staatssammlung München (SNSB).

### Morphological study

This study is based on the results of the morphological study of a large amount of collected material deposited in the ZSM and MWM museums, developed by de Freina and Nardelli (2007) and de Freina (2011). New material was added and 115 adult specimens of the *Arctia villica* complex (Fig. 1) were examined externally to evaluate possible differences in their colouration, spot size, and wing shape based on the taxonomic keys provided by de Freina and Nardelli (2007), Ylla et al. (2010), de Freina (2011) and Witt and Ronkay (2011), and were dissected using the standard

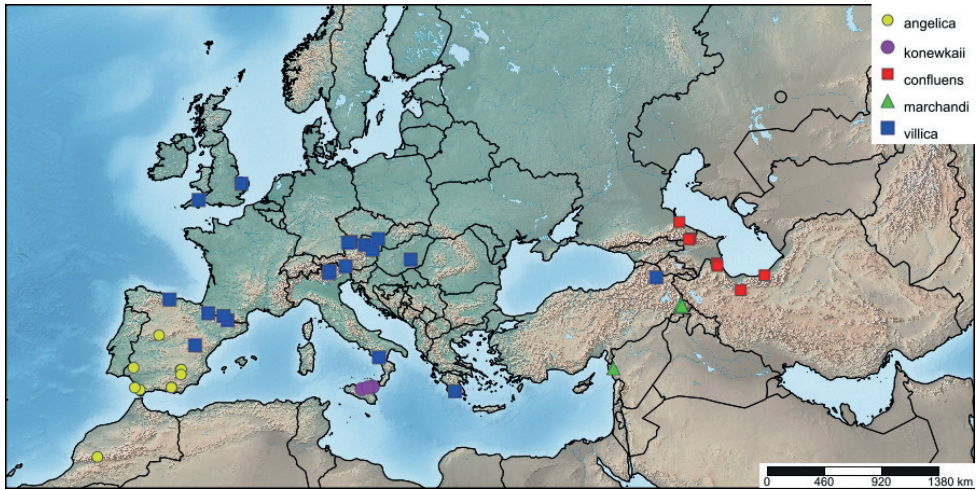


**Figure 1.** Distribution of *Arctia* samples sequenced. Note that each point may represent more than one specimen. The map was created using [www.simplemapp.net](http://www.simplemapp.net).

procedure (Fibiger 1997) with minor modifications. Adult images were taken with a Nikon D70 digital camera and were z-stacked using Zerene software. Genital structures were examined using a Zeiss Stemi 508 stereomicroscope with a Zeiss Axio-cam ICc5 digital camera and were compared with those published by de Freina and Nardelli (2007), de Freina (2011), and Witt and Ronkay (2011). Specimens were deposited in RCBA-UMU, in the Department of Zoology and Physical Anthropology of the University of Murcia (Spain), and in the Bavarian State Collection of Zoology in the ZSM (Germany).

## Molecular study

Thirty-four adult specimens of the *Arctia villica* complex were processed and sequenced at the Canadian Centre for DNA Barcoding (CCDB, Guelph) to obtain DNA barcodes using the standard high-throughput protocol described by deWaard et al. (2008), which can be accessed at [www.dnabarcoding.ca/page/research/protocols](http://www.dnabarcoding.ca/page/research/protocols). The study was completed with publicly available sequences downloaded from The Barcode of Life (BOLD: [www.boldsystem.org](http://www.boldsystem.org)) (Ratnasingham and Hebert 2007). Ultimately, the analysis involved 55 *Arctia villica* sensu lato COI sequences from Europe and countries around the Caucasus, with more than 500 bp for calculations and tree constructions (Table 1). Voucher data, GPS coordinates, images, sequences, GenBank accession numbers, and trace files are publicly available through the public data set (<https://doi.org/10.5883/DS-VILLICA>) in BOLD.

Sequence divergences for the barcode region were calculated using the Kimura 2-parameter (K2P) model (Kimura 1980) and the degrees of interspecific genetic variation were calculated using the analytical tools of BOLD. All the new and public

**Table 1.** Taxon names, old (BIN1) and present BINs (BIN2), BOLD accession numbers for the specimens used in distance estimations (Process ID), haplotype, and locality information (Country and Territory).

Taxon	BIN1	BIN2	Process ID	Haplotype	Country	Territory	
<i>Arctia villica</i>	ACP7520	AAC8627	ABOLA146-14	1	Austria	Kaernten	
	ACP7520	AAC8627	ABOLC051-16	1	Austria	Niederösterreich	
	ACP7520	AAC8627	ABOLD441-16	1	Austria	Niederösterreich	
	ACP7520	AAC8627	FBLMZ558-12	1	Germany	Bavaria	
	ACP7520	AAC8627	GWOSI563-10	1	Germany	Bavaria	
	ACP7520	AAC8627	IBLAO1063-14	1	Hungary	Bacs-Kiskun	
	ACP7520	AAC8627	NOENO403-17	1	Austria	Niederösterreich	
	ACP7520	AAC8627	LEASW136-19	2	Greece	Peloponnese	
	<i>Arctia marchandi</i>	ACP7520	AAC8627	VNMB685-08	3	Syria	Aleppo
		AAC8627	AAC8627	IBLAO1080-14	4	Turkey	Hakkari
AAC8627		AAC8627	VNMB690-08	4	Turkey	Hakkari	
AAC8627		AAC8627	VNMB689-08	5	Turkey	Hakkari	
<i>Arctia villica</i>	ACP7477	AAC8627	CGUKD205-09	6	U. Kingdom	Devon	
	ACP7477	AAC8627	CGUKD277-09	6	U. Kingdom	Norfolk	
<i>Arctia angelica</i>	ACP7477	AAC8627	IBLAO1060-14	6	Spain	Castilla-León	
	ACP7477	AAC8627	IBLAO1061-14	6	Spain	Castilla-León	
<i>Arctia villica</i>	ACP7477	AAC8627	IBLAO1073-14	6	Spain	Cataluña	
	ACP7477	AAC8627	IBLAO1124-14	6	Spain	Aragon	
	ACP7477	AAC8627	IBLAO1125-14	6	Spain	Asturias	
	ACP7477	AAC8627	IBLAO1126-14	6	Spain	Asturias	
	ACP7477	AAC8627	IBLAO951-14	6	Spain	Aragón	
	ACP7477	AAC8627	IBLAO952-14	6	Spain	Aragón	
	ACP7477	AAC8627	LEATC649-13	6	Italy	Südtirol	
	ACP7477	AAC8627	GWORZ116-10	7	Italy	Basilicata	
	ACP7477	AAC8627	IBLAO553-12	8	Spain	Cataluña	
	ACP7477	AAC8627	PHLAC475-10	9	Italy	Südtirol	
<i>Arctia confluens</i>	ACP7477	AAC8627	VNMB688-08	10	Turkey	Kars	
	ACP7477	AAC8627	IBLAO1077-14	11	Azerbaijan	Masally	
	ACP7477	AAC8627	IBLAO1078-14	11	Azerbaijan	Lerik	
	ACP7477	AAC8627	VNMB686-08	11	Russia	Dagestan	
	ACP7477	AAC8627	IBLAO1082-14	12	Russia	Dagestan	
	ACP7477	AAC8627	IBLAO1081-14	13	Russia	Dagestan	
	ACP7477	AAC8627	IBLAO1083-14	14	Russia	Dagestan	
	ACP7477	AAC8627	VNMB687-08	15	Kyrgyzstan	Namagan	
	ACP8428	AAC8627	IBLAO1064-14	16	Iran	Zanjan	
	<i>Arctia angelica</i>	ABY6789	ABY6789	GBMIN80080-17	17	n/a	n/a
ABY6789		ABY6789	IBLAO1068-14	17	Spain	Andalusia	
ABY6789		ABY6789	IBLAO1069-14	17	Spain	Andalusia	
ABY6789		ABY6789	IBLAO1070-14	17	Spain	Andalusia	
ABY6789		ABY6789	IBLAO1246-20	17	Spain	Andalusia	
ABY6789		ABY6789	IBLAO733-12	17	Spain	Andalusia	
ABY6789		ABY6789	IBLAO734-12	17	Spain	Andalusia	
ABY6789		ABY6789	IBLAO1067-14	18	Spain	Andalusia	
ABY6789		ABY6789	IBLAO1071-14	18	Spain	Castilla-La Mancha	
ABY6789		ABY6789	IBLAO1107-14	18	Spain	Castilla-La Mancha	
ABY6789		ABY6789	IBLAO1127-14	18	Spain	Castilla-La Mancha	
ABY6789		ABY6789	IBLAO1128-14	18	Spain	Castilla-La Mancha	
ABY6789		ABY6789	IBLAO1058-14	19	Morocco	Marrakech-Tensift-Al Hauz	
ABY6789		ABY6789	IBLAO1059-14	19	Morocco	Marrakech-Tensift-Al Hauz	
<i>Arctia konevskii</i>		ACL5457	ACL5457	GBMIN80081-17	20	Italy	Sicily
	ACL5457	ACL5457	IBLAO1074-14	21	Italy	Sicily	

Taxon	BIN1	BIN2	Process ID	Haplotype	Country	Territory
<i>Arctia konewkaii</i>	ACL5457	ACL5457	IBLAO1076-14	21	Italy	Sicily
	ACL5457	ACL5457	IBLAO1188-19	21	Italy	Sicily
	ACL5457	ACL5457	IBLAO1075-14	22	Italy	Sicily
<i>Arctia confluens</i>	AAC8628	AAC8628	VNMB693-08	23	Iran	Mazandaran
<i>Arctia caja</i>	AAA8530	AAA8530	IBLAO551-12		Spain	Catalonia
<i>Arctia festiva</i>	ABW9262	ABW9262	IBLAO1091-14		Spain	La Rioja
<i>Arctia flavia</i>	AAV9830	AAV9830	ABOLA435-14		Austria	NordTirol
<i>Arctia lapponica</i>	ACF2201	ACF2201	LON720-09		Norway	Sor-Varanger

species sequences were downloaded and aligned with the CLUSTAL algorithm of the MEGA6 software (Tamura et al. 2013). Bootstrap values were calculated with 1000 replicates, and initial Neighbour-Joining (NJ) and Maximum Likelihood (ML) trees based on distance were constructed with the MEGA6 software. A phylogenetic hypothesis with Maximum Likelihood as an optimality criterion was generated using IQ-TREE v. 1.6.12 (Nguyen et al. 2015). An alignment of 658 bps for 59 samples was partitioned into codon positions with ModelFinder software (Kalyaanamoorthy et al. 2017) and the codon position was modelled with GTR+F. Support values were calculated by 1,000 replications of both ultrafast bootstraps (UFBoot; Hogan et al. 2017) and Shimodaira-Hasegawa-like approximate likelihood ratio test (SH-aLRT; Guindon et al. 2010), as well as approximate Bayes branch test (aBayes; Anisimova et al. 2011). We selected *Arctia flavia*, *A. caja*, *A. festiva* and *A. lapponica* (Thunberg, 1791) which are taxonomically related to *A. villica* in the subtribe Arctiina, as outgroups to root the tree (Table 1). To assess the COI divergences between the taxa in the *A. villica* species complex and the other *Arctia* species from Europe, we included all sites with the pairwise deletion option. The number of haplotypes was calculated with DnaSP 5.10 software (Rozas et al. 2003).

To elucidate the taxonomic status of some of the *A. villica* species complex studied, two molecular species delimitation methods were applied to reveal the potential Molecular Operational Taxonomic Units (MOTUs) that could represent putative cryptic species. The two methods were distance-based: Barcode Index Number (BIN) System (Ratnasingham and Hebert 2013), and the hierarchical clustering algorithm that only considers a pairwise genetic distances approach using the Assemble Species by Automatic Partitioning (ASAP) (Puillandre et al. 2021).

The BIN method (Ratnasingham and Hebert 2013) is implemented as part of the Barcode of Life Data system (BOLD; Ratnasingham and Hebert 2007). Newly submitted sequences are compared together with sequences already available in BOLD. Sequences are clustered according to their molecular divergence using algorithms that aim at finding discontinuities between clusters and each cluster is assigned a globally unique and specific identifier Barcode Index Number (BIN) registered in BOLD.

The ASAP method (Puillandre et al. 2021) build species partitions from single locus sequence alignments (i.e., barcode data sets). Grounded in evolutionary theory, ASAP is the implementation of a hierarchical clustering algorithm that uses pairwise genetic distances, avoiding the computational burden of phylogenetic reconstruction

and proposing species partitions by neglecting the use of biological a priori insight of intraspecific diversity. This method has greater potential than the other programs assessed, for instance the barcode-gap approach Automatic Barcode Gap Discovery (ABGD) (Puillandre et al. 2012), the General Mixed Yule-Coalescent model (GMYC) (Pons et al. 2006) and the Poisson Tree Process (PTP) (Zhang et al. 2013), both first developed in a Maximum Likelihood framework, and later extended to a Bayesian framework (Reid and Carstens 2012) according to Puillandre et al. (2021).

## Results

### Molecular analysis

In the dataset composed of 59 sequences, 55 specimens of the *A. villica* complex were sequenced or their conspecific sequences were acquired from the databases (BOLD) to analyse taxonomic identity and geographical species grouping, obtaining more than 572 bp for the barcode region (48 of them with 658 bp). In total, 23 different haplotypes were found in the 55 barcode sequences analysed of the five lineages of *A. villica* species complex ranging from eleven haplotypes in *A. villica* to three in *A. marchandi* (Table 1). The overall haplotype diversity (Hd) was  $0.922 \pm 0.02$  in 56 polymorphic sites and nucleotide diversity per site (Pi) was 0.01679. Nucleotide composition showed a A+T of 68.8%. No insertions or deletions were found.

Neighbour-Joining (NJ) and Maximum Likelihood (ML) trees of COI barcode region generated using MEGA software recovered the same topology and were practically identical, and all haplotypes could be unequivocally assigned to one of the eight major clades (Table 1). A phylogenetic hypothesis with ML as an optimality criterion was generated using IQ-TREE software and the topology obtained was chosen as the basis for our discussion with branch support values (Fig. 2). The monophyly of the *A. villica* species complex was recovered by all those methods and was corroborated with the inclusion of *A. flavia*, *A. caja*, *A. festiva*, and *A. lapponica* as outgroups to root the tree.

Three well-supported clades (bootstrap values higher than 70%) were found and were thereafter treated as three MOTUs considered as species, namely *A. villica*, *A. angelica*, and *A. konewkaii*. The divergence between these three groups varies between 2.4% and 3.5% (mean 2.8%; Table 2). The highest interspecific value was found between *A. villica* and *A. konewkaii* (3.5%) and between *A. angelica* and *A. konewkaii* (3.1%), whereas the lowest one was found between *A. villica* and *A. angelica* (2.4%). The total number of nucleotide substitutions between species is 56 variable sites (Table 2; a complete similarity matrix can be accessed in Suppl. material 1).

The *A. villica* clade shows five different sub-clades with genetic differences of less than 2% among them including the clade 1 sequences from Northern Spain, Italy, and the United Kingdom (15 samples with 6 haplotypes); the clade 2, with samples from Germany, Austria, and Hungary (7 samples with 1 haplotype); another clade with

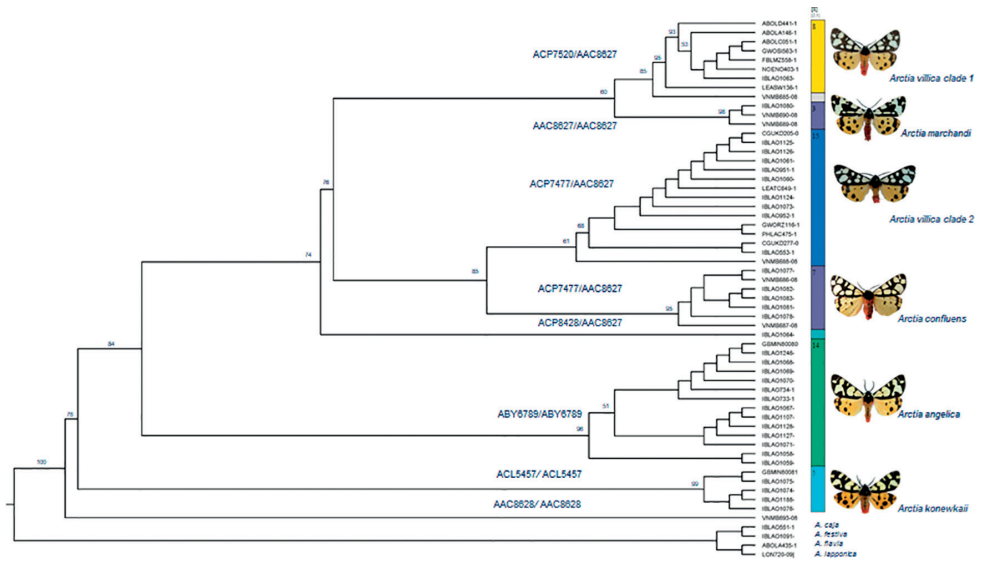


**Figure 2.** Maximum Likelihood tree of *Arctia* species, obtained from 59 nucleotide COI sequences. Bootstrap values > 50% are provided at major nodes. Old and new BINs are indicated for each node. ASAP species delimitation result is indicated by vertical and coloured bars.

**Table 2.** Interspecific mean K2P (Kimura 2-Parameter) divergences (mean pairwise distances) based on the analysis of COI fragments (> 500 bp) among *Arctia* species.

	<i>A. angelica</i>	<i>A. confluens</i>	<i>A. konewkaii</i>	<i>A. marchandi</i>	<i>A. villica01</i>
<i>A. confluens</i>	2.7				
<i>A. konewkaii</i>	3.2	3.5			
<i>A. marchandi</i>	2.2	1.8	2.7		
<i>A. villica01</i>	2.4	1.9	3.3	1.3	
<i>A. villica02</i>	2.4	1.5	3.0	1.4	1.5

samples from Russia, Kyrgyzstan, and Azerbaijan (7 samples with 6 haplotypes); the Turkey clade (3 samples with 2 haplotypes); and the one from Syria (1 sample with one haplotype). West and Central European specimens initially identified as *A. villica* clades 1 and 2 differed up to 1.5% while *A. villica* clade 2 from Central Europe differed at 1.5% and 1.4% from *A. confluens* and *A. marchandi*, respectively (Table 2). Initially, the samples from Russia, Kyrgyzstan, and Azerbaijan were identified as *A. confluens*, and specimens from Turkey as *A. marchandi*, between which a difference of 1.8% was found. The highest interspecific values were found between both clades of *A. villica* and *A. marchandi* (1.8%) and *A. confluens* (1.5%), whereas the lowest one was found between both clades of *A. villica* and *A. marchandi* (1.4% and 1.3%) (Table 2). One specimen from Iran (IBLAO1064-14) identified as *A. confluens* differed up to 1.5% from the other subgroups.

## Delimitation of species

The mean K2P values between the morphologically determined species were used to study species delimitation using two different methods. The BIN System is an online framework that clusters barcode sequences algorithmically and is recalculated from time to time as the number of sequences of each species increases.

All the COI sequences from the five lineages were uploaded and examined into the Barcode of Life Data System (BOLD), resulting in four BINs (AAC8627, ABY6789, ACL5457, and AAC8628) ( $n = 55$  seqs; 23 COI haplotypes). The BIN AAC8627 was attributed to 35 sequences (15 COI haplotypes: 577–658 bp) from different continuous localities along Europe, from Spain and the United Kingdom, to Asia Minor, Caucasus, and Iran; ABY6789 was associated with 14 sequences, and three COI haplotypes (658 bp) located in the southern half of the Iberian Peninsula and Morocco; ACL5457 is unique from Sicily, with five sequences and three haplotypes (658 bp); and AAC8628 for one specimen identified as *A. confluens* (Table 1; field BIN2; Fig. 2). In previous recalculations, six different BINs were related to the five species with singles BIN for *A. angelica* (ABY6789), *A. konewkaii* (ACL5457), *A. marchandi* (AAC8627), two BINs for *A. villica* (ACP7520 and ACP7477) and three BINs for *A. confluens* (ACP7477, ACP8428, and AAC8628) sharing BIN ACP7477 with the *A. villica* clade 2 (Table 1; field BIN1; Fig. 2). This variation in the BIN values, suggesting the presence of different species with unique and specific identifier BIN within the studied *Arctia villica* complex, should be updated with the results of this study.

ASAP method was performed on the data set of 54 sequences, representing all specimens sequenced. For the ASAP analysis, the sequence of a specimen identified as *A. confluens* from Iran (VNMB693-08; BIN: AAC8628) was excluded from further analysis because of the doubtful sequence that separates it from the rest of the groups. The analysis resulted in partitioning all COI sequences into eight MOTUs (hypothetical species) corresponding to five main lineages: *A. angelica*, *A. konewkaii*, *A. villica* (2 groups), *A. marchandi* (2 groups, one of them with only one barcode), and *A. confluens* (2 groups, one of them with only one barcode). ASAP score 2.5 was the smallest within the range of genetic distances and was calculated as the average among two values: the fourth largest p-value (0.255) and the smallest rank of relative barcode gap width ( $1.22e-04$ ). The value of probability (p-value) quantifies the chances that each of its new groups represents a single species, and the rank calculates the width of the barcode gap between the previous and this new partition. Both metrics are combined into a single ASAP-score that is used to rank the partitions (see Puillandre et al. 2021). The graphical output shows each node of the hierarchical clustering with the same probability of being a panmictic species ( $p > 0.1$ ) (Fig. 2).

The two methods used for species delimitation are congruent in recognizing the five main lineages as distinct from any other species studied. The exception are the specimens identified as *A. confluens*, since they are related to two different BINs: specimens collected from Iran with BIN AAC8628 and the general *A. villica* BIN

AAC8627 including specimens from Caucasus and Syria. This high genetic variation needs to be further investigated with additional samples, particularly from Turkey, Caucasus, and Transcaucasia.

## Discussion

### Morphological and ecological traits

The contemporary species definitions and the properties upon which they are based were presented and discussed by e.g., de Queiroz (2007). Among them, biological, ecological, evolutionary, phylogenetic, phenotypic, and genotypic were noted as alternative species concepts, and a “Unified Species Concept” was presented by treating the species exists as a separately evolving metapopulation lineage and the definitions of species mentioned above as operational criteria for different lines of evidence to assessing lineage separation.

The *Arctia villica* complex is a species group with high morphological and colour variability, characterized by the extensive black forewing background with small, well-defined, and rather distinct white patches partly or fully fused, but do not show clearly distinctive differences in the genitalia except in the slight variation of the aedeagus angle, although within each of the species, there is a wide range of variation of the characters with singular overlaps between the peripheric populations where introgression processes probably appear.

In this group of species, wing morphology, zoogeographical distribution, and maternal mitochondrial DNA (barcoding) are properties of lineage separation. Analysis of extensive samples of European and Asian populations of the *Arctia villica* species complex based on morphological features and zoogeographical and biological information revealed the presence of five species, including different forms and varieties, named *A. villica*, *A. angelica*, *A. konewkaii*, *A. marchandi*, and *A. confluens* (de Freina and Nardelli 2007; de Freina 2011). Subsequently, Witt and Ronkay (2011) considered that their distinctive differences in morphology fit well into the range of variation of their characters and all the taxa were considered at subspecific taxonomic rank.

Nevertheless, de Freina and Nardelli (2007) noted that the genital morphology of the entire *A. villica* group is strikingly uniform in both sexes with an insignificant individual variability that is not relevant for the systematics and without signs of regionally deviating structures that could indicate existing subspecies or development processes leading to such. The absence of notable differences in the male and female genitalia, which is the basic feature of the biological species concept for interbreeding, reproductive isolation, and specific mate recognition or fertilization system does not constitute evidence contradicting a hypothesis of lineage separation since the lineage simply may not yet have evolved that properties, as might be expected if they are still in the divergence process, or do not need them because recognition among sexes is due to chemical mechanisms. There are many other such examples in the Noctuoidea (e.g.,

several species complexes in the genera *Euxoa* Hübner, [1821], *Agrotis* Ochsenheimer, 1816, *Cucullia* Schrank, 1802, *Apamea* Ochsenheimer, 1816, and so on).

Although the main criterion to separate Lepidoptera species is genital morphology, other pre- and post-reproductive isolation mechanisms must be considered that prevent the forthcoming of fertile offspring, even though mating may occur (e.g., Yela 2002). De Freina and Nardelli (2007) performed mating experiments between *A. villica* and *A. konewkaii*, from which a F1 was obtained without a fertile F2, suggesting that the reproductive barrier could be related to the pheromone chemistry and not to the genital structure. In the only case where mating was achieved between F2 specimens, the female spawned sterile eggs. The presence in nature of hybrid specimens with morphological characteristics of the male and barcoding of the female has been detected in the area where the populations of *A. villica* and *A. angelica* overlap in the Iberian Peninsula (Table 1; IBLAO1060-14 and IBLAO1061-14).

### BIN discrepancies and species

Detailed morphological, ecological, and genetic analysis can discriminate closely related species that show slight sequence divergence from their nearest neighbour. Molecular analyses enable initial biodiversity evaluation in such taxa, but there is no objective way to select the algorithm or input parameters that best recover actual species boundaries. In different groups of invertebrate taxa, a sequence divergence in the barcode region lower than 2% often corresponds to intraspecific differences, while higher values are typical of interspecific variation and recognized as distinct MOTUs (Hausmann et al. 2011). However, the divergence between young sister species may fall below the 2% threshold, while unusually variable species may exceed it. This is an immediate consequence of the gradual process of speciation, and nominal species do not always correspond to the same divergence stage.

The discrimination of divergences involving these young species requires more algorithmic finesse, and the selection of an effective algorithm for MOTU recognition is necessary. In our study, BIN and ASAP methods were selected to analyse the *Arctia villica* complex sequences.

The Barcode Index Number (BIN) system is a persistent registry for animal MOTUs recognized through sequence variation in the barcode region. The BIN pipeline analyzes new sequence data for the barcode region as they are uploaded to BOLD, and BIN metadata are dynamic because key elements of specimen records on BOLD, especially taxonomic assignments, are frequently revised by data providers and because of the high flow of new records (Ratnasingham and Hebert 2013).

In 2017, BOLD calculated seven different BINS for the five species with singleton BINS for *A. angelica*, *A. konewkaii*, and *A. marchandi*, two for *A. villica* and three for *A. confluens*. Currently, four BINS have been calculated clearly differentiating *A. konewkaii* and *A. angelica*, while *A. villica* formed a group that includes *A. villica*, *A. marchandi*, and *A. confluens*. This variation in the BIN values suggests the presence of different species with unique and specific identifiers within the studied *Arctia villica* complex.

This case of discordance between BIN assignments and the *Arctia villica* species taxonomy proposed can reflect the inability of sequence variation at COI to diagnose species because of introgression or their young age. These “merged species” have diagnostic nucleotide substitutions in the barcode region that can be correlated with the morphological or ecological traits used in species diagnosis. BIN sharing can be made when algorithms used as ABGD (Automatic Barcode Gap Discovery, Puillandre et al. 2012), CROP (Clustering 16S rRNA for OTU Prediction; Hao et al. 2011), RESL (Refined Single Linkage; Ratnasingham and Hebert 2013), GMCY (Generalized Mixed Yule Coalescent; Fujisawa and Barraclough 2013), and jMOTU (Java Program to define MOTU; Jones et al. 2011) fail to partition very young species because of their limited sequence divergence that cannot be separated completely (Ratnasingham and Hebert 2013).

Dellicour and Flot (2018) noted that some methods generally perform well and mostly congruently providing similar species partitions inferred from independent data as other molecular markers, morphological data, or ecological data although they perform poorly when the number of sampled individuals per species or intra- versus interspecific divergences is too low (see Ahrens et al. 2016). Increased sample size and taxonomic and geographic coverage are critical to recognizing species boundaries from barcode sequence information, in addition to other species characteristics.

## Integration of molecular and morphological data

Concerning the species delimitation analyses, Puillandre et al. (2021) assessed ASAP power along with three other programs (ABGD, PTP, and GMYC) on real COI barcode data sets noticing the ASAP potential to become a relevant tool to test the hypothesis in an integrative taxonomy process. ASAP identifies a species partition ranked with different scores that must be subsequently tested against other evidence in an integrative taxonomy framework, especially when a single-locus data is used.

The ASAP procedure of the barcoding data obtained in our study indicates the existence of five *Arctia* species within the formerly known *Arctia villica* subspecies distributed from the Iberia Peninsula to the areas around Transcaucasia and Iran. Two well-supported and reciprocally monophyletic groups were found in the Iberian Peninsula, *A. angelica*, and Sicily, *A. konewkaii*. The other group was made up by sequences of the polymorphic *A. villica* within two clusters which show notable sequence variability as expected from its wide geographic distribution across many European and Asian localities. These two groups represent two *A. villica* populations related to both species *A. marchandi* and *A. confluens*, respectively. The *A. villica* populations (clade 1) from Austria, Germany, and Hungary were related to the *A. marchandi* population from Turkey while one specimen from Syria identified as *A. villica* is equally related to both groups. The other *A. villica* population (clade 2) from Great Britain, Italy, and half of the Iberian Peninsula was related to the polymorphic *A. confluens* (Fig. 2). The polymorphic *A. confluens* group has three different BINs in the same area of distribution.

Hence, with the combined evidence from comparative morphological studies and the DNA barcode results presented above, *Arctia* species belonging to the *villica* group could be considered as metapopulations lineages separately evolving extended through

time and including connected subpopulations according to the Unified Species Concept and Species Delimitation (de Queiroz, 2007). In our study, these *Arctia* species must have evolved separately from other lineages with separated historical biogeographic processes (Fig. 2).

The current distributions of *A. villica* species complex is likely to be the result of multiple range shifts driven by past climatic changes. Cyclic climatic change during the Pleistocene has caused repeated range shifts in most European taxa, profoundly influencing the biodiversity of Europe (for reviews, see Hewitt 1996, 1999, 2000, 2004; Taberlet et al. 1998; Schmitt 2007).

Three peninsular refugia in the south of the continent, Iberia, Italy, and Balkan harbour high biodiversity and endemism rates due in large part to their long-term environmental stability, which enables the persistence of palaeoendemic taxa (e.g., Jansson 2003; Graham et al. 2006). Isolation among refugial populations promotes genetic and phenotypic differentiation as a result of independent adaptation to local environments and genetic drift, with consequences for reproductive isolation between discrete refugial lineages and the creation of hybrid zones where diverged lineages come into secondary contact (Hewitt 1999).

The major lineage of *A. villica* may have diversified in four complexes represented by a widespread group of ancient *A. villica* from Spain to Russia and three species groups restricted to known areas in the Iberian Peninsula (*A. angelica*), Sicily (*A. konewkaii*), and around the Caucasus (*A. confluens* and *A. marchandi*), showing a pattern that could be considered evidence for similar ecological preferences or parallel histories for these species during the Quaternary. The fact that these four taxa with more restricted distribution make up separated clades to the broadly distributed *A. villica* suggests that all clades share it as their recent common ancestor. This phylogeographic pattern has been suggested for other Lepidoptera (e.g. those of the genera *Polyommatus* Latreille, 1804, *Erebia* Dalman, 1816, *Melitaea* Fabricius, 1807, *Parnassius* Latreille, 1804, *Chelis* Rambur, [1866]), in which it is postulated a marked role of climatic oscillations during the Pleistocene on population isolation and differentiation (Haubrich and Schmitt 2007; Albre et al. 2008; Lenevea et al. 2009; Vila et al. 2010; Todisco et al. 2012; Ortiz et al. 2015).

The apparent absence of a clear lineage sorting between *A. villica* and *A. confluens*-*A. marchandi* may be due to relatively recent radiation. Preliminary information in Kizildağ et al. (2019) suggested that *A. marchandi* should be considered at the subspecific level, although the *A. confluens*-*A. marchandi* divergence must be further evaluated when more specimens from all over their distributional ranges have been sequenced.

However, an increasing number of studies indicate that many endemic taxa inhabiting refugial regions are of Pleistocene origin and formed by allopatric fragmentation. In some cases, they are described as distinct species and, in other cases, these taxa are considered to be subspecies or lineages within species. The present occurrence of *A. angelica*, *A. confluens* and *A. marchandi* in the Iberian Peninsula and around the Caucasus, respectively, showing a sympatric distribution with *A. villica*, is thought to be the result of a range expansion of *A. villica* since the last glaciation events, due to the high ecological plasticity of this species and the finding of many suitable habitats, including *A. konewkaii* in Sicily.

Additional information from nuclear markers and a greater number of samples from the Caucasus will be crucial for the resolution of the different questions that are currently unresolved, such as *A. confluens* and *A. marchandi* intraspecific variability and whether they can be delimited and recognized as species utilizing integrated taxonomy.

## Acknowledgements

We are very grateful to the staff at the Canadian Centre for DNA Barcoding for sequence analysis. Paul D.N. Hebert and many other colleagues of the Barcode of Life project (Biodiversity Institute of Ontario, Guelph, Canada) contributed to the success of this study. We are particularly grateful to Ramón Macià, Carlos Antonietty and Pablo Valero for loaning specimens and to Peter Huemer from Tiroler Landesmuseum in Innsbruck (Austria) and Axel Hausmann from Bavarian State Collection of Zoology, of Munich (Germany), for granting access to their projects on BOLD. Thanks are also due to Alejandro López, Ana Isabel Asensio, and Manuel González Veiga for their comments, suggestions and technical support. John Girdley and Claire Ward also helped with comments and linguistic advice.

Environmental Authorities in the National Park of Sierra Nevada (Andalusia), National Park of Picos de Europa (Asturias), Aragón Region, Castilla-La Mancha Region, Natural Park of Alt Pirineu, and Aran Valley (Catalonia) permitted collection and access to field sites. We also thank to Reza Zahiri and various anonymous referees for their comments. We are very grateful for this collegial and kind support. This study has been supported by the project Fauna Ibérica XII – Lepidoptera: Noctuoidea I (PGC2018-095851-B-C63) of the Spanish Ministry of Research and Science and part of DNA sequencing was supported by Genome Canada (Ontario Genomics Institute) in the framework of the iBOL program, WP 1.9. The Instituto de Ciencias Ambientales de Toledo (ICAM-UCLM) provided infrastructure and collaborated in logistic tasks; we thank its director, Prof. Federico Fernández González, for his kind support.

## References

- Ahrens D, Fujisawa T, Krammer HJ, Eberle J, Fabrizi S, Vogler AP (2016) Rarity and incomplete sampling in DNA-based species delimitation. *Systematic Biology* 65(3): 478–494. <https://doi.org/10.1093/sysbio/syw002>
- Albre J, Gers C, Legal L (2008) Molecular phylogeny of the *Erebia tyndarus* (Lepidoptera, Rhopalocera, Nymphalidae, Satyrinae) complex of species combining CoxII and ND5 mitochondrial genes: A case study of recent radiation. *Molecular Phylogenetics and Evolution* 47(1): 196–210. <https://doi.org/10.1016/j.ympev.2008.01.009>
- Anisimova M, Gil M, Dufayard J, Dessimoz C, Gascuel O (2011) Survey of Branch Support Methods Demonstrates Accuracy, Power, and Robustness of Fast Likelihoodbased Approximation Schemes. *Systematic Biology* 60(5): 685–699. <https://doi.org/10.1093/sysbio/syr041>

- de Freina JJ (2011) Revision des *Arctia villica*-Komplexes – 2. Teil. Nomenklatur und Systematik der osteuropäisch-asiatischen Arten *Arctia villica* (Linnaeus, 1758) (partim), *Arctia marchandi* De Freina, 1983 stat. n. und *Arctia confluens* Romanoff, 1884 stat. n. (Lepidoptera: Arctiidae, Arctiinae). *Entomofauna* 32(4): 93–124.
- de Freina JJ, Nardelli U (2007) Revision des *Arctia villica*-Komplexes – 1. Teil. Nomenklatur und Systematik der adriato- und atlantomediterranen Arten *Arctia villica* (Linnaeus, 1758 (partim), *Arctia angelica* (Boisduval, 1829) stat. n. und *Arctia konewkaii* (Freyer, 1831) stat. rev. (Lepidoptera: Arctiidae, Arctiinae). *Entomologische Zeitschrift Stuttgart* 117(3): 105–123.
- de Freina JJ, Witt TJ (1987) Die Bombyces und Sphinges der Westpalaerktis (Insecta, Lepidoptera) Band 1. Forschung and Wissenschaft, München, Germany, 708 pp.
- de Queiroz K (2007) Species concept and species delimitation. *Systematic Biology* 56(6): 879–886. <https://doi.org/10.1080/10635150701701083>
- Dellicour S, Flot J (2018) The hitchhiker's guide to single-locus species delimitation. *Molecular Ecology Resources* 18(6): 1234–1246. <https://doi.org/10.1111/1755-0998.12908>
- deWaard JR, Ivanova NV, Hajibabaei M, Hebert PDN (2008) Assembling DNA barcodes: Analytical Protocols. In: Martin C (Ed.) *Methods in Molecular Biology: Environmental Genetics*. Humana Press, Totowa, 275–293. [https://doi.org/10.1007/978-1-59745-548-0\\_15](https://doi.org/10.1007/978-1-59745-548-0_15)
- Fibiger M (1997) Noctuidae Europaeae. Noctuinae III. *Entomological Press, Soro*, 418 pp.
- Fujisawa T, Barraclough TG (2013) Delimiting species using Single-Locus Data and the Generalized Mixed Yule Coalescent approach: A revised method and evaluation on simulated data sets. *Systematic Biology* 62(5): 707–724. <https://doi.org/10.1093/sysbio/syt033>
- Graham CH, Moritz C, Williams SE (2006) Habitat history improves prediction of biodiversity in rainforest fauna. *Proceedings of the National Academy of Sciences of the United States of America* 103(3): 632–636. <https://doi.org/10.1073/pnas.0505754103>
- Guindon S, Dufayard J, Lefort V, Anisimova M, Hordijk W, Gascuel O (2010) New Algorithms and Methods to Estimate Maximum-Likelihood Phylogenies: Assessing the Performance of PhyML 3.0. *Systematic Biology* 59(3): 307–321. <https://doi.org/10.1093/sysbio/syq010>
- Hao X, Jiang R, Chen T (2011) Clustering 16S rRNA for OTU prediction: A method of unsupervised Bayesian clustering. *Bioinformatics* 27(5): 611–618. <https://doi.org/10.1093/bioinformatics/btq725>
- Haubrich K, Schmitt T (2007) Cryptic differentiation in alpine endemic, high-altitude butterflies reveals down-slope glacial refugia. *Molecular Ecology* 16(17): 3463–3658. <https://doi.org/10.1111/j.1365-294X.2007.03424.x>
- Hausmann A, Huemer P (2011) Taxonomic decision as a compromise: *Acasis appensata* (Eversmann, 1832) in Central Italy—a case of conflicting evidence between DNA barcode and morphology (Lepidoptera: Geometridae). *Zootaxa* 3070(1): 60–68. <https://doi.org/10.11646/zootaxa.3070.1.7>
- Hausmann A, Haszprunar G, Hebert PDN (2011) DNA barcoding the Geometrid fauna of Bavaria (Lepidoptera): successes, surprises, and questions. *PLoS ONE* 6(2): e17134. <https://doi.org/10.1371/journal.pone.0017134>
- Hebert PDN, Penton EH, Burns JM, Janzen DH, Hallwachs W (2004) Ten species in one: DNA barcoding reveals cryptic species in the neotropical skipper butterfly *Astraptes fulgerator*. *Proceedings of the National Academy of Sciences of the United States of America* 101(41): 14812–14817. <https://doi.org/10.1073/pnas.0406166101>

- Hewitt GM (1996) Some genetic consequences of ice ages, and their role in divergence and speciation. *Biological Journal of the Linnean Society* 58(3): 247–276. <https://doi.org/10.1006/bijl.1996.0035>
- Hewitt GM (1999) Post-glacial re-colonization of European biota. *Biological Journal of the Linnean Society* 68(1–2): 87–112. <https://doi.org/10.1111/j.1095-8312.1999.tb01160.x>
- Hewitt GM (2000) The genetic legacy of the Quaternary ice ages. *Nature* 405(6789): 907–913. <https://doi.org/10.1038/35016000>
- Hewitt GM (2004) Genetic consequences of climatic oscillations in the Quaternary. *Philosophical Transactions of the Royal Society of London, Series B, Biological Sciences* 359(1442): 183–195. <https://doi.org/10.1098/rstb.2003.1388>
- Hogan D, Chernomor O, Haeseler A, Mihn B, Vihn L (2017) UFBBoot2: Improving the ultra-fast bootstrap approximation. *Molecular Biology and Evolution* 35(2): 518–522. <https://doi.org/10.1093/molbev/msx281>
- Huemer P, Hausmann A (2009) A new expanded revision of the European high mountain *Sciadia tenebraria* species group (Lepidoptera: Geometridae). *Zootaxa* 2117(1): 1–30. <https://doi.org/10.11646/zootaxa.2117.1.1>
- Jansson R (2003) Global patterns in endemism explained by past climatic change. *Proceedings of the Royal Society B, Biological Sciences* 270(1515): 583–590. <https://doi.org/10.1098/rspb.2002.2283>
- Jones M, Ghoorah A, Blaxter M (2011) jMOTU and Taxonator: Turning DNA barcode sequences into annotated operational taxonomic units. *PLoS ONE* 6(4): e19259. <https://doi.org/10.1371/journal.pone.0019259>
- Kalyaanamoorthy S, Minh B, Wong T, Haeseler A, Jermini L (2017) ModelFinder: Fast model selection for accurate phylogenetic estimates. *Nature Methods* 14(6): 587–589. <https://doi.org/10.1038/nmeth.4285>
- Kimura M (1980) A simple model for estimating evolutionary rates of base substitutions through comparative studies of nucleotide sequences. *Journal of Molecular Evolution* 16(2): 111–120. <https://doi.org/10.1007/BF01731581>
- Kizildağ S, Kemal M, Koçak AÖ (2019) Comments on the taxonomic status of “*marchandi* De Freina” in SE Turkey (Lepidoptera, Arctiidae). *Miscellaneous Papers* 189: 1–3.
- Lenevea J, Chichvarkhin A, Wahlberg N (2009) Varying rates of diversification in the genus *Melitaea* (Lepidoptera: Nymphalidae) during the past 20 million years. *Biological Journal of the Linnean Society. Linnean Society of London* 97(2): 346–361. <https://doi.org/10.1111/j.1095-8312.2009.01208.x>
- Lumley LM, Sperling FAH (2010) Integrating morphology and mitochondrial DNA for species delimitation within the spruce budworm (*Choristoneura fumiferana*) cryptic species complex (Lepidoptera: Tortricidae). *Systematic Entomology* 35(3): 416–428. <https://doi.org/10.1111/j.1365-3113.2009.00514.x>
- Murzin VS (2003) *The Tiger Moths of the Former Soviet Union* (Insecta: Lepidoptera: Arctiidae). Pensoft Publishers, Sofia, 243 pp.
- Mutanen M, Aarvik L, Huemer P, Kaila L, Karsholt O, Tuck K (2012) DNA barcodes reveal that the widespread European tortricid moth *Phalonidia manniana* (Lepidoptera: Tortricidae) is a mixture of two species. *Zootaxa* 3262(1): 1–21. <https://doi.org/10.11646/zootaxa.3262.1.1>

- Nguyen L, Schmidt H, Haeseler A, Minh B (2015) A fast and effective stochastic algorithm for estimating maximum likelihood phylogenies. *Molecular Biology and Evolution* 32(1): 268–274. <https://doi.org/10.1093/molbev/msu300>
- Ortiz AS, Rubio RM, Guerrero JJ, Garre M, Hausmann A (2015) Integrated taxonomy, phylogeography and conservation in the genus *Chelis* Rambur, [1866] in the Iberian Peninsula (Lepidoptera, Erebidae, Arctiinae). *Spixiana* 39: 273–286.
- Padial JM, De La Riva I (2010) A response to recent proposals for integrative taxonomy. *Biological Journal of the Linnean Society* 101(3): 747–756. <https://doi.org/10.1111/j.1095-8312.2010.01528.x>
- Pons J, Barraclough TG, Gomez-Zurita J, Cardoso A, Duran DP, Hazell S, Kamoun S, Sumlin WD, Vogler P (2006) Sequence-based species delimitation for the DNA taxonomy of undescribed insects. *Systematic Biology* 55(4): 595–609. <https://doi.org/10.1080/10635150600852011>
- Puillandre N, Lambert A, Brouillet S, Achaz G (2012) ABGD, Automatic Barcode Gap Discovery for primary species delimitation. *Molecular Ecology* 21(8): 1864–1877. <https://doi.org/10.1111/j.1365-294X.2011.05239.x>
- Puillandre N, Brouillet S, Achaz G (2021) ASAP: Assemble species by automatic partitioning. *Molecular Ecology Resources* 21(2): 609–620. <https://doi.org/10.1111/1755-0998.13281>
- Ratnasingham S, Hebert PDN (2007) The Barcode of Life Data System. *Molecular Ecology Notes* 7(3): 355–364. <https://doi.org/10.1111/j.1471-8286.2007.01678.x>
- Ratnasingham S, Hebert PDN (2013) A DNA-Based Registry for All Animal Species: The Barcode Index Number (BIN) System. *PLoS ONE* 8(8): e66213. <https://doi.org/10.1371/journal.pone.0066213>
- Reid NM, Carstens BC (2012) Phylogenetic estimation error can decrease the accuracy of species delimitation: A Bayesian implementation of the general mixed Yule-coalescent model. *BMC Evolutionary Biology* 12(1): e196. <https://doi.org/10.1186/1471-2148-12-196>
- Rönkä K, Mappes J, Kaila L, Wahlberg N (2016) Putting *Parasemia* in its phylogenetic place: A molecular analysis of the subtribe Arctiina (Lepidoptera). *Systematic Entomology* 41(4): 844–853. <https://doi.org/10.1111/syen.12194>
- Rozas J, Sanchez-Delbarrio JC, Messeguer X, Rozas R (2003) DnaSP, DNA polymorphism analyses by the coalescent and other methods. *Bioinformatics* 19(18): 2496–2497. <https://doi.org/10.1093/bioinformatics/btg359>
- Schlick-Steiner BC, Steiner FM, Seifert B, Stauffer C, Christian E, Crozier RH (2010) Integrative taxonomy: A multisource approach to exploring biodiversity. *Annual Review of Entomology* 55(1): 421–438. <https://doi.org/10.1146/annurev-ento-112408-085432>
- Schmitt T (2007) Molecular biogeography of Europe: Pleistocene cycles and Postglacial trends. *Frontiers in Zoology* 4(1): 1–11. <https://doi.org/10.1186/1742-9994-4-11>
- Schrank F (1802) Fauna Boica. Durchgedachte Geschichte der in Baiern einheimischen und zahmen Thiere. Zweyter Band zweyte Abtheilung 2(2). Johann Wilhelm Krüll, Ingolstadt, 152 pp.
- Smith MA, Fernandez-Triana J, Roughley R, Hebert PDN (2009) DNA barcode accumulation curves for understudied taxa and areas. *Molecular Ecology Resources* 9: 208–216. <https://doi.org/10.1111/j.1755-0998.2009.02646.x>
- Taberlet P, Fumagalli L, Wust-Saucy AG, Cosson JF (1998) Comparative phylogeography and postglacial colonization routes in Europe. *Molecular Ecology* 7(4): 453–464. <https://doi.org/10.1046/j.1365-294x.1998.00289.x>

- Tamura K, Stecher G, Peterson D, Filipski A, Kumar S (2013) MEGA6: Molecular Evolutionary Genetics Analysis Version 6.0. *Molecular Biology and Evolution* 30(12): 2725–2729. <https://doi.org/10.1093/molbev/mst197>
- Todisco V, Gratton P, Zakharov EV, Wheatm CW, Sbordoni V, Sperling FAH (2012) Mitochondrial phylogeography of the Holarctic *Parnassius phoebus* complex supports a recent refugial model for alpine butterflies. *Journal of Biogeography* 39(6): 1058–1072. <https://doi.org/10.1111/j.1365-2699.2011.02675.x>
- Vila R, Lukhtanov V, Talavera G, Gil TF, Pierce NE (2010) How common are dot-like distributions? Taxonomical oversplitting in western European *Agrodiaetus* (Lepidoptera: Lycaenidae) revealed by chromosomal and molecular markers. *Biological Journal of the Linnean Society* 101(1): 130–154. <https://doi.org/10.1111/j.1095-8312.2010.01481.x>
- Witt TJ, Ronkay L (2011) Noctuidae Europaeae. Lymantriinae-Arctiinae, Including Phylogeny and Check List of the Quadrifid Noctuoidea of Europe (Vol. 13). Entomological Press, Sorø, 448 pp.
- Witt TJ, Speidel W, Ronkay G, Ronkay L, László GM (2011) Arctiinae. In: Witt TJ, Ronkay L (Eds) Noctuidae Europaeae (Vol. 13). Lymantriinae and Arctiinae Including Phylogeny and Check List of the Quadrifid Noctuoidea of Europe. Entomological Press, Sorø, 81–217.
- Yela J (2002) The internal genitalia as a taxonomic tool: description of the relict endemic moth, *Coranarta restricta* sp. n., from the Iberian Peninsula (Lepidoptera: Noctuidae: Hadeninae). *Entomologica Fennica* 13(1): 1–12. <https://doi.org/10.33338/ef.84131>
- Ylla J, Macià R, Gastón FJ (2010) Manual de Identificación y Guía de Campo de los Ártidos de la Península Ibérica y Baleares. Argania edition, Barcelona, 290 pp.
- Zhang J, Kapli R, Pavlidis P, Stamatakis A (2013) A general species delimitation method with applications to phylogenetic placements. *Bioinformatics* 29(22): 2869–2876. <https://doi.org/10.1093/bioinformatics/btt499>

## Supplementary material I

### Complete similarity matrix

Authors: Antonio S. Ortiz, Rosa M. Rubio, Josef J. de Freina, Juan J. Guerrero, Manuel Garre, José Luis Yela

Data type: Similarity index matrix

Explanation note: Complete similarity index matrix among *Arctia villica* species.

Copyright notice: This dataset is made available under the Open Database License (<http://opendatacommons.org/licenses/odbl/1.0/>). The Open Database License (ODbL) is a license agreement intended to allow users to freely share, modify, and use this Dataset while maintaining this same freedom for others, provided that the original source and author(s) are credited.

Link: <https://doi.org/10.3897/zookeys.1159.95225.suppl1>

# A review of *Microdytes* J. Balfour-Browne, 1946 from Thailand, Laos, and Cambodia with descriptions of five new species and new records (Coleoptera, Dytiscidae)

Ryohei Okada<sup>1,2</sup>, Weeyawat Jaitrong<sup>1</sup>, Günther Wewalka<sup>3</sup>

**1** Thailand Natural History Museum, National Science Museum, Technopolis, Pathum Thani, Thailand  
**2** Coleopterological Society of Japan, National Museum of Nature and Science, Tsukuba, Japan  
**3** Starkfriedgasse 16/1/3, A – 1190 Vienna, Austria

Corresponding author: Ryohei Okada ([wasserinsekt@kub.biglobe.ne.jp](mailto:wasserinsekt@kub.biglobe.ne.jp))

---

Academic editor: Mariano Michat | Received 6 January 2023 | Accepted 3 April 2023 | Published 25 April 2023

---

<https://zoobank.org/CD97DD12-0549-412F-9765-08D8DE21605B>

---

**Citation:** Okada R, Jaitrong W, Wewalka G (2023) A review of *Microdytes* J. Balfour-Browne, 1946 from Thailand, Laos, and Cambodia with descriptions of five new species and new records (Coleoptera, Dytiscidae). ZooKeys 1159: 87–119. <https://doi.org/10.3897/zookeys.1159.99218>

---

## Abstract

The diving beetle genus *Microdytes* J. Balfour-Browne, 1946 in Thailand, Laos, and Cambodia is reviewed, and five new species are described: *Microdytes eliasi* Wewalka & Okada, **sp. nov.** (Thailand, Cambodia), *M. jeenthongi* Okada & Wewalka, **sp. nov.** (Thailand), *M. maximiliani* Wewalka & Okada, **sp. nov.** (Laos, China), *M. sekaensis* Okada & Wewalka, **sp. nov.** (Thailand, Laos), *M. ubonensis* Okada & Wewalka, **sp. nov.** (Thailand, Laos). Two species are the first country records: *M. balkei* Wewalka, 1997 (Laos, Cambodia) and *M. wewalkai* Bian & Ji, 2009 (Laos). For 12 and 8 species, the first provincial records from Thailand and Laos, respectively, are given. A checklist, a key to the 25 known *Microdytes* species from these countries, and habitus images and illustrations of diagnostic characters are provided. Distribution maps of the recorded species are presented, and species distribution patterns are also briefly discussed.

## Keywords

Diving beetles, faunistics, key to species, Southeast Asia, taxonomy, zoogeography

## Introduction

The dytiscid genus *Microdytes* J. Balfour-Browne, 1946 contains 47 described species classified in the tribe Hyphyrini of the subfamily Hydroporinae (Nilsson and Hájek

2023). These minute diving beetles (adult length up to 2.3 mm) generally occur in small seeps, springs, and streams, and a few are also known to inhabit subterranean and hypogepetric environments (Wewalka 1997; Wewalka et al. 2007; Sheth et al. 2020). *Microdytes* species occur throughout southern and southeastern Asia from Nepal to southern India to southern China, southern Japan, Philippines, and Indonesia (Miller and Wewalka 2010). So far, 16 species were recorded from Thailand, and this country was regarded as the center of distribution of the genus by Wewalka (1997, 2011).

During 2018–2022, as part of the field survey by the senior author to reveal diversity of Thailand diving beetles, a total of 228 *Microdytes* specimens were collected from 30 localities. For comparative purposes, we also studied specimens from Thailand, Laos, and Cambodia, mainly collected as part of the “NHMB Basel, Laos Expeditions” in 2011 and 2012 (Geiser and Nagel 2013).

In this paper, we describe five new species from Thailand, Laos, and Cambodia, increasing the number of known *Microdytes* species to 52. New and first regional records from those countries are also given. A checklist and a key to all *Microdytes* species known from these countries are provided. To facilitate the identification of the species, photographs of habitus and discriminant characters are provided for the first time. Distribution maps of the recorded *Microdytes* species are also presented, and their distribution patterns and microhabitat preferences are briefly discussed.

## Materials and methods

The study was based on the examination of 695 specimens: 241 from Thailand, 420 from Laos, and 34 from Cambodia. These specimens are deposited in the following institutions and private collections:

<b>CGW</b>	Collection Günther Wewalka, Vienna, Austria;
<b>CRO</b>	Collection Ryohei Okada, Tokyo, Japan;
<b>MNHN</b>	Muséum National d’Histoire Naturelle, Paris, France;
<b>NMB</b>	Naturhistorisches Museum, Basel, Switzerland;
<b>NMP</b>	National Museum (Natural History), Prague, Czech Republic;
<b>NMW</b>	Naturhistorisches Museum Wien, Vienna, Austria;
<b>THNHM</b>	Thailand Natural History Museum, Pathum Thani, Thailand.

Beetles were pin mounted on square or triangular card points. Male genitalia were dissected, then put on cards for detailed observation. The holotypes, paratypes, and lectotype of the closely related species were examined. Specimens from Myanmar were also used for comparisons.

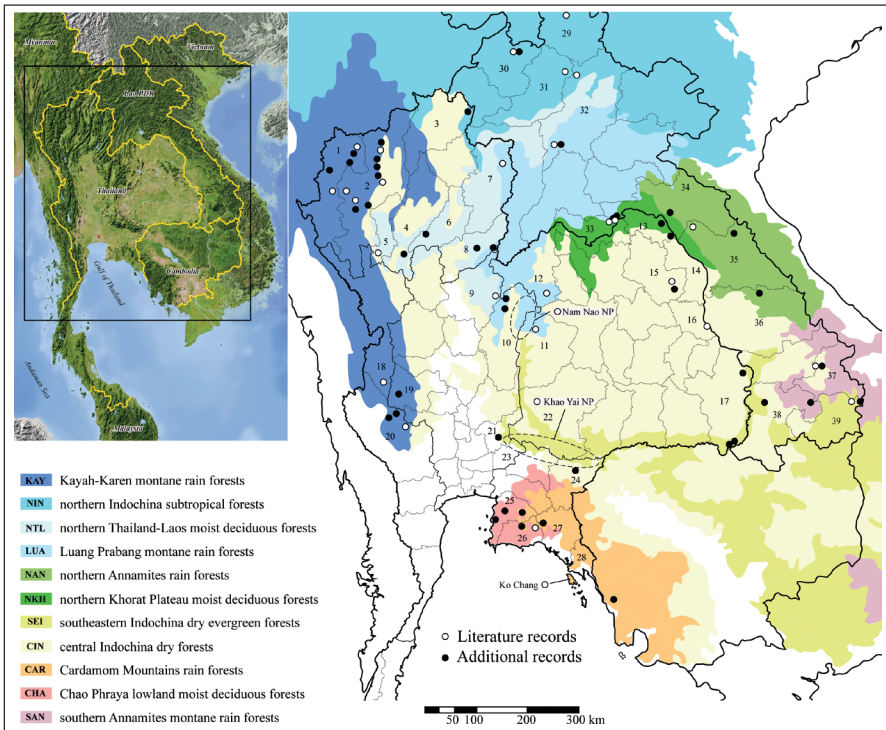
The beetles were studied with an Olympus SZX10 compound microscope equipped with Nomarsky optics up to 1000×. Habitus photographs were taken using a Canon EOS 7D Mark II digital camera with attached Canon MP-E65 mm f/2.8 macro lens with 5:1 optics. Male genitalia were illustrated wet, using an Olympus BHT transmitted light microscope with a RICOH GX6 attachment. Composite images were created using the

image stacking software Helicon Focus (Helicon Soft Ltd., Kharkov), and subsequently edited with Adobe Photoshop elements (2008) (Adobe Systems Inc., USA) where necessary.

The terminology to denote the orientation of the genitalia follows Miller and Nilsson (2003); the style of the descriptive notes follows Wewalka (1997, 2011) and Miller and Wewalka (2010).

Body measurements were made with a compound microscope equipped with a micrometer eyepiece. The abbreviations of measurements used in this study are as follows: **TL** (total body length), **TL-H** (body length without head), **MW** (maximum width of body). The ratio **TL/MW** was also calculated. Measurements of holotypes are added between round brackets. Label data of holotype specimens are cited between quotation marks. A backslash (\) indicates separate labels. Our comments are given between square brackets.

All localities where *Microdytes* species were recorded in Thailand, Laos, and Cambodia are shown in Fig. 1. Literature records (Wewalka 1997, 2011) and additional



**Figure 1.** Known localities of *Microdytes* species in Thailand, Laos, and Cambodia, including literature records, sampling sites and additional records in this study. For those records where specific information of province was not reported, the location was mapped by dotted lines. Ecoregion classification is given following Olson et al. (2001). Thailand: 1 Mae Hong Son 2 Chiang Mai 3 Chiang Rai 4 Lampang 5 Lamphun 6 Phrae 7 Nan 8 Uttaradit 9 Phitsanulok 10 Phetchabun 11 Chaiyaphum 12 Loei 13 Bueng Kan 14 Nakhon Phanom 15 Sakon Nakhon 16 Mukdahan 17 Ubon Ratchathani 18 Tak 19 Uthai Thani 20 Kanchanaburi 21 Saraburi 22 Nakhon Ratchasima 23 Nakhon Nayok 24 Sa Kaeo 25 Chonburi 26 Rayong 27 Chanthaburi 28 Trat. Laos: 29 Phongsaly 30 Luang Namtha 31 Oudomxay 32 Luang Prabang 33 Vientiane 34 Bolikhamxay 35 Khammouane 36 Savannakhet 37 Sekong 38 Champasak 39 Attapeu.

records in this study are symbolized separately. For interpretation of distribution patterns of *Microdytes*, we mapped the recorded localities onto terrestrial ecoregions as defined by Olson et al. (2001). The main ecoregions for the distributions of species in Thailand, Laos, and Cambodia are abbreviated as follows:

<b>T</b>	Thailand;
<b>L</b>	Laos;
<b>C</b>	Cambodia;
<b>KAY</b>	Kayah-Karen montane rain forest;
<b>NIN</b>	northern Indochina subtropical forests;
<b>LUA</b>	Luang Prabang montane rain forests;
<b>NAN</b>	northern Annamites rain forests;
<b>NKH</b>	northern Khorat Plateau moist deciduous forests;
<b>SEI</b>	southeastern Indochina dry evergreen forests;
<b>CIN</b>	central Indochina dry forests;
<b>CAR</b>	Cardamom Mountains rain forests;
<b>CHA</b>	Chao Phraya lowland moist deciduous forests.

## Results

### Descriptions

#### *Microdytes eliasi* Wewalka & Okada, sp. nov.

<https://zoobank.org/8C12C23B-3B90-4F46-9D48-F5ABD6625734>

Figs 2, 7, 12, 42C, 43C

**Type locality.** Cambodia, Koh Hong Province, 20 km SW Koh Hong, Tatai River, 11°34'N, 103°07'E, alt. 50–300 m.

**Type material.** *Holotype* (NMB): ♂ “Cambodia SW, Tatai riv. 20 km SE Koh Hong 11°34'N, 103°07'E, 3.–19.v.2005, 50–300 m, E. Jendek, O. Šauša leg.” [printed white label] \ “HOLOTYPUS *Microdytes eliasi* sp. nov. Wewalka & Okada 2022” [printed red label]. *Paratypes*: (47 exs.): 7♂♂, 14♀♀, with same data as the holotype (CGW, CRO, NMB, NMP); 2♂♂, Thailand, Saraburi Province, Kaeng Khoi District, Ched Khot St. 122 (alt. 140 m), 14°28'26"N, 101°09'59"E, 30.V.2020, R. Okada leg. (CRO, THNHM); 4♂♂, 4♀♀, Thailand, Sa Kaeo Province, Mueang Sa Kaeo District, Ban Kaeng St. 277 (alt. 80 m), 13°58'47"N, 102°11'29"E, 30.I.2022, R. Okada leg. (CGW, CRO, THNHM); 2♂♂, 3♀♀, Thailand, Chonburi Province, Bo Thong District, That Thong St. 107 (alt. 100 m), 13°15'01"N, 101°22'34"E, 14.III.2020, R. Okada leg. (CGW, CRO, THNHM); 2♂♂, 2♀♀, same locality St. 298 (alt. 100 m), 13.VII.2022, R. Okada leg. (CGW, CRO); 1♀, same province, Si Racha District, Bang Phra St. 269 (alt. 90 m), 13°14'39"N, 101°02'20"E, 26.XII.2021, R. Okada leg.

(CRO); 3♂♂, 2♀♀, Thailand, Chanthaburi Province, Khaeng Hong Maeo District, Kaeng Hong waterfall St. 257 (alt. 160 m), 13°02'57"N, 101°45'35"E, 26.VI.2021, R. Okada leg. (CGW, CRO, THNHM); 1♀, same district, Kha riv. St. 258 (alt. 90 m), 12°57'38"N, 101°46'30"E, 26.VI.2021, R. Okada leg. (CRO). All paratypes are provided with printed red paratype labels.

**Diagnosis.** *Microdytes eliasi* sp. nov. very closely resembles *M. maculatus* (Motschulsky, 1860) (Figs 25, 41) in size and coloration but differs from this species by the more regularly oval habitus, the laterally expanded median lobe at apex and constricted tips of paramere (Figs 12, 42C, 43C) (see also comments in *M. maculatus*). It is also similar to *M. feryi* Wewalka, 2011 (Fig. 21) in habitus and coloration, but it is smaller and can be distinguished by male genitalia [compared with a male paratype from Myanmar, "Tenasserim, Birma Coll. V. Helfer National Museum Prague" (CGW)].

**Description. Measurements.** TL = 1.64–1.85 mm (1.76 mm), TL-H = 1.49–1.65 mm (1.55 mm), MW = 1.12–1.25 mm (1.24 mm), TL/MW = 1.33–1.44 (1.42). Body regularly oval, moderately convex (Fig. 2).

**Coloration.** Head reddish brown. Pronotum reddish brown, narrowly dark brown along anterior and posterior margins. Elytron dark brown with yellowish brown markings forming a distinct transverse band near base not reaching suture connected along lateral margin with a post-median transverse lateral band, with a small post-median spot near suture, and a triangular spot near apex (Figs 2, 7). Ventral surface of head, prothorax and elytral epipleuron yellowish brown; thorax and abdominal ventrites reddish brown to dark brown. Legs, antennae and palpi yellowish brown.

**Sculpture and structure.** Head finely, sparsely, and relatively regularly punctured; anterior half to two-thirds finely microreticulate; clypeus not bordered. Pronotum quite regularly, sparsely, and fairly strongly punctured, with coarser punctures along posterior margin; without microreticulation; lateral margins finely bordered, regularly rounded. Elytron quite regularly, moderately densely and fairly strongly punctured, progressively finer and sparser towards lateral margin; without longitudinal rows of stronger punctures; highly polished and shining; without microreticulation. Ventral surface: metacoxae and metasternum strongly but sparsely punctured, abdomen finely and sparsely punctured; without microreticulation.

**Male.** The two parts of the median lobe expanded laterally at apex in ventral aspect (Figs 12A, 42A); slightly curved in lateral aspect (Fig. 12B). The tips of parameres twisted in lateral aspect (Fig. 12C, D); constricted in ventral aspect (Fig. 43C).

**Female.** Without secondary sexual characters. Sclerotized spermatheca not found.

**Variation.** Variation of markings is shown in Fig. 7.

**Etymology.** This species is dedicated to Elias Bramböck, Vienna, Austria. The species epithet is a name in the genitive singular.

**Habitat.** In Thailand, this species was collected in small streams at low altitude lower than 200 m (Fig. 45).

**Distribution.** Thailand: Saraburi, Sa Kaeo, Chonburi, and Chanthaburi provinces; Cambodia: Koh Hong Province.

***Microdytes jeenthongi* Okada & Wewalka, sp. nov.**

<https://zoobank.org/D3B3AE52-D18B-49E8-AAB7-E0DC2F5E6CD1>

Figs 3, 8, 13, 39E

**Type locality.** Thailand, Chiang Mai Province, Mae Chaem District, Tha Pha, 18°30'46"N, 98°25'25"E, alt. 720 m.

**Type material.** *Holotype* (THNHM): ♂, “THAI: Chiang Mai Mae Chaem Dist., Tha Pha St. 166 (alt. 720 m) 15.VIII.2020” [printed white label] \ “HOLOTYPE *Microdytes jeenthongi* sp. nov. Okada & Wewalka 2022 [printed red label]”. *Paratypes* (3 exs.): 2♂♂, same data as the holotype (CGW, NMW); 1♂, same locality, 4.VII.2020, R Okada leg (CRO). All paratypes are provided with printed red paratype labels.

**Diagnosis.** *Microdytes jeenthongi* sp. nov. resembles *M. shunichii* Satō, 1995 (Fig. 36) and *M. zetteli* Wewalka, 1997 (Fig. 37) in habitus, coloration and very finely punctured metasternum and metacoxae. From *M. shunichii* it differs by the reddish brown pronotum and very finely and sparsely punctured elytra. From *M. zetteli* it can be distinguished by larger size, less finely and sparsely punctured head.

**Description. Measurements.** TL = 1.77–1.82 mm (1.79 mm), TL-H = 1.23–1.26 mm (1.26 mm), MW = 1.18–1.23 mm (1.23 mm), TL/MW = 1.46–1.50 (1.49). Body regularly oval, moderately convex (Fig. 3).

**Coloration.** Head reddish brown. Pronotum reddish brown, along the anterior margin narrowly and along the posterior margin more widely dark brown, especially medially. Elytron dark brown with a distinct transverse band at the base not reaching suture, continuing along the margin to a post-median transverse band and a triangular spot near the apex, and a small round post-median spot near suture (Figs 3, 8). Ventral surface of head and prothorax yellowish brown; thorax, abdominal ventrites and elytral epipleuron reddish brown to dark brown. Legs, antennae and palpi yellowish brown.

**Sculpture and structure.** Head finely and sparsely, slightly irregularly punctured; anterior fourth finely microreticulate; clypeus not bordered. Pronotum punctured moderately irregularly, finely, and sparsely, very coarsely along posterior margin; without microreticulation; lateral margins finely bordered, regularly rounded. Elytron very sparsely and finely punctured, progressively finer and sparser towards lateral margin; one longitudinal row of punctures distinct; highly polished and shining; without microreticulation. Ventral surface: metasternum and metacoxae very finely, sparsely, and irregularly punctured; abdomen almost without punctures; without microreticulation.

**Male.** The two parts of the median lobe expanded and pointed at apex forming the unique arrowhead shape in ventral aspect (Fig. 13A); almost straight and slightly expanded downwards at apex in lateral aspect (Fig. 13B). Parameres moderate triangular in lateral aspect (Figs 13C, D).

**Female.** Unknown.

**Variation.** Variation of markings is shown in Fig. 8.

**Etymology.** This species is dedicated to Tadsanai Jeenthong, collection manager of National Science Museum, Thailand. The species epithet is a name in the genitive singular.



**Figures 2–6.** Habitus of **2** *Microdytes eliasi* sp. nov., female, paratype **3** *M. jeenthongi* sp. nov., male, holotype **4** *M. maximiliani* sp. nov., male, holotype **5** *M. sekaensis* sp. nov., male, holotype **6** *M. ubonensis* sp. nov., male, holotype. Scale bar: 1.0 mm.

**Habitat.** This species was collected in a small, shallow stream with gravel bottom flowing through a small valley. In this stream, specimens were collected from a restricted point where tree roots were exposed along the river bottom (Fig. 46).

**Distribution.** Thailand: Chiang Mai Province.

***Microdytes maximiliani* Wewalka & Okada, sp. nov.**

<https://zoobank.org/E1377AC3-9A63-4D0A-BEEF-FEEFA69E26F3>

Figs 4, 9, 14, 38

**Type locality.** Laos, Louang Namtha Province, 10 km E Muang Sing, 21°09–10'N, 101°13–15'E, alt. 750–1400 m.

**Type material.** *Holotype* (NMB): ♂, “LAOS, Louang Namtha prov., 10 km E Muang Sing, 750–1400 m, Ban Oudonsinh B. Nam Det \ B. Nam Mai, 21°09–10'N \ 101°13–15'E, 14.–20.V.2011” \ “NHMB Basel Laos 2011 Expedition D. Hauk & M. Geiser” [printed white labels] \ “HOLOTYPUS *Microdytes maximiliani* sp. nov. Wewalka & Okada 2022” [printed red label]. *Paratypes* (4 exs.): 2♂♂, 1♀, with same data as the holotype (CGW, NMB, NMP); 1♀, CHINA: Yunnan, Xishuangbanna, ca. 10 km NW Menglun, ca. 700–800 m, 7.XI.1999, M. Jäch et al. (CWBS 360) (NMW). All paratypes are provided with printed red paratype labels.

**Diagnosis.** *Microdytes maximiliani* sp. nov. resembles *M. satoi* Wewalka, 1997 in coloration of pronotum and elytra but differs from this species by darker head, larger size, a distinct impression on lateral side in anterior third of elytron (Fig. 38) and male genitalia. It is similar to *M. paoloi* Wewalka, 2011 in size and coloration of pronotum but can be distinguished by elytral markings, the impression on lateral side of elytron and male genitalia. The shape of median lobe of aedeagus of *M. maximiliani* is very similar to that of *M. schoenmanni* Wewalka, 1997, but this species is much smaller and differs in coloration, punctuation and a missing impression on lateral side of elytron.

**Description. Measurements.** TL = 1.60–2.00 mm (1.86 mm), TL-h = 1.40–1.80 mm (1.61 mm), MW = 1.30–1.35 mm (1.30 mm), TL/MW = 1.23–1.43 (1.43). Body broad and regularly oval, quite convex (Figs 4, 38).

**Coloration.** Head dark reddish brown, darker on vertex and along eyes. Pronotum dark brown. Elytron dark brown with yellowish brown markings forming a distinct transverse band near base not reaching suture and lateral margin, a post-median lateral spot often connected with a triangular spot near apex (Figs 4, 9). Elytral epipleuron and ventral surface dark brown to black. Legs, antennae and palpi reddish brown.

**Sculpture and structure.** Head finely and sparsely punctured, stronger punctures along eyes and on vertex; with fine microreticulation missing on vertex; clypeus not bordered. Pronotum irregularly punctured with sparse fine punctures and strong punctures concentrated along posterior margin and sparsely on disc; without microreticulation; lateral margins finely bordered, scarcely rounded. Elytron quite regularly, moderately densely and fairly strongly punctured, with traces of two longitudinal rows of punctures; highly polished and shining; without microreticulation; with a distinct impression on lateral side in anterior third (Fig. 38). Ventral surface: metacoxae, metasternum and abdomen moderately strongly but very sparsely punctured; without microreticulation.

**Male.** Median lobe of aedeagus in ventral aspect slightly tapered from base to apex, expanded before apex, apex truncate (Fig. 14A); in lateral aspect straight, tapered in apical ninth, apex bent downwards (Fig. 14B). Parameres narrow triangular in lateral aspect (Fig. 14C, D).

**Female.** Without secondary sexual characters. Sclerotized spermatheca not found.

**Variation.** Variation of markings is shown in Fig. 9.

**Etymology.** This species is dedicated to Maximilian Bramböck, Vienna, Austria. The species epithet is a name in the genitive singular.

**Habitat.** The species was collected in Yunnan in a 1–2-m wide stream flowing through dense primary forest (Jäch and Ji 2003).

**Distribution.** Laos: Louang Namtha Province; China: Yunnan Province.

***Microdytes sekaensis* Okada & Wewalka, sp. nov.**

<https://zoobank.org/FC40E421-E223-493B-A4C8-9F9B94978DE2>

Figs 5, 10, 15

**Type locality.** Thailand, Bueng Kan Province, Seka District, Ban Tong, 18°08'16"N, 103°59'35"E, alt. 190 m.

**Type material.** *Holotype* (THNHM): ♂, “THAI: Bueng Kan Seka Dist., Ban Tong St. 206 (alt. 190 m) 28.XII.2020 R. Okada leg. \ HOLOTYPE *Microdytes sekaensis* sp. nov. Okada & Wewalka 2022” [printed red label]. *Paratypes* (37 exs.): 1♂, with same data as the holotype (CGW); 36 exs., Laos, Bolikhamsay Province, Nam Kading NPA, Tad Paloy campsite, 18°21–23'N, 104°09'E, alt. 250–400 m, 24.–28.V.2011, NHMB Basel Laos 2011 Expedition, M. Geiser, D. Hauk, A. Phantala & E. Vongphachan leg. (CGW, CRO, NMB, NMP). All paratypes are provided with printed red paratype labels.

**Diagnosis.** *Microdytes sekaensis* sp. nov. resembles *M. hainanensis* Wewalka, 1997 and *M. schwendingeri* Wewalka, 1997 (Figs 34, 40B) in habitus and size but differs by elytral markings and clypeus not bordered. Size and coloration of *M. sekaensis* sp. nov. is also similar to those of *M. gabrielae* Wewalka, 1997 (Fig. 23), but it is distinguishable from the latter by the more rounded-oval body and finely and sparsely punctured ventral surface.

**Description. Measurements.** TL = 1.34–1.36 mm (1.36 mm), TL-h = 0.92–0.93 mm (0.93 mm), MW = 0.99–1.01 mm (1.01 mm), TL/MW = 1.35–1.36 (1.35). Body broadly oval, strongly convex (Fig. 5).

**Coloration.** Head yellowish brown. Pronotum yellowish brown, along posterior margin narrowly dark brown. Elytron reddish brown to dark brown with two yellowish brown spots: one basal spot not reaching base, one anterior lateral spot continuing along the lateral margin to a post-median lateral spot and a transverse spot near apex, also with a round median spot near suture (Figs 5, 10). Ventral surface predominantly yellowish brown. Legs, antennae and palpi yellowish brown.

**Sculpture and structure.** Head very finely and sparsely, slightly irregularly punctured; entirely and distinctly microreticulate; clypeus not bordered. Pronotum quite irregularly, finely, and sparsely punctured on the disc, additionally with coarser punctures at medial part of posterior margin; without microreticulation; lateral margins finely bordered, regularly rounded. Elytron fairly finely, regularly, and moderately densely punctured, progressively finer and sparser towards lateral margin; two longitudinal rows of

punctures moderately distinct; highly polished and shining; without microreticulation. Ventral surface: metacoxae and metasternum finely and sparsely punctured, epipleura and abdomen almost without punctures; without microreticulation.

**Male.** Median lobe of aedeagus in ventral aspect slightly tapered from base to apex and narrowly constricted before apex, apex spoon shaped (Fig. 15A); in lateral aspect slightly curved with an arrowhead shaped apical expansion (Fig. 15B). Paramere narrowly trapezoid in lateral aspect (Fig. 15C, D).

**Female.** Without secondary sexual characters. Sclerotized spermatheca not found.

**Variation.** Variation of markings is shown in Fig. 10.

**Etymology.** This species is named after the district name of the type locality.

**Habitat.** This species was collected in the remaining water pools in a dried-up stream which had a sandy bottom with rich leaf deposits (Fig. 47).

**Distribution.** Thailand: Bueng Kan Province; Laos: Bolikhamxay Province.

***Microdytes ubonensis* Okada & Wewalka, sp. nov.**

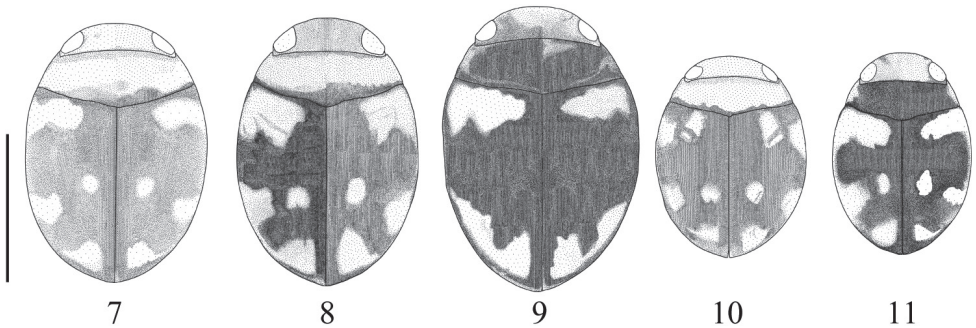
<https://zoobank.org/007C27AC-BD23-48EE-9659-05448237A6EE>

Figs 6, 11, 16, 40A

**Type locality.** Thailand, Ubon Ratchathani Province, Si Mueang Mai Dist., Nam Thaeng, 15°32'19"N, 105°24'08"E, alt. 200 m.

**Type material. Holotype** (THNHM): ♂, “THAI: Ubon Ratchathani Si Mueang Mai Dist., Nam Thaeng St. 242 (alt. 200 m) 23.V.2021 R. Okada leg.” [printed white label] / HOLOTYPE *Microdytes ubonensis* sp. nov. Okada & Wewalka 2022” [printed red label]. **Paratypes** (52 exs.): 3♂♂, 1♀, with same data as the holotype (CGW, CRO); 4♀♀, Thailand, Ubon Ratchathani Province, Nam Yuen Dist., Dom Pradit St. 221 (alt. 190 m), 14.402°N, 104.215°E, 26.II.2021 R Okada leg. (THNHM); 4♂♂, 4♀♀, Thailand, Ubon Ratchathani Province, Nam Yuen District, Dom Pradit St. 240 (alt. 260 m), 14°23'22"N, 105°09'25"E, 22.V.2021, R. Okada leg. (CRO); 18 exs., Laos, Savannakhet Province, Phou Xang He NBCA, ca. 5 km SW Ban Pa Phaknau, 17°00'N, 105°38'E, alt. 250–400 m, 31.V.–6.VI. 2011, NHMB Basel, Laos 2011 Expedition, M. Brancucci, M. Geiser, D. Hauk, Z. Kraus, A. Phantala & E. Vongphachan leg. (CGW, NMB, NMP); 1♂, Laos, Champasak Province, Bolavens Plateau, waterfall ca. 2 km E Tad Katamtok, 15°08.1'N, 106°38.8'E, alt. 415 m, 10.–12.V.2010, J. Hájek leg. (NMP); 15 exs., Laos, Champasak Province, Bolavens Plateau, ca. 1 km S Ban Lak 40 [vill.] Tad Yueang waterfall, 15°10.8'N, 106°08.3'E, alt. 900–970 m, 28.IV.2010, J. Hájek leg. (CGW, CRO, NMP); 1♂, Laos, Vientiane Province, Phou Khao Khouay NBCA ca. 46 km N Vientiane (waterfall), 18°22.4'N, 102°42.4'E, alt. 270 m, 18.V.2010, J. Hájek leg. (NMP); 1♀, Laos, Vientiane Province, 90 km E Vientiane, Phou Khao Khouay NP, Nam Leuk, 1.–8.VI.1996, H. Schillhammer leg (NMW). All paratypes are provided with printed red paratype labels.

**Diagnosis.** *Microdytes ubonensis* sp. nov. is similar to *M. boukali* Wewalka, 1997 and *M. lotteae* Wewalka, 1998 in habitus, size, and pronotal coloration but differs from these species by having yellowish head and the elytral markings with distinct post-me-



**Figures 7–11.** Variation of markings of **7** *Microdytes eliasi* sp. nov. **8** *M. jeenthongi* sp. nov. **9** *M. maximiliani* sp. nov. **10** *M. sekaensis* sp. nov. **11** *M. ubonensis* sp. nov. Scale bar: 1.0 mm.

dian spot near suture and finely and sparsely punctured ventral surface. *M. ubonensis* sp. nov. also resembles *M. huangyongensis* Bian et al., 2015 in habitus and coloration but it differs in size and male genitalia.

**Description. Measurements.** TL = 1.25–1.40 mm (1.37 mm), TL-h = 1.08–1.19 mm (1.18 mm), MW = 0.87–0.95 mm (0.95 mm), TL/MW = 1.42–1.47 (1.44). Body regularly oval, moderately convex (Fig. 6).

**Coloration.** Head yellowish brown. Pronotum dark brown, indistinctly yellowish brown at lateral sides. Elytron dark brown with yellowish brown markings forming a distinct transverse band at base not reaching suture, with a post-median lateral spot and a triangular spot near apex and often with a distinct longitudinal post-median spot near suture (Figs 6, 11). Ventral surface of head and prothorax yellowish brown; thorax, abdominal ventrites and elytral epipleuron reddish brown to dark brown. Legs, antennae and palpi yellowish brown.

**Sculpture and structure.** Head finely, sparsely, and relatively regularly punctured; almost entirely microreticulate; clypeus not bordered (Fig. 40A). Pronotum quite regularly, sparsely, and fairly strongly punctured, coarser punctures along the posterior margin; without microreticulation; lateral margins very finely bordered, regularly rounded. Elytron moderately regularly and densely punctured, progressively finer and sparser towards lateral margin; longitudinal rows of stronger punctures not distinct; highly polished and shining; without microreticulation. Ventral surface: metacoxae and metasternum finely and sparsely punctured, abdomen without punctures; without microreticulation.

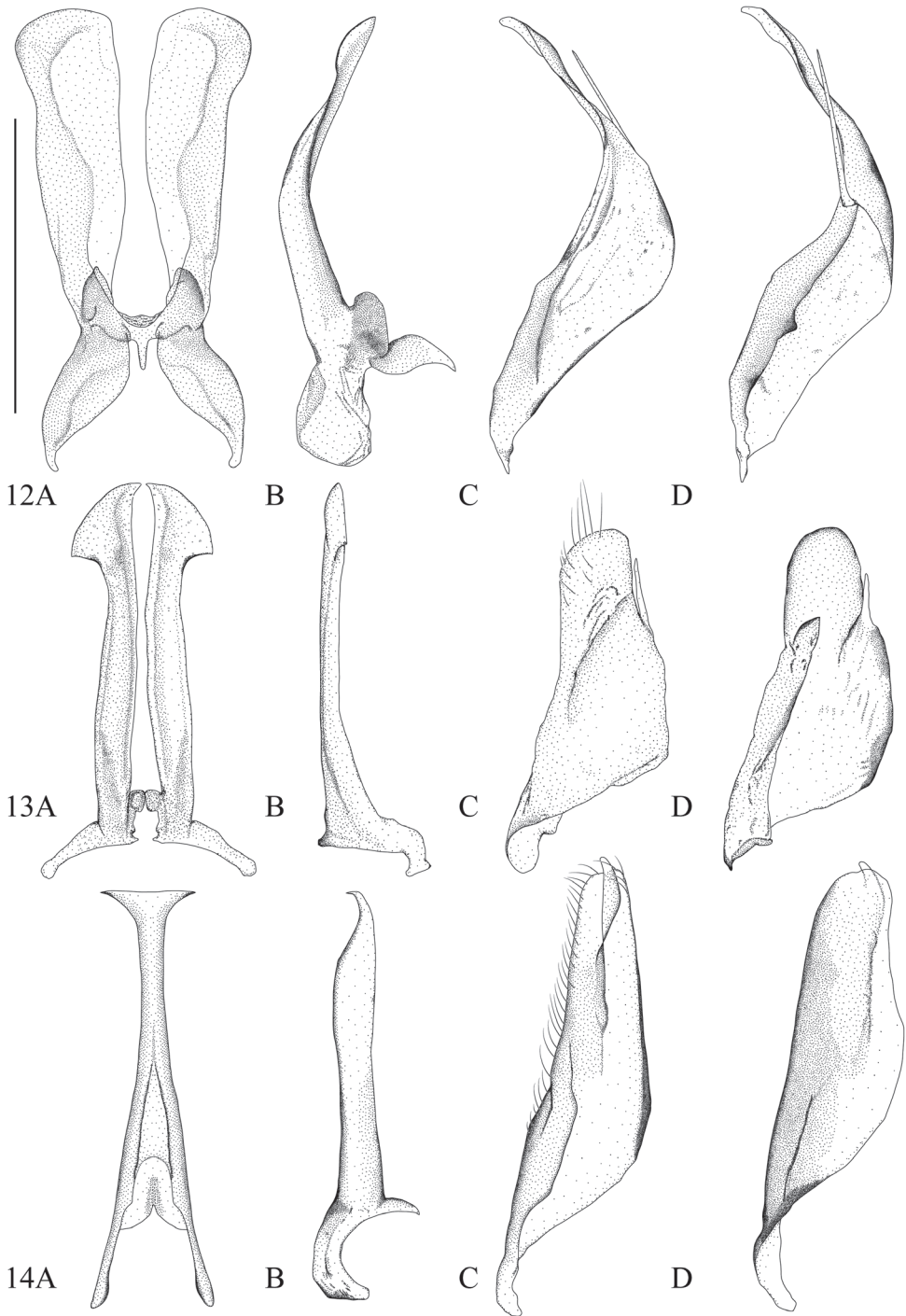
**Male.** Median lobe of aedeagus in ventral aspect equally tapered from base to apex, with a small swelling at apex (Fig. 16A); in lateral aspect tapered from base to apex, with a small ventral hook at apex (Fig. 16B). Paramere narrow triangular in lateral aspect (Fig. 16C, D).

**Female.** Without secondary sexual characters. Sclerotized spermatheca not found.

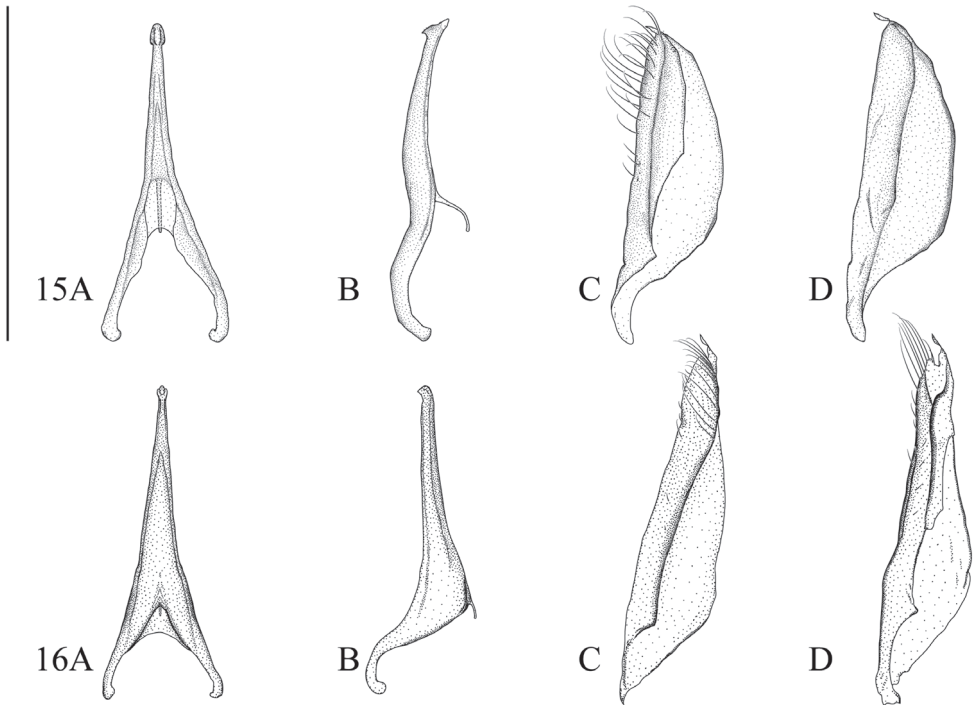
**Variation.** Variation of markings is shown in Fig. 11.

**Etymology.** This species is named after the popular provincial name of the type locality.

**Habitat.** This species was collected in a variety of habitats. At the type locality, specimens were collected from a small stream on a more or less deforested bedrock



**Figures 12–14.** **12** *Microdytes eliasi* sp. nov. **13** *M. jeenthongi* sp. nov. **14** *M. maximiliani* sp. nov. **A** median lobe in ventral aspect **B** median lobe in lateral aspect **C** left paramere in lateral aspect **D** right paramere in medial aspect. Scale bar: 0.25 mm.



**Figures 15, 16.** 15 *Microdytes sekaensis* sp. nov. 16 *M. ubonensis* sp. nov. **A** median lobe in ventral aspect **B** median lobe in lateral aspect **C** left paramere in lateral aspect **D** right paramere in medial aspect. Scale bar: 0.25 mm.

(Fig. 48). At other localities, specimens were collected in small pit holes near small forest streams with rich leaf deposits.

**Distribution.** Thailand: Ubon Ratchathani Province; Laos: Savannakhet, Champasak, and Vientiane provinces.

### New faunistic records from Thailand, Laos, and Cambodia

#### *Microdytes akitai* Wewalka, 1997

Fig. 18

*Microdytes akitai* Wewalka, 1997: 17; Wewalka 2011: 37; Nilsson and Hájek 2023: 211.

**Type locality.** Laos, Vientiane Province, Mt. Phou Khao Khouay.

**Material examined.** Laos: Bolikhamsay Province. 22 exs., Nam Khading National Bio-Diversity Conservation Area, Tad Paloy campsite, 18°23.17'N, 104°09.65'E, alt. 300 m, forest stream, 8.–11.VII.2010 & 24.–28.V.2011, NHMB Basel Laos 2010 & 2011 Expeditions, M. Brancucci, M. Geiser, D. Hauk, A. Phantala & E. Vongphachan leg. (CGW, CRO, NMB, NMP) (Fig. 18).

**Comments.** Specimens from Bolikhamsay have more distinct elytral markings and darker head color than in the specimens from the type locality but no other differences have been observed, in particular, in the male genitalia.

**Distribution.** Laos: Vientiane and Bolikhamsay (first record) provinces.

***Microdytes balkei* Wewalka, 1997**

Figs 17, 19, 39D

*Microdytes balkei* Wewalka, 1997: 18; Wewalka 2011: 29; Nilsson and Hájek 2023: 211.

**Type locality.** Thailand, Rayong Province, Khao Chamao NP.

**Material examined.** THAILAND: Mukdahan Province. 1♂, Phu Pha Thoep N.P., small pools (23), 1.I.2000, Mazzoldi leg. (CGW); Ubon Ratchathani Province. 1♂, 1♀, Nam Yuen District, Dom Pradit St. 240 (alt. 260 m), 22.V.2021, R. Okada leg. (CRO, THNHM); Saraburi Province. 1♀, Kaeng Khoi District, Ched Khot St. 122 (alt. 140 m), 30.V.2020, R. Okada leg. (CRO); Chonburi Province. 2♂♂, 1♀, Ban Bueng District, Khlong Kiu St. 261 (alt. 200 m), 6.XI.2021, R. Okada leg. (CGW, CRO) (Fig. 17); 2♂♂, 1♀, Si Racha District, Bang Phra St. 269 (alt. 90 m), 26.XII.2021, R. Okada leg. (CRO); Rayong Province. 4♂♂, Wang Chan District, Pa Yup Nai St 299 (alt. 200 m), 17.VII.2022, R. Okada leg. (CRO, THNHM).

LAOS: Savannakhet Province. 203 exs., Phou Xang He NBCA, ca. 5 km SW Ban Pa Phaknau, 17°00'N, 105°38'E, alt. 250–400 m, 31.V.–6.VI. 2011, NHMB Basel, Laos 2011 Expedition, M. Brancucci, M. Geiser, D. Hauk, Z. Kraus, A. Phantala & E. Vongphachan leg. (CGW, CRO, NMB, NMP); Sekong Province. 3♀♀, ca. 51 km N Sekong (river) Ho Chi Minh trail, 15°49.6'N, 106°39.8'E, alt. 410 m, 14.–15.V.2010, J. Hájek leg. (NMP).

CAMBODIA: Koh Hong Province. 12 exs., 20 km SW Koh Hong, Tatai River, 11°34'N, 103°07'E, alt. 50–300 m, 3.–19.V.2005, E. Jendek & O. Šauša leg. (CGW, NMB).

**Comments.** Since the figure of the median lobe of this species was not depicted clearly in Wewalka (1997), we present a new figure of the aedeagus including parameres (Fig. 17).

**Distribution.** Thailand: Mukdahan, Rayong, Trat, Ubon Ratchathani (first record), Saraburi (first record), and Chonburi (first record) provinces, Khao Yai NP [Nakhon Ratchasima or Nakhon Nayok Province]; Laos (first record): Savannakhet and Sekong provinces; Cambodia (first record): Koh Hong Province.

***Microdytes dimorphus* Wewalka, 1997**

Fig. 20

*Microdytes dimorphus* Wewalka, 1997: 22; Wewalka 2011: 37; Nilsson and Hájek 2023: 211.

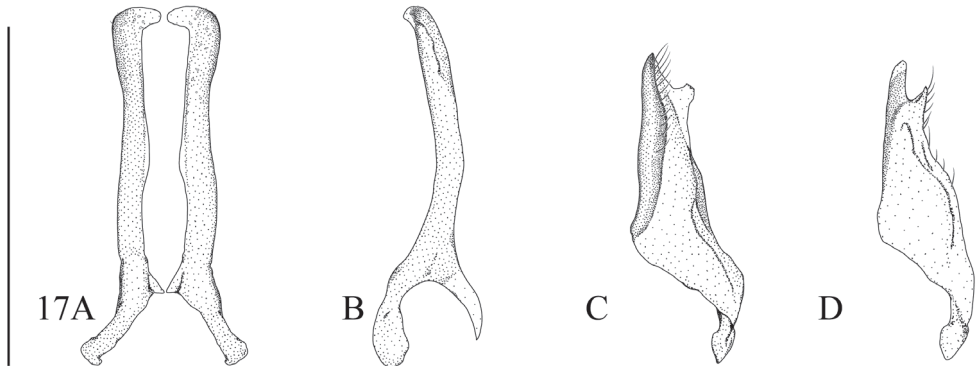


**Figure 17.** *Microdytes balkei* **A** median lobe in ventral aspect **B** median lobe in lateral aspect **C** left paramere in lateral aspect **D** right paramere in medial aspect. Scale bar: 0.25 mm.

**Type locality.** Thailand, Nakhon Ratchasima or Nakhon Nayok Province, Khao Yai NP.

**Material examined.** THAILAND: Chonburi Province. 1♂, Si Racha District, Bang Phra St. 269 (alt. 90 m), 26.XII.2020, R. Okada leg. (CRO) (Fig. 20).

**Comments.** *Microdytes dimorphus* was described based on a single male specimen from Khao Yai National Park and no additional records are known so far. Therefore, this is the second record of this species. Wewalka (1997) suggested *M. dimorphus* is more closely related to *M. menopausis* Wewalka, 1997 (Fig. 27) but differs by having coarser punctures on the elytra similar in size, a punctured abdomen, a more produced clypeus, and larger second segment of antennae. The specimen examined in this study corresponds with *M. dimorphus* due to the status of punctures on the elytra and abdomen, although the characteristics of clypeus and antenna are intermediate between *M. dimorphus* and *M. menopausis*. This species can be distinguished from *M. menopausis* in having a more slender body shape and indistinct elytral markings at both shoulders and post-median part (Fig. 20).

**Distribution.** Thailand: Khao Yai NP [Nakhon Ratchasima or Nakhon Nayok Province] and Chonburi (first record) Province.

### *Microdytes franzi* Wewalka & Wang, 1998

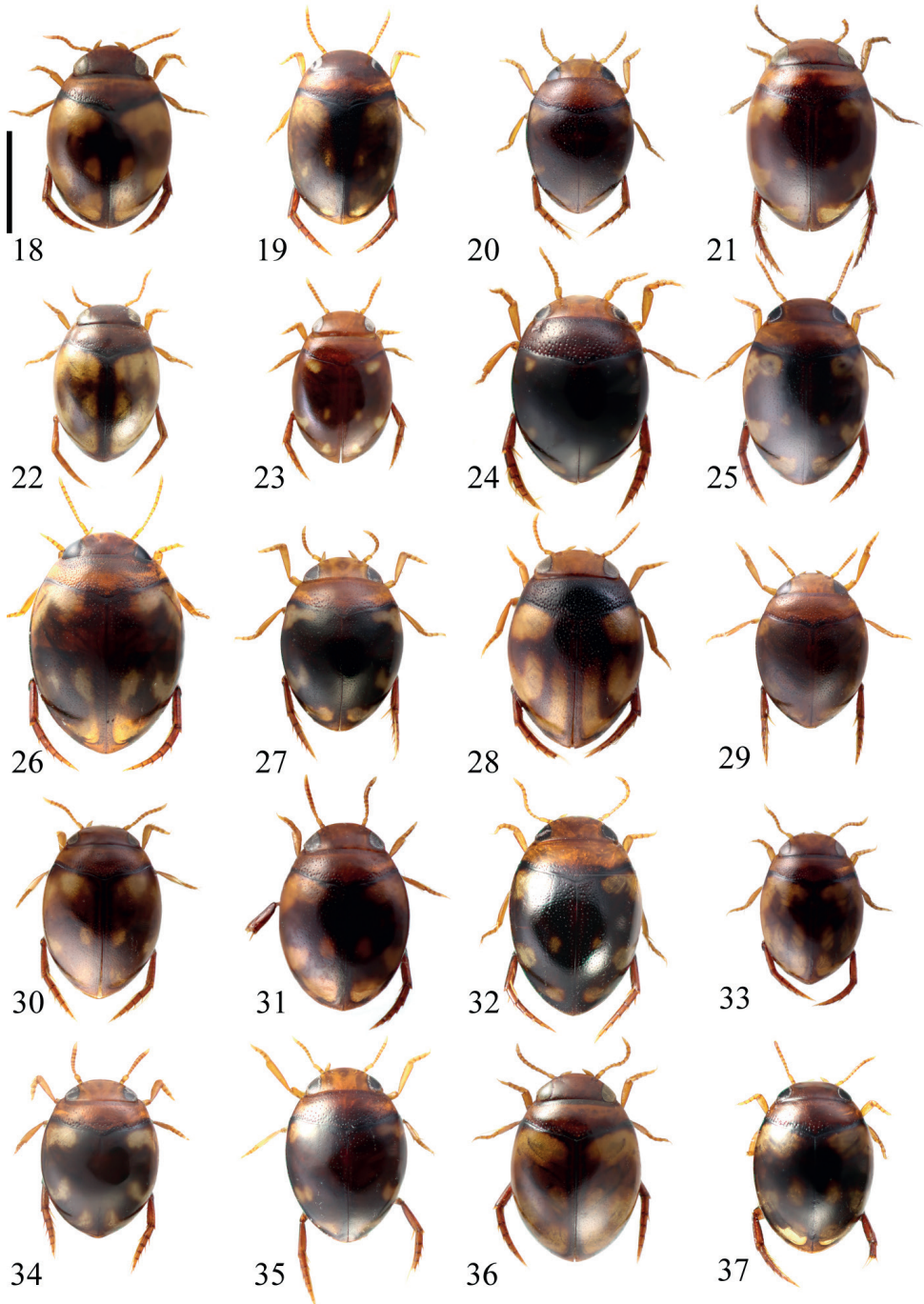
Fig. 22

*Microdytes franzi* Wewalka & Wang, 1998: 65; Wewalka 2011: 38; Nilsson and Hájek 2023: 211.

**Type locality.** Laos, Vientiane Province, Mt. Phou Khao Khouay.

**Material examined.** LAOS: Bolikhamsay Province. 20 exs., Nam Khading National Bio-Diversity Conservation Area, Tad Paloy campsite, 18°23.17'N, 104°09.65'E, alt. 300 m, forest stream, 8.–11.VII.2010 & 24.–28.V.2011, NHMB Basel Laos 2010 & 2011 Expeditions, M. Brancucci, M. Geiser, D. Hauk, A. Phantala & E. Vongphachan leg. (CGW, CRO, NMB, NMP) (Fig. 22).

**Distribution.** Laos: Vientiane and Bolikhamsay (first record) provinces.



**Figures 18–37.** Habitus of **18** *Microdytes akitai* **19** *M. balkei* **20** *M. dimorphus* **21** *M. feryi* (paratype, from Myanmar) **22** *M. franzi* **23** *M. gabrielae* **24** *M. heineri* **25** *M. maculatus* **26** *M. mariannae* **27** *M. menopausis* **28** *M. paoloi* **29** *M. pasiricus* **30** *M. pederzani* **31** *M. rocchii* **32** *M. schoedli* **33** *M. schoenmanni* (from Myanmar) **34** *M. schwendingeri* **35** *M. shepardi* **36** *M. shunichii* **37** *M. zetteli*. Scale bar: 1.0 mm.

***Microdytes gabrielae* Wewalka, 1997**

Fig. 23

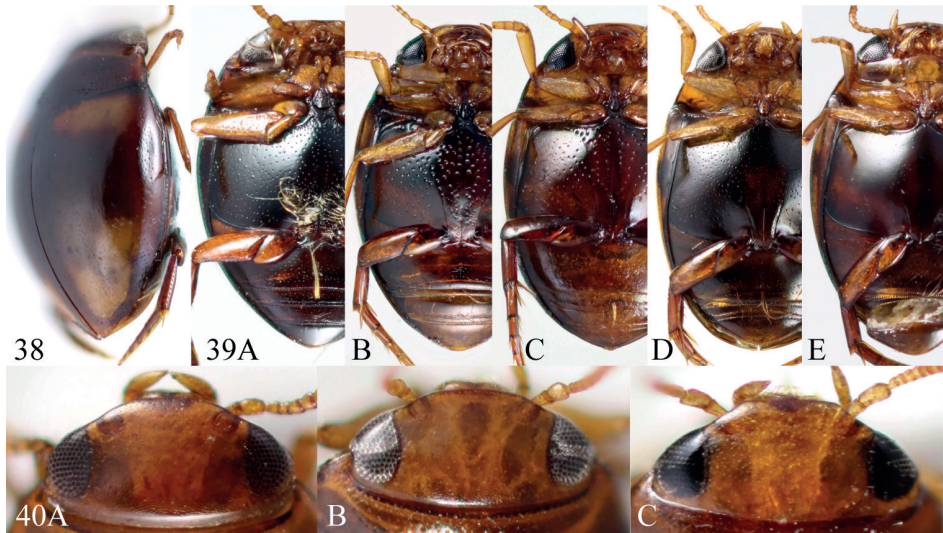
*Microdytes gabrielae* Wewalka, 1997: 24; Wewalka 2011: 29; Nilsson and Hájek 2023: 211.**Type locality.** Thailand, Phetchabun Province, Huai Nam Phang.**Material examined.** THAILAND: Phetchabun Province. 1♂, Phu Hin Rongkla NP, small stream (7), 25.XII.1999, Mazzoldi leg. (CGW) (Fig. 23); 4♂♂, 3♀♀, Lom Kao District, Ban Noen St. 294 (alt. 1620 m), 18.VI.2022, R. Okada leg. (CGW, CRO, THNHM); Phitsanulok Province. 1♂, Nakhon Thai Distr., Phu Hin Rong Kla NP, in waterfall, 16°59'49.1"N, 101°00'34.8"E, 7.III.2016, A. Damaška leg. (NMP).**Distribution.** Thailand: Phetchabun and Phitsanulok provinces.***Microdytes heineri* Wewalka, 2011**

Figs 24, 39A

*Microdytes heineri* Wewalka, 2011: 23; Nilsson and Hájek 2023: 211.**Type locality.** China, Yunnan Province, Simao Prefecture.**Material examined.** THAILAND: Chiang Mai Province. 8 exs., Mae Taeng District, Pa Pae St. 49 (alt. 1000 m), 15.VI.2019, R. Okada leg. (CGW, CRO, THNHM); 1♂, same district, Kuet Chang St. 170 (alt. 520 m), 16.VIII.2020, R. Okada leg. (CRO) (Fig. 24).**Comments.** Male specimens have distinct setae on the metacoxae (Fig. 39A).**Distribution.** Thailand: Nan and Chiang Mai (first record) provinces; Laos: Luang Namtha and Luang Prabang provinces; China: Yunnan Province.***Microdytes maculatus* (Motschulsky, 1860)**

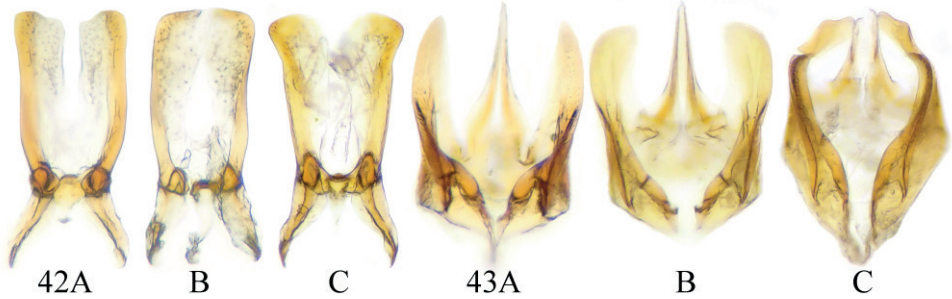
Figs 25, 39C, 41

*Hydrovatus maculatus* Motschulsky, 1860: 42; Sharp 1882: 814, 973; Régimbart 1899: 231; Zaitzev 1915: 293; Zimmermann 1920: 34.*Desmopachria maculatus*: Gschwendtner 1936: 367; Balfour-Browne 1946: 106 (uncertain assignment).*Microdytes maculatus*: Vazirani 1969: 301; Vazirani 1977: 24; Satô 1981: 68; Wewalka 1997: 27; Biström et al. 1997: 75; Miller and Wewalka 2010: 35; Wewalka 2011: 29; Nilsson and Hájek 2023: 211.**Type locality.** “Ind or”, “Dohen [a place with this name exists in Pakistan, Jammu and Kashmir Province, but it is very unlikely that this is the type locality]”.**Material examined.** THAILAND: Chiang Mai Province. 6♂♂, 1♀, Chom Thong District, Ban Luang St. 165 (alt. 360 m), 15.VIII.2020, R. Okada leg. (CGW, CRO)



**Figures 38–40.** Diagnostic characters of *Microdytes* species. **38** Impression of lateral side (*M. maxmilianii* sp. nov.) **39** ventral surface **A** with setae (*M. heinerti*) **B** with very coarse punctures (*M. schoedli*) **C** with coarse punctures (*M. maculatus*) **D** with fine punctures (*M. balkei*) **E** with very fine punctures (*M. jeenthongi* sp. nov.) **40** clypeus bead **A** not bordered (*M. ubonensis* sp. nov.) **B** finely bordered (*M. schwendingeri*) **C** produced (*M. dimorphus*).

(Fig. 25); 9 exs., Mae Chaem District, Tha Pha St. 166 (alt. 720 m), 15.VIII.2020, R. Okada leg. (CGW, CRO); 1♂, 1♀, Chiang Dao District, Ping Khong St. 226 (alt. 430 m), 20.III.2021, R. Okada leg. (CRO); Chiang Rai Province. 3♀♀, Wiang Kaen District, Muang Yai St. 70 (alt. 470 m), 2.VIII.2019, R. Okada leg. (CRO); Lampang Province. 5♂♂, 9♀♀, Thoen District, Mae Pa St. 197 (alt. 200 m), 15.XI.2020, R. Okada leg. (CGW, CRO); Mae Hong Son Province. 3♂♂, Pai District, Mueang Paeng St. 93 (alt. 760 m), 1.XII.2019, R. Okada leg. (CRO); 3♂♂, 2♀♀, Pha Bong, ca. 12 km S Mae Hong Son, 12.XI.1995, H. Zettel leg (CGW, NMW); Phrae Province. 1♂, 15 km E Phrae, Mae Khaem, 16.XI.1995, H. Zettel leg. (NMW); Uttaradit Province. 2♂♂, 1♀, Nam Pat District, Saen To St. 184 (alt. 210 m), 13.IX.2020, R. Okada leg. (CRO); Phetchabun Province. 1♀, Huai Nam Phang, S Ban Nam Nao, 25.XI.1995, H. Zettel leg. (NMW); Bueng Kan Province. 2♂♂, Seka District, Ban Tong St. 206 (alt. 190 m), 27.XII.2020, R. Okada leg. (CGW, CRO); Nakhon Phanom Province. 12 exs., Bang Phaeng District, Phai Lom St. 203 (alt. 200 m), 27.XII.2020, R. Okada leg. (CGW, CRO); Sakon Nakhon Province. 1♀, Charoen Sin District, Huai Yang St. 208 (alt. 320 m), 29.XII.2020, R. Okada leg. (CRO); 2♂♂, 2♀♀, Tao Ngoi District, Nan Tan St. 210 (alt. 310 m), 29.XII.2020, R. Okada leg. (CGW, CRO); Ubon Ratchathani Province. 1♂, 1♀, Si Mueang Mai District, Nam Thaeng St. 221 (alt. 190 m), 26.II.2021, R. Okada leg. (CRO); 1♂, 1♀, Nam Yuen District, Dom Pradit St. 224 (alt. 190 m), 27.II.2021, R. Okada leg. (CRO); Kanchanaburi Province. 1♂, Si Sawat District, Na Suan St. 28 (alt. 310 m), 12.I.2019, R. Okada leg. (CRO).



**Figures 41–43.** 41 Lectotype of *Microdytes maculatus* (photograph by Christophe Rivier, Muséum national d'histoire naturelle, Paris) 42 median lobe of **A** *M. maculatus* from northern Thailand **B** from northeastern Thailand **C** *M. eliasi* sp. nov. 43 paramere of **A** *M. maculatus* from northern Thailand **B** from northeastern Thailand **C** *M. eliasi* sp. nov.

Laos: Luang Prabang Province. 4 exs., Thong Khan, 19°35'N, 101°58'E, alt. ca. 750 m, 11–12.V.2002, V. Kubáň leg. (CGW, NMB).

**Comments.** The lectotype of *Microdytes maculatus* (Fig. 41) has a rhomboid-like habitus similar to that of most specimens from Myanmar, northern Thailand, and China, while most specimens from northeastern Thailand and Laos have a more regularly rounded habitus, but this is not a discriminant character.

There is also a geographic variation in the shapes of the median lobe and the apical part of the parameres. In specimens from Myanmar, northern Thailand, and China, the two parts of the median lobe have obtuse apical medial angles (Fig. 42A), and the parameres have narrow tips (Fig. 43A), while in those of northeastern Thailand and western Laos the two parts of the median lobe have almost right apical medial angles (Fig. 42B) and the parameres have rounded tips (Fig. 43B). Because some specimens show an intermediate status and no other distinguishing character can be found, they

are treated as geographic variations belonging to the same species. Molecular biological studies are required to establish if they are different species within a complex.

**Distribution.** India: southern Andaman Islands; Myanmar: Chin and Shan states, Saganing Division; Thailand: Chiang Mai, Chiang Rai (first record), Lampang (first record), Lamphun, Mae Hong Son, Uttaradit (first record), Phetchabun (first record), Bueng Kan (first record), Mukdahan, Nakhon Phanom (first record), Sakon Nakhon (first record), Ubon Ratchathani (first record), and Kantchanaburi provinces, Khao Yai NP [Nakhon Ratchasima or Nakhon Nayok Province]; Laos: Vientiane, Luang Prabang (first record) and Khammouan provinces; China: Yunnan Province.

***Microdytes mariannae* Wewalka, 1997**

Fig. 26

*Microdytes mariannae* Wewalka, 1997: 28; Wewalka 2011: 30; Nilsson and Hájek 2023: 211.

**Type locality.** Thailand, Phetchabun Province, Nam Nao.

**Material examined.** THAILAND: Phetchabun Province. 8♂♂, 10♀♀, Lom Kao District, Ban Noen St. 187 (alt. 1620 m), 20.IX.2020, R. Okada leg. (CGW, CRO, THNHM) (Fig. 26); 2♂♂, 2♀♀, same locality, St. 294, 18.VI.2022, R. Okada Leg. (CRO, THNHM).

**Distribution.** Thailand: Phetchabun and Loei provinces.

***Microdytes menopausis* Wewalka, 1997**

Fig. 27

*Microdytes menopausis* Wewalka, 1997: 29; Wewalka 2011: 30; Nilsson and Hájek 2023: 211.

**Type locality.** Thailand, Khao Yai NP.

**Material examined.** THAILAND: Nakhon Phanom Province. 1♂, 2♀♀, Bang Phaeng District, Phai Lom St. 203 (alt. 200 m), 27.XII.2020, R. Okada leg. (CGW, CRO); Sakon Nakhon Province. 1♀, Tao Ngoi District, Nan Tan St. 210 (alt. 310 m), 29.XII.2020, R. Okada leg. (CRO) (Fig. 27); Ubon Ratchathani Province. 1♀, Nam Yuen District, Dom Pradit St. 224 (alt. 190 m), 27.II.2021, R. Okada leg. (CGW); 1♂, Si Mueang Mai District, Nam Thaeng St. 241 (alt. 190 m), 23.V.2021, R. Okada leg. (THNHM).

LAOS: Khammouan Province. 1♂, Nakai-Nam Theun NPA, Ban Navang env., 17°57–59'N, 105°13–16'E, alt. 600–750 m, 18.–21.V.2012, NHMB Basel, Laos 2012 Expedition, M. Brancucci, M. Geiser, K. Phanthavong & S. Xayalath leg. (NMB); Savannakhet Province. 3 exs., Phou Xang He NBCA, ca. 5 km SW Ban Pa Phaknau, 17°00'N, 105°38'E, alt. 250–400 m, 31.V.–6.VI. 2011, NHMB Basel, Laos

2011 Expedition, M. Brancucci, M. Geiser, D. Hauk, Z. Kraus, A. Phantala & E. Vongphachan leg. (CGW, NMB).

**Distribution.** Thailand: Trat, Nakhon Phanom (first record), Sakon Nakhon (first record), and Ubon Ratchathani (first record) provinces, Khao Yai NP [Nakhon Ratchasima or Nakhon Nayok Province]; Laos: Khammouan, Savannakhet (first record) and Sekong provinces.

***Microdytes paoloi* Wewalka, 2011**

Fig. 28

*Microdytes paoloi* Wewalka, 2011: 24; Nilsson and Hájek 2023: 211.

**Type locality.** Thailand, Phetchabun Province, Phu Hin Rongkla NP.

**Material examined.** THAILAND: Phetchabun Province. 1♂, paratype, Phu Hin Rongkla NP, small stream, alt. 1250 m (4), 25.XII.1999, Mazzoldi leg. (CMW) (Fig. 28).

**Distribution.** Thailand: Phetchabun and Loei provinces.

***Microdytes pasiricus* (Csiki, 1938)**

Fig. 29

*Hydrovatus pasiricus* Csiki, 1938: 126 (including var. *simplicor* and var. *unicolor*).

*Microdytes pasiricus*: Biström et al. 1997: 75; Wewalka 1997: 30; Wewalka 2011: 30; Freitag et. al. 2016: 185; Nilsson and Hájek 2023: 212.

**Type locality.** Indonesia, Central Java, Sarangan near Lake Pasir.

**Material examined.** THAILAND: Chiang Rai Province. 3♂♂, Wiang Kaen District, Muang Yai St. 71 (alt. 440 m), 11.VIII.2019, R. Okada leg. (CGW, CRO) (Fig. 29); Chiang Mai Province. 2♀♀, Mae Chaem District, Tha Pha St. 166 (alt. 720 m), 15.VIII.2020, R. Okada leg. (CRO, THNHM).

**Distribution.** Thailand: Chiang Rai (first record), Chiang Mai (first record) and Phetchabun provinces; Philippines: Busuanga, Luzon, Mindoro, Palawan; Singapore; Indonesia: Java.

***Microdytes pederzanii* Wewalka, 2011**

Fig. 30

*Microdytes pederzanii* Wewalka, 2011: 25; Nilsson and Hájek 2023: 212.

**Type locality.** Thailand, Phetchabun Province, Phu Hin Rongkla NP.

**Material examined.** THAILAND: Phetchabun Province. 2♀♀, Lom Kao District, Ban Noen St. 187 (alt. 1620 m), 20.IX.2020, R. Okada leg. (CRO); Uttaradit Prov-

ince. 1♂, 1♀, Nam Pad District, Phu Soi Dao NP, pine forest, 12.VII.2020, T. Jeenthong leg. (THNHM) (Fig. 30).

**Distribution.** Thailand: Phetchabun and Uttaradit (first record) provinces.

***Microdytes rocchii* Wewalka, 2011**

Fig. 31

*Microdytes rocchii* Wewalka, 2011: 26; Nilsson and Hájek 2023: 212.

**Type locality.** Laos, Khammuan Province, Ban Khoun Ngeun.

**Material examined.** LAOS: Khammouan Province. 1♀, Ban Khon Ngeun, 18°07'N, 104°29'E, alt. ca 200 m, 19.–31.V.2001, Pacholátko leg. (CGW) (Fig. 31); Savannakhet Province. 1♂, Phou Xang He NBCA, ca. 5 km SW Ban Pa Phaknau, 17°00'N, 105°38'E, alt. 250–400 m, 31.V.–6.VI. 2011, NHMB Basel, Laos 2011 Expedition, M. Brancucci, M. Geiser, D. Hauk, Z. Kraus, A. Phantala & E. Vongphachan leg. (NMB).

**Distribution.** Laos: Khammuan and Savannakhet (first record) provinces.

***Microdytes schoedli* Wewalka, 1997**

Figs 32, 39B

*Microdytes schoedli* Wewalka, 1997: 33; Wewalka 2011: 31; Nilsson and Hájek 2023: 212.

**Type locality.** Thailand, Phetchabun Province, Nam Nao NP.

**Material examined.** THAILAND: Chiang Mai Province. 2♀♀, Chiang Dao District, Ping Khong St. 226 (alt. 430 m), 20.III.2021, R. Okada leg. (CRO); Lampang Province. 1♂, 1♀, Thoen District, Mae Pa St. 197 (alt. 200 m), 15.XI.2020, R. Okada leg. (CRO); Mae Hong Son Province. 1♂, Pai District, Thung Yao St. 50 (alt. 610 m), 15.VI.2019, R. Okada leg. (CRO); 2♂♂, 2♀♀, Muang Mae Hong Son District, Pha Bong St. 250 (alt. 480 m), 13.VI.2021, R. Okada leg. (CGW, CRO) (Fig. 32); Phetchabun Province. 1♂, 2♀♀, Lom Sak District, Nam Chun St. 296 (alt. 200 m), 19.VI.2022, R. Okada leg. (CRO); Kanchanaburi Province. 2♂♂, 1♀, Si Sawat District, Khao Chot St. 27 (alt. 420 m), 12.I.2019, R. Okada leg. (CRO); 1♀, same district, Na Suan St. 28 (alt. 310 m), 12.I.2019, R. Okada leg. (CRO).

LAOS: Khammouan Province. 1♂, 2♀♀, Nakai-NamTheun NPA, Ban Navang env., 17°57–59'N, 105°13–16'E, alt. 600–750 m, 18.–21.V.2012, NHMB Basel, Laos 2012 Expedition, M. Brancucci, M. Geiser, K. Phanthavong & S. Xayalath leg. (NMB); Savannakhet Province. 1♂, Phou Xang He NBCA, ca. 5 km SW Ban Pa Phaknau, 17°00'N, 105°38'E, alt. 250–400 m, 31.V.–6.VI. 2011, NHMB Basel, Laos 2011 Expedition, M. Brancucci, M. Geiser, D. Hauk, Z. Kraus, A. Phantala & E. Vongphachan leg. (NMB).

**Distribution.** Thailand: Chiang Mai, Lampang (first record), Mae Hong Son (first record), Phetchabun, Tak, Mukdahan, and Kanchanaburi (first record) provinces; Laos: Khammouan (first record), Savannakhet (first record) and Sekong provinces.

***Microdytes schwendingeri* Wewalka, 1997**

Figs 34, 40B

*Microdytes schwendingeri* Wewalka, 1997: 36; Wewalka 2011: 37; Nilsson and Hájek 2023: 212.

**Type locality.** Thailand, Sakon Nakhon Province, Phu Pan NP.

**Material examined.** THAILAND: Nakhon Phanom Province. 1♂, 1♀, Bang Phaeng District, Phai Lom St. 203 (alt. 200 m), 27.XII.2020, R. Okada leg. (CRO, THNHM) (Fig. 34).

LAOS: Savannakhet Province, 1♀, Phou Xang He NBCA, ca. 5 km SW Ban Pa Phaknau, 17°00'N, 105°38'E, alt. 250–400 m, 31.V.–6.VI. 2011, NHMB Basel, Laos 2011 Expedition, M. Brancucci, M. Geiser, D. Hauk, Z. Kraus, A. Phantala & E. Vongphachan leg. (NMB); Champasak Province. 2♂♂, 1♀, Bolavens Plateau, waterfall ca. 2 km E Tad Katamtok, 15°08.1'N, 106°38.8'E, alt. 415 m, 10.–12.V.2010, J. Hájek leg. (CGW, NMP).

**Comments.** Some specimens from Laos have less distinct elytral markings but no other differences from typical specimens have been observed.

**Distribution.** Thailand: Nakhon Phanom (first record) and Sakon Nakhon provinces; Laos (first record): Savannakhet and Champasak provinces.

***Microdytes shepardi* Wewalka, 1997**

Fig. 35

*Microdytes shepardi* Wewalka, 1997: 37; Wewalka 2011: 33; Nilsson and Hájek 2023: 212.

**Type locality.** Thailand, Phetchabun Province, Nam Nao NP.

**Material examined.** THAILAND: Chiang Mai Province. 1♂, 1♀, Chiang Dao District, Ping Khong St. 226 (alt. 430 m), 20.III.2021, R. Okada leg. (CRO); Chiang Rai Province. 1♂, Wiang Kaen District, Muang Yai St. 71 (alt. 440 m), 2.VIII.2019, R. Okada leg. (CRO); Uthai Thani Province. 5♂♂, 2♀♀, Ban Rai District, Kaen Makrut St. 128 (alt. 440 m), 20.VI.2020, R. Okada leg. (CGW, CRO, THNHM) (Fig. 35).

LAOS: 1♂, Luang Prabang Province, Thong Khan, 19°35'N, 101°58'E, alt. ca. 750 m, 11.–12.V.2002, V. Kubáň leg. (NMB).

**Distribution.** Thailand: Chiang Mai, Chiang Rai (first record), Mae Hong Son, Phetchabun, Uthai Thani (first record), Chaiyaphum and Sakon Nakhon provinces; Laos: Luang Prabang Province; China: Yunnan Province.

***Microdytes shunichii* Satô, 1995**

Fig. 36

*Microdytes shunichii* Satô, 1995: 313; Wewalka 1997: 38; Wewalka 2011: 33; Nilsson and Hájek 2023: 212.

*Microdytes holzmanni* Wewalka & Wang, 1998: 66.

*Microdytes holzmannorum*: Nilsson 2007: 51 (as unjustified emendation of *holzmanni*).

**Type locality.** Vietnam, Vinh Phuc Province, Mt. Tam Dao.

**Material examined.** THAILAND: Phetchabun Province. 1♀, Lom Kao District, Ban Noen St. 187 (alt. 1620 m), 20.IX.2020, R. Okada leg. (CRO); 3♂♂, 2♀♀, same locality, St. 294, 18.VI.2022, R. Okada leg. (CGW, CRO, THNHM).

LAOS: Luang Namtha Province. 62 exs., 10 km E Muang Sing, Ban Oudomsinh / B. Nam Det / B. Nam Mai, 21°09–10'N, 101°13–15'E, 750–1400 m, 14.–20.V.2011, NHMB Basel, Laos 2011 Expedition, D. Hauk & M. Geiser (CGW, CRO, NMB, NMP) (Fig. 36); Luang Prabang Province. 1♂, 5 km W Ban Song Cha, 20°33–34'N, 102°14'E, 1200 m, 24.–30. IV.1999, V. Kubáň leg. (NMB); Khammouan Province. 2♂♂, Nakai-Nam Theun NPA, Ban Navang env., 17°57–59'N, 105°13–16'E, alt. 600–750 m, 18.–21.V.2012, NHMB Basel, Laos 2012 Expedition, M. Brancucci, M. Geiser, K. Phanthavong & S. Xayalath leg. (NMB); Savannakhet Province. 1♀, Phou Xang He NBCA, ca. 5 km SW Ban Pa Phaknau, 17°00'N, 105°38'E, alt. 250–400 m, 31.V. – 6.VI. 2011, NHMB Basel, Laos 2011 Expedition, M. Brancucci, M. Geiser, D. Hauk, Z. Kraus, A. Phantala & E. Vongphachan leg. (CGW, NMB, NMP); Attapeu Province. 1♂, 1♀, Dong Amphan National Biodiversity Conservation Area, Nong Fa (crater lake) env., 15°05.9'N, 107°25.6'E, alt. ca. 1160 m, 30.IV.–6.V.2010, J. Hájek leg. (NMP); 1♀, Thong Kai Ohk, Ban Kachung (Mai) env., 15°01–02'N, 107°26–27'E, 1200–1450 m, 10.–24.VI.2011, NHMB Basel Laos 2011 Expedition, M. Geiser, D. Hauk, A. Phantala & E. Vongphachan leg. (NMB).

**Distribution.** Thailand: Nan, Chiang Mai, and Phetchabun (first record) provinces; Laos: Phongsali (first record), Luang Namtha (first record), Oudomxai, Luang Prabang (first record), Vientiane, Khammouan, Savannakhet (first record), and Attapeu (first record) provinces; China: Yunnan Province, Hong Kong; Vietnam: Vinh Phuc Province.

***Microdytes wewalkai* Bian & Ji, 2009**

*Microdytes wewalkai* Bian & Ji, 2009: 37; Wewalka 2011: 36; Nilsson and Hájek 2023: 212.

**Type locality.** China, Hainan, Lingtou (Ledong) County, Jianfengling NR.

**Material examined.** LAOS: Attapeu Province. 3♂♂, 2♀♀, Dong Amphan National Bio-Diversity Conservation Area, Nong Fa (crater lake) env., 15°05.9'N, 107°25.6'E, alt. ca. 1160 m, 30.IV.–6.V.2010, J. Hájek leg. (CGW, NMP).

**Comments.** Specimens from Laos have two transverse yellowish red markings on both sides of the middle of pronotum while in specimens from China (Hainan) it is completely black, but no other differences have been observed.

**Distribution.** Laos (first record): Attapeu Province; China: Hainan Province.

### *Microdytes zetteli* Wewalka, 1997

Fig. 37

*Microdytes zetteli* Wewalka, 1997: 41; Wewalka 2011: 34; Nilsson and Hájek 2023: 212.

**Type locality.** Thailand, Chiang Mai Province, Doi Suthep.

**Material examined.** THAILAND: Chiang Mai Province. 12 exs., Mae Taeng District, Pa Pae St. 49 (alt. 1000 m), 15.VI.2019, R. Okada leg. (CGW, CRO, THN-HM); 2♂♂, Mae Chaem District, Tha Pha St. 136 (alt. 720 m), 4.VII.2020, R. Okada leg. (CGW, CRO); 1♂, same locality St. 166 (alt. 720 m), 15.VIII.2020, R. Okada leg. (THNHM) (Fig. 37); Chiang Rai Province. 1♀, Wiang Kaen District, Muang Yai St. 71 (alt. 440 m), 2.VIII.2019, R. Okada leg. (CRO).

LAOS: 4 exs., Luang Prabang Province, 5 km W Ban Song Cha, 20°33–4'N, 102°14'E, alt. ca. 1200 m, 1.–16.V.1999, V. Kubáň leg. (CGW, NMB).

**Distribution.** Myanmar: Shan State; Thailand: Chiang Mai, Chiang Rai (first record) and Mae Hong Son provinces; Laos: Luang Prabang Province.

### Additional species known from Thailand, Laos, or Cambodia

#### *Microdytes schoenmanni* Wewalka, 1997

Fig. 33

*Microdytes schoenmanni* Wewalka, 1997: 34; Miller and Wewalka 2010: 35; Wewalka 2011: 31; Nilsson and Hájek 2023: 212.

**Type locality.** Thailand, Trat Province, Koh Chang Island, Klong Prao.

**Material examined.** MYANMAR: 1♂, Shan State, N Aungban, halfway between Pindaya and Ye'ngan, 20°58.271'N, 96°32.488'E, ca. alt. 1241 m, stream, 10.VI.2004, Shaverdo leg. (CGW) (Fig. 33).

**Distribution.** India: Darjeeling; Nepal; Myanmar: Chin and Shan states, Saganing and Tanintharyi divisions; Thailand: Trat Province, Khao Yai NP [Nakhon Ratchasima or Nakhon Nayok Province]; Laos: Attapeu Province; China: Yunnan Province.

## Checklist of the species of *Microdytes* from Thailand, Laos, and Cambodia

- Microdytes akitai* Wewalka, 1997 Laos  
*Microdytes balkei* Wewalka, 1997 Thailand, Laos, Cambodia  
*Microdytes dimorphus* Wewalka, 1997 Thailand  
*Microdytes eliasi* Wewalka & Okada, sp. nov. Thailand, Cambodia  
*Microdytes franzi* Wewalka & Wang, 1998 Laos  
*Microdytes gabrielae* Wewalka, 1997 Thailand  
*Microdytes heineri* Wewalka, 2011 Thailand, Laos, China  
*Microdytes jeenthongi* Okada & Wewalka, sp. nov. Thailand  
*Microdytes maculatus* (Motschulsky, 1860) India, Myanmar, Thailand, Laos, China  
*Microdytes mariannae* Wewalka, 1997 Thailand  
*Microdytes maximiliani* Wewalka & Okada, sp. nov. Laos, China  
*Microdytes menopausis* Wewalka, 1997 Thailand, Laos  
*Microdytes paoloi* Wewalka, 2011 Thailand  
*Microdytes pasiricus* (Csiki, 1938) Thailand, Philippines, Singapore, Indonesia  
*Microdytes perdezanii* Wewalka, 2011 Thailand  
*Microdytes rocchii* Wewalka, 2011 Laos  
*Microdytes schoedli* Wewalka, 1997 Thailand, Laos  
*Microdytes schoenmanni* Wewalka, 1997 India, Nepal, Myanmar, Thailand, Laos, China  
*Microdytes schwendingeri* Wewalka, 1997 Thailand, Laos  
*Microdytes sekaensis* Okada & Wewalka, sp. nov. Thailand, Laos  
*Microdytes shepardii* Wewalka, 1997 Thailand, Laos, China  
*Microdytes shunichii* Satô, 1995 Thailand, Laos, China, Vietnam  
*Microdytes ubonensis* Okada & Wewalka, sp. nov. Thailand, Laos  
*Microdytes wewalkai* Bian & Ji, 2009 Laos, China  
*Microdytes zetteli* Wewalka, 1997 Myanmar, Thailand, Laos

## Key to the species of *Microdytes* from Thailand, Laos, and Cambodia

- 1 Elytron with a distinct impression on lateral side in anterior third (Fig. 38); TL: 1.60–2.00 mm ..... ***M. maximiliani* sp. nov.**  
 – Elytron without impression on lateral side ..... **2**  
 2 Punctures on metacoxae very coarse (Fig. 39B) to moderately coarse (Fig. 39C) ... **3**  
 – Punctures on metacoxae fine (Fig. 39D) or very fine (Fig. 39E) ..... **18**  
 3 Elytra with two postmedian longitudinal bands (Fig. 28); TL: 1.90–2.00 mm ..  
 ..... ***M. paoloi***  
 – Elytra without longitudinal band ..... **4**  
 4 Pronotum dark brown to black with a transverse reddish-brown band on each side. TL: 1.90–2.10 mm ..... ***M. wewalkai***  
 – Pronotum without transverse band ..... **5**  
 5 Body oval or rhomboid (Figs 20, 24, 27, 29, 35); medium to large species TL: 1.40–2.10 mm ..... **6**  
 – Body oval; small species TL: 1.30–1.40 mm ..... **11**

6	Elytra without a post-median spot near suture .....	7
–	Elytra with a post-median spot near suture .....	13
7	Pronotum predominantly reddish brown to dark brown; metacoxae of male with distinct setae (Fig. 39A); TL: 1.85–1.95 mm .....	<i>M. heineri</i>
–	Pronotum predominantly yellowish brown; metacoxae without setae.....	8
8	Body regularly oval; clypeus not bordered; TL: 1.70–2.00 mm .....	<i>M. shepardii</i>
–	Body rhomboid; clypeus bordered at least in the middle.....	9
9	Elytra predominantly yellowish brown; clypeus rounded and finely bordered; TL: 1.40–1.60 mm .....	<i>M. pasiricus</i>
–	Elytra predominantly dark brown; clypeus straightened and slightly bordered in the middle (Fig. 40C) .....	10
10	Apical three sternites distinctly punctured; the coarser punctures on the elytra similar in size; TL: 1.75–1.85 mm .....	<i>M. dimorphus</i>
–	Apical three sternites almost without punctures; the coarser punctures on the elytra distinctly of two kinds; TL: 1.40–1.70 mm .....	<i>M. menopaensis</i>
11	Body oblong oval; pronotum predominantly dark brown; TL: 1.25–1.40 mm....	<i>M. ubonensis</i> sp. nov.
–	Body broadly oval; pronotum predominantly yellowish brown .....	12
12	Elytral markings with distinct transversal band at the base and without a post-median spot near the suture; TL: 1.30–1.40 mm .....	<i>M. schwendingeri</i>
–	Elytral markings with two indistinct spots at the base and with a post-median spot near the suture; TL: 1.34–1.36 mm.....	<i>M. sekaensis</i> sp. nov.
13	Elytral punctures consisting of one kind .....	14
–	Elytral punctures consisting of two kinds (e.g., Fig. 32) .....	15
14	Body regularly oval; the two parts of the median lobe obtuse to right apical medial angles but not expanded laterally at apex; the tips of paramere narrow to rounded but not constricted; TL: 1.60–1.90 mm.....	<i>M. maculatus</i>
–	Body more regularly oval; the two parts of the median lobe expanded laterally at apex; the tips of paramere constricted; TL: 1.64–1.85 mm .....	<i>M. eliasi</i> sp. nov.
15	Body oblong oval; TL: 1.90–2.15 mm .....	<i>M. schoedli</i>
–	Body regularly oval .....	
16	Elytral marking near the base indistinct; bigger punctures on elytra coarser; TL: 1.60–1.75 mm.....	<i>M. pederzani</i>
–	Elytral marking near the base distinct; bigger punctures on elytra less coarse.....	17
17	Post-median spot near the suture rounded; TL: 1.80–1.85 mm .....	<i>M. rocchii</i>
–	Post-median spot near the suture longitudinal; TL: 2.10–2.25 mm .....	<i>M. mariannae</i>
18	Body oblong oval; TL: 1.70–1.80 mm .....	<i>M. balkei</i>
–	Body regularly oval .....	19
19	Elytral marking near the base indistinct and small spot; TL: 1.45–1.55 .....	<i>M. gabrielae</i>
–	Elytral marking near the base distinct .....	20

- 20 Elytral marking dilated or waved at the shoulder; TL: 1.40–1.65 mm.....**21**  
 – Elytral marking broad transverse band at the shoulder; TL: 1.60–1.90 mm.... **22**  
 21 Head dark brown; pronotum dark brown; TL: 1.40–1.60 mm .....*M. franzi*  
 – Head yellowish brown; pronotum reddish brown; 1.40–1.65 mm .....  
 ..... *M. schoenmanni*  
 22 Pronotal punctures coarser; elytral punctures stronger; TL: 1.60–1.70 mm.....  
 ..... *M. akitai*  
 – Pronotal punctures sparser; elytral punctures finer ..... **23**  
 23 Pronotum predominantly yellowish brown; elytral punctures fine but distinct;  
 TL: 1.65–1.90 mm ..... *M. shunichii*  
 – Pronotum predominantly reddish brown; elytral punctures very fine and very  
 sparse ..... **24**  
 24 Head moderately finely and sparsely punctured; TL: 1.55–1.70 mm....*M. zetteli*  
 – Head finely and sparsely punctured; TL: 1.79–1.82 mm....*M. jeenthongi* sp. nov.

## Discussion

### Distribution patterns

The discovery of five new species with three first country records and 40 first regional records from Thailand, Laos, and Cambodia shows how poorly the Dytiscidae fauna of these countries is known. The data on species diversity of *Microdytes* species are summarized in Table 1 and Fig. 44. A total of 25 *Microdytes* species were recorded from these three countries. Among the recorded species, 20 are known from Thailand, 17 from Laos, and two from Cambodia; 16 species (64%) are known to occur only from those three countries, whereas nine species (36%) are also recorded in adjacent countries. This result makes Thailand and Laos the most and second-most fauna-rich countries for this genus.

In view of species diversity by ecoregions, LUA has the highest number of species (13 species, 52% of total fauna). This region comprises four species which occur only in one ecoregion. NAN has the second highest number of species (10 species, 40%), including the two new species *M. sekaensis* sp. nov. and *M. ubonensis* sp. nov. KAY, NIN, SEI, and CIN also have high numbers of species (8 species, 32%), including *M. jeenthongi* sp. nov., *M. maximiliani* sp. nov., *M. ubonensis* sp. nov., and *M. eliasi* sp. nov., respectively.

The distribution pattern of *Microdytes* species recorded from the three countries represents four types: 1) widespread type, occurring throughout continental South-east Asia to adjacent countries (5 species, 20%); 2) northern type, distributed mainly from northern Thailand and Laos to adjacent countries (9 species, 36%); 3) central type, recorded only from northeastern Thailand to southern Laos (6 species, 24%); 4) eastern type, occurring in northeastern and eastern Thailand and southern Laos (5 species, 20%). The conclusions made above are not definitive because there are still many unexplored areas.

**Table 1.** Summary of distribution types of *Microdytes* species in main ecoregions in Thailand, Laos, and Cambodia. **T** Thailand **L** Laos **C** Cambodia **KAY** Kayah-Karen montane rain forest **NIN** northern Indochina subtropical forests **LUA** Luang Prabang montane rain forests **NAN** northern Annamites rain forests **NKH** northern Khorat Plateau moist deciduous forests **SEI** southeastern Indochina dry evergreen forests **CIN** central Indochina dry forests **CAR** Cardamom Mountains rain forests **CHA** Chao Phraya lowland moist deciduous forests.

Distribution pattern	<i>Microdytes</i> species	Distribution records			Limited to three countries	Main ecoregions in Thailand, Laos, and Cambodia										N	Ratio	
		Thailand	Laos	Cambodia		KAY	NIN	LUA	NAN	NKH	SEI	CIN	CAR	CHA				
Widespread	<i>maculatus</i>	+	+			T	T	L	T	T	T	T					5	20%
	<i>pasivicus</i>	+				T	T											
	<i>schoedli</i>	+	+		+	T	T	L			T/L							
	<i>schuichii</i>	+	+			T	L	L	L									
	<i>schoenmanni</i>	+	+			T	L	L	L									
	<i>heineri</i>	+	+			T	T/L										9	36%
	<i>jeenbhongi</i> sp. nov.	+			+	T												
	<i>maximiliani</i> sp. nov.	+					L											
	<i>shepardi</i>	+	+			T	T				T/L							
	<i>zetteli</i>	+	+		+	T	T	L										
(limited to N Thailand)	<i>gabrielae</i>	+																
	<i>marianneae</i>	+																
	<i>paobi</i>	+																
	<i>poderzani</i>	+																
	<i>aktinai</i>	+																
	<i>franzi</i>	+																
	<i>rocchii</i>	+																
	<i>schuendingeri</i>	+																
	<i>sekaensis</i> sp. nov.	+																
	<i>tubonensis</i> sp. nov.	+																
NE and E Thailand to S Laos	<i>balkei</i>	+	+	+	+		L	L	L								6	24%
	<i>dimorphus</i>	+					L	L	L									
	<i>elias</i> sp. nov.	+																
	<i>menopausis</i>	+																
	<i>ueuwalkai</i>	+																
	<i>ueuwalkai</i>	+																
	<i>ueuwalkai</i>	+																
	<i>ueuwalkai</i>	+																
	<i>ueuwalkai</i>	+																
	<i>ueuwalkai</i>	+																
Total recorded species	20	17	2	16	8	8	13	10	6	8	8	4	3	25	100%			
Ratio				64%	32%	32%	52%	40%	24%	32%	32%	16%	12%					

**Notes.** Ecoregions where only 1 or 2 *Microdytes* species were recorded are excluded in the list (i.e., northern Thailand-Laos moist deciduous forests, southern Annamites montane rain forests, and Chao Phraya lowland moist deciduous forests).

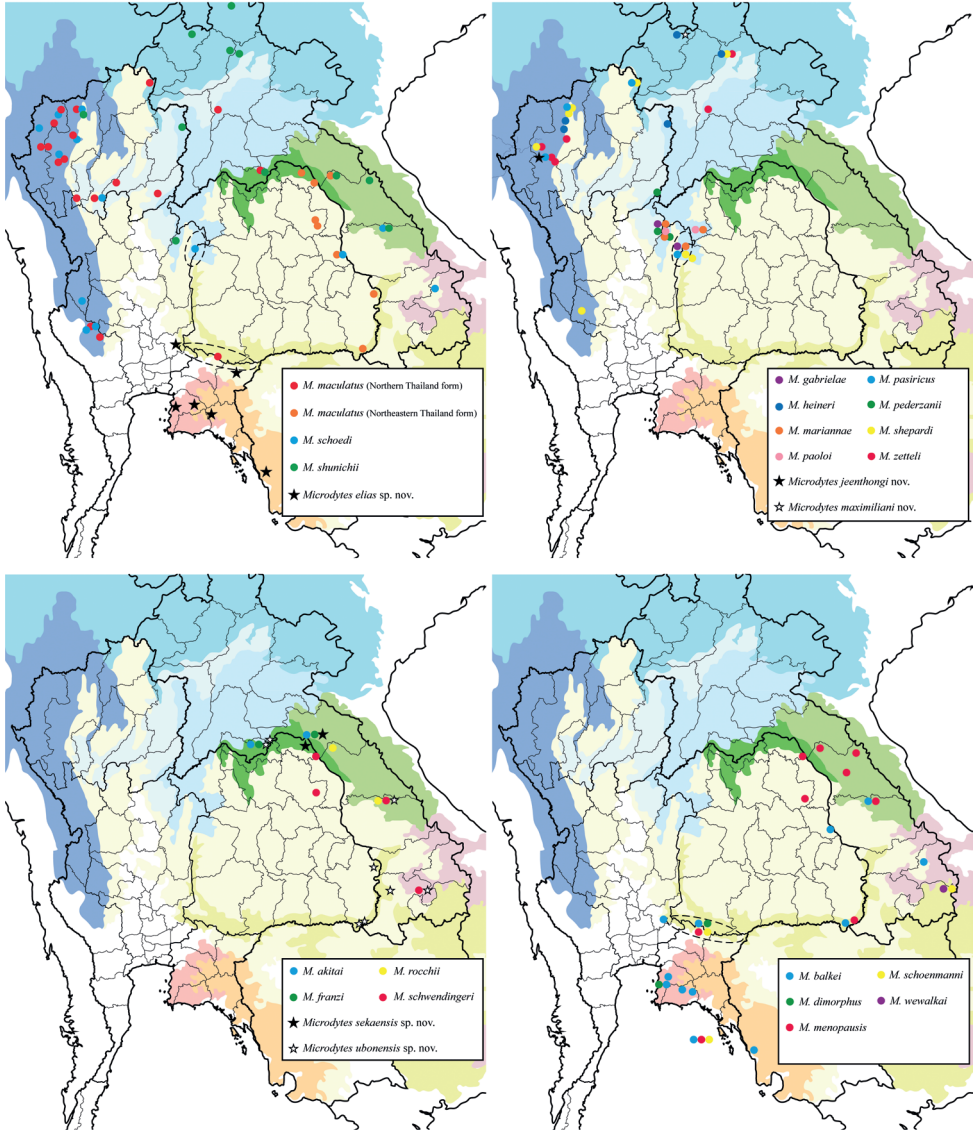


**Figure 44.** Distribution map of *Microdytes* species in Thailand, Laos, and Cambodia.

Most of the *Microdytes* specimens examined in this study were collected at lotic habitats associated with running water flowing under primary or secondary forests, and many species were sympatric. At one locality of Tha Pha, northern Thailand, located at Kayah-Karen montane rain forests, four species were collected from the same small stream (Fig. 46). In this stream, *M. maculatus*, which shows a wide distribution, was found at several sites: at the edge of a water body, among roots of trees in the gaps between stone and gravel. The other species, however, were collected only in restricted areas: *M. jeenthongi* sp. nov. from a shallow, relatively fast-flowing area where tree roots



**Figures 45–48.** Collecting localities of *Microdytes* species in Thailand **45** Ban Kaeng, Sa Kaeo Province, one of the localities of *M. eliasi* sp. nov. **46** Tha Pha, Chiang Mai Province, type locality of *M. jeenthongi* sp. nov. **47** Ban Tong, Bueng Kan Province, type locality of *M. sekaensis* sp. nov. **48** Nam Thaeng, Ubon Ratchathani Province, type locality of *M. ubonensis* sp. nov.

were exposed at bottom of the river, *M. zetteli* from calm pool areas associated with slowly running water, and *M. pasiricus* among gravel under big stones in fast streams. Although our field surveys were conducted only two times at this site, it is worth noting that *M. jeenthongi* sp. nov. and *M. zetteli*, which morphologically resemble each other, were collected each time at the same places which are only one meter from each other. This result suggests that microhabitat preferences for some *Microdytes* species are very strict, and it may lead to the discovery of the richest fauna in this area.

Unlike the northern region of Thailand, where diving beetle surveys have been carried out relatively many times (e.g., by Dr. William D. Shepard, Dr. Manfred A. Jäch, Dr. Herbert Zettel; pers. comm.), a large part of this country remained poorly explored, especially Isan (northeastern region) and the eastern regions. Our study detected three new *Microdytes* species from these unexplored areas. From the southern region no *Microdytes* species have been reported so far, although two species (*Microdytes elgae* Hendrich, Balke & Wewalka, 1995 and *M. pasiricus*) were recorded from Singapore, situated at the southern end of the Malay Peninsula (Wewalka 1997; Hendrich et al. 2004). Further new species can be expected from Thailand, particularly by collecting in unexplored provinces and repeated sampling at the microhabitat levels.

## Acknowledgements

We thank Jiří Hájek (Prague, Czech Republic), Isabelle Zürcher-Pfander (Basel, Switzerland), Manfred A. Jäch (Vienna, Austria), and Tadsanai Jeenthong (Pathum Thani, Thailand) for providing study material. Sincere gratitude to Antoine Mantilleri (Paris, France) for checking type material. Thanks also go to Michael Cota (Pathum Thani, Thailand) for correcting the English of this manuscript. We also offer thanks to Helena Shaverdo (Vienna, Austria) and Veera Vilasri (Pathum Thani, Thailand) for their supporting loan material.

## References

- Balfour-Browne J (1946) *Microdytes* gen. nov. Dytiscidarum (Hyphydrini). Journal of the Bombay Natural History Society 46: 106–108.
- Bian D, Ji L (2009) Two new species of Dytiscidae from Hainan, China. Coleopterists Bulletin 63(1): 35–40. <https://doi.org/10.1649/0010-065X-63.1.35>
- Bian D, Zhang Y, Ji L (2015) *Microdytes huangyongensis* sp. n. and new records of *Allopachria* Zimmermann, 1924 from Zhejiang Province, China (Coleoptera: Dytiscidae). Zootaxa 4040(4): 469–471. <https://doi.org/10.11646/zootaxa.4040.4.7>
- Biström O, Nilsson AN, Wewalka G (1997) A systematic review of the tribes Hyphydrini Sharp and Pachydrini n. trib. (Coleoptera, Dytiscidae). Entomologica Fennica 8(2): 57–82. <https://doi.org/10.33338/ef.83921>
- Csiki E (1938) Die Schwimmkäfer (Haliplidae und Dytiscidae) von Sumatra, Java und Bali der Deutschen Limnologischen Sunda-Expedition. Archiv für Hydrobiologie Supplement 15(1937): 121–130.
- Freitag H, Jäch MA, Wewalka G (2016) Diversity of aquatic and riparian Coleoptera of the Philippines: Checklist, state of knowledge, priorities for future research and conservation. Aquatic Insects 37(3): 177–213. <https://doi.org/10.1080/01650424.2016.1210814>
- Geiser M, Nagel P (2013) Coleopterology in Laos – an introduction to the nature of the country and its coleopterological exploration. Entomologica Basiliensia et Collectionis Frey 34: 11–46.
- Hendrich L, Balke M, Yang CM (2004) Aquatic Coleoptera of Singapore – Species Richness, Ecology and Conservation. The Raffles Bulletin of Zoology 52: 97–141.
- Jäch MA, Ji L (2003) China Water Beetle Survey (1999–2003), 20 pp. In: Jäch MA, Ji L (Eds) Water Beetles of China (Vol. III). Zoologisch-Botanische Gesellschaft and Wiener Coleopterologenverein, Wien, [vi +] 572 pp.
- Miller KB, Nilsson AN (2003) Homology and terminology: Communicating information about rotated structures in water beetles. Latissimus 17: 1–4.
- Miller KB, Wewalka G (2010) *Microdytes* Balfour-Browne of India with description of three new species (Coleoptera: Dytiscidae: Hydroporinae). Zootaxa 2420(1): 26–36. <https://doi.org/10.11646/zootaxa.2420.1.2>
- Motschulsky Vde (1860) Insectes des Indes orientales, et de contrées analogues. 2:de Série. Études Entomologiques Motschulsky 8(1859): 25–48.

- Nilsson AN, Hájek J (2023) A world catalogue of the family Dytiscidae, or the diving beetles (Coleoptera, Adephaga). Version 1.I.2023. <http://www.norrent.se>; [www.waterbeetles.eu](http://www.waterbeetles.eu) [Accessed 07 January 2023]
- Olson DM, Dinerstein E, Wikramanyake ED, Burgess ND, Powell GVN, Underwood EC, D'Amico JA, Itoua I, Strand HE, Morrison JC, Loucks CJ, Allnutt TF, Ricketts TH, Kura Y, Lamoreux JF, Wettengel WW, Hedao P, Kassem KR (2001) Terrestrial ecoregions of the world: A new map of life on Earth. *Bioscience* 51(11): 933–938. [https://doi.org/10.1641/0006-3568\(2001\)051\[0933:TEOTWA\]2.0.CO;2](https://doi.org/10.1641/0006-3568(2001)051[0933:TEOTWA]2.0.CO;2)
- Régimbart M (1899) Révision des Dytiscidae de la région Indo-Sino-Malaise. *Annales de la Société Entomologique de France* 68: 186–367.
- Satô M (1981) Notes on the genus *Microdytes* (Coleoptera, Dytiscidae) and its ally from Nepal. *Annotationes Zoologicae Japonenses* 54: 67–72.
- Satô M (1995) A new species of the genus *Microdytes* (Coleoptera, Dytiscidae) from Northern Vietnam. *Special Bulletin of the Japanese Society of Coleopterology* 4: 313–315.
- Sharp D (1882) On aquatic carnivorous Coleoptera or Dytiscidae. *The Scientific Transactions of the Royal Dublin Society, Series II* 2: 179–1003. [+ pls 7–18]
- Sheth SD, Ghate HV, Dahanukar N, Hájek J (2020) The First Hygropetric Species of *Microdytes* J. Balfour-Browne, 1946 (Coleoptera: Dytiscidae) from the Western Ghats, India. *Oriental Insects* 55(2): 254–266. <https://doi.org/10.1080/00305316.2020.1787903>
- Vazirani TG (1969) Contribution to the study of aquatic beetles (Coleoptera), 2. A Review of the Subfamilies Noterinae, Laccophilinae, Dytiscinae and Hydroporinae (in Part) from India. *Oriental Insects* 2(3–4): 221–341. <https://doi.org/10.1080/00305316.1968.10433885>
- Vazirani TG (1977) Records of the Zoological Survey of India; Catalogue of Oriental Dytiscidae. *Miscellaneous Publication, Occasional Paper No. 6*: 1–111.
- Wewalka G (1997) Taxonomic revision of *Microdytes* Balfour-Browne. (Coleoptera: Dytiscidae). *Koleopterologische Rundschau* 67: 13–51.
- Wewalka G (1998) DYTISCIDAE: I. The Chinese species of *Microdytes* Balfour-Browne with description of a new species (Coleoptera). In: Jäch MA, Ji L (Eds) *Water Beetles of China II*. Zoologisch-Botanische Gesellschaft and Wiener Coleopterologenverein, Vienna, 61–67.
- Wewalka G (2011) New species, new records and taxonomic updates on *Microdytes* Balfour-Browne, 1946. *Koleopterologische Rundschau* 81: 21–39.
- Wewalka G, Wang LJ (1998) Three new species of *Microdytes* Balfour-Browne from Laos and Borneo (Coleoptera, Dytiscidae). *Koleopterologische Rundschau* 68: 65–69.
- Wewalka G, Ribera I, Balke M (2007) Description of a new subterranean hyphydrine species from Hainan (China), based on morphology and DNA sequence data. *Koleopterologische Rundschau* 77: 61–66.
- Zaitzev FA [Ph] (1915) Les coléoptères aquatiques de la collection Motschulsky. I. Haliplidae, Dytiscidae, Gyridae. *Ezegodnik Zoologiceskago Muzeja Akademii Nauk* 20: 239–295.
- Zimmermann A (1920) Pars 71. Dytiscidae, Haliplidae, Hygrobiidae, Amphizoidae. In: Schenkling S (Ed.) *Coleopterorum Catalogus (Vol. IV)*. Junk, Berlin, 326 pp.



# Description of a new nematode species, *Chromadorina communis* sp. nov. (Nematoda, Chromadoridae), from Changdao Island, China and phylogenetic analysis of Chromadorida based on small subunit rRNA gene sequences

Wen Guo<sup>1</sup>, Mengna Wang<sup>1</sup>, Haotian Li<sup>1</sup>, Chunming Wang<sup>1</sup>

<sup>1</sup> College of Life Sciences, Liaocheng University, Liaocheng, 252059, China

Corresponding author: Chunming Wang ([wangchunming@lcu.edu.cn](mailto:wangchunming@lcu.edu.cn))

---

Academic editor: Sergei Subbotin | Received 23 January 2023 | Accepted 11 April 2023 | Published 25 April 2023

---

<https://zoobank.org/2B1C9783-E2BA-45B9-8234-A3875135A323>

---

**Citation:** Guo W, Wang M, Li H, Wang C (2023) Description of a new nematode species, *Chromadorina communis* sp. nov. (Nematoda, Chromadoridae), from Changdao Island, China and phylogenetic analysis of Chromadorida based on small subunit rRNA gene sequences. ZooKeys 1159: 121–131. <https://doi.org/10.3897/zookeys.1159.100908>

---

## Abstract

*Chromadorina communis* sp. nov. is described from Changdao Island at the confluence of the Yellow and the Bohai seas. The new species is characterized by its medium-sized body; finely striated cuticle with homogeneous punctations; absence of ocelli; buccal cavity with three equal-sized, solid teeth; four cephalic setae; oval amphidial fovea which is positioned between cephalic setae; curved spicules with tapered distal ends; simple, boat-shaped gubernaculum; five or six cup-shaped preloacal supplements; and conical tail with a very short spinneret. A phylogenetic analysis of small subunit rRNA gene sequences using maximum-likelihood and Bayesian inference confirmed the taxonomic position of *Chromadorina communis* sp. nov. within Chromadorinae. Tree topology in Chromadorida shows six morphological families clustered into a monophyletic clade and verifies the taxonomic position of the family Neotonchidae based on morphological and molecular analysis.

## Keywords

Chromadorida, free-living marine nematodes, phylogenetic analysis, SSU, taxonomy

## Introduction

Nematodes are one of the most widely distributed and diverse groups of the animal phyla, and half a million to 10 million nematode species have been estimated (Hodda 2022). However, a large number of species remain undescribed. Phylogenetic analyses based on molecular sequences, especially the small subunit rRNA gene (SSU), combined with morphological characters has updated the classification of Nematoda (De Ley and Blaxter 2002, 2004), revealed relationships among nematode groups (Holterman et al. 2006; Meldal et al. 2007), and elucidated the transition between marine, freshwater, and terrestrial different habitats (Holterman et al. 2008, 2019). However, due to the scarcity of nematode sequences, especially those of marine nematodes, relationships among nematodes are far from understood.

Species of the order Chromadorida Chitwood, 1993 are mainly marine species, and freshwater and limnetic–terrestrial species are also present among them. The Chromadorida are characterized by the combined characters of a punctate cuticle and a female reproductive system with reflexed ovaries (Lorenzen 1981), which distinguish this order from other nematode orders. Lorenzen (1994) summarized the superfamily Chromadoroidea (corresponding to Chromadorida) systematically and gave a phylogenetic analysis of this group based on morphological features. Tchesunov (2014) reviewed the six families of Chromadorida and provided diagnoses of the families and genera; he listed Chromadoridae with five subfamilies and 38 genera, Cyatholaimidae with four subfamilies and 21 genera, Achromadoridae with a single genus (*Achromadora*), Ethmolaimidae with three genera, Neotonchidae with six genera, and Selachinematidae with two subfamilies and 11 genera. Venekey et al. (2019) reviewed the family Chromadoridae, provided polytomous identification keys for subfamilies and genera, listed valid species of each genus, and provided a phylogenetic analysis based SSU rRNA gene sequences of 11 genera and large subunit (LSU) rRNA gene sequences of eight genera. Phylogenetic relationships within Chromadorida based on full-length sequences of the SSU rRNA gene has been analyzed for 4 families by Holterman et al. (2008) and six families (22 genera) by Leduc et al. (2017). As more Chromadorida SSU rRNA gene sequences have been deposited in the GenBank, an updated and more detailed phylogenetic analysis is needed.

Until now, 29 species of *Chromadorina* Filipjev, 1918 have been described, among which 25 species are marine and four are limnetic (*C. astacicola* W. Schneider, 1932, *C. bercziki* Andrassy, 1962, *C. bioculata* (Schultze, 1857) Wieser, 1954, and *C. viridis* (Linstow, 1876) Wieser, 1954). A new species, *C. communis* sp. nov., is described here and a molecular phylogeny based on SSU rRNA gene sequences within Chromadora is analyzed. The new species was found during a study of the diversity of free-living marine nematodes of Changdao Island. This is the first new species of *Chromadorina* from the China Sea.

## Materials and methods

### Sample collection and nematode identification

From Changdao Island in June 2022, undisturbed samples were collected from rock surfaces with *Ulva lactuca* and *U. prolifera* (Fig. 1). Samples used for morphological analysis were fixed with 10% formalin in seawater, and samples used for molecular analysis were fixed with 95% alcohol. In the laboratory, sediment samples fixed with formalin were washed through two sieves (mesh sizes 500  $\mu\text{m}$  and 45  $\mu\text{m}$ ) to separate meiofauna from macrofauna larger than 500  $\mu\text{m}$ . Meiofauna were transferred into a grid-lined Petri dish and sorted under a stereoscopic microscope. Nematodes were transferred into a mixture of ethanol (50%) and glycerin (ratio 1:9 by volume), the ethanol was allowed to slowly evaporate (McIntyre and Warwick 1984), and the specimens were mounted in glycerin on permanent slides. Descriptions were made using an Axiscope-5 differential interference contrast microscope (Zeiss, Germany). Line drawings were made with the aid of iPad (Apple, USA), and photographs were taken with the aid of ZEN software (Zeiss).

### DNA extraction, PCR amplification, and phylogenetic analysis

Samples used for molecular analysis were washed and separated as with formalin-fixed samples. Species of *C. communis* sp. nov. were selected and confirmed on the temporary slides based mainly on buccal cavity, spicules, and numbers of pre-loacal supplements. Genomic DNA of seven nematode specimens were extracted with DNeasy Blood & Tissue kit (Qiagen, Germany) and used as templates of nearly full-length SSU rRNA gene amplification with two sets of primers, 1096F (5' – GGT AAT TCT GGA GCT AAT AC – 3') / 1912R (5' – TTT ACG GTC

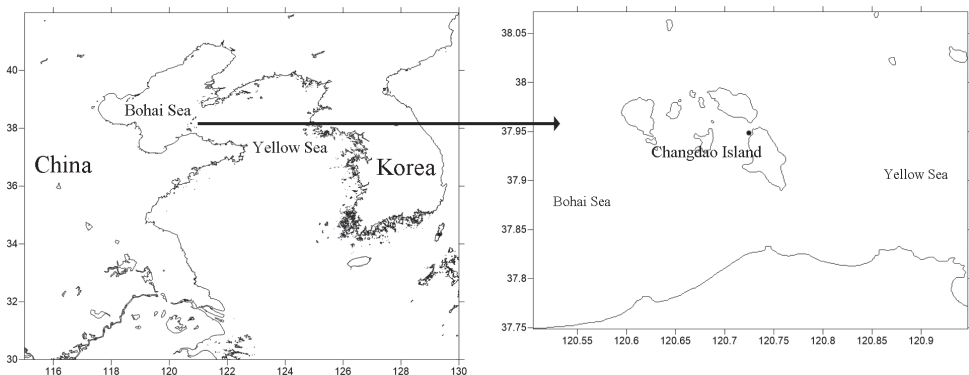


**Figure 1.** Sampling site (dot) on Changdao Island.

AGA ACT AGG G – 3') and 1813F (5' – CTG CGT GAG AGG TGA AAT – 3') / 2646R (5' – GCT ACC TTG TTA CGA CTT TT – 3') (Holterman et al. 2006). PCR was conducted as described by Zhao et al. (2015). The PCR product was sequenced by Genewiz (China). The sequences were assembled in Genious v. 6.1.2. The new SSU sequence was deposited in GenBank under accession number OP680597. Near full-length SSU rRNA sequences of Chromadorida and Desmodorida (genus *Prodesmodora* Micoletzky, 1923) were retrieved from GenBank with BLAST; other sequences in GenBank from Chromadorida and longer than 600 bp were also used in the phylogenetic analysis.

Sequences were aligned with the Clustal W algorithm, and the final alignment consisted of 76 sequences from 34 genera. Substitution models of (GTR (general time-reversible) + G (gamma distribution) + I (proportion of invariable sites)) were selected as the best-fit model for SSU alignments. A ML analysis was performed with Mega X with 1000 bootstrap replicates. A BI analysis was constructed with CIPRES (<http://www.phylo.org/>) and MrBayes on XSEDE v. 3.2.7a was used; the trees were run with chain length of 10,000,000, burn-in frac = 0.25, and the analysis was rooted with *Enoplolaimus* sp. (accession number KR265034). The topology of the resulting tree was viewed in FigTree v. 1.4.3 and edited with PowerPoint.

## Results and discussion

### Taxonomy

#### Order Chromadorida Chitwood, 1933

#### Family Chromadoridae Filipjev, 1917

#### Genus *Chromadorina* Filipjev, 1918

#### *Chromadorina communis* sp. nov.

<https://zoobank.org/63F40161-62AA-4836-8F27-9AAF48185A28>

Figs 2, 3, Table 1

**Diagnosis.** *Chromadorina communis* sp. nov. is characterized by its medium-sized body, finely striate cuticle with punctuations, buccal cavity with three equally sized teeth, absent ocelli, four cephalic setae 6–8 µm long, oval amphidial fovea level with cephalic setae, curved spicules with tapered distal end, boat-shaped gubernaculum, five or six cup-shaped preloacal supplements, and a conical tail with a short spinneret.

**Material examined.** Four males and two females were measured and studied.

**Holotype:** m#1 on slide 22YTCD6-2-17; **paratypes:** m#2 on 22YTCD6-2-15, m#3 on 22YTCD6-2-18, m#4 on 22YTCD6-2-11, f#1 on 22YTCD6-2-1, and f#2 on 22YTCD6-2-18. Type specimens were deposited in the Institute of Oceanology, Chinese Academy of Sciences, Qingdao.

**Measurements.** Detailed measurements information of individual specimens are shown in the Table 1.

**Table 1.** Measurements of *Chromadorina communis* sp. nov. (in  $\mu\text{m}$  except for ratios).

Characters	Holotype	Paratypes	Paratypes
	male	males ( $n = 3$ )	females ( $n = 2$ )
Total body length	711	741.0 $\pm$ 73.6 (696–851)	753.5 $\pm$ 47.4 (720, 787)
Maximum body diameter	32	27.8 $\pm$ 2.9 (26–32)	31.5 $\pm$ 0.7 (31, 32)
Head diameter	11	10.5 $\pm$ 0.6 (10–11)	10.5 $\pm$ 0.7 (10, 11)
Length of cephalic setae	8	6.5 $\pm$ 1.0 (6–8)	6.5 $\pm$ 0.7 (6, 7)
Diameter of amphidial fovea	5	4.5 $\pm$ 0.6 (4–5)	5.0 $\pm$ 0.0 (5, 5)
Amphidial fovea*	2	2.5 $\pm$ 0.6 (2–3)	2.0 $\pm$ 0.0 (2, 2)
Nerve ring*	71	71.5 $\pm$ 4.7 (67–78)	72.0 $\pm$ 0.0 (72, 72)
Body diameter at nerve ring	24	21.8 $\pm$ 1.5 (21–24)	21.5 $\pm$ 0.7 (21, 22)
Pharynx length	119	122.5 $\pm$ 5.1 (118–129)	125.5 $\pm$ 4.9 (122, 129)
Pharynx bulb length	26	24.8 $\pm$ 1.5 (23–26)	27.5 $\pm$ 0.7 (27, 28)
Body diameter at the base of pharynx	28	24.5 $\pm$ 2.4 (23–28)	25.5 $\pm$ 0.7 (25, 26)
Anal body diameter	22	22.0 $\pm$ 1.4 (21–24)	17.5 $\pm$ 2.1 (16, 19)
Spicules length along arc	28	27.5 $\pm$ 0.6 (27–28)	-
Gubernaculum length	17	17.5 $\pm$ 1.3 (16–19)	-
Vulva*	-	-	360.0 $\pm$ 11.3 (352, 368)
Body diameter at vulva	-	-	31.5 $\pm$ 0.7 (31, 32)
V%	-	-	47.9 $\pm$ 1.5 (46.8, 48.9)
Precloacal supplements	5	5.5 $\pm$ 0.6 (5–6)	-
Tail length	89	92.0 $\pm$ 5.7 (87–100)	115.5 $\pm$ 12.0 (107, 124)
a	22.2	26.9 $\pm$ 3.8 (22.2–27.1)	23.9 $\pm$ 1.0 (23.2, 24.6)
b	6.0	6.1 $\pm$ 0.4 (5.6–6.6)	6.0 $\pm$ 0.1 (5.9, 6.1)
c	8.0	8.1 $\pm$ 0.3 (7.7–8.5)	6.5 $\pm$ 0.3 (6.3, 6.7)
c'	4.0	4.2 $\pm$ 0.2 (4.0–4.4)	6.6 $\pm$ 0.1 (6.5, 6.7)

Abbreviations are as follows: a = body length/maximum body diameter; b = body length/pharynx length; c = body length/tail length; c' = tail length/anal body diameter; V% = position of vulva from anterior body end expressed as a percentage of total body length.

\*Distance from anterior body end.

**Description. Males.** Body cylindrical and medium-sized. Inner and outer cephalic setae inconspicuous. Four cephalic setae 6–8  $\mu\text{m}$  in length (0.55–0.73 head diameter long), two pairs of sublateral cervical setae (4–5  $\mu\text{m}$  long) present. Somatic setae (3–4  $\mu\text{m}$  long) scarcely present in pharynx and on caudal region. Cuticle faintly striate, with homogeneous punctuations without longitudinal differentiation. Ocelli absent. Amphidial fovea oval, level with cephalic setae, in some specimens difficult to observe. Buccal cavity slightly cuticularized and funnel-shaped, with three equally sized, solid teeth. Pharynx cylindrical, with posterior end widened into obvious bulb (20.1–21.8% of pharynx length). Nerve ring slightly posterior to middle pharynx region (54–63% of pharynx length). Secretory–excretory system pore on anterior end of body (3–4  $\mu\text{m}$  from anterior end).

Reproductive system monorchic, with anterior testis outstretched, located to right of intestine. Spicules paired, curved, 1.2–1.3 cloacal body diameters long; proximal end slightly cephalate and distal end tapered. Gubernaculum simple, boat-shaped, parallel to the distal end of spicules. Five or six cup-shaped precloacal supplements, 12  $\mu\text{m}$  from cloacal opening and 12–16  $\mu\text{m}$  apart. Tail conical, with short spinneret, with three caudal glands in line.

**Females.** Similar to males in most characteristics. Reproductive system didelphic and amphidelphic, with reflexed ovaries. Anterior ovary to right of intestine and posterior ovary to left of intestine. Vulva slightly anterior to mid-body. Vagina short and sclerotized.

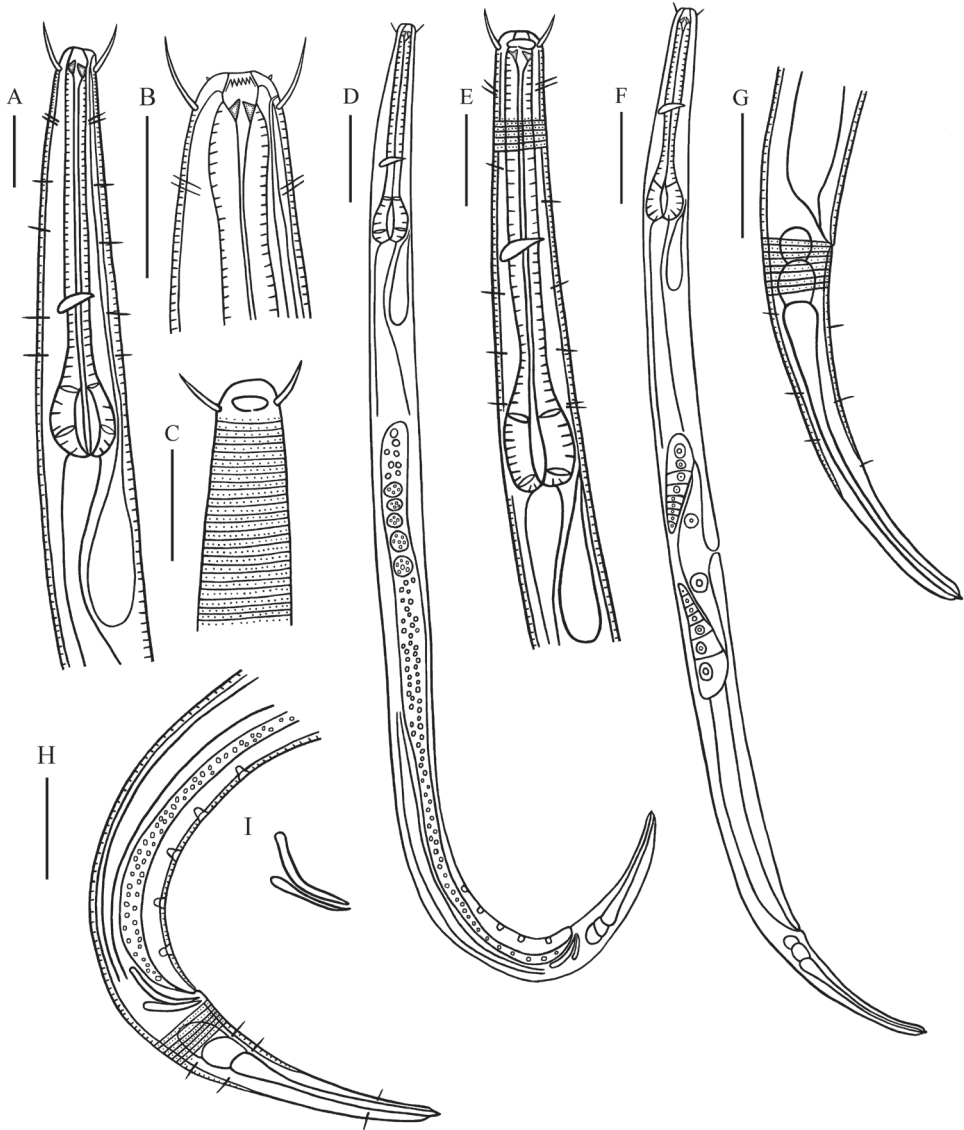


**Figure 2.** *Chromadorina communis* sp. nov. **A** lateral view of male anterior region showing buccal cavity and pharyngeal region (holotype) **B** lateral view of male anterior region showing buccal cavity (holotype) **C** lateral view of male anterior region showing cuticle and amphids (holotype) **D** lateral view of male whole body (holotype) **E** lateral view of female anterior body showing buccal cavity and pharyngeal region (22YTCD6-2-1) **F** lateral view of female entire body showing vulva (22YTCD6-2-1) **G** lateral view of female posterior body (22YTCD6-2-1) **H** lateral view of male posterior body, showing preloocal supplements and tail (holotype) **I** lateral view of spicules and gubernaculum. Scale bars: 20  $\mu\text{m}$  (**A–C, E**); 50  $\mu\text{m}$  (**D, F**); 30  $\mu\text{m}$  (**G, H**).

**Type locality and habitat.** Changdao Island, Shandong Province, China, 37°57'N, 120°43'E, at the confluence of the Yellow and the Bohai seas. Salinity 28.1‰  $\pm$  0.36.

**Distribution.** Occurred on rock surfaces with *Ulva lactuca* and *U. prolifera*.

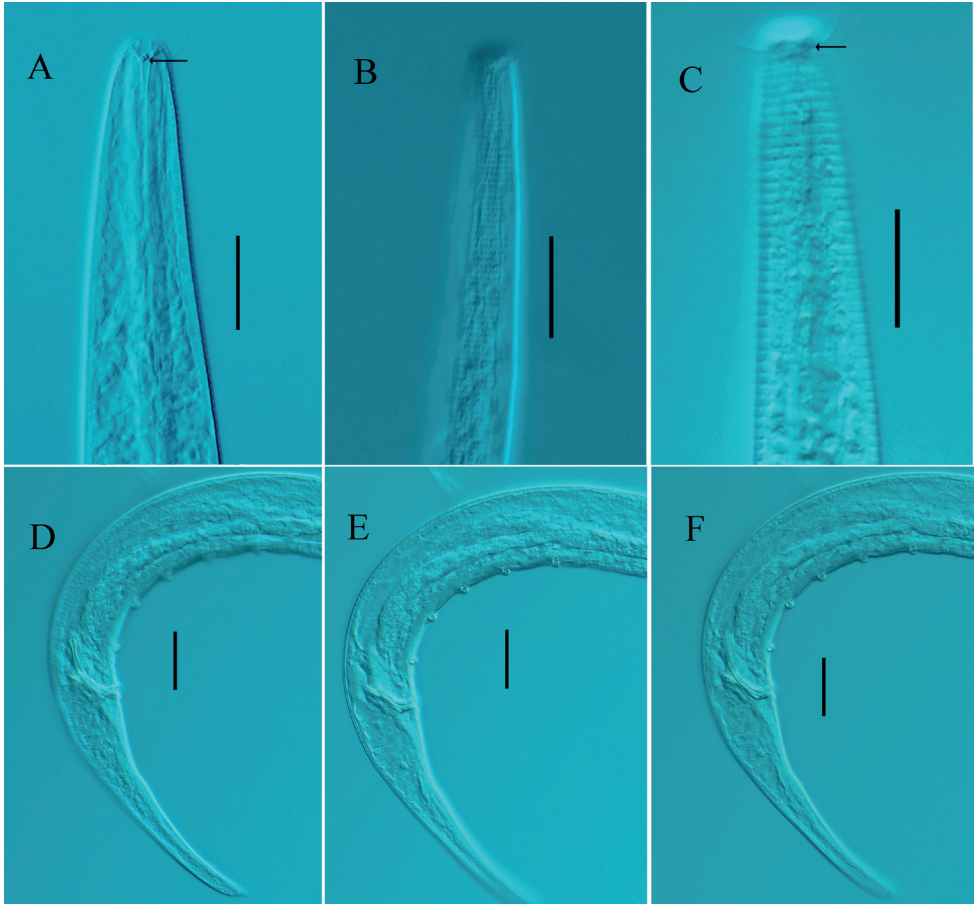


**Figure 3.** *Chromadorina communis* sp. nov. **A** lateral view of male anterior region showing buccal cavity and teeth (arrow) (holotype) **B** lateral view of male anterior region showing cuticle (holotype) **C** lateral view of female anterior region showing amphids (arrow) and cephalic setae (22YTCD6-2-1) **D-F** lateral view of male posterior body showing spicules, preloacal supplements, and gubernaculum (holotype). Scale bars: 20  $\mu$ m.

**Etymology.** Latin, *communis*, “common”.

**Differential diagnosis.** *Chromadorina communis* sp. nov. is similar to the cultured species *C. hirommi* Kito & Nakamura, 2001 in body length, length of cephalic setae, and numbers of preloacal supplements, but it differs in tooth shape (three equally sized teeth vs dorsal tooth large and subventral teeth small), absence of ocelli (brownish pigment present in *C. hirommi*), position of excretory pore (0.3 head diameter from anterior body end vs 1.8 head diameter from anterior body end), spicule length and shape (27–28  $\mu$ m, distal end tapered vs 22–25  $\mu$ m, distal end blunt and bifurcate), and gubernaculum shape (slightly cuticularized and boat-shaped vs well cuticularized with wavy dorsal fringe, distal parts of lateral pieces distinct and directed ventrad).

Eleven sequences of *Chromadorina* are included in the phylogenetic analysis, but only three species (*C. bioculata*, *C. germanica*, and *C. communis* sp. nov.) are identified to species, and *C. bioculata* was found in freshwater. *Chromadorina communis* sp. nov. shows a close relationship with *Chromadorina* sp. (KJ636255), but it differs by 3.1% (52 in 1678 bp, including three gaps). *Chromadorina communis* sp. nov. is supported as a new species by both phylogenetic and morphological analyses.

## Molecular phylogenetic relationships and analysis

The ML topology obtained with the SSU rRNA gene sequence is in accordance with the BI topology, and only the BI tree is shown (Fig. 4). The main Chromadorida clade is split into two major clades: Clade A composed of Selachinematidae and Chromadoridae and Clade B composed of Cyatholaimidae, Achromadoridae, Neotonchidae, and *Prodesmodora* (100% posterior probability and 74% bootstrap value). Ethmolaimidae (with one species only, *Ethmolaimus pratensis*) splits early from the main Chromadorida clade. Six Chromadorida families constitute well-supported monophyletic clades.

In clade A1, nine genera of Selachinematidae form a well-supported monophyletic group (100% posterior probability and 83% bootstrap value), but Selachinematinae and Choniolaiminae are not shown as monophyletic clades at the subfamily level. In Clade A2, Chromadoridae forms a well-supported monophyletic group (100% posterior probability and 96% bootstrap value). In the subfamily level, only Chromadorinae constitutes a monophyletic clade based on the BI analysis (93% posterior probability); however, it is weakly supported by the ML analysis (39% bootstrap value). Hypodontolaiminae and the genus *Endeolophos* (Euchromadorinae) constituted a monophyletic clade (97% posterior probability and 85% bootstrap value). *Endeolophos* shows a close relationship with the genus *Chromadorita*, which was highly supported by the BI analysis (100% posterior possibility), and it clustered with Hypodontolaiminae. The morphological characters of *Endeolophos*—cuticle homogeneous, amphidial fovea at the level of the cephalic setae, and gubernaculum without telamons—conform to the subfamily Hypodontolaiminae, while other characters—outer labial sensillar setiform, cuticular with complex structure, pharyngeal bulb absent, and precloacal supplements absent—conform to the Euchromadorinae (Tchesunov 2014). We prefer to keep *Endeolophos* in Euchromadorinae despite the molecular evidence.

*Chromadora* shows a close relationship with *Chromadorina* in clade A2, and Venekey et al. (2019) also noted this and explained this relationship as a result of a misidentification; there are great morphological similarities between *Chromadora* and *Chromadorina* (Venekey et al. 2019).

In clade B, *Gomphonema parvum* (clade B1) of family Neotonchidae split early, but it is weakly supported (65% posterior probability and 40% bootstrap value). The position of Neotonchidae has been uncertain for a long time. Platt (1982) united Neotonchinae and Ethmolaiminae into Ethmolaimidae with the holapomorphy of “cup-shaped precloacal supplements with an external articulated flange”, but this character was doubted by Lorenzen (1994), as it also occurs in *Dichromadora*. Tchesunov (2014) also considered the validity of the family Neotonchidae due to its mixed characters of

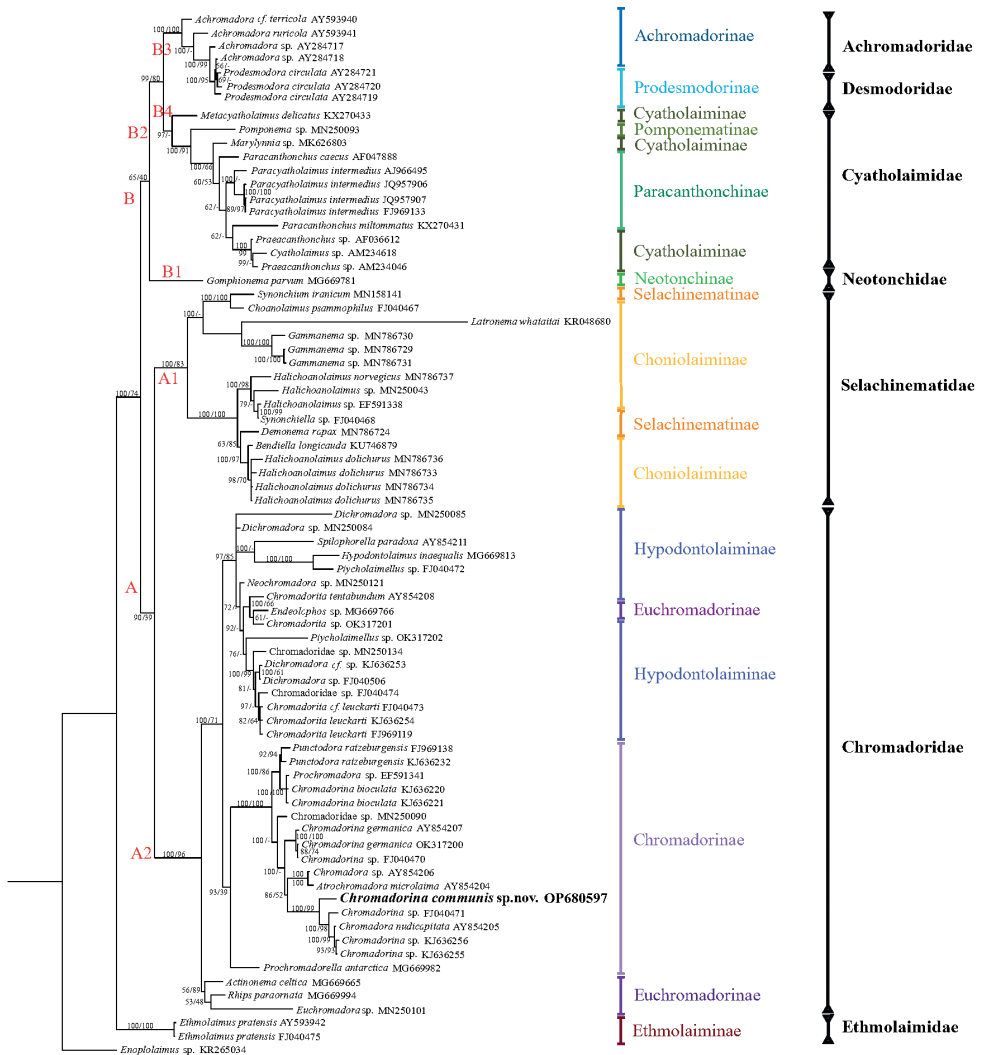


**Figure 4.** Bayesian inference tree of the order Chromadorida inferred from small subunit (SSU) sequences under the general time-reversible (GTR) + proportion of invariable sites (I) + gamma distribution (G) model. Posterior probability (left) and bootstrap values (right) are given on corresponding clades. The sequence obtained in this study is shown in bold. Subfamilies and families are listed on the right. Main clades are shown by red letters or letters with numbers. The scale stands for substitutions per site.

Chromadoridae, Cyatholaimidae, and Microlaimidae. According to our BI and ML analyses, Neotonchinae (clade B1) is a sister taxon to Achromadoridae (clade B2), *Prodesmodora* (clade B3), and Cyatholaimidae (clade B4), but there is no close relationship with Ethmolaiminae. This is in accordance with the topology tree by Leduc et al. (2017), but it is contrary to Bezerra et al.'s (2013) results based on morphological characters. We prefer to retain Neotonchidae until more molecular evidence is available.

In clade B3, two freshwater genera, *Achromadora* and *Prodesmodora*, form a highly supported clade (100% posterior probability and 100% bootstrap value). Lorenzen (1981, 1994) concluded that *Achromadora* is a holophyletic based on the the position of the ovary and prevailing parthenogenetic reproduction, and holapomorphy was presented in *Prodesmodora*. Taxonomic position of *Prodesmodora* should be reconsidered.

## Conclusions

*Chromadorina communis* sp. nov. is described based on morphological characteristics and distinguished from allied species by the absence of ocelli, a buccal cavity with three equally sized, solid teeth, curved spicules with a tapered distal end, simple and boat-shaped gubernaculums, and a conical tail with a very short spinneret. A phylogenetic analysis also supports the validity of the new species. With the description of *C. communis* sp. nov., 30 species of *Chromadorina* have been identified.

The phylogenetic analysis of Chromadorida show six families clustered into a monophyletic clade, and this conforms to the morphological taxonomy at the family level. The genus *Endeolophos* should be kept in Euchromadorinae based on morphological characters, and the position of family Neotonchidae should be considered as valid until further data are available.

## Acknowledgements

This work was supported by A Project of Shandong Province Higher Educational Science and Technology Program (no. J18KA152) and Open Project of Liaocheng University Animal Husbandry Discipline (319312101). We are very grateful to Dr Sergei Subbotin and two anonymous reviewers for their kind reviews and valuable suggestions, and Dr Wang Yanting for improvement of the manuscript.

## References

- Bezerra TN, Pape E, Hauquier F, Vanreusel A, Ingels J (2013) New genus and two new species of the family Ethmolaimidae (Nematoda: Chromadorida), found in two different cold-seep environments. *Zootaxa* 3692(1): 7–27. <https://doi.org/10.11646/zootaxa.3692.1.4>
- De Ley P, Blaxter ML (2002) Systematic position and phylogeny. In: Lee DL (Ed.) *The Biology of Nematodes*. Taylor & Francis, London. <https://doi.org/10.1201/b12614-2>
- De Ley P, Blaxter ML (2004) A new system for Nematoda: Combining morphological characters with molecular trees, and translating clades into ranks and taxa. *Nematology Monographs and Perspectives* 2: 633–653. [https://doi.org/10.1163/9789004475236\\_061](https://doi.org/10.1163/9789004475236_061)
- Hodda M (2022) Phylum Nematoda: A classification, catalogue and index of valid genera, with a census of valid species. *Zootaxa* 5114(1): 1–289. <https://doi.org/10.11646/zootaxa.5114.1.1>

- Holterman M, van der Wurff A, van den Elsen S, van Megen H, Bongers T, Holovachov O, Bakker J, Helder J (2006) Phylum-wide analysis of SSU rDNA reveals deep phylogenetic relationships among nematodes and accelerated evolution toward crown clades. *Molecular Biology and Evolution* 23(9): 1792–1800. <https://doi.org/10.1093/molbev/msl044>
- Holterman M, Holovachov O, van den Elsen S, van Megen H, Bongers T, Bakker J, Helder J (2008) Small subunit ribosomal DNA-based phylogeny of basal Chromadoria (Nematoda) suggests that transitions from marine to terrestrial habitats (and vice versa) require relatively simple adaptations. *Molecular Phylogenetics and Evolution* 48(2): 758–763. <https://doi.org/10.1016/j.ympev.2008.04.033>
- Holterman M, Schratzberger M, Helder J (2019) Nematodes as evolutionary commuters between marine, freshwater and terrestrial habitats. *Biological Journal of the Linnean Society* 128(3): 756–767. <https://doi.org/10.1093/biolinnean/blz107>
- Kito K, Nakamura T (2001) A new species of *Chromadorina* (Nematoda: Chromadoridae) discovered in a laboratory aquarium. *Species Diversity* 6(2): 111–116. <https://doi.org/10.12782/specdiv.6.111>
- Leduc D, Verdon V, Zhao ZQ (2017) Phylogenetic position of the Paramicrolaimidae, description of a new *Paramicrolaimus* species and erection of a new order to accommodate the Microlaimoidea (Nematoda: Chromadorea). *Zoological Journal of the Linnean Society* 183(1): 52–69. <https://doi.org/10.1093/zoolinnean/zlx072>
- Lorenzen S (1981) Entwurf eines phylogenetischen Systems der freilebenden Nematoden. Veröffentlichungen des Institut für Meeresforschung in Bremerhaven 7.
- Lorenzen S (1994) The Phylogenetic Systematics of Free-living Nematodes. The Ray Society, London.
- McIntyre AD, Warwick RM (1984) Meiofauna techniques. In: Holme NA, McIntyre AD (Eds) *Methods for the Study of Marine Benthos*. Blackwell Scientific Publications, Oxford, 217–244.
- Meldal BH, Debenham NJ, De Ley P, De Ley IT, Vanfleteren JR, Vierstraete AR, Bert W, Boronie G, Moens T, Tyler PA, Blaxter ML, Rogers AD, Lamshead PJD (2007) An improved molecular phylogeny of the Nematoda with special emphasis on marine taxa. *Molecular Phylogenetics and Evolution* 42(3): 622–636. <https://doi.org/10.1016/j.ympev.2006.08.025>
- Platt HM (1982) Revision of the Ethmolaimidae (Nematoda: Chromadorida). *Bulletin of the British Museum (Natural History). Zoology* 43(4): 185–252.
- Tchesunov AV (2014) Order Chromadorida Chitwood, 1933. In: Schmidt-Rhaesa A (Ed.) *Gastrotricha, Cycloneuralia, Gnathifera (Vol. 2), Nematoda. Handbook of Zoology*. De Gruyter, Berlin, 373–398. <https://doi.org/10.1515/9783110274257.373>
- Venekey V, Gheller PF, Kandraticus N, Cunha BP, Vilas-Boas AC, Fonseca G, Maria TF (2019) The state of the art of Chromadoridae (Nematoda, Chromadorida): a historical review, diagnoses and comments about valid and dubious genera and a list of valid species. *Zootaxa* 4578(1): 1–67. <https://doi.org/10.11646/zootaxa.4578.1.1>
- Wieser W (1954) Free-living marine nematodes II. Chromadoroidea. *Lunds Universitets Årsskrift (N.F.2)* 50(16): 1–148.
- Zhao Z, Li D, Davies KA, Ye W (2015) *Schistonchus zealandicus* n. sp. (Nematoda: Aphelenchoididae) associated with *Ficus macrophylla* in New Zealand. *Nematology* 17(1): 53–66. <https://doi.org/10.1163/15685411-00002851>



# Two new species of *Sinopoda* from China, with first description of the male of *S. horizontalis* Zhong, Cao & Liu, 2017 (Araneae, Sparassidae)

Jianshuang Zhang<sup>1</sup>, Yuanqian Xing<sup>2</sup>, Jinghui Yang<sup>2</sup>, Hao Yu<sup>1,2</sup>, Yang Zhong<sup>3,4</sup>

**1** The State Key Laboratory of Southwest Karst Mountain Biodiversity Conservation of Forestry, Administration, School of life sciences, Guizhou Normal University, Guiyang, China **2** School of Biological Sciences, Guizhou Education University, Guiyang, Guizhou, China **3** School of Nuclear Technology and Chemistry & Biology, Hubei University of Science and Technology, Xianning, Hubei, China **4** Administrative Commission of Jiugongshan National Nature Reserve of Hubei Xianning, Xianning, Hubei, China

Corresponding author: Yang Zhong ([hubeispider@aliyun.com](mailto:hubeispider@aliyun.com))

---

Academic editor: Gergin Blagoev | Received 6 February 2023 | Accepted 29 March 2023 | Published 2 May 2023

---

<https://zoobank.org/85B4CC9F-6985-4193-8B17-0257600CF650>

---

**Citation:** Zhang J, Xing Y, Yang J, Yu H, Zhong Y (2023) Two new species of *Sinopoda* from China, with first description of the male of *S. horizontalis* Zhong, Cao & Liu, 2017 (Araneae, Sparassidae). ZooKeys 1159: 133–155. <https://doi.org/10.3897/zookeys.1159.101535>

---

## Abstract

Three species of spider genus *Sinopoda* Jäger, 1999 are reported from southern China. Two of them are described as new to science: *S. guiyang* Zhang, Yu & Zhong, **sp. nov.** and *S. xishui* Zhang, Yu & Zhong, **sp. nov.**, both from Guizhou Province. The male of *S. horizontalis* Zhong, Cao & Liu, 2017 is described for the first time based on new material from the type locality, Wuyishan National Nature Reserve, Fujian Province, China. Detailed descriptions, diagnoses, photographs and a distribution map of the three species are provided.

## Keywords

Huntsman spider, morphology, new species, southern China, taxonomy

## Introduction

*Sinopoda* Jäger, 1999 is the fourth most species-rich genus of huntsman spider family Sparassidae after *Pseudopoda* Jäger, 2000 (251 species), *Heteropoda* Latreille, 1804 (189 species), and *Olios* Walckenaer, 1837 (166 species) (World Spider Catalog 2023; Zhang et al. 2023), including 139 species so far. *Sinopoda* is mainly distributed in eastern Asia, with 86 species recorded from East Asia, 50 species reported from Southeast Asia, and a single species described from India (Zhang et al. 2021; Zhong et al. 2022). Currently, a total of 73 *Sinopoda* species are known from China, representing 52.5% of the global species, making China the country with the most *Sinopoda* species (Zhang et al. 2021; Zhong et al. 2022; World Spider Catalog 2023). Despite this fact, the diversity of this genus in China is still not fully discovered as several new species have been described in each of the last few years (Zhong et al. 2017, 2018, 2019, 2022; Grall and Jäger 2020; Zhu et al. 2020; Wang et al. 2021).

While examining spiders collected from southern China, we have found some *Sinopoda* specimens that belong to three species: two of them from Guizhou Province, belong to undescribed species new to science; the remaining one from Wuyishan National Nature Reserve of Fujian Province, was identified as *Sinopoda horizontalis* Zhong, Cao & Liu, 2017 based on comparison with the type specimens (previously described based on a holotype female only). The goal of this paper is to describe the two new species under the names of *S. guiyang* Zhang, Yu & Zhong, sp. nov. and *S. xishui* Zhang, Yu & Zhong, sp. nov. and to redescribe *S. horizontalis*, describing the male for the first time.

## Materials and methods

Specimens in this study were collected by hand. The type specimens are deposited in the Museum of Guizhou Normal University, Guiyang, China. Specimens were preserved in 75 or 95% alcohol and examined using an Olympus SZX7 stereomicroscope. Left male palps were examined and illustrated after dissection. Epigynes were removed and cleared in a warm 10% potassium hydroxide (KOH) solution. The vulva was imaged after being embedded in Arabic gum. Images were captured with a Canon EOS 70D digital camera (20.2 megapixels) mounted on an Olympus CX41 compound microscope, and assembled using Helicon Focus ver. 6.80 image stacking software. All measurements were obtained using an Olympus SZX7 stereomicroscope and are given in millimetres. Eye diameters were measured at the widest part. The total body length does not include the chelicerae or spinnerets. Leg lengths are given as total length (femur, patella + tibia, metatarsus, tarsus). Numbers of macrosetae are listed for each segment in the following order: prolateral, dorsal, retrolateral and ventral (in femora and patellae ventral spines are absent and fourth digit is omitted in the setation formula). The distribution map was generated with ArcGIS ver. 10.5 (Environmental Systems Research Institute, Inc.). The terminology used in the text and figure legends follows Grall and Jäger (2020) and Zhong et al. (2019, 2022), and the abbreviations used in the text or figures are given in Table 1.

**Table 1.** List of abbreviations used in the text or figures.

Male palp	
C = conductor	EA = embolic apophysis
Cy = cymbium	EB = embolic base
RTA = retrolateral tibial apophysis	Sp = spermophor
dRTA = dorsal branch of RTA	St = subtegulum
vRTA = ventral branch of RTA	T = tegulum
E = embolus	
Epigyne	
AB = anterior band	LL = lateral lobe
FD = fertilization duct	LS = lobal septum
GA = glandular appendage	MS = membranous sac
ID = internal duct	PP = posterior part of spermathecae
Ocular area	
AER = anterior eye row	CH = clypeus height
ALE = anterior lateral eye	PER = posterior eye row
AME = anterior median eye	PLE = posterior lateral eye
AME–ALE = distance between AME and ALE	PME = posterior median eye
AME–AME = distance between AMEs	PME–PLE = distance between PME and PLE
AME–PLE = distance between AME and PLE	PME–PME = distance between PMEs
AME–PME = distance between AME and PME	

## Taxonomy

### Family Sparassidae Bertkau, 1872

### Subfamily Heteropodinae Thorell, 1873

### Genus *Sinopoda* Jäger, 1999

**Type species.** *Sarotes forcipatus* Karsch, 1881 from China and Japan.

**Diagnosis.** See Jäger (1999), Liu et al. (2008), Zhang et al. (2015) and Grall and Jäger (2020).

**Composition and infrageneric groupings.** See WSC (2023) and Zhang et al. (2021).

### *Sinopoda guiyang* Zhang, Yu & Zhong, sp. nov.

<https://zoobank.org/425C8C5A-625C-4344-A882-373C7D5F440B>

Figs 1–3, 9

**Type material.** *Holotype* ♂ (YHSPA001), CHINA: Guizhou Province: Guiyang City: Xinpu Town, Xiangzhigou, Nanjing temple, 26.75°N, 106.93°E, c. 1092 m, by hand, 14.VI.2017, H. Yu et al. leg. *Paratypes*: 2♂3♀ (YHSPA002–006), same data as holotype.

**Etymology.** The species name is derived from the name of the type locality; noun in apposition.

**Diagnosis.** The males of new species resemble those of *S. ovata* Zhong, Jäger, Chen & Liu, 2019 and *S. triangula* Liu, Li & Jäger, 2008 in having a short vRTA with rough apex, and a long, finger-like dRTA (Fig. 1A, B, D; Zhong et al. 2019: figs 43B, C, 44B, C; Liu et al. 2008: fig. 7B, C), but differ by: (1) subdistal embolus without triangular

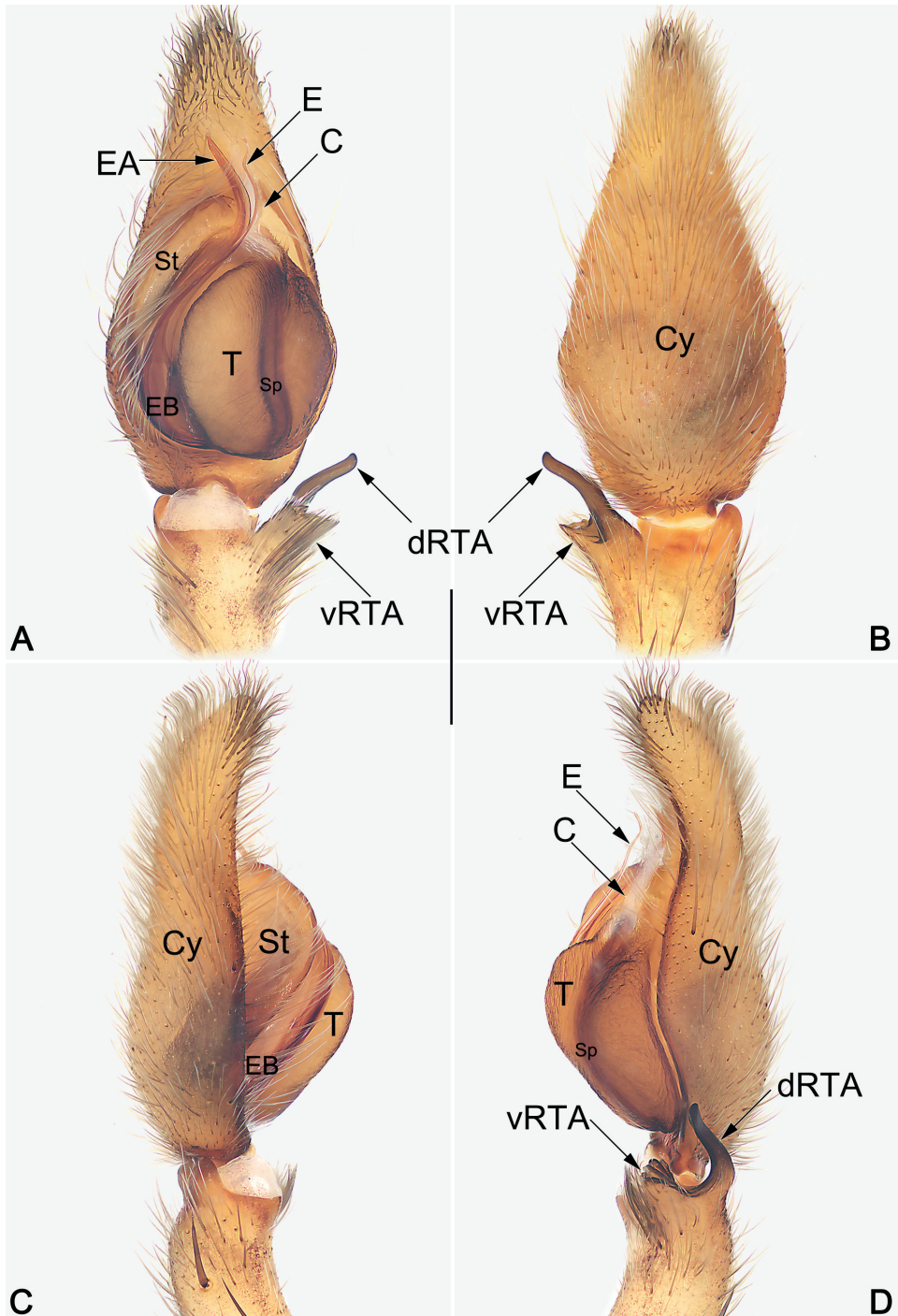


**Figure 1.** Male palp of the holotype of *Sinopoda guiyang* sp. nov. **A** ventral view **B** dorsal view **C** pro-lateral view **D** retrolateral view. Abbreviations: C = conductor; Cy = cymbium; dRTA = dorsal branch of RTA; E = embolus; EA = embolic apophysis; EB = embolic base; Sp = spermophor; St = subtegulum; T = regulum; vRTA = ventral branch of RTA. Scale bar: 0.5 mm (equal for **A–D**).

projection (vs. with a triangular projection) (cf. Figs 1A, D, 2A–C and Zhong et al. 2019: figs 43A, B, 44A, B and Liu et al. 2008: fig. 7A, B, D–F); (2) embolus whip-like or filiform, distinctly thin (vs. relatively thicker, distally wide) (cf. Figs 1A, D, 2A–C and Zhong et al. 2019: figs 43A, B, 44A, B and Liu et al. 2008: fig. 7A, B, D–F); (3) apex of vRTA with four ridges (vs. without ridges) (cf. Fig. 1D and Zhong et al. 2019: figs 43C, 44C and Liu et al. 2008: fig. 7C). Females also resemble those of *S. ovata* and *S. triangula* by the general shape of vulva but can be recognized by the thumb-like glandular appendages extend transversally (vs. finger-like and descend obliquely) (cf. Fig. 3C and Zhong et al. 2019: figs 43E, 45B and Liu et al. 2008: fig. 7H).

**Description. Male (YHSPA001).** Total length 8.4. Prosoma 4.0 long, 3.4 wide, anterior width of prosoma 2.6. Opisthosoma 4.4 long, 2.6 wide. **Eye sizes and interdistances:** AME 0.18, ALE 0.26, PME 0.18, PLE 0.27, AME–AME 0.19, AME–ALE 0.09, PME–PME 0.24, PME–PLE 0.35, AME–PME 0.33, ALE–PLE 0.28, CH AME 0.21, CH ALE 0.23. **Spination:** Palp: 131, 101, 1021; Fe: I–III 323, IV 321; Pa: I–IV 101; Ti: I 2024, II–III 2126, IV 2226; Mt: I–II 2024, III–IV 3036. **Measurements of palp and legs:** Palp 6.3 (2.2, 1.3, 1.1, 1.7), I 15.5 (3.8, 1.9, 4.4, 4.0, 1.4), II 17.5 (4.8, 1.9, 4.7, 4.5, 1.6), III 14.1 (4.4, 1.5, 3.6, 3.3, 1.3), IV 15.4 (4.4, 1.7, 3.6, 4.1, 1.6). Leg formula: II-I-IV-III. Cheliceral furrow with three anterior and four posterior teeth, and with ~ 35 denticles.

**Colouration in ethanol (Fig. 2D, E).** Prosoma yellowish-brown, anteriorly and medially yellowish, lateral and posterior margin dark brown, with shallow fovea and radial furrows. Chelicerae light brown. Sternum yellowish-white, margin yellowish. Endites and labium uniformly yellowish-white. Legs dark yellowish-brown, covered by short spines. Opisthosoma oval, dorsum brown, marginally with two longitudinal and dark brown bands reaching posterior half, median part with four pairs of inconspicuous purplish dots; venter uniformly gray.

**Palp (Figs 1, 2A–C).** Cymbium distinctly longer than tibia. Embolus filiform, 2-shaped in ventral view, arising at approximately the 8–9 o'clock position, terminating at c. 12 o'clock position. Conductor long, membranous, c. 2/3 of the tegulum length, originating at 12–1 o'clock position portion of tegulum. Tegulum oval, slightly bulged, medially with distinct and slightly curved spermophore, proximally covering embolic base. RTA arising mesially to distally from tibia, ventrally with distinct brush of stiff setae. dRTA slender, finger-shaped; vRTA round, apex with four ridges.

**Female (YHSPA002).** Total length 10.3. Prosoma 4.2 long, 3.6 wide, anterior width of prosoma 2.8. Opisthosoma 6.1 long, 4.6 wide. **Eye sizes and interdistances:** AME 0.17, ALE 0.24, PME 0.20, PLE 0.29, AME–AME 0.21, AME–ALE 0.10, PME–PME 0.27, PME–PLE 0.39, AME–PME 0.39, ALE–PLE 0.34, CH AME 0.23, CH ALE 0.26. **Spination:** Palp: 131, 101, 2026, 1014; Fe: I–III 323, IV 321; Pa: I–IV 000; Ti: I–III 2026, IV 2126; Mt: I–II 1014, III 2026, IV 3036. **Measurements of palp and legs:** Palp 5.0 (1.5, 0.9, 1.0, 1.6), I 12.2 (3.3, 1.5, 3.0, 3.2, 1.2), II 12.7 (3.8, 1.8, 3.2, 2.8, 1.1), III 10.3 (3.0, 1.6, 2.7, 2.1, 0.9), IV 11.9 (3.5, 1.7, 2.9, 2.7, 1.1). Leg formula: II-I-IV-III. Cheliceral furrow with three anterior and four posterior teeth, and with ~ 42 denticles. Colouration in ethanol as in males, but generally slightly darker (Fig. 3D, E).

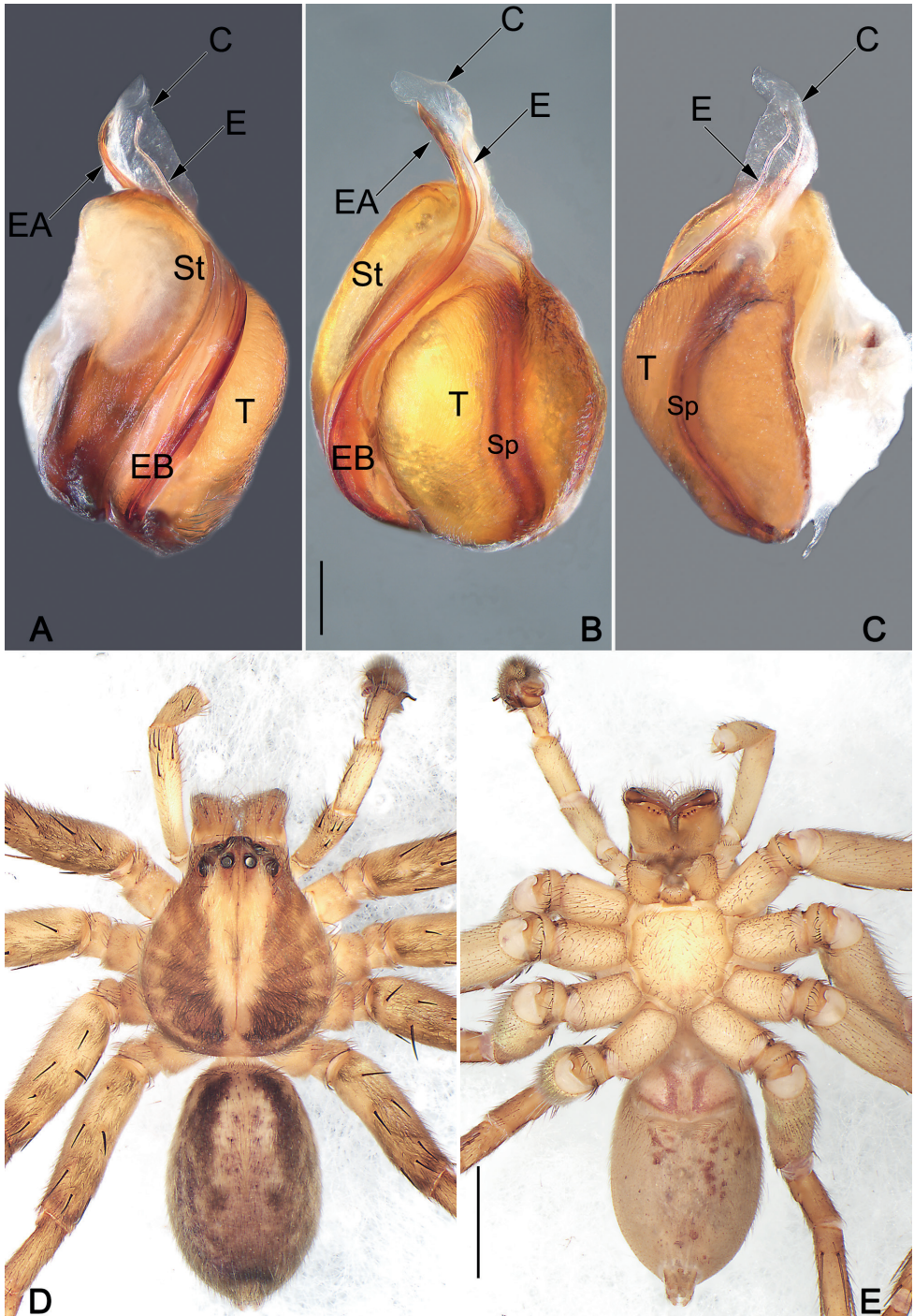


**Figure 2.** *Sinopoda guiyang* sp. nov., male holotype, palpal bulb (**A–C**) and habitus (**D, E**) **A** prolateral view **B** ventral view **C** retrolateral view **D** dorsal view **E** ventral view. Abbreviations: C = conductor; E = embolus; EA = embolic apophysis; EB = embolic base; Sp = spermophor; St = subtegulum; T = tegulum. Scale bars: 0.2 mm (equal for **A–C**); 2 mm (equal for **D, E**).

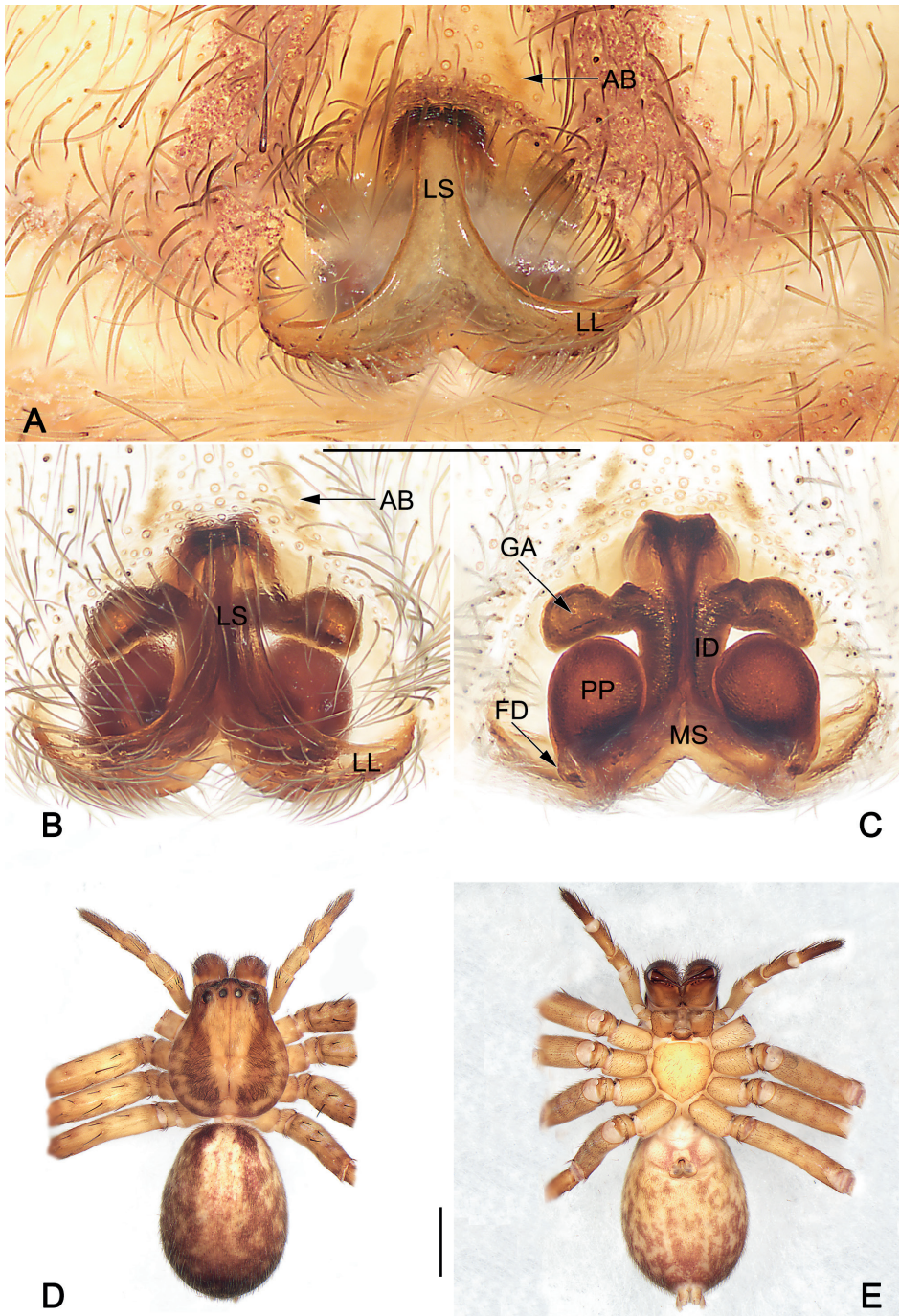


**Figure 3.** *Sinopoda guiyang* sp. nov., female paratype, epigyne (**A–C**) and habitus (**D, E**) **A** intact, ventral view **B** cleared and macerated, ventral view **C** cleared and macerated, dorsal view **D** dorsal view **E** ventral view. AB = anterior band; FD = fertilization duct; GA = glandular appendage; ID = internal duct; LL = lateral lobe; LS = lobal septum; MS = membranous sac; PP = posterior part of spermathecae. Scale bars: 0.5 mm (equal for **A–C**); 2 mm (equal for **D, E**).

**Copulatory organ (Fig. 3A–C).** Epigynal field wider than long, with short and indistinct anterior bands, slit sensillum absent. Lobal septum wide, anterior part about 1/10 width of epigynal plate, gradually wider to the posterior. Lateral lobes fused, with small median incision and posterior margin slightly bilobed. Internal ducts running parallel along median line. Glandular appendages thumb-like, extend transversally. Posterior part of spermathecae balloon-shaped, relatively large, c. 1.6 times longer than wide; the two PP separated by about 0.8 width. Fertilization ducts acicular, membranous, located on dorsal-basal surface of spermathecae. Membranous sac between fertilization ducts, more or less triangular.

**Distribution.** Known only from the type locality, Guiyang City, Guizhou, China (Fig. 9).

**Comments.** *Sinopoda guiyang* sp. nov. possesses several characters associated with the *globosa*-group (currently comprises six species, see Zhang et al. 2021: 15, fig. 4) and resembles *S. ovata* and *S. triangula* (the core species of the *globosa*-group) for their characteristic genital organs (for a detailed diagnosis, see above), but can be distinguished from all members of the *globosa*-group by the absence of triangular projection in the embolus. Because the embolus of all *S. globosa*-group species has a subdistally triangular projection, there remains considerable uncertainty about placing this new species into the *globosa*-group.

### ***Sinopoda horizontalis* Zhong, Cao & Liu, 2017**

Figs 4–6, 9

*Sinopoda horizontalis* Zhong, Cao & Liu, 2017: 157, figs 5A, B, 6A, B, 15A, B (♀).

**Holotype examined.** ♀ (ZY-2013-SPA007), CHINA: Fujian Province: Wuyishan City, Wuyishan National Nature Reserve, 27.35°N, 117.29°E, c. 1152 m, by hand, 16 VI 2013, Y. Zhong and X.W. Cao leg.

**New material examined.** 3♂, 1♀ (ZY-2021-SPA011–014). Same locality as holotype, by hand, 16.VI.2021, Y. Zhong leg.

**Diagnosis.** Males of *S. horizontalis* resemble those of *S. hamata* (Fox, 1937) and *S. liui* Zhong, Cao & Liu, 2017 in the general shape of the male palp. The palps of the three species share the similarly shaped conductor and embolus, and the distinctly long, ribbon-shaped dRTA which with lumpy margins, but differ in the following: the vRTA digitiform, distinctly longer than wide, apex blunt in *S. horizontalis* (vs. laminar, distinctly wider than long in *S. hamata*, thumb-shaped, apex beak-shaped and relatively sharper in *S. liui*) (cf. Fig. 4A, B, D and Zhong et al. 2018: figs 6C, 7C and Zhong et al. 2019: figs 31C, 32C). Females also resemble those of *S. hamata* and *S. liui* in having the strongly narrow lobal septum anteriorly, and the distinctly bilobed posterior margin of epigynal plate, but can be recognised from *S. hamata* by the internal ducts running parallel along median line (vs. convergent anteriorly but distinctly oblique posteriorly) (cf. Fig. 6C–F and Zhong et al. 2018: figs 6D, E, 7D, E); and from *S. liui* can be recognised by the posterior part of spermathecae are proportionately longer, nearly 2/5 length of internal

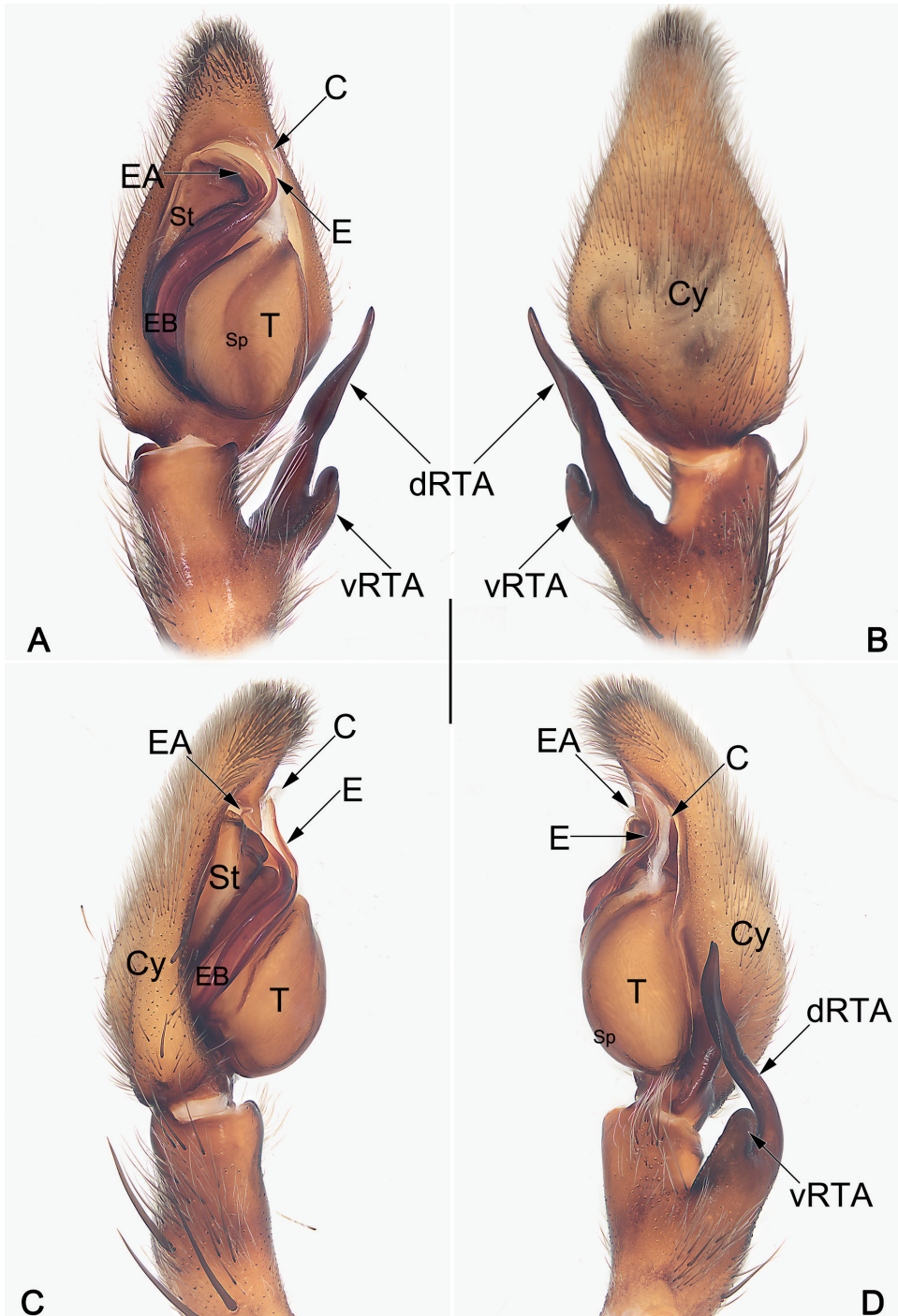


**Figure 4.** Male palp of the toptype of *Sinopoda horizontalis* **A** ventral view **B** dorsal view **C** prolateral view **D** retrolateral view. Abbreviations: C = conductor; Cy = cymbium; dRTA = dorsal branch of RTA; E = embolus; EA = embolic apophysis; EB = embolic base; Sp = sperophor; St = subtegulum; T = tegulum; vRTA = ventral branch of RTA. Scale bar: 1 mm (equal for **A–D**).

ducts (vs. proportionately much shorter, no more than 1/4 length of internal ducts) (cf. Fig. 6C–F and Zhong et al. 2019: fig. 33B and Zhong et al. 2017: figs 5D, 6D).

**Description. Male (ZY-2021-SPA011).** Total length 14.8. Prosoma 7.0 long, 6.7 wide, anterior width of prosoma 3.4. Opisthosoma 7.8 long, 5.2 wide. **Eye sizes and interdistances:** AME 0.24, ALE 0.45, PME 0.22, PLE 0.50, AME–AME 0.21, AME–ALE 0.13, PME–PME 0.41, PME–PLE 0.38, AME–PME 0.48, ALE–PLE 0.40, CH AME 0.29, CH ALE 0.35. **Spination:** Palp: 131, 101, 1021; Fe: I–III 323, IV 321; Pa: I–IV 101; Ti: I–IV 2226; Mt: I–II 1014, III 2026, IV 3036. **Measurements of palp and legs:** Palp 9.7 (2.8, 2.0, 2.1, 2.8), I 34.0 (9.9, 3.8, 8.4, 8.9, 3.0), II 35.8 (10.6, 3.8, 9.0, 9.5, 2.9), III 27.7 (7.8, 3.6, 7.2, 7.0, 2.1), IV 28.9 (8.6, 3.1, 7.0, 7.7, 2.5). Leg formula: II-I-IV-III. Cheliceral furrow with three anterior and four posterior teeth, and with ~ 32 denticles.

**Colouration in ethanol (Fig. 5D, E).** Prosoma dark yellowish to brown, with yellow submarginal transversal band at posterior part. Median band of prosoma bright yellowish-brown, lateral bands brown and not distinctly delimited to median band. Fovea and radial furrows distinctly marked. Chelicerae dark reddish-brown. Sternum light yellow, margin slightly darker. Endites and labium yellowish, both with distal parts brighter. Legs dark yellowish-brown, covered by short spines. Dorsal opisthosoma brown, with an irregular yellow media band, reaching 2/3 of abdomen length, with five pairs of inconspicuous black dots on each side; ventral opisthosoma yellowish-brown with irregular pattern and two longitudinal yellow lines between epigastric furrow and spinnerets.

**Palp (Figs 4, 5A–C).** Cymbium distinctly longer than tibia. Embolus filiform, 2-shaped, arising from tegulum at nearly the 7–8 o'clock position in ventral view, terminating at c. 12 o'clock position. Conductor long, c. 2/3 of the tegulum length, curving medially, arising at 12–1 o'clock position from tegulum. Tegulum oval, slightly bulged, medially with distinct spermophore, proximally covering embolic base; spermophore <-shaped in ventral view. RTA arising mesially to distally from tibia, ventrally with distinct brush of stiff setae. dRTA ribbon-shaped, distinctly long, curved and tapering, almost extending media part of cymbium; vRTA digitiform, relatively short, about 1/2 of tibia length, apex round.

**Female (ZY-2021-SPA014).** Total length 14.9. Prosoma 7.6 long, 7.3 wide, anterior width of prosoma 4.5. Opisthosoma 9.3 long, 5.8 wide. **Eye sizes and interdistances:** AME 0.30, ALE 0.48, PME 0.36, PLE 0.58, AME–AME 0.25, AME–ALE 0.17, PME–PME 0.45, PME–PLE 0.61, AME–PME 0.62, ALE–PLE 0.66, CH AME 0.31, CH ALE 0.45. **Spination:** Palp: 131, 101, 2121, 1014; Fe: I–III 323, IV 321; Pa: I–IV 101; Ti: I–III 2024, IV 2124; Mt: I–II 1014, III 2026, IV 3036. **Measurements of palp and legs:** Palp 9.6 (2.8, 1.4, 2.2, 3.2), I 24.3 (6.3, 2.6, 6.3, 6.6, 2.5), II 25.9 (8.3, 3.3, 7.1, 5.2, 2.0), III 20.2 (7.7, 3.4, 3.6, 3.8, 1.7), IV 22.2 (7.1, 2.5, 5.8, 4.9, 1.9). Leg formula: II-IV-III-I. Cheliceral furrow with three anterior and four posterior teeth, and with ~ 40 denticles. Colouration in ethanol as in males, but body slightly darker (Fig. 6A, B; see Zhong et al. (2017) for others described). Copulatory organ as in Fig. 6C, D (topotype) and Fig. 6E, F (holotype).

**Distribution.** Known only from the type locality, Wuyishan National Nature Reserve, Fujian, China (Fig. 9).

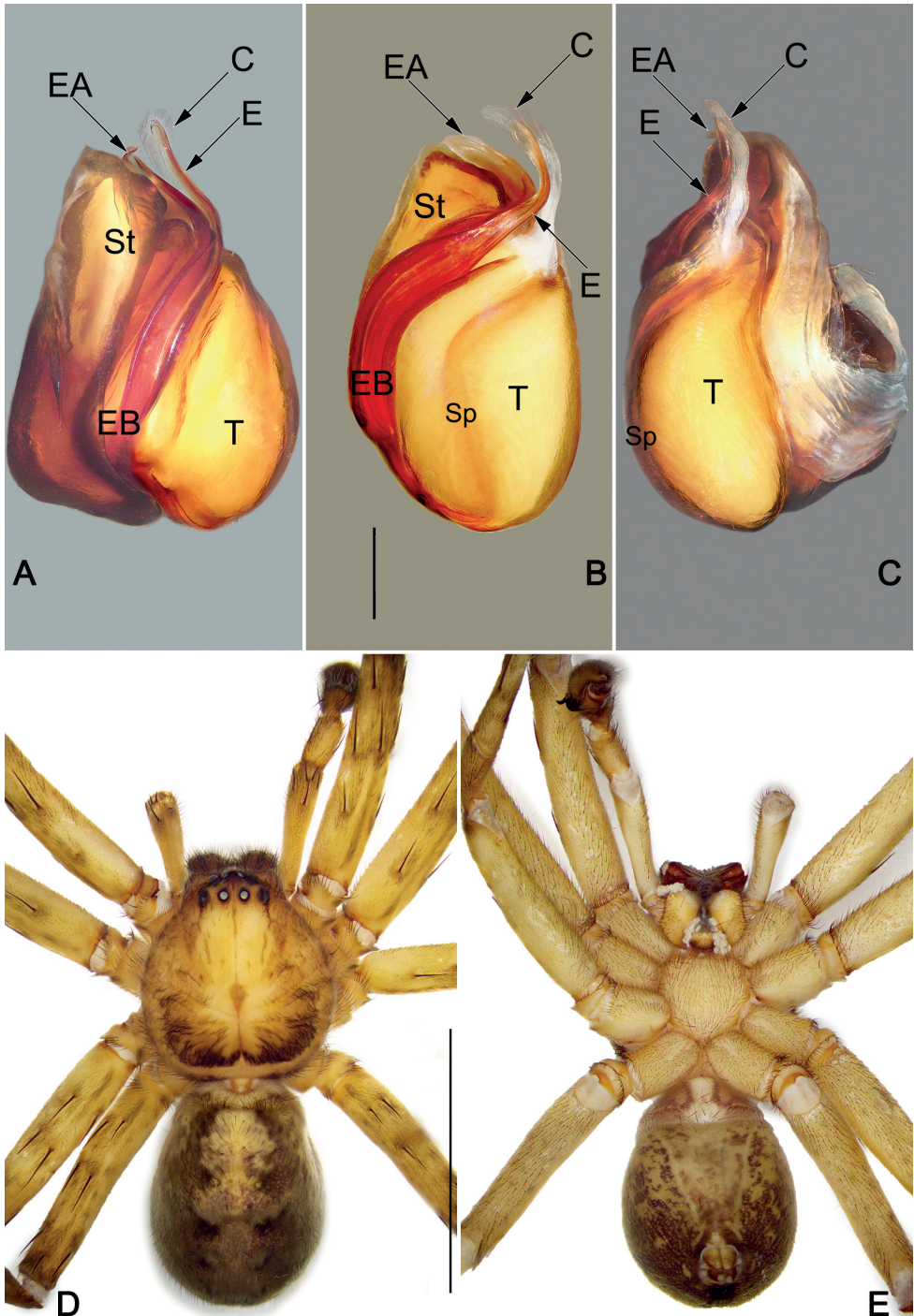


**Figure 5.** *Sinopoda horizontalis*, male topotype, palpal bulb (**A–C**) and habitus (**D, E**) **A** prolateral view **B** ventral view **C** retrolateral view **D** dorsal view **E** ventral view. Abbreviations: C = conductor; E = embolus; EA = embolic apophysis; EB = embolic base; Sp = spermophor; St = subtegulum; T = tegulum. Scale bars: 0.2 mm (equal for **A–C**); 5 mm (equal for **D, E**).

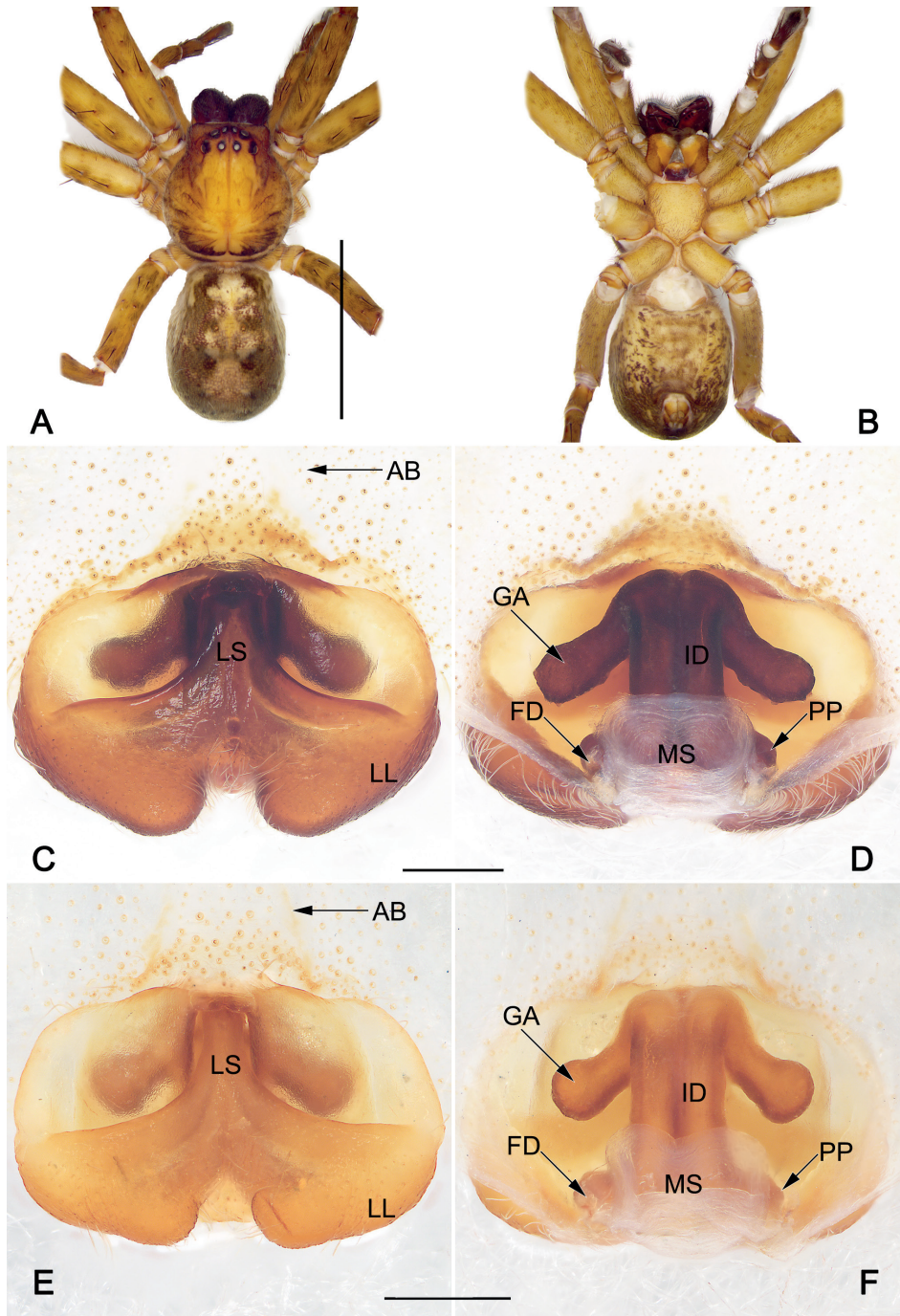


**Figure 6.** *Sinopoda horizontalis*, habitus (A,B) and epigyne (C,D) of female topotype, and epigyne (E,F) of female holotype **A** dorsal view **B** ventral view **C, E** cleared and macerated, ventral view **D, F** cleared and macerated, dorsal view. AB = anterior band; FD = fertilization duct; GA = glandular appendage; ID = internal duct; LL = lateral lobe; LS = lobal septum; MS = membranous sac; PP = posterior part of spermathecae. Scale bars: 5 mm (equal for A, B); 0.5 mm (equal for C, D, equal for E, F).

***Sinopoda xishui* Zhang, Yu & Zhong, sp. nov.**

<https://zoobank.org/75A10745-DBF5-4845-905C-D2CB6DE32005>

Figs 7–9

**Type material.** *Holotype* ♀ (YHSPA007), CHINA: Guizhou Province: Zunyi City: Xishui County, Xishui National Nature Reserve, Sanchahe Town, Hongyangou Village, 28.50°N, 106.40°E, c. 934 m, by hand, 23.V.2022, H. Yu et al. leg. *Paratype*: 1 ♀, same data as holotype.

**Etymology.** The species name is derived from the name of the type locality; noun in apposition.

**Diagnosis.** Females of this new species resembles those of *S. yaanensis* Zhong, Jäger, Chen & Liu, 2019 in having similar vulva with swollen, globular glandular appendages, and oval shaped posterior part of spermathecae, but can be distinguished by: (1) lobal septum distinctly wider, its anterior part about 1/5 width of epigynal plate (Fig. 7A, B) (vs. relatively narrower, its anterior part about 1/8–1/9 width of epigynal plate; Zhang et al. 2015: figs 40, 46; Zhong et al. 2019: fig. 57E); and (2) the anterior part of internal ducts far from the anterior margin of epigynal plate (Fig. 7C) (vs. reach the anterior margin of epigynal plate; Zhang et al. 2015: fig. 41; Zhong et al. 2019: fig. 57J).

**Description. Female (YHSPA007).** Total length 16.4. Prosoma 7.7 long, 6.8 wide, anterior width of prosoma 4.2. Opisthosoma 8.7 long, 6.1 wide. **Eye sizes and interdistances:** AME 0.35, ALE 0.44, PME 0.38, PLE 0.48, AME–AME 0.28, AME–ALE 0.14, PME–PME 0.44, PME–PLE 0.53, AME–PME 0.52, ALE–PLE 1.44, CH AME 0.32, CH ALE 0.37. **Spination:** Palp: 131, 101, 2121, 1014; Fe: I–III 323, IV 321; Pa: I–IV 101; Ti: I–III 2026, IV 2126; Mt: I–II 1014, III 2026, IV 3036. **Measurements of palp and legs:** Palp 9.8 (3.0, 1.6, 2.1, 3.1), I 26.8 (7.8, 2.4, 7.8, 6.5, 2.3), II 29.1 (8.9, 2.8, 8.2, 7.1, 2.1), III 24.2 (7.6, 3.1, 6.3, 5.1, 2.1), IV 24.7 (6.7, 2.4, 7.3, 6.1, 2.2). Leg formula: II-I-IV-III. Cheliceral furrow with two anterior and four posterior teeth, and with ~ 38 denticles.

Colour of the living holotype female was uniformly dark except brown femur (Fig. 8A). Colouration in ethanol (Fig. 7D, E): Prosoma dark yellowish to brown, with bright yellow submarginal transversal band at posterior part. Median band of prosoma bright yellowish, anteriorly as wide as PER, gradually narrowing posteriorly; lateral bands brown, distinctly delimited to median band, starting from PLE, reaching dark reddish submarginal transversal band. Fovea and radial furrows distinctly marked. Chelicerae yellowish-brown. Sternum bright yellow, margin slightly darker. Endites and labium yellowish. Legs yellowish-brown, covered by short spines. Dorsal opisthosoma dark brown, anteriorly with a small ‘)‘(-shaped yellow pattern, with three pairs of inconspicuous dots on each side; ventral opisthosoma dark, with several transversal folds.

**Copulatory organ (Fig. 7A–C).** Epigynal field wider than long, anterior bands nearly invisible indistinct, slit sensillum absent. Lobal septum wide, anterior part about 1/5 width of epigynal plate, gradually wider to the posterior. Lateral lobes fused, posterior margin slightly bilobed, medially with small incision. Internal ducts running parallel along the middle line. Glandular appendages distinctly inflated, globular; the

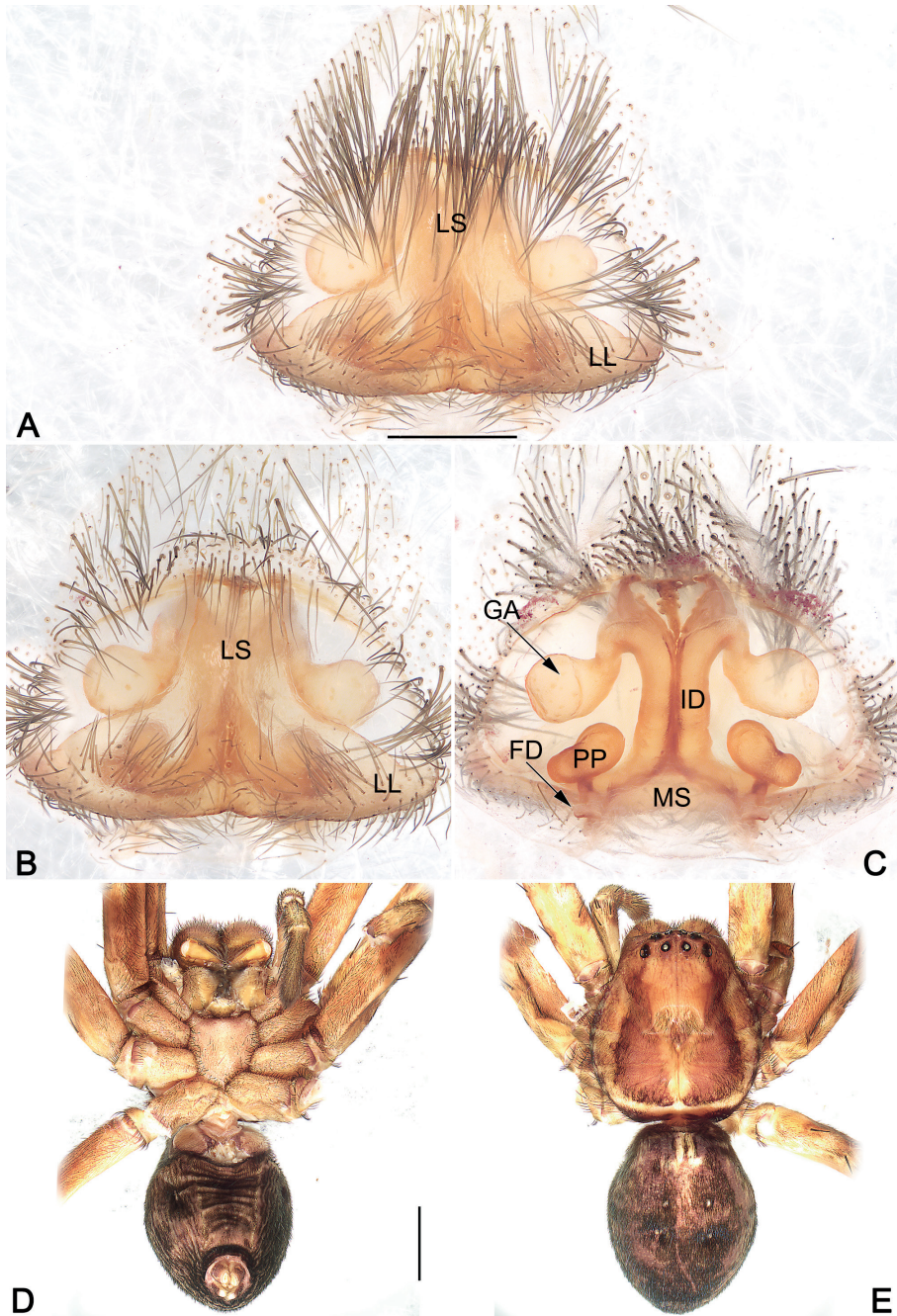


**Figure 7.** *Sinopoda xishui* sp. nov., female holotype, epigyne (**A–C**) and habitus (**D, E**) **A** macerated, ventral view **B** cleared and macerated, ventral view **C** cleared and macerated, dorsal view **D** dorsal view **E** ventral view. FD = fertilization duct; GA = glandular appendage; ID = internal duct; LL = lateral lobe; LS = lobal septum; MS = membranous sac; PP = posterior part of spermathecae. Scale bars: 0.5 mm (equal for **A–C**); 3 mm (equal for **D, E**).



**Figure 8.** *Sinopoda xishui* sp. nov., female holotype (A) and paratype (B), live specimens. Photographs by Qianle Lu (Shenzhen, Guangdong).

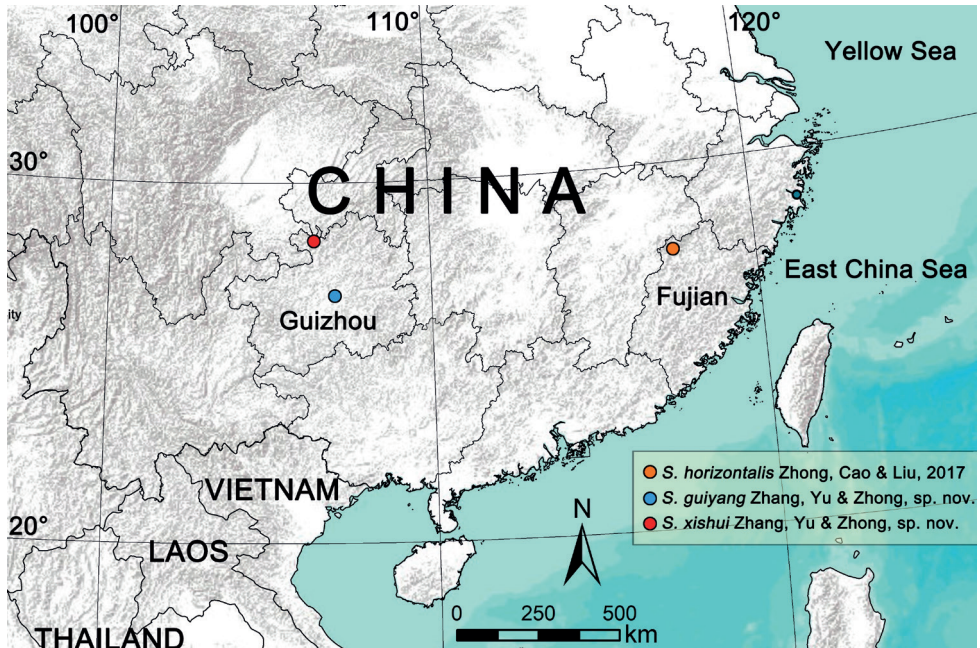


**Figure 9.** Distribution records of the *Sinopoda* species treated in this paper: *S. horizontalis* Zhong, Cao & Liu, 2017 (orange circle: Fujian Province: Wuyishan City, Wuyishan National Nature Reserve), *S. guiyang* sp. nov. (blue circle: Guizhou Province, Guiyang City, Xinpu Town, Xiangzhigou), *S. xishui* sp. nov. (red circle: Guizhou Province, Zunyi City, Xishui National Nature Reserve).

two GA widely separated by about  $3\times$  diameters. Posterior part of spermathecae more or less bean-shaped, c. 1.9 times longer than wide; the two PP separated by about 2.3 width. Fertilization ducts acicular, membranous, located on posterior surface of spermathecae. Membranous sac between fertilization ducts, nearly trapezoidal.

**Male.** Unknown.

**Distribution.** Known only from the type locality, Xishui National Nature Reserve, Guizhou, China (Fig. 9).

**Comments.** The females of *S. xishui* sp. nov. exhibit typical *globosa*-group features (internal ducts running parallel along median line, and with ovate posterior parts of spermathecae, as diagnosed in Zhang et al. (2021)), and resembles *S. yaanensis* (the core species of the *globosa*-group) (for a detailed diagnosis, see above). However, this species is not readily assignable to the *globosa*-group due to the lack of an available male specimen.

## Acknowledgements

We thank Jie Liu (Wuhan, China), and Tamás Szűts (Budapest, Hungary) for providing constructive comments on an earlier version of the manuscript. We are espe-

cially grateful to Gergin Blagoev (Guelph, Canada), the subject editor of this manuscript. This work was supported by the National Natural Sciences Foundation of China (NSFC-32060113/31702006/32000303), the Natural Science Foundation of Guizhou Province (J [2020] 1Y081), the Project of Biodiversity Survey and Assessment in Guiyang (GZZC-2021-018), the Joint Fund of the National Natural Science Foundation of China and the Karst Science Research Center of Guizhou Province (Grant No. U1812401), the Natural Sciences Foundation of Xianning City (2022ZRKX063), the Scientific Research Project of Education Department of Hubei Province (Q20222806), and the program of Hubei University of Science and Technology (2021ZX12), the Guizhou Education University Academic Discipline Project (2019YLPYXKB01), the Second Scientific Expedition Project of Xishui National Nature Reserve, and Guizhou provincial first-class major (biological science) project (Education department of Guizhou Province [2019] 46).

## References

- Grall E, Jäger P (2020) Forty-seven new species of *Sinopoda* from Asia with a considerable extension of the distribution range to the south and description of a new species group (Sparassidae: Heteropodinae). *Zootaxa* 4797(1): 1–101. <https://doi.org/10.11646/zootaxa.4797.1.1>
- Jäger P (1999) *Sinopoda*, a new genus of Heteropodinae (Araneae, Sparassidae) from Asia. *The Journal of Arachnology* 27: 19–24.
- Liu J, Li SQ, Jäger P (2008) New cave-dwelling huntsman spider species of the genus *Sinopoda* (Araneae: Sparassidae) from southern China. *Zootaxa* 1857(1): 1–20. <https://doi.org/10.11646/zootaxa.1857.1.1>
- Wang ZY, Liang W, Li SQ (2021) Five new *Sinopoda* species (Araneae, Sparassidae) from China and Thailand. *ZooKeys* 1012: 1–19. <https://doi.org/10.3897/zookeys.1012.59854>
- World Spider Catalog WSC (2023) World Spider Catalog, version 24.0. Natural History Museum, Bern. <https://doi.org/10.24436/2> [Accessed on 02 April 2023]
- Zhang BS, Zhang ZS, Zhang F (2015) Three new *Sinopoda* species (Araneae: Sparassidae) from southern China. *Zootaxa* 3974(1): 59–75. <https://doi.org/10.11646/zootaxa.3974.1.4>
- Zhang H, Zhong Y, Zhu Y, Agnarsson I, Liu J (2021) A molecular phylogeny of the Chinese *Sinopoda* spiders (Sparassidae, Heteropodinae): implications for taxonomy. *PeerJ* 9: e11775. [26 pp] <https://doi.org/10.7717/peerj.11775>
- Zhang H, Zhu Y, Zhong Y, Jäger P, Liu J (2023) A taxonomic revision of the spider genus *Pseudopoda* Jäger, 2000 (Araneae: Sparassidae) from East, South and Southeast Asia. *Megataxa* 9(1): 1–304. <https://doi.org/10.11646/megataxa.9.1.1>
- Zhong Y, Cao XW, Liu J (2017) Six *Sinopoda* species (Araneae: Sparassidae) from Fujian and Yunnan Provinces in China. *Zootaxa* 4227(2): 151–172. <https://doi.org/10.11646/zootaxa.4227.2.1>
- Zhong Y, Jäger P, Chen J, Liu J (2018) Taxonomic review of the *Sinopoda okinawana*-group (Araneae: Sparassidae) in China. *Zootaxa* 4388(3): 328–346. <https://doi.org/10.11646/zootaxa.4388.3.2>

- Zhong Y, Jäger P, Chen J, Liu J (2019) Taxonomic study of *Sinopoda* spiders from China (Araneae: Sparassidae). *Zootaxa* 4607(1): 1–81. <https://doi.org/10.11646/zootaxa.4607.1.1>
- Zhong Y, Zeng MY, Gu CL, Yu HL, Yang JY (2022) A new species of *Sinopoda* from China, with first description of the male of *S. wuyiensis* Liu, 2021 (Araneae, Sparassidae). *ZooKeys* 1116: 121–132. <https://doi.org/10.3897/zookeys.1116.85303>
- Zhu Y, Zhong Y, Yang TB (2020) One new species of the genus *Sinopoda* from Hubei Province, with description of the male of *Sinopoda angulata* (Araneae, Sparassidae). *Biodiversity Data Journal* 8: e55377. <https://doi.org/10.3897/BDJ.8.e55377>

# Systematic notes on three new *Luthela* (Mesothelae, Heptathelidae) spiders from China, with their descriptions

Mian Wei<sup>1,2</sup>, Shuqiao Wang<sup>1,2</sup>, Yucheng Lin<sup>1,2</sup>

**1** Key Laboratory of Bio-resources and Eco-environment (Ministry of Education), College of Life Sciences, Sichuan University, Chengdu, Sichuan 610064, China **2** The Sichuan Key Laboratory for Conservation Biology of Endangered Wildlife, Sichuan University, Chengdu, Sichuan 610064, China

Corresponding author: Yucheng Lin ([linyucheng@scu.edu.cn](mailto:linyucheng@scu.edu.cn))

Academic editor: Peter Michalik | Received 8 July 2022 | Accepted 17 April 2023 | Published 2 May 2023

<https://zoobank.org/DEC4657E-FE24-45DB-B132-E916EC4E3A10>

**Citation:** Wei M, Wang S, Lin Y (2023) Systematic notes on three new *Luthela* (Mesothelae, Heptathelidae) spiders from China, with their descriptions. ZooKeys 1159: 151–168. <https://doi.org/10.3897/zookeys.1159.90120>

## Abstract

Three new segmented trapdoor spider species belonging to the family Heptathelidae Kishida, 1923, i.e., *Luthela asuka* **sp. nov.** (♂♀, Sichuan), *L. beijing* **sp. nov.** (♂♀, Beijing), and *L. kagami* **sp. nov.** (♂♀, Sichuan), are described from China. Their phylogenetic position and relationships within Heptathelidae are tested and assessed using a combination available COI data downloaded from GenBank with new DNA sequences obtained in this study. The results show that the new species form a clade with eight known and one undescribed species of *Luthela*. High-definition illustrations of the male palps and female genitalia, diagnoses, and DNA barcodes are provided for these three new species, and their distributions are mapped.

## Keywords

Burrowing spider, COI, heptathelids, molecular analysis, new species, taxonomy

## Introduction

Mesotheles, commonly known as primitively segmented spiders, are characterized by having a series of plates on the abdomen and the spinnerets situated in the middle of ventral abdomen. The suborder Mesothelae previously included only one extant family Liphistiidae Thorell, 1869 (*s.l.*), which has now been split into two closely related families, Heptathelidae Kishida, 1923 and Liphistiidae Thorell, 1869 (*s.s.*) (Petrunkevitch 1939).

The family Heptathelidae currently consists of 107 extant species in seven genera, whose range is limited to the Far East, such as in Japan, the Ryukyu Islands, China, and Vietnam (Xu et al. 2021; WSC 2023). This family was originally described as a tribe (Heptatheleae) of Liphistiidae (*s.l.*) by Kishida (1923), and subsequently was elevated to the level of a family by Petrunkevitch (1939) and confirmed by Haupt (1983). Raven (1985) synonymized Heptathelidae with Liphistiidae (*s.l.*). Recent molecular phylogenetic studies (Xu et al. 2015a, 2015b, 2021) have confirmed the monophyly of Liphistiidae (*s.l.*) as well as that of its two subfamilies, Heptathelinae and Liphistiinae. Li (2022) restored the subfamily Heptathelinae to the family level and circumscribed Liphistidae (*s.s.*) to include only all extant species of *Liphistius* Schiødte, 1849. Based on extensive comparisons of the estimated divergence time in extant spider families and known fossils, Breitling (2022) suggested that it would make more sense to reunite both families into Liphistiidae (*s.l.*). WSC (2023) took note of Breitling's viewpoint, but at present rejected his proposal on the grounds that the age of splitting is not sufficient reason to reunite the families.

*Luthela* Xu & Li, 2022, an endemic genus of northern China, was newly erected and delimited on the basis of morphological characters and molecular data, and it was transferred from Liphistiidae to Heptathelidae (Li 2022; Xu et al. 2022). At present, *Luthela* includes eight known extant species, which are distributed almost exclusively north of the Yangtze River to the Yellow river basin in China, but no species have been recorded in Beijing and Sichuan.

The aims of this paper are 1) to describe and illustrate the three new species; 2) to provide the COI sequences of them for verifying their sex pairing; 3) to test their phylogenetic position and relationships within heptathelids; and 4) to map the geographic distributions of these extant *Luthela* species. This paper expands the knowledge of species diversity of Chinese Heptathelidae.

## Materials and methods

### Specimens sampling

Specimens studied here were collected from Beijing City and Sichuan provinces, China, on 8 October 2019, 15 June 2022, 16 October 2022, and 30 January to 1 February 2023. All specimens were captured by hand and stored in 95% ethanol at  $-20^{\circ}\text{C}$ .

### Molecular data

To test the taxonomic position of the three *Luthela* species, five individuals were selected from the examined materials for molecular data collection. The first and second legs on the right were used to extract genomic DNA and sequence the gene fragments COI. The rest of the bodies were kept as vouchers. All molecular data were obtained from specimens collected at the type localities of the species, although not from the type specimens themselves. Whole genomic DNA was extracted from tissue samples with the Universal Genomic DNA Kit (CW BIO, Beijing, China) following the manufacturer's protocol

for animal tissue. The COI gene fragments were amplified in 50  $\mu$ L reactions. Primer pairs and PCR protocols are given in Table 1. Raw sequences were edited and assembled using Mesquite v. 3.02 (Maddison and Maddison 2011). New sequences were deposited in GenBank (Table 2). All molecular vouchers and examined materials are stored in the Natural History Museum of Sichuan University in Chengdu, China (NHMSU).

To place these new species in a proper taxonomic position within Heptathelidae and verify their sexual pairing, we used these sequences and a selection from previously sequenced taxa to assemble a phylogeny of heptathelid spiders: *Ganthela* Xu & Kuntner, 2015, *Heptathela* Kishida, 1923, *Luthela*, *Qionghela* Xu & Kuntner, 2015, *Ryuthela* Haupt, 1983, *Songthela* Ono, 2000, and *Vinathela* Ono, 2000. In addition, a *Liphistius* species was used as the outgroup (Table 2). Sequences were aligned with MAFFT v. 7.505 (Katoh and Standley 2013) using ‘-auto’ strategy and normal alignment mode. Best partitioning scheme and evolutionary models for three predefined partitions were selected using PartitionFinder2 v. 2.1.1 (Lanfear et al. 2017), with all algorithms and Akaike information criterion (AIC). SYM+I+G, HKY+I+G, and GTR+G were selected for the first, second, and third codon positions of COI, respectively.

Bayesian phylogenetic inference (BI) was performed using MrBayes v. 3.2.7 (Ronquist et al. 2012) through Phylosuite v. 1.2.3 (Zhang et al. 2020) using four Markov Chain Monte Carlo (MCMCs) chains with default heating parameters for 50,000,000 generations or until the average standard deviation of split frequencies was <0.01. Markov chains were sampled every 5000 generations, and the first 25% of sampled trees were burn-in. The website iTOL v. 6.7 (Letunic and Bork 2021) was used to analyse the performance of our BI analyses. Maximum-likelihood (ML) phylogenies were also inferred using IQ-TREE v. 2.0 (Nguyen et al. 2015) through Phylosuite v. 1.2.3 (Zhang et al. 2020) under Edge-linked partition model for 1000 ultrafast (Minh et al. 2013) bootstraps, as well as the Shimodaira–Hasegawa-like approximate likelihood-ratio test (Guindon et al. 2010).

## Morphological data

Specimens were examined and measured with a Leica M205 C stereomicroscope. All male palps and female genitalia were dissected from the bodies before being examined and photographed. To reveal the internal structure, female genitalia were boiled for 5 min in KOH solution (1 mol/L) at 45 °C, and then a dissection needle was used to remove the remaining soft tissue before being photographed. Photographs of male palps and female genitalia were taken with a Canon EOS 60D wide zoom digital camera (8.5 megapixels) mounted on an Olympus BX 43 compound microscope. The

**Table 1.** Loci, primer pairs, and PCR protocols used here.

Locus	Annealing temperature/time	Direction	Primer	Sequence 5' → 3'	Reference
COI	49 °C/15 s	F	LCO1409	GGTCAACAAATCATAAAGATATTGG	Folmer et al. 1994
		R	HCO2198	TAAACTTCAGGGTGACCAAAAAATCA	

**Table 2.** List of segmented spider taxa and their COI data used for phylogenetic analysis of heptathelids (including five new DNA sequence data obtained here).

Species	Identifier	COI	Species	Identifier	COI
<i>Liphistius desultor</i>	LS054	KR028518	<i>Vinathela cucphuongensis</i>	XUX-2013-008	KT767580
<i>Ganthela cipingensis</i>	XUX-2013-516	KP875509	<i>Vinathela nenglianggu</i>	DQ-2018-036	MN400648
<i>Ganthela jianensis</i>	XUX-2013-534	KP875503	<i>Luthela badong</i>	XUX-2012-140	KP229863
<i>Ganthela qingyuanensis</i>	XUX-2012-288	KP875525	<i>Luthela dengfeng</i>	XUX-2012-031	MH172686
<i>Ganthela venus</i>	XUX-2013-160	KP875483	<i>Luthela handan</i>	XUX-2011-214	KP229810
<i>Ganthela wangjiangensis</i>	XUX-2012-278	KP875508	<i>Luthela luotianensis</i>	XUX-2012-079	KP229881
<i>Ganthela xianyouensis</i>	XUX-2013-153	KP875526	<i>Luthela schensiensis</i>	XUX-2011-273	MH172701
<i>Heptathela kimurai</i>	XUX-2013-356	MN274707	<i>Luthela</i> sp.	XUX-2016-110	MH172699
<i>Heptathela tokashiki</i>	XUX-2014-051	MN274727	<i>Luthela taian</i>	XUX-2014-143A	MH172722
<i>Qionghela baishensis</i>	XUX-2012-087	KP229805	<i>Luthela yiyuan</i>	XUX-2012-051	MH172727
<i>Qionghela qiongzong</i>	XUX-2017-156	MN911987	<i>Luthela yuncheng</i>	XUX-2011-235	MH172738
<i>Ryuthela nishibirai</i>	OKR19	AB778138	<i>Luthela asuka</i> sp. nov.	WM-2019-A002	OQ661856
<i>Ryuthela unten</i>	XUX-2012-531	MF078619	<i>Luthela asuka</i> sp. nov.	WM-2023-A003	OQ661857
<i>Songthela bristowei</i>	XUX-2012-256	KP229808	<i>Luthela beijing</i> sp. nov.	WM-2022-B001	OQ661858
<i>Songthela ciliensis</i>	XUX-2012-177	KP229918	<i>Luthela kagami</i> sp. nov.	WM-2023-K001	OQ661859
<i>Songthela hangzhouensis</i>	XUX-2013-171	KT767579	<i>Luthela kagami</i> sp. nov.	WM-2023-K002	OQ661860

images were montaged using Helicon Focus v. 7.0.2 image stacking software (Khmelik et al. 2006). All measurements are given in millimeters. Eye diameters were measured as the maximum diameter in either dorsal or frontal views. Leg measurements are given in the following sequence: total length (femur, patella + tibia, metatarsus, tarsus). Body length was measured only from the anterior edge of prosoma to the posterior edge of opisthisoma, excluding the chelicerae.

Abbreviations used in the text or figures as follows:

<b>ALE</b>	anterior lateral eyes;	<b>MA</b>	marginal apophysis of tegulum;
<b>AME</b>	anterior median eyes;	<b>MH</b>	middle haematodocha;
<b>ASC</b>	apical spine of conductor;	<b>PC</b>	paracymbium;
<b>BSC</b>	basal spine of conductor;	<b>PLE</b>	posterior lateral eyes;
<b>Co</b>	conductor;	<b>PME</b>	posterior median eyes;
<b>CT</b>	contrategulum;	<b>RC</b>	receptacular cluster;
<b>DT</b>	dorsal extension of TA;	<b>ST</b>	subtegulum;
<b>E</b>	embolus;	<b>T</b>	tegulum
<b>EO</b>	embolus opening;	<b>TA</b>	terminal apophysis of tegulum.

## Results

### Phylogenetic analysis

The BI analysis of the dataset of COI genes recovered a single parsimonious tree topology. This tree shows heptathelids are monophyletic but with low support. All 29 heptathelid species included are divided into two major clades, and the seven genera

they represent formed the following phylogenetic relationships: (*Songthela* + (*Vinathela* + (*Ganthela*))) + (*Luthela* + (*Qionghela* + (*Ryuthela* + *Heptathela*))). These seven genera are also monophyletic, with high support in clades of *Songthela*, *Vinathela*, *Qionghela*, *Ryuthela*, and *Heptathela*, but low support in the *Ganthela* and *Luthela* clades. Three new species (Fig. 1, indicated by red font) are nested within *Luthela*, which is a clade composed of 12 *Luthela* species (Fig. 1, indicated by a pink box). The sex pairing of all three new species were confirmed to be correct and highly supported as separate clades and belong to the genus *Luthela*. The sister group relationship of *Luthela asuka* sp. nov. and *Luthela kagami* sp. nov. has high support. The same relationship occurs between *Luthela beijing* sp. nov. and *Luthela handan* Xu et al., 2022. These results support our taxonomic decision to recognise them as new species and confirm their higher affinities.

The result of ML is consistent with that of the BI on some major clades, but there are some differences (Fig. 2). In the ML tree, all 29 heptathelid species also clustered into a monophyletic group. Different from the topology structure of BI tree, the phylogenetic relationships of the seven genera they represent are as follows:

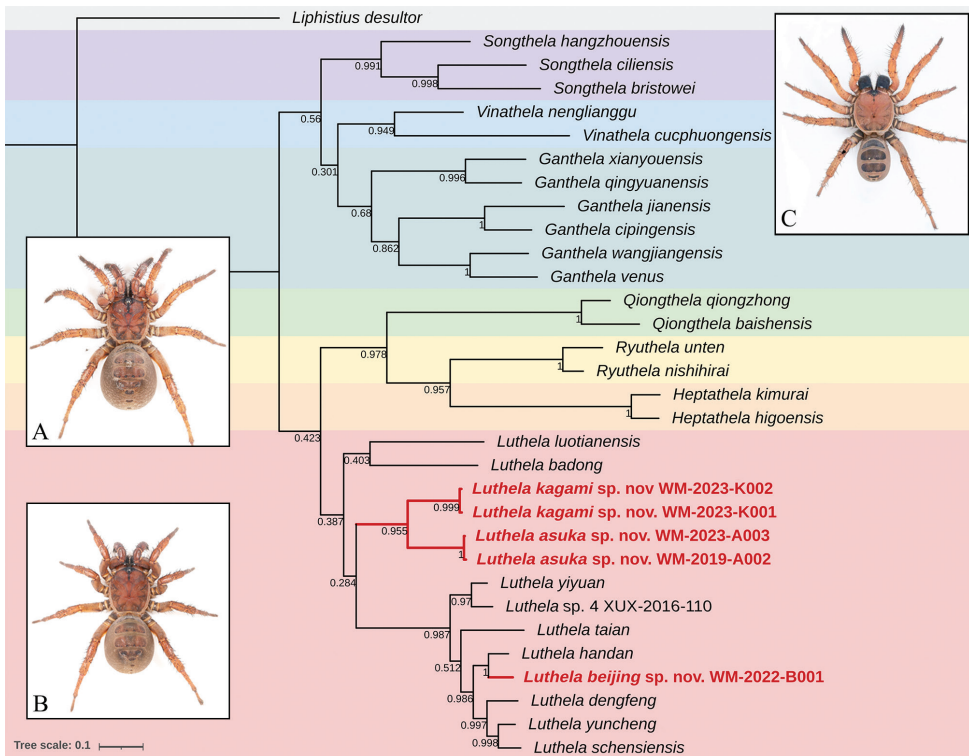


**Figure 1.** Tree topology obtained by Bayesian analysis in MrBayes v. 3.2.7. Numerical values at nodes indicate posterior probabilities. Note: 29 species representing the family Heptathelidae were clustered into a monophyletic group; the high support of three new species (red font) in the genus *Luthela* (pink box), and the low support of monophyly of 12 *Luthela* species. *Liphistius desultor* (light grey box) of Liphistiidae was selected as outgroup for this phylogenetic analysis. Habitus images: **A** *Luthela asuka* sp. nov. **B** *Luthela kagami* sp. nov. **C** *Luthela beijing* sp. nov. Photographs by Yejie Lin.

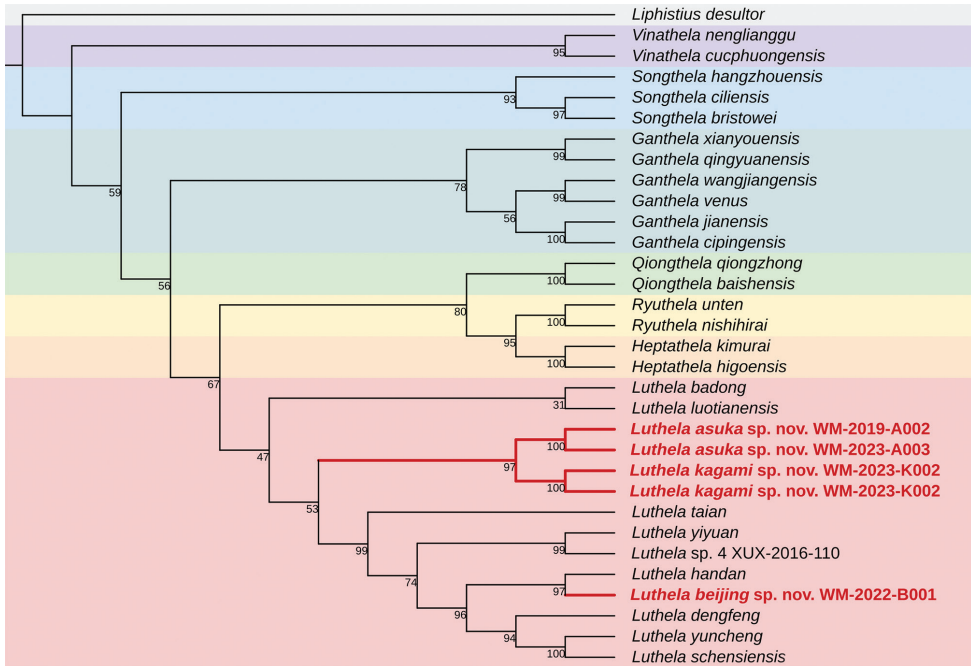


**Figure 2.** Tree topology obtained by maximum likelihood in IQ-TREE v. 2.0. Numbers at nodes are bootstrap values; other conventions as in Fig. 1. The clade of the three new *Luthela* species (red font) is nested within *Luthela* (pink box). Further clades are other genera of Heptathelidae (*Heptathela*, *Ryuthela*, *Qionghthela*, *Ganthela*, *Songthela*, and *Vinathela* are from the bottom up).

(*Vinathela* + (*Songthela* + (*Ganthela* + (*Luthela* + (*Qionghthela* + (*Ryuthela* + *Heptathela*)))))). Also, as in the BI tree, the clades of *Vinathela*, *Songthela*, *Qionghthela*, *Ryuthela*, and *Heptathela* have high support, but the clades of *Ganthela* and *Luthela* have low support. As a sister group, the clade of *Luthela* is delimited to include eight known, three new, and one still undescribed species. Both BI and ML analyses show that the three new species form a clade which is the sister group to remaining *Luthela* species. The available molecular evidence supports the taxonomic placement of the three new *Luthela* species.

## Taxonomy

### Family Heptathelidae Kishida, 1923

#### Genus *Luthela* Xu & Li, 2022

#### *Luthela* Xu & Li, 2022: 134.

**Type species.** *Luthela yiyuan* Xu, Yu, Liu & Li, 2022 by original designation, from Yiyuan Co., Shandong Province, China.

**Diagnosis.** Males of *Luthela* differ from those of other heptathelid genera except *Songthela*, by the smooth conductor with one or two long spines (see ASC and BSC in Figs 3C, 4B, 5B, 6B), and they can be distinguished from the males of *Songthela* in having regular larger teeth on the contrategular margin (see CT in Figs 3B, 3C, 4B, 5D, 6B, 6C). Females of *Luthela* can be recognized from those of other genera by the middle pair of the receptacular clusters being situated at the anterior margin of the bursa copulatrix and the lateral ones at the dorsolateral position of the bursa copulatrix (Fig. 3H, 5F, 5H, 6H).

**Composition.** *Luthela asuka* Wei & Lin, sp. nov. (♂♀, Sichuan), *Luthela badong* Xu et al., 2022 (♂♀, Hubei), *L. beijing* Wei & Lin, sp. nov. (♂♀, Beijing), *L. dengfeng* Xu et al., 2022 (♂♀, Henan), *L. handan* Xu et al., 2022 (♂♀, Henan), *Luthela kagami* Wei & Lin, sp. nov. (♂♀, Sichuan), *L. luotianensis* (Yin et al., 2002) (♀, Hubei), *L. schensiensis* (Schenkel, 1953) (♂♀, Shaanxi), *L. taian* Xu et al., 2022 (♂♀, Shandong), *L. yiyuan* Xu et al., 2022 (♂♀, Shandong), and *L. yuncheng* Xu et al., 2022 (♂♀, Shanxi).

**Distribution.** Northern China, from the Yangtze River to the Yellow river basin.

***Luthela asuka* Wei & Lin, sp. nov.**

<https://zoobank.org/917ACCF0-7506-496C-8C29-0CF53D0C710D>

Figs 3A, B, G, 4

**Type material.** *Holotype* ♂, CHINA: Sichuan Province, Chengdu City, Longquanyi District, Longquan Mountain Forest Park, near Tiangong Temple, 30.5305°N, 104.2709°E, 636 m elev., 8.X.2019, M. Wei and Y. Shen leg. *Paratypes* 1 ♀, CHINA: Sichuan Province, Chengdu, Longquan District, Longquan Mountain Forest Park, near the expressway of Chengdu to Jianyang, 30.5381°N, 104.3015°E, 740 m elev., 16.X.2022, S. Wang leg.; 1 ♀, CHINA: Sichuan Province, Chengdu, Longquan District, Longquan Mountain Forest Park, near the expressway of Chengdu to Jianyang, 30.5381°N, 104.3015°E, 740 m elev., 1.II.2023, S. Wang and M. Wei leg. Deposited in NHMSU.

**Etymology.** The specific epithet is from “Asuka Langley Soryu”, a fictional character wearing a red combat suit from the animation “Evangelion” (by the Japanese creator Hideaki Anno), refers to the body color; noun (name) in apposition.

**Diagnosis.** Males can be distinguished from those of congeners, except *L. kagami* Wei & Lin, sp. nov., in lacking the BSC (Fig. 4A), contrary to other species (cf. Xu et al. 2022: figs 3B, 5E, 6B, 7E, 10B, 12B, 14D), and in having the contrategulum bearing relatively dense, smaller serrated teeth (Fig. 4B, E), rather than sparse and larger teeth in other species (cf. Xu et al. 2022: figs 3A, 5D, 6B, 7D, 10H, 12D, 14H). Males also differ from *L. kagami* sp. nov. in having two nearly invisible lateral teeth on the middle portion of the conductor and the longer TA (Fig. 4A–C, E, F), rather than two relatively larger teeth and a shorter TA in the latter (Fig. 7B–D, F). Females differ from those of congeners in having the paired receptacular clusters situated at the relatively short genital stalks and in the relatively smaller size (Fig. 4G, H), rather

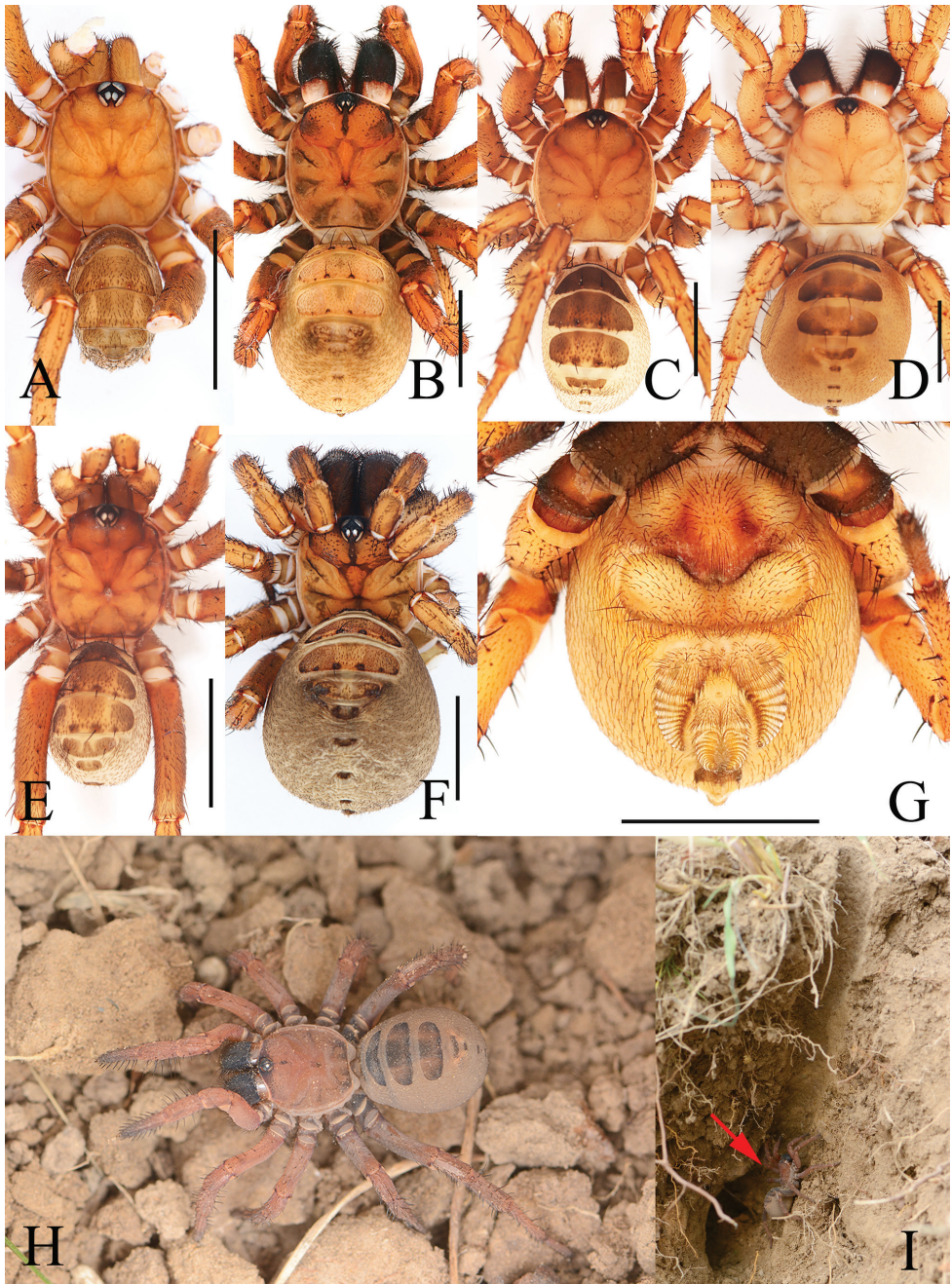


**Figure 3.** New species of *Luthela* **A, B, G** *L. asuka* sp. nov. from Longquanyi District, Chengdu **C, D, H, I** *L. beijing* sp. nov. from Zizhuyuan Park, Beijing **E, F** *L. kagami* sp. nov. from Guihua Township, Pengzhou City **A, C, E** male habitus, dorsal view **B, D, F** female habitus, dorsal view **G** female habitus, ventral view **H** living female, dorsal view **I** burrow, vertical section, with red arrow pointing to the spider. Photographs by Chao Wu (**H, I**). Scale bars: 5.00 mm.

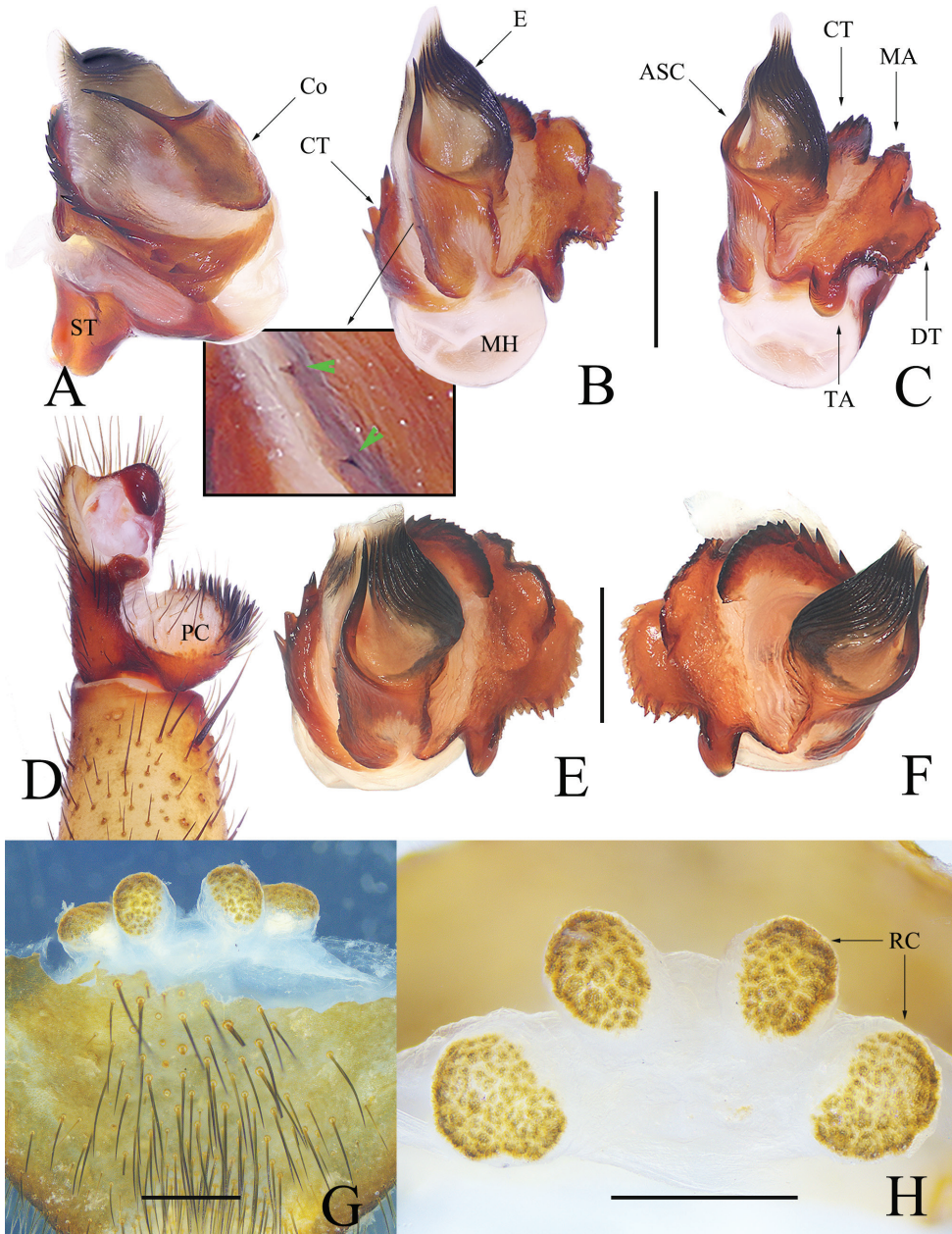


**Figure 4.** *Luthela asuka* sp. nov. **A** male left palp bulb, prolateral view **B** male left palp bulb, ventral view **C** male left palp bulb, retrolateral view **D** left cymbium, ventral view **E** left palpal bulb, apical view **F** right palpal bulb, apical view **G** vulva, ventral view **H** vulva, dorsal view. Green arrows indicate small teeth on conductor. Scale bars: 0.50 mm.

than the long genital stalks and the larger size (cf. Xu et al. 2022: figs 4, 5H, I, 6H–M, 8, 9, 11, 13, 14H–M). Females differ from those of *L. kagami* sp. nov. in having the receptacular clusters relatively separated and the lateral pair larger than the middle pair (Fig. 4G, H), rather than closer and nearly equal in size (Fig. 7G, H).

**Description. Male** (holotype) (Fig. 3A). Carapace red; cervical and radial groove distinct. Cephalic region moderately raised. Chelicerae robust; fang furrow with 11 promarginal teeth of variable size. Sternum longer than wide. Abdomen pale yellow, with 5 large dorsal and 2 small posterior tergites, 4 tapering setae near posteromargin of 5 large tergites, and 2 on the rest. Seven spinnerets. Measurements: body 12.06 long. Carapace 5.59 long, 5.09 wide. Abdomen 5.92 long, 4.51 wide. Sternum 2.49 long, 1.91 wide. ALE > PLE > PME > AME. Leg I 18.00 (4.90 + 5.58 + 4.66 + 2.86), leg II 18.08 (4.54 + 5.42 + 5.04 + 3.08), leg III 19.31 (4.20 + 5.41 + 5.87 + 3.83), leg IV 26.76 (6.21 + 7.70 + 8.10 + 4.76).

**Palp** (Fig. 4A–F): prolateral paracymbium pale, weakly sclerotized, with numerous setae and spines at distal and retrolateral surface. Contrategular margin denticulate, with large teeth on proximal part and smaller but denser teeth on distal part. Marginal apophysis of tegulum serrated, with tapering terminal apophysis of tegulum, margin of dorsal extension of terminal apophysis with teeth varied in size and distance. Conductor smooth, fused to embolic base, with large apical spine and 2 tiny lateral spines on middle portion. Embolus with translucent, flat opening and several ribbed ridges distally.

**Female** (one of paratypes) (Fig. 3B, G). Carapace red, with dark pattern; cervical and radial grooves distinct, with sparse spines. Cephalic region slightly elevated. Chelicerae more robust than male, fang furrow with 12 promarginal teeth of variable size, larger than male. Sternum longer than wide. Abdomen pale, with five large and five small tergites; chaetotaxy on tergites as in male. Seven spinnerets. Measurements: body 16.12 long. Carapace 7.02 long, 6.94 wide. Abdomen 8.93 long, 8.08 wide. Sternum 3.39 long, 1.86 wide. ALE > PLE > PME > AME. Leg I 14.84 (4.80 + 5.50 + 2.57 + 1.97), leg II 14.96 (4.59 + 4.66 + 3.32 + 2.39), leg III 14.70 (4.64 + 4.61 + 2.94 + 2.51), leg IV 22.24 (6.57 + 6.64 + 5.83 + 3.20).

**Female genitalia** (Fig. 4G, H). Two pairs of receptacular clusters situated on short and thick stalks; lateral pair relatively larger than middle pair. Middle pair of receptacular clusters separated from each other, situated on anteromargin of bursa copulatrix; lateral receptacular clusters situated slightly dorsolaterally.

**Distribution.** Known only from the type locality (Fig. 8).

***Luthela beijing* Wei & Lin, sp. nov.**

<https://zoobank.org/AEB13509-6970-44FE-8CC9-40963F20B516>

Figs 3C, D, H, I, 5, 6

**Material examined.** *Holotype* ♂ and *paratypes* 1♂ 2♀, CHINA: Beijing, Haidian District, near Baishi Bridge, Zizhuyuan Park, 39.9393°N, 116.3110°E, 55 m elev., 15.VI.2022, H. Yang leg. Deposited in NHMSU.

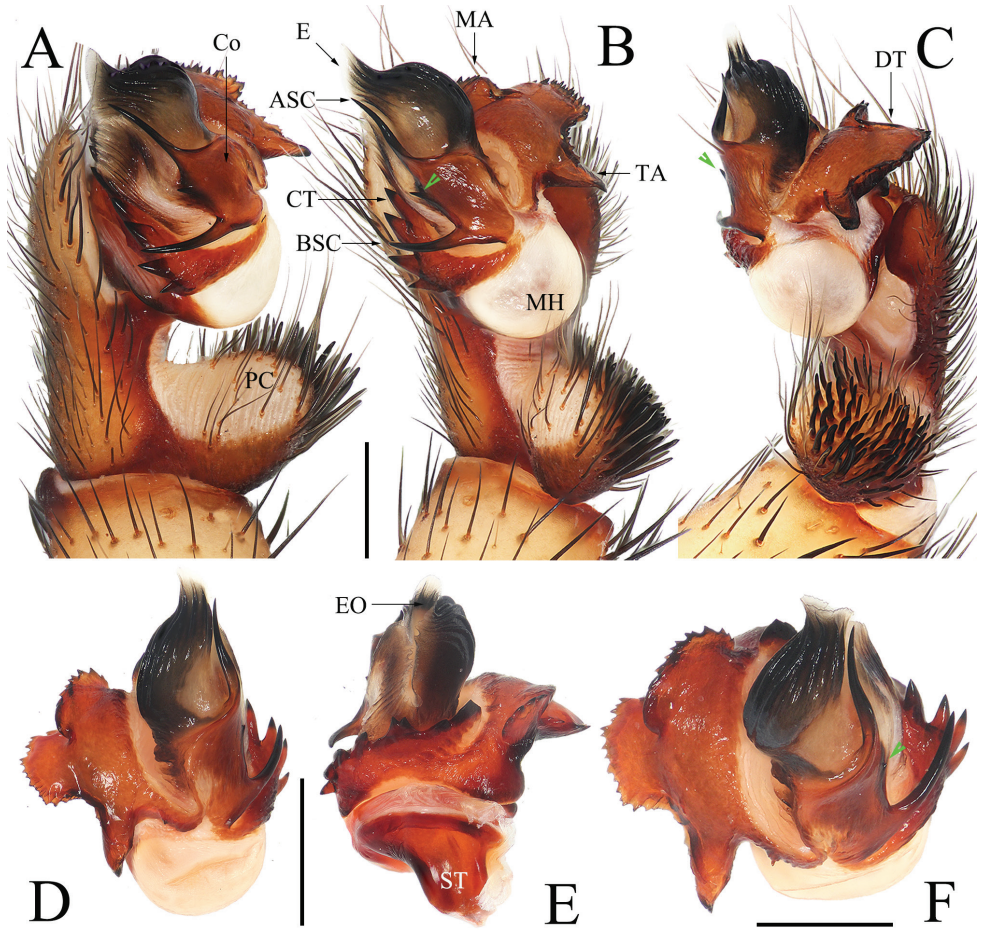


**Figure 5.** *Luthela beijing* sp. nov., male holotype **A** left palp, prolateral view **B** left palp, ventral view **C** left palp, retrolateral view **D** right palpal bulb, ventral view **E** right palpal bulb, dorsal view **F** right palpal bulb, apical view. Green arrows in **B**, **C**, and **F** indicate small teeth on conductor. Scale bars: 0.50 mm.

**Etymology.** The specific epithet derives from the type locality; noun in apposition.

**Diagnosis.** Males of this new species can be recognized from those of other congeners, except *L. handan*, *L. schensiensis*, *L. yiyuan*, and *L. yuncheng*, by the conductor having 2 spines of nearly equal length and by having a lateral tooth on the middle portion of conductor (Fig. 5B, F), rather than 2 spines in unequal length or lacking a lateral tooth on the conductor (cf. Xu et al. 2022: figs 5B, D, 6A, E, 12A, B, D). Males differ from those of *L. schensiensis* and *L. yuncheng* in having 6 or 7 large teeth on the contrategular (Figs 5F, 6A), rather than 7–10 in *L. schensiensis* and 8 in *L. yuncheng*. (cf. Xu et al. 2022: figs 10G, K, 14D). Males differ from those of *L. yiyuan* by the margin of the contrategular having relatively longer teeth and the distal tooth bifurcated (Figs 5B, 6A, D), rather than shorter teeth on contrategular and the distal tooth with 3 serrations. (cf. Xu et al. 2022: fig. 3G, K). And males differ from those of *L. handan* in having the

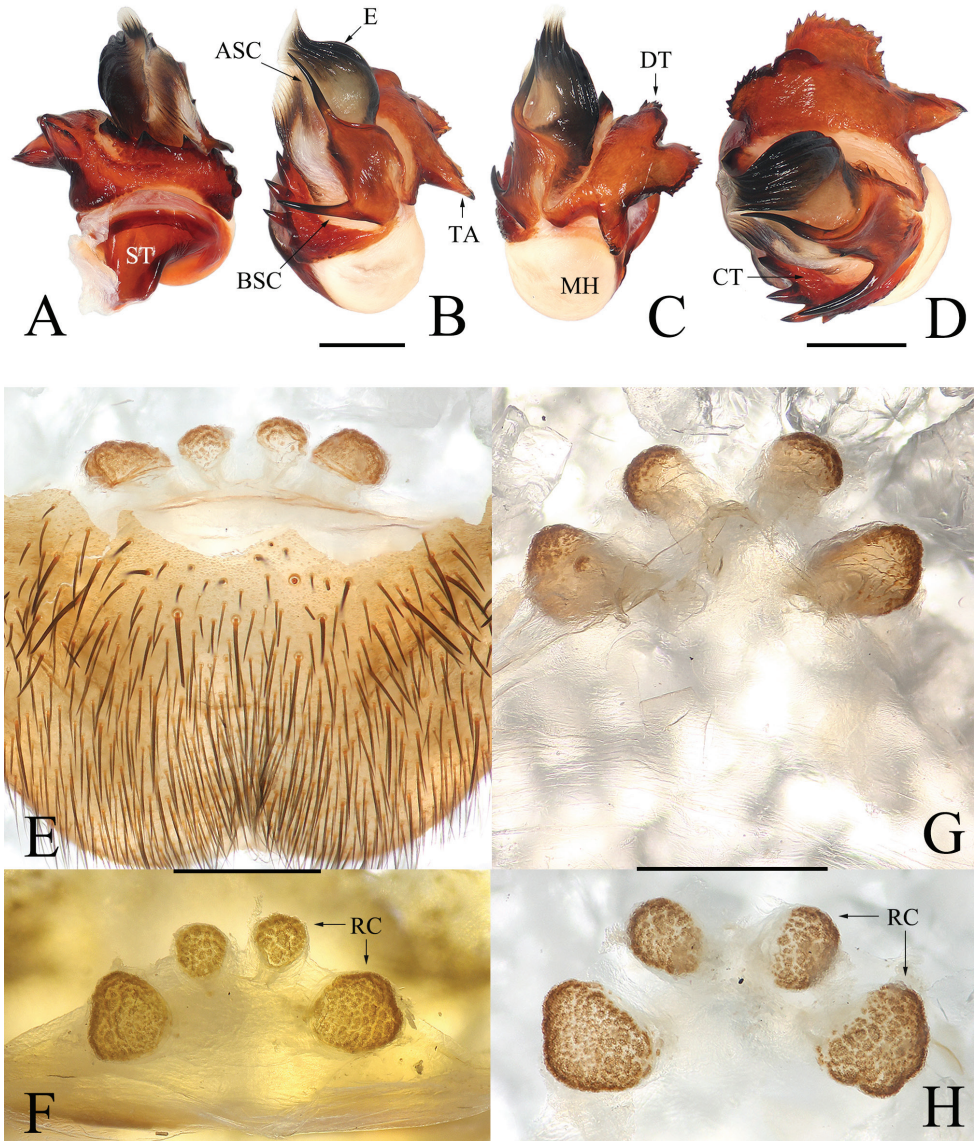


**Figure 6.** *Luthela beijing* sp. nov. **A–D** left palpal bulb **E–H** female genitalia **A, F, H** dorsal view **B, E, G** ventral view **C** retrolateral view **D** apical view. Scale bars: 0.50 mm.

basal spine of conductor thinner and shorter and the promixal part of the margin of the marginal apophysis with a row of smaller teeth (Figs 5B, F, 6B, D), rather than with a thick, long basal spine on the conductor and the proximal margin of the marginal apophysis with 3 larger teeth. (cf. Xu et al. 2022: fig. 7E, G). Females can be distinguished from those of congeners in having the 2 paired receptacular clusters with longer genital stalks and the lateral pair equal to ca 2× size the middle ones (Fig. 6E–H), rather than

shorter genital stalks and the lateral receptacular clusters greater than 3× or less than 2× the middle ones in size (cf. Xu et al. 2022: figs 4, 5H, I, 6H–M, 8, 9, 11, 13, 14).

**Description. Male** (holotype) (Fig. 3C). Carapace black in life; cervical and radial grooves distinct, with sparse spines. Cephalic region moderately raised. Chelicerae robust; fang furrow with 9 promarginal teeth of variable size. Sternum longer than wide. Abdomen pale, with short setae, with 4 large dorsal and 6 small posterior tergites. Four tapering setae near posteromargin of large tergites, 2 on the rest. Seven spinnerets. Measurements: body 14.89 long. Carapace 6.22 long, 5.38 wide. Abdomen 7.82 long, 4.08 wide. Sternum 2.99 long, 1.86 wide. ALE > PLE > PME > AME. Leg I 17.62 (5.13 + 5.26 + 4.46 + 2.77), leg II 17.93 (5.26 + 5.49 + 4.36 + 2.82), leg III 19.34 (4.89 + 5.62 + 5.47 + 3.36), leg IV 25.27 (6.04 + 7.29 + 7.79 + 4.15).

**Palp** (Figs 5A–F, 6A–D): prolateral paracymbium pale, weakly sclerotized; distal and retrolateral sides with numerous setae and spines. Contrategulum with denticulate margin, with 7 teeth, the fifth bifurcated, and only 4 large teeth visible in dorsal view. Posterior part of marginal apophysis of tegulum serrated, with regular, small denticles; terminal apophysis of tegulum relatively long, apex pointed in distal view, margin of dorsal extension of terminal apophysis with teeth nearly equal in size and distance. Conductor smooth, fused to embolic base, 2 long spines separated at a wide angle, a small tooth located between upper spines and lower spines of conductor. Embolus with translucent, flat opening, and several ribbed ridges distally.

**Female** (one of paratypes) (Fig. 3D, H, I). Carapace red; cervical and radial grooves distinct, with sparse spines. Cephalic region slightly elevated. Chelicerae more robust than male; fang furrow with 10 promarginal teeth of variable size; larger than male. Sternum longer than wide. Abdomen pale, with 4 large and 6 small tergites; chaetotaxy on tergites as in male. Seven spinnerets. Measurements: body 18.12 long. Carapace 7.36 long, 7.29 wide. Abdomen 9.72 long, 7.28 wide. Sternum 3.62 long, 2.49 wide. ALE > PLE > PME > AME. Leg I 15.63 (5.01 + 5.54 + 3.05 + 2.03), leg II 14.80 (4.90 + 4.72 + 3.08 + 2.10), leg III 16.22 (4.99 + 5.29 + 3.70 + 2.24), leg IV 23.23 (6.22 + 7.10 + 6.27 + 3.64).

**Female genitalia** (Fig. 6E–H). Two pairs of receptacular clusters situated on stalks, middle pair of receptacular clusters separated from each other, on anteromargin of bursa copulatrix, distinctly smaller than lateral pair. Lateral receptacular clusters dorsolateral, stalks thick.

**Distribution.** Known only from the type locality (Fig. 8).

***Luthela kagami* Wei & Lin, sp. nov.**

<https://zoobank.org/20078EAE-3269-428C-8640-54398ACBC00F>

Figs 3E, F, 7

**Type material. Holotype** ♂, CHINA: Sichuan Province, Pengzhou, Guihua County, 31.0548°N, 103.8100°E, 664 m elev., 4.X.2021, Y. He leg.; **paratypes** 2♀, same data as holotype, 30.I.2023, S. Wang and M. Wei leg. Deposited in NHMSU.

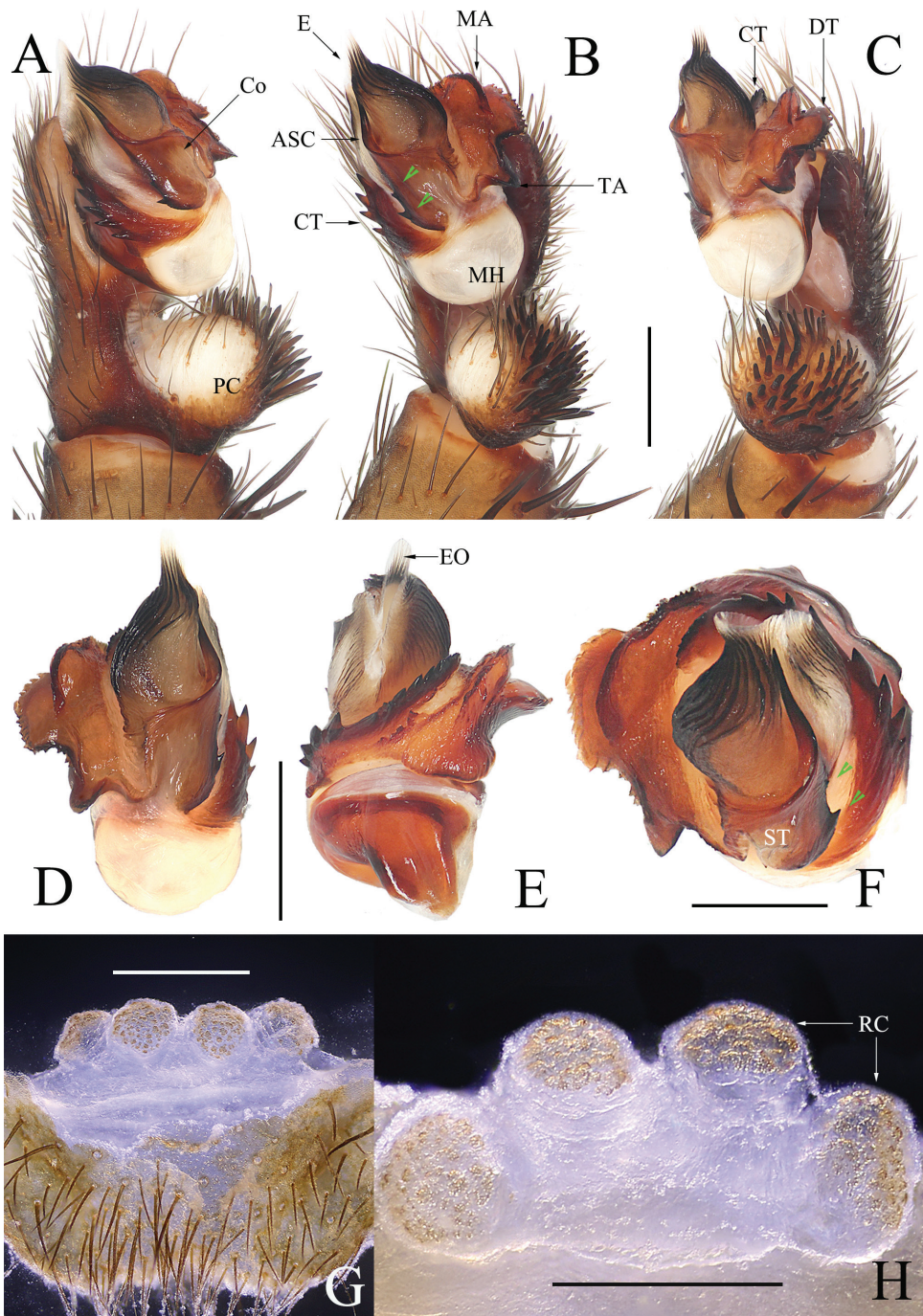


**Figure 7.** *Luthela kagami* sp. nov. **A** male left palp, prolateral view **B** male left palp, ventral view **C** male left palp, retrolateral view **D** right palpal bulb, ventral view **E** right palpal bulb, dorsal view **F** right palpal bulb, apical view **G** vulva, ventral view **H** vulva, dorsal view. Green arrows in **B** and **F** indicate small teeth on conductor. Scale bars: 0.50 mm.

**Etymology.** The specific epithet is from “Hiiragi Kagami”, a fictional character from the comic “Lucky Star” (written and illustrated by the Japanese cartoonist Yoshimizu Kagami) with haircut similar to “Asuka Langley Soryu” (see Etymology of *Luthela asuka* sp. nov.); the name refers to the great similarity between these two new species; noun (name) in apposition.

**Diagnosis.** Males can be distinguished from those of other congeners, except *L. asuka* sp. nov., in lacking BSC (Fig. 7A), in contrast to other species (cf. Xu et al. 2022: figs 3B, 5E, 6B, 7E, 10B, 12B, 14D), and in the contrategulum having relatively dense, smaller serrated teeth (Fig. 7B, F), rather sparse but larger teeth in other species (cf. Xu et al. 2022: figs 3A, 5D, 6B, 7D, 10H, 12D, 14H). Males differ from those of *L. asuka* sp. nov. in having two relatively large teeth on the middle portion of conductor and a shorter TA (Fig. 7B–D, F), rather than with two tiny, nearly invisible teeth and a longer TA (Fig. 4A, B, E). Females differ from congeners, except *L. asuka* sp. nov., in having the paired receptacular clusters with relatively short genital stalks and in their relatively smaller size (Fig. 7G, H), rather than long genital stalks and large size (cf. Xu et al. 2022: figs 4, 5H, I, 6H–M, 8, 9, 11, 13, 14H–M). Females can be distinguished from *L. asuka* sp. nov. in having the receptacular clusters close and nearly equal in size (Fig. 7G, H), rather than separated and with the lateral pair larger than the middle pair (Fig. 4G, H).

**Description. Male** (holotype) (Fig. 3E). Carapace red; cervical and radial grooves distinct. Cephalic region moderately raised. Chelicerae robust; fang furrow with 12 promarginal teeth of variable size. Sternum longer than wide. Abdomen pale yellow, with 5 large dorsal and 2 small posterior tergites, 4 tapering setae near posteromargin of 5 large tergites and 2 on the rest. Seven spinnerets. Measurements: body 11.27 long. Carapace 5.50 long, 4.97 wide. Abdomen 5.77 long, 4.28 wide. Sternum 2.41 long, 1.89 wide. ALE > PLE > PME > AME. Leg I 17.84 (4.87 + 5.53 + 4.62 + 2.82), leg II 17.89 (4.50 + 5.37 + 4.97 + 3.05), leg III 19.19 (4.19 + 5.38 + 5.83 + 3.79), leg IV 26.62 (6.18 + 7.67 + 8.05 + 4.72).

**Palp** (Fig. 7A–F): prolateral paracymbium pale, weakly sclerotized, with numerous setae and spines at distal and retrolateral sides. Contrategular margin denticulate, with large teeth on proximal part, and smaller but denser teeth distally. Marginal apophysis of tegulum serrated, with relatively short terminal apophysis of tegulum; margin of dorsal extension of terminal apophysis with teeth varied in size and distance. Conductor smooth, fused to embolic base, with large apical spine and 2 small lateral spines on middle portion. Embolus with translucent, flat opening and several ribbed ridges distally.

**Female** (one of paratypes) (Fig. 3F). Carapace red, with dark pattern, cervical and radial grooves distinct, with sparse spines. Cephalic region slightly elevated. Chelicerae more robust than male, fang furrow with 12 promarginal teeth of variable size, larger than male. Sternum longer than wide. Abdomen pale, with 5 large and five 5 tergites; chaetotaxy on tergites as in male. Seven spinnerets. Measurements: body 15.74 long. Carapace 7.00 long, 6.93 wide. Abdomen 8.89 long, 8.21 wide. Sternum 3.24 long, 1.79 wide. ALE > PLE > PME > AME. Leg I 14.70 (4.77 + 5.47 + 2.55 + 1.91), leg II 14.85 (4.57 + 4.63 + 3.30 + 2.35), leg III 14.61 (4.61 + 4.59 + 2.92 + 2.49), leg IV 22.15 (6.54 + 6.63 + 5.82 + 3.16).

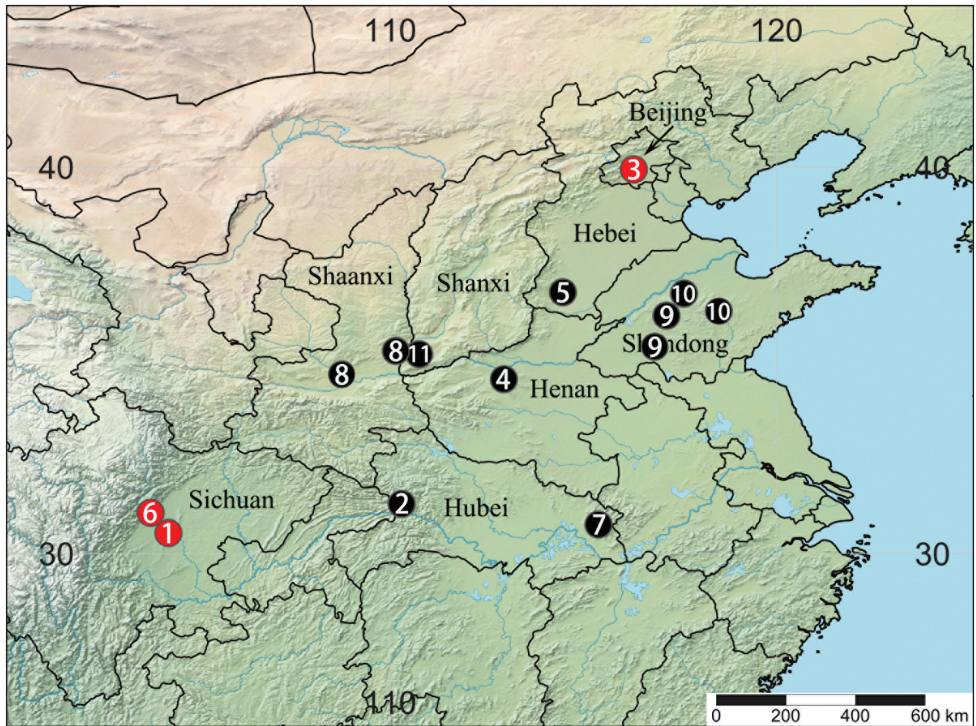


**Figure 8.** Distribution records of 11 *Luthela* species. 1 = *L. asuka* sp. nov., 2 = *L. badong*, 3 = *L. beijing* sp. nov., 4 = *L. dengfeng*, 5 = *L. handan*, 6 = *L. kagami* sp. nov., 7 = *L. luotianensis*, 8 = *L. schensiensis*, 9 = *L. taian*, 10 = *L. yiyuan*, 11 = *L. yuncheng*.

**Female genitalia** (Fig. 7G–H). Two pairs of receptacular clusters on short, thick stalks, close to each other, nearly equal in size. Middle pair of receptacular clusters separated from each other, on anteromargin of bursa copulatrix; lateral receptacular clusters set slightly dorsolaterally.

**Distribution.** Known only from the type locality (Fig. 8).

## Acknowledgements

We thank Dr Robert Raven and an anonymous referee for constructive comments on this manuscript. Special thanks to the subject editor, Prof. Peter Michalik, for his kind help. Yiting He, Yunxiao Shen, and Zixu Yin helped collect samples during the field work. Haocong Yang donated specimens collected in Beijing. Yejie Lin and Chao Wu donated high-quality photographs. This study was supported by the National Natural Science Foundation of China (NSFC-31972870, 31750002).

## References

- Breitling R (2022) On the taxonomic rank of the major subdivisions of the extant segmented spiders (Arachnida: Araneae: Mesothelae: Liphistiidae *s. lat.*). *Miscellanea Araneologica* 2022: 1–4.
- Folmer O, Black M, Hoeh W, Lutz R, Vrijenhoek R (1994) DNA primers for amplification of mitochondrial cytochrome *c* oxidase subunit I from diverse metazoan invertebrates. *Molecular Marine Biology and Biotechnology* 3: 294–299.
- Guindon S, Dufayard J, Lefort V, Anisimova M, Hordijk W, Gascuel O (2010) New algorithms and methods to estimate maximum-likelihood phylogenies: Assessing the performance of PhyML 3.0. *Systematic Biology* 59(3): 307–321. <https://doi.org/10.1093/sysbio/syq010>
- Haupt J (1983) Vergleichende Morphologie der Genitalorgane und Phylogenie der liphistiomorphen Webspinnen (Araneae: Mesothelae). I. Revision der bisher bekannten Arten. *Journal of Zoological Systematics and Evolutionary Research* 21(4): 275–293. <https://doi.org/10.1111/j.1439-0469.1983.tb00296.x>
- Katoh K, Standley D (2013) MAFFT multiple sequence alignment software version 7: Improvements in performance and usability. *Molecular Biology and Evolution* 30(4): 772–780. <https://doi.org/10.1093/molbev/mst010>
- Khmelik VV, Kozub D, Glazunov A (2006) Helicon Focus 3.10.3. <http://www.heliconsoft.com/heliconfocus.html> [Accessed on 6 August 2022]
- Kishida K (1923) *Heptathela*, a new genus of liphistiid spiders. *Annotationes Zoologicae Japonenses* 10: 235–242.
- Lanfear R, Frandsen B, Wright A, Senfeld T, Calcott B (2017) PartitionFinder 2: New methods for selecting partitioned models of evolution for molecular and morphological phylogenetic analyses. *Molecular Biology and Evolution* 34(3): 772–773. <https://doi.org/10.1093/molbev/msw260>
- Letunic I, Bork P (2021) Interactive Tree of Life (iTOL) v5: An online tool for phylogenetic tree display and annotation. *Nucleic Acids Research* 49(W1): 293–296. <https://doi.org/10.1093/nar/gkab301>
- Li S (2022) On the taxonomy of spiders of the suborder Mesothelae. *Acta Arachnologica Sinica* 31(1): 71–72. <https://doi.org/10.3969/j.issn.1005-9628.2022.01.013>
- Maddison D, Maddison W (2011) Mesquite: a modular system for evolutionary analysis. <https://www.mesquiteproject.org/>
- Minh B, Nguyen M, von Haeseler A (2013) Ultrafast approximation for phylogenetic bootstrap. *Molecular Biology and Evolution* 30(5): 1188–1195. <https://doi.org/10.1093/molbev/mst024>
- Nguyen L, Schmidt H, von Haeseler A, Minh B (2015) IQ-TREE: A fast and effective stochastic algorithm for estimating maximum-likelihood phylogenies. *Molecular Biology and Evolution* 32(1): 268–274. <https://doi.org/10.1093/molbev/msu300>
- Petrunkovitch A (1939) Catalogue of American spiders. Part one. *Transactions of the Connecticut Academy of Arts and Sciences* 33: 133–338.

- Raven R (1985) The spider infraorder Mygalomorphae (Araneae): Cladistics and systematics. *Bulletin of the American Museum of Natural History* 182: 1–180.
- Ronquist F, Teslenko M, van der Mark P, Ayres D, Darling A, Höhna S, Larget B, Liu L, Suchard M, Huelsenbeck J (2012) MrBayes 3.2: Efficient Bayesian phylogenetic inference and model choice across a large model space. *Systematic Biology* 61(3): 539–542. <https://doi.org/10.1093/sysbio/sys029>
- WSC (2023) World Spider Catalog. Version 24. Natural History Museum Bern. [Online at] <http://wsc.nmbe.ch> [Accessed on 18 April 2023]
- Xu X, Liu F, Chen J, Li D, Kuntner M (2015a) Integrative taxonomy of the primitively segmented spider genus *Ganthela* (Araneae: Mesothelae: Liphistiidae): DNA barcoding gap agrees with morphology. *Zoological Journal of the Linnean Society* 175(2): 288–306. <https://doi.org/10.1111/zoj.12280>
- Xu X, Liu F, Chen J, Ono H, Li D, Kuntner M (2015b) A genus-level taxonomic review of primitively segmented spiders (Mesothelae, Liphistiidae). *ZooKeys* 488: 121–151. <https://doi.org/10.3897/zookeys.488.8726>
- Xu X, Kuntner M, Bond J, Ono H, Ho S, Liu F, Yu L, Li D (2020) Molecular species delimitation in the primitively segmented spider genus *Heptathela* endemic to Japanese islands. *Molecular Phylogenetics and Evolution* 151: 106900. <https://doi.org/10.1016/j.ympev.2020.106900>
- Xu X, Su Y, Ho S, Kuntner M, Ono H, Liu F, Chang C, Warrit N, Sivayyapram V, Aung K, Pham D, Norma-Rashid Y, Li D (2021) Phylogenomic analysis of ultraconserved elements resolves the evolutionary and biogeographic history of segmented trapdoor spiders. *Systematic Biology* 70(6): 1110–1122. <https://doi.org/10.1093/sysbio/syaa098>
- Xu X, Yu L, Liu F, Li D (2022) Delimitation of the segmented trapdoor spider genus *Luthela* gen. nov., with comments on the genus *Sinothela* from northern China (Araneae, Mesothelae, Liphistiidae). *Zootaxa* 5091(1): 131–154. <https://doi.org/10.11646/zootaxa.5091.1.5>
- Zhang D, Gao F, Jakovčić I, Zou H, Zhang J, Li W, Wang G (2020) PhyloSuite: An integrated and scalable desktop platform for streamlined molecular sequence data management and evolutionary phylogenetics studies. *Molecular Ecology Resources* 20(1): 348–355. <https://doi.org/10.1111/1755-0998.13096>

# Two new thomisid species (Arachnida, Araneae, Thomisidae) from China and Vietnam, with the first descriptions of the males of *Borboropactus longidens* Tang & Li, 2010 and *Stephanopsis xiangzhouica* Liu, 2022

Cong-zheng Li<sup>1\*</sup>, Yan-bin Yao<sup>2\*</sup>, Yong-hong Xiao<sup>1</sup>, Ke-ke Liu<sup>1</sup>

**1** College of Life Science, Jingtangshan University, Ji'an 343009, Jiangxi, China **2** Jinshan College of Fujian Agriculture and Forestry University, Fuzhou 350007, Fujian, China

Corresponding author: Ke-ke Liu ([kekeliu@jgsu.edu.cn](mailto:kekeliu@jgsu.edu.cn))

---

Academic editor: Miquel A. Arnedo | Received 24 February 2023 | Accepted 6 April 2023 | Published 2 May 2023

---

<https://zoobank.org/9B90D030-9C99-43ED-AF4D-B729CDB89D75>

---

**Citation:** Li C-z, Yao Y-b, Xiao Y-h, Liu K-k (2023) Two new thomisid species (Arachnida, Araneae, Thomisidae) from China and Vietnam, with the first descriptions of the males of *Borboropactus longidens* Tang & Li, 2010 and *Stephanopsis xiangzhouica* Liu, 2022. ZooKeys 1159: 169–187. <https://doi.org/10.3897/zookeys.1159.102601>

---

## Abstract

Collections of thomisid spiders by amateur and professional arachnologists in China have led to the discovery of some interesting crab spiders (Thomisidae). Two new species in two genera of thomisid spiders are described and illustrated with photographs and SEMs: *Pharta xizang* Liu & Yao, **sp. nov.** (♀) and *Stephanopsis qiong* Liu & Yao, **sp. nov.** (♀). The previously unknown males of *Borboropactus longidens* Tang & Li, 2010 and *Stephanopsis xiangzhouica* Liu, 2022 were also collected and are described for the first time. The genus *Borboropactus* Simon, 1884 is reported for the first time from Vietnam. The new *Stephanopsis* species is also recorded for only the second time from the Asian mainland. Distributions of all these species are mapped.

## Keywords

Crab spider, distribution, new species, single sex, taxonomy

---

\* These authors contributed equally to this work.

## Introduction

The family Thomisidae, the crab spiders, is the seventh largest spider family with a global distribution, comprising 2165 extant species belonging to 171 genera (WSC 2022). Of these, 312 species from 53 genera were recorded from China (WSC 2022). More than 50% of the Chinese species are from southern provinces of this country, such as Yunnan, Hainan and Hunan. Only a few percent of the total Chinese number of species have been reported in the past ten years (Li and Lin 2016; Liu et al. 2017, 2022b, 2022c; Yu and Zhang 2017; Yu et al. 2017; Tian et al. 2018; Lin et al. 2019, 2022; Huang and Lin 2020; Wang et al. 2020; Liu et al. 2021; Zhang et al. 2022). China not only has the most species- and genus-rich thomisid fauna, but for approximately 65%, only one of the sexes has been described, which represents a challenge for future taxonomic revisions (Li 2020). However, only a few papers (Meng et al. 2019; Wang et al. 2020; Liu et al. 2022c; Lin et al. 2022) have revised the species of these single-sex species, and there are still many poorly known species from southern China with unusual morphological characteristics (Liu et al. 2022a).

In the past five years, specimens have been collected by spider enthusiasts and colleagues. When examining these spider specimens collected from Tibet, Guangdong, Fujian and Hainan provinces, two new thomisid species were identified, two males of *Borboropactus longidens* Tang & Li, 2010 and *Stephanopsis xiangzhouica* Liu, 2022 were found for the first time. The aims of the present paper are (1) to provide detailed descriptions of two new species, (2) to provide descriptions of previously unknown males of these two species and (3) to provide the second record of the genus *Stephanopsis* from the Asian mainland.

## Materials and methods

Specimens were examined using a SZ6100 stereomicroscope. Both male and female copulatory organs were dissected and examined in 95% ethanol using an Olympus CX43 compound microscope with a KUY NICE CCD camera. The epigynes were cleared with pancreatin solution (Álvarez-Padilla and Hormiga 2007). Specimens, including dissected male palps and epigynes, were preserved in 75% ethanol after examination. For SEM photographs, the specimens were dried under natural conditions and photographed with a ZEISS EVO LS15 scanning electron microscope. Specimens, including the detached male palps or female genitalia, were stored in 75% ethanol after examination. Types are deposited in the Animal Specimen Museum, College of Life Science, Jinggangshan University (ASM-JGSU).

All morphological measurements were taken using a Zeiss Stereo Discovery V12 stereomicroscope with Zoom Microscope System (Software: AxioVision SE64 Version 4.8.3) and are given in millimetres. The body length of all specimens was taken from the anterior margin of the clypeus to the posterior end of the abdomen, excluding the

spinnerets. Terminology of the male and female genitalia follows Benjamin (2011), Meng et al. (2019), and Liu et al. (2022c). Leg measurements are given as total length (femur, patella, tibia, metatarsus, tarsus). Leg spines were documented by dividing each leg segment into four aspects: dorsal (d), prolateral (p), retrolateral (r) and ventral (v).

The abbreviations used in the figures and text are as follows:

<b>ALE</b>	anterior lateral eye;
<b>AME</b>	anterior median eye;
<b>At</b>	atrium;
<b>CD</b>	copulatory duct;
<b>CO</b>	copulatory opening;
<b>Con</b>	conductor;
<b>d</b>	dorsal;
<b>Em</b>	embolus;
<b>ET</b>	epigynal tooth;
<b>FD</b>	fertilization duct;
<b>GA</b>	glandular appendage;
<b>IZCAS</b>	Institute of Zoology, Chinese Academy of Sciences in Beijing;
<b>MA</b>	median apophysis;
<b>MF</b>	median field;
<b>MOA</b>	median ocular area;
<b>MS</b>	membranous sac;
<b>p</b>	prolateral;
<b>PLE</b>	posterior lateral eye;
<b>PME</b>	posterior median eye;
<b>r</b>	retrolateral;
<b>RTA</b>	retrolateral tibial apophysis;
<b>Sp</b>	spermatheca;
<b>St</b>	subtegulum;
<b>TR</b>	transverse ridge of copulatory opening;
<b>v</b>	ventral;
<b>VTA</b>	ventral tibial apophysis.

## Taxonomy

### Family Thomisidae Sundevall, 1833

#### Genus *Borboropactus* Simon, 1884

**Comments.** This genus includes 17 species, all of which are distributed in tropical Africa and Asia (WSC 2022). Most species (10 species) are described based either on

single females or single males (Li and Lin 2016) and taxonomic species identification is therefore challenging. In China, two species are known only from a single sex, *B. biprocessus* Tang, Yin & Peng, 2012 (male) and *B. longidens* Tang & Li, 2010 (female) (Tang and Li 2010; Yin et al. 2012).

### ***Borboropactus longidens* Tang & Li, 2010**

Figs 1–3

*Borboropactus longidens* Tang & Li, 2010: 21, figs 15A–D, 16A, B (♀).

**Material examined.** 1 ♂, 1 ♀, CHINA, Hainan, Ledong County, Jianfengling National Natural Reserve, Mingfenggu Scenic Spot, 18°44'25.87"N, 108°50'47.83"E, 1–31 May 2021, Yunhu Mo leg. (Tho-293, ASM-JGSU); 1 ♂, 2 ♀, Vietnam, Tam Dao National Park, Vinh Phuc, Vietnam Natural Forest, 21°29.55'N, 105°37.42'E, 1063 m, 12 September. 2007, Pham Dinh Sac leg. (IZCAS, examined by Yejie Lin).

**Diagnosis.** The male of this species resembles that of *Borboropactus edentatus* Tang & Li, 2010 (see Tang and Li 2010: 12, fig. 6A–D) by having the embolus lacking the spiralling tip, but can be easily distinguished by the round median apophysis (vs. oval in *B. edentatus*), the tibia with a horn-like retrolateral apophysis as long as the tibia (vs. triangular, shorter than tibia in *B. edentatus*), and lacking the dorsal apophysis (vs. present in *B. edentatus*) (Figs 1G–J, 2). The female of this new species differs from that of *B. edentatus* (see Tang and Li 2010: 12, fig. 7B, C) by the narrow median field (vs. lacking), the slender epigynal teeth (vs. lacking), and the L-shaped copulatory ducts (vs. oval) (Fig. 3I, J).

**Description. Male. Habitus** as in Fig. 1A, B. Total length 7.15, prosoma length 3.36, width 3.00, anteriorly narrowed to 0.41× its maximum width. Eye diameters (Fig. 1C): AME 0.16, ALE 0.17, PME 0.15, PLE 0.20; interdistances: AME–AME 0.12, AME–ALE 0.14, PME–PME 0.17, PME–PLE 0.31, AME–PME 0.21, AME–PLE 0.45, ALE–ALE 0.73, PLE–PLE 1.03, ALE–PLE 0.20. MOA 0.51 long, front width 0.43, back width 0.44. Chelicerae (Fig. 1D, E) with four promarginal teeth, three retromarginal teeth, including a vestige tooth, and four small denticles in-between the teeth. Endites (Fig. 1B) nearly quadrilateral, with dense setae on surface. Labium (Fig. 1B) rectangular, anteriorly with strong setae. Sternum (Fig. 1B) broadly oval, with dense setae around margin. Legs measurements: I 10.58 (3.1, 1.55, 3, 2.02, 0.91); II 7.45 (2.5, 0.88, 2.32, 1.19, 0.56); III 7.63 (1.88, 0.95, 2.11, 1.91, 0.78); IV 9.22 (2.01, 1.91, 2.01, 2.16, 1.13); spination (Fig. 1A, B, F): I Fe: p2, v2; Ti: d4, v10; Mt: d3, v6; II Pa: d1; Ti: d4, v10; Mt: d2, v6; III Fe: d1; Ti: d3; Mt: d3; IV: Fe: d2; Ti: d4; Mt: d3; cusps: I Fe: 8; II Fe: 1. Opisthosoma (Fig. 1A, B) length 3.79, width 3.22, dorsally with abundant macrosetae on posterior part.

**Colouration** (Fig. 1A, B). Prosoma yellow to dark brown, densely covered white feathery setae, with an approximate U-shaped yellowish marking medially and dark

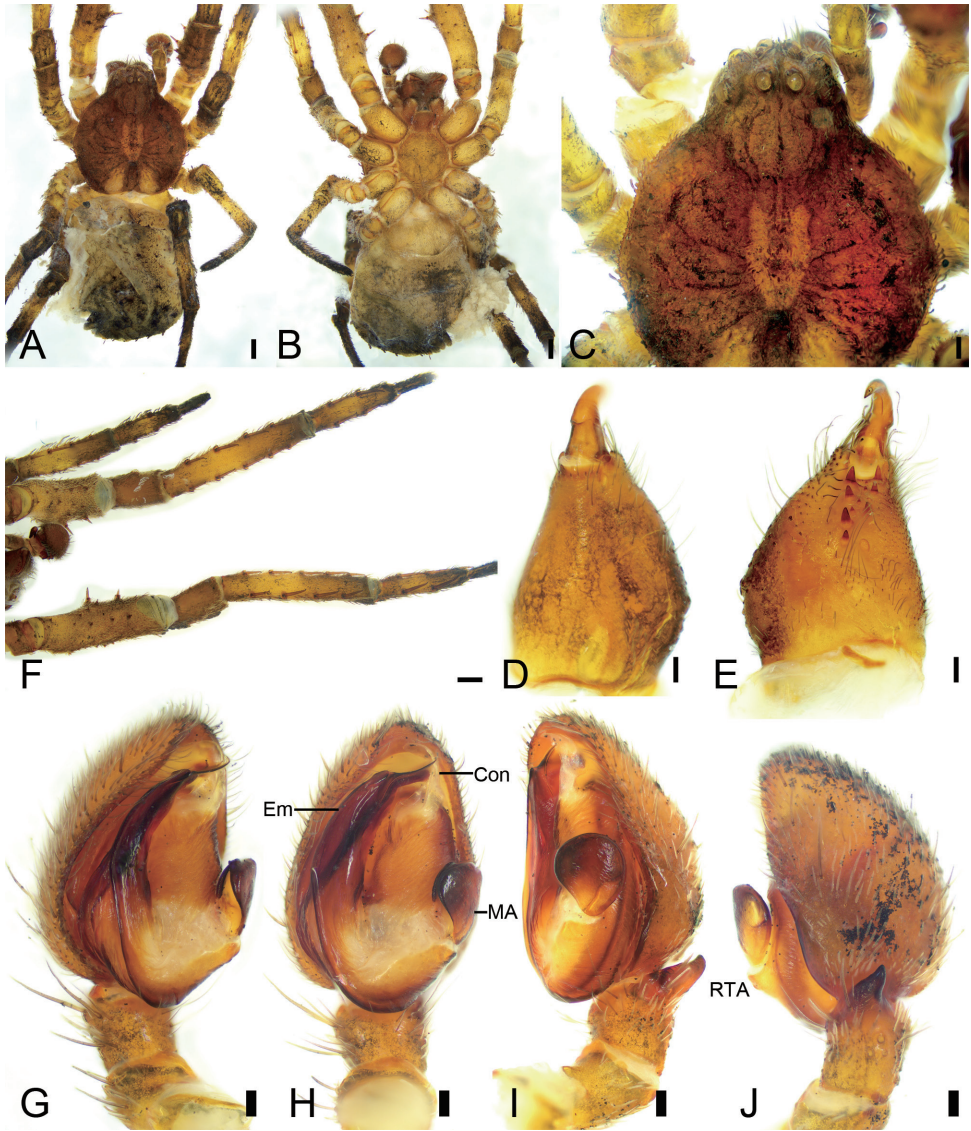


**Figure 1.** *Borboropactus longidens* Tang & Li, 2010, male **A** habitus, dorsal view **B** same, ventral view **C** eyes, dorsal view **D** chelicera, dorsolateral view **E** same, ventral view **F** leg I, ventral view **G** palp, ventro-prolateral view **H** same, ventral view **I** same, ventro-retrolateral view **J** same, retro-dorsal view. Abbreviations: Con – conductor, Em – embolus, MA – median apophysis, RTA – retrolateral tibial apophysis. Scale bars: 0.5 mm (**A**, **B**); 0.2 mm (**C**); 0.1 mm (**D**–**J**).

thin radial markings around the fovea. Chelicerae, endites, and labium yellow-brown. Sternum yellow. Legs from yellow to dark brown, mottled. Opisthosoma yellow to greyish black.

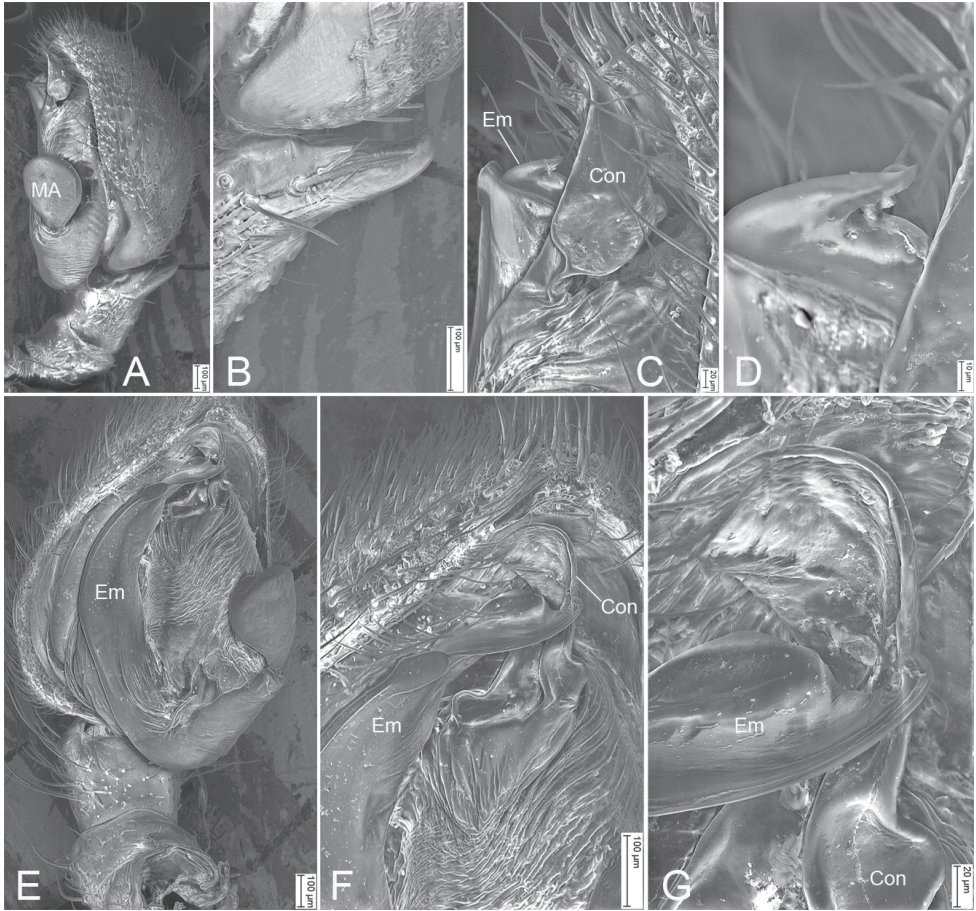


**Figure 2.** SEM micrographs of *Borboropactus longidens* Tang & Li, 2010, male palp **A** retrolateral view **B** same, details of retrolateral tibial apophysis **C** same, details of conductor and embolus **D** same, details of embolic tip **E** ventral view **F** same, detail of conductor and embolus **G** same, details of conductor and embolic tip. Abbreviations: Con – conductor, Em – embolus, MA – median apophysis, RTA – retrolateral tibial apophysis.

**Palp** (Figs 1G–J, 2). Palp with a relative long and strong retrolateral tibial apophysis (*RTA*), extending dorsally, as long as tibia in retrolateral view; median apophysis (*MA*) pear-shaped, located at submedian-retrolateral of tegulum; conductor (*Con*) translucent, with broad base and apex, nearly as long as 1/3 of tegulum; embolus (*Em*) flatted-shaped, slightly less than tegular length, originating at the 6 o'clock position of tegulum, with a membranous anterior part and spine-like apex.

**Female. Habitus** as in Fig. 3A–D. As in male except as follows. Total length 10.67, prosoma length 4.46, width 4.32, anteriorly narrowed to 0.44× its maximum width. Eye diameters (Fig. 3E): AME 0.16, ALE 0.19, PME 0.17, PLE 0.20; interdistances:

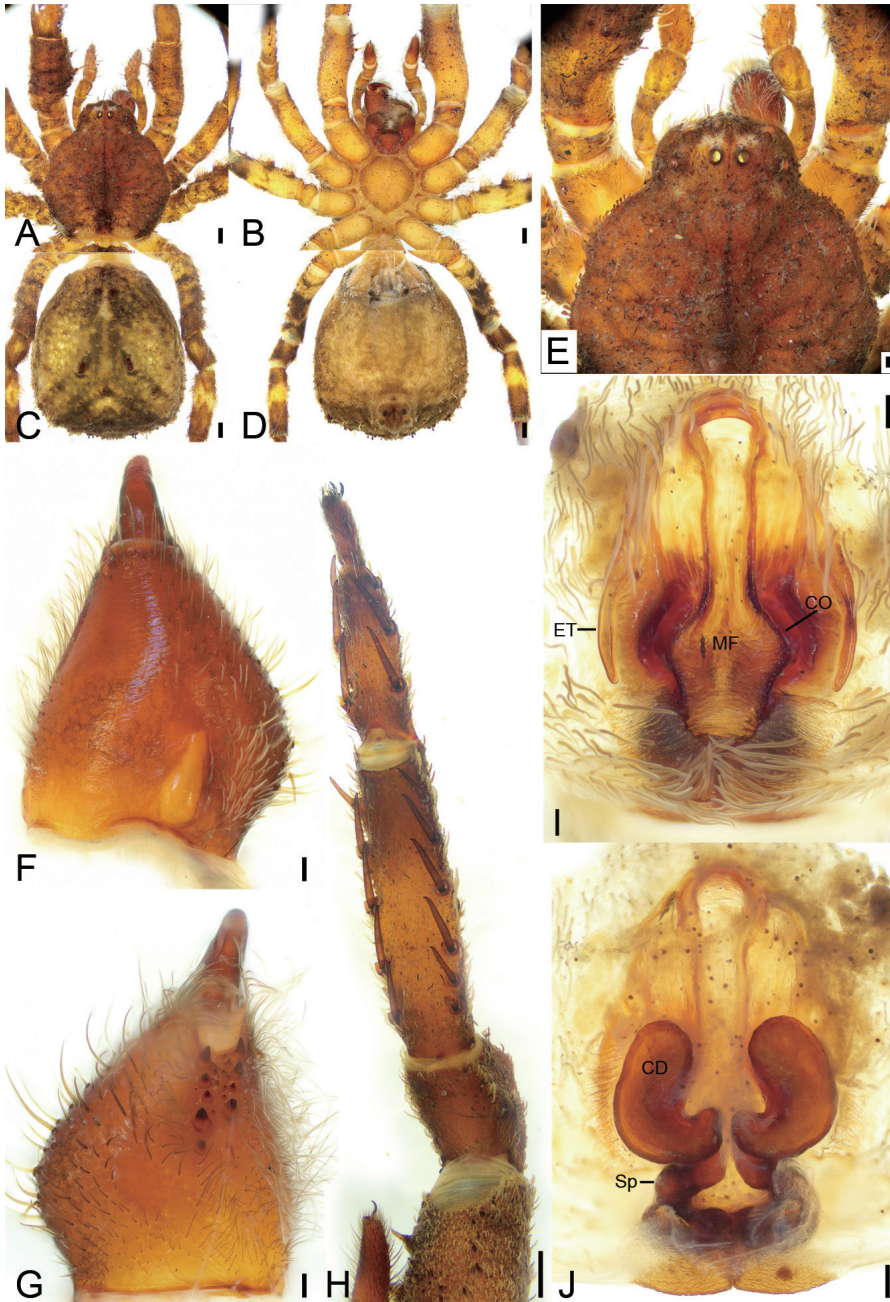


**Figure 3.** *Borboropactus longidens* Tang & Li, 2010, female **A** prosoma, dorsal view **B** same, ventral view **C** opisthosoma, dorsal view **D** same, ventral view **E** eyes, dorsal view **F** chelicera, dorsal view **G** same, ventral view **H** leg I, ventral view **I** epigyne, dorsal view **J** same, ventral view. Abbreviations: CD – copulatory duct, CO – copulatory opening, ET – epigynal tooth, MF – median field, Sp – spermatheca. Scale bars: 0.5 mm (**A–D**); 0.2 (E); 0.1 mm (**F–J**).

AME–AME 0.15, AME–ALE 0.27, PME–PME 0.24, PME–PLE 0.47, AME–PME 0.34, AME–PLE 0.68, ALE–ALE 0.99, PLE–PLE 1.44, ALE–PLE 0.36. MOA 0.64 long, front width 0.45, back width 0.54. Chelicerae (Fig. 3F, G) with five promarginal teeth, four retromarginal teeth, including a vestige tooth, and nine small denticles in-between teeth. Labium (Fig. 3B) wider than long. Legs (Fig. 3A–D, H) measurements: I 10.91 (3.45, 1.35, 3.35, 2.01, 0.75); II 8.73 (2.5, 1.25, 2.41, 1.88, 0.69); III 9.95 (2.67, 1.11, 2.5, 2.53, 1.14); IV 10.3 (2.75, 1.52, 2.38, 2.44, 1.21); spination (Fig. 3A–D, H): I Fe: p2; Ti: v11; Mt: d3, v6; II Ti: d3, v9; Mt: d3, v6; III Fe: d1; Ti: d4; Mt: d3; cusps: I Fe: 18; II Fe: 1; IV Fe: 1. Opisthosoma (Fig. 3C, D) length 6.21, width 5.32.

**Colouration** (Fig. 3A–D). Prosoma medially with a fine dark mark. Chelicerae, endites, and labium red-brown. Opisthosoma white to dark brown.

**Epigyne** (Fig. 3I, J). Median field (*MF*) flask-like, subposterior part broader than other parts; epigynal teeth (*ET*) very long, as long as 1/2 of median field, arising median-bilaterally; copulatory openings (*CO*) arising from anterior part of maximum median field; copulatory ducts (*CD*) broad, wider than spermathecae, both ends swollen, sloping C-shaped, located at median of vulva, anterior part widely separated by its maximum width, and posterior part are approaching each other; spermathecae (*Sp*) C-shaped, median part have a constriction, posterior part close touching, both ends slightly swollen.

**Distribution.** Known from China (Hainan) and Vietnam (Fig. 10).

## Genus *Pharta* Thorell, 1891

**Comments.** This genus includes ten species distributed in Asia (Benjamin 2014; WSC 2022). Half of them (5 species) are recorded from China, where it is known from Yunnan, Guizhou, and Jiangxi provinces (Tang et al. 2009; Wang et al. 2016; Liu et al. 2022c). No species were recorded from Tibet Province.

### *Pharta xizang* Liu & Yao, sp. nov.

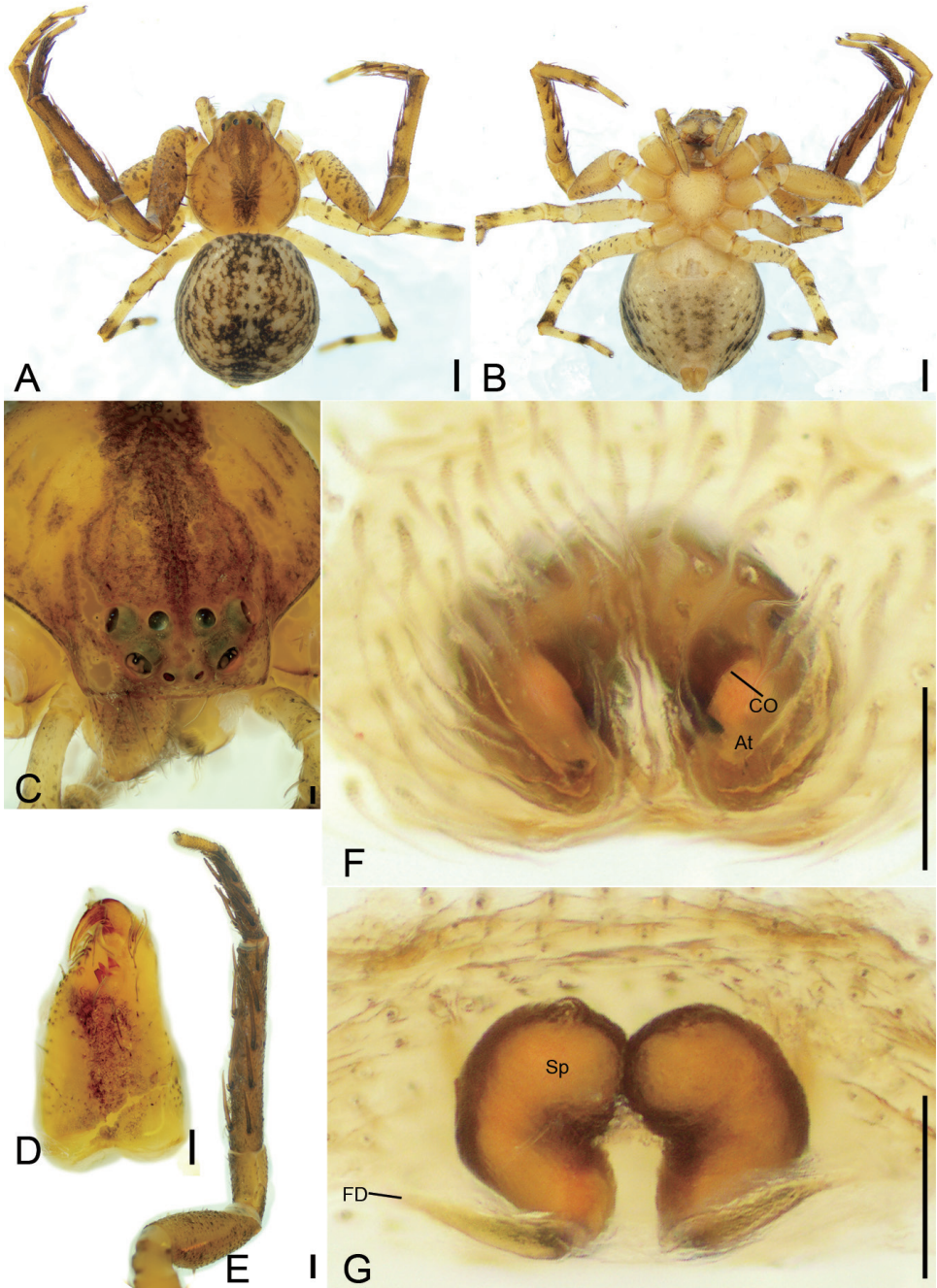
<https://zoobank.org/4B8E9C66-615E-4DCC-93A5-5A439C23ADB3>

Fig. 4

**Type material.** *Holotype* ♀: CHINA, Tibet, Linzhi City, Motuo County, near Lianhua Hotel, 29°19'31.07"N, 95°19'59.51"E, 1101 m, 17 July 2017, Jian Chen, Jie Liu, Man Fang, Zengtao Zhang and Fengxiang Liu leg. (Tho-296, ASM-JGSU).

**Etymology.** The specific name derived from the Chinese Pinyin for Tibet; noun in apposition.

**Diagnosis.** The male of this new species resembles *Pharta tengchong* (Tang, Griswold & Yin, 2009) (see Tang et al. 2009: 47, fig. 6A–F) in having the prosoma with an



**Figure 4.** *Pharta xizang* sp. nov., female holotype, preserved **A** habitus, dorsal view **B** same, ventral view **C** eyes, dorsal view **D** chelicera, ventrolateral view **E** leg I, ventro-retrolateral view **F** epigyne, dorsal view **G** same, ventral view. Abbreviations: At – atrium, CO – copulatory opening, FD – fertilisation duct, Sp – spermatheca. Scale bars: 0.5 mm (**A, B**); 0.2 mm (**C**); 0.1 mm (**D–G**).

inverted triangular black-brown marking and the touching anterior spermathecae with a bent part, but differs from it by the copulatory openings being hidden by cambered atrial lateral margins directed medially (vs. bilaterally in *P. tengchong*) and the separated posterior spermathecae (vs. closely touching in *P. tengchong*) (Fig. 4F, G).

**Description. Female. Habitus** as in Fig. 4A, B. Total length 4.62, prosoma length 1.98, width 1.89, anteriorly narrowed to 0.50× its maximum width. Eye diameters (Fig. 4C): AME 0.05, ALE 0.13, PME 0.10, PLE 0.11; interdistances: AME–AME 0.10, AME–ALE 0.07, PME–PME 0.13, PME–PLE 0.14, AME–PME 0.19, AME–PLE 0.32, ALE–ALE 0.32, PLE–PLE 0.59, ALE–PLE 0.14. MOA 0.32 long, front width 0.20, back width 0.31. Chelicerae (Fig. 4D) with three small promarginal teeth and three retromarginal teeth (median and distal touching). Endites (Fig. 4B) nearly quadrilateral, slightly longer than wide. Labium (Fig. 4B) rectangular, wider than long, anteriorly with strong setae. Sternum (Fig. 4B) oval, longer than wide, with notch anteromedially. Legs measurements (Fig. 4A, B, E): I 6.12 (1.73, 0.78, 2.21, 1.04, 0.36); II 7.21 (2.27, 0.86, 2.09, 1.4, 0.59); III 3.19 (0.88, 0.4, 1.02, 0.45, 0.44); IV 4.67 (1.51, 0.58, 1.17, 0.91, 0.5); spination (Fig. 4A, B, E): I Fe: d5, p2, r1; Ti: p2, r2, v10; Mt: p1, r1, v8; II Fe: d2; Pa: p1; Ti: p3, r3, v10; Mt: p1, r1, v8; III Fe: d2; Pa: p1; Ti: d2, v2; Mt: d5, v1; IV: Fe: d1; Pa: d1; Ti: d2, p2, v1; Mt: d1, p2. Opisthosoma (Fig. 4A, B) length 2.63, width 2.40.

**Colouration** (Fig. 4A, B). Prosoma yellow-brown, medially with single broad, dark brown, mottled band, laterally with fringe-shaped dark brown, mottled stripe. Chelicerae yellowish to dark brown. Endites yellow. Labium yellow-brown. Sternum yellow. Legs: tibia and metatarsus I yellow-brown, other segments yellow with a few dark spots, distal parts of tibiae and metatarsi III and IV with dark brown annulations. Opisthosoma grey to dark, with net-like mottled markings and sparse white guanine spots; venter yellow to dark brown, laterally with sparse white guanine spots.

**Epigyne** (Fig. 4F, G). Epigyne heart-shaped, 1.2× wider than long. Copulatory openings (*CO*) visible, hidden by hood-shaped atrium (*At*). Copulatory ducts not visible, possibly absent. Spermathecae (*Sp*) C-shaped, ca. 2× longer than wide, anterior part of spermathecae closely touching, posterior parts slightly separated. Fertilisation ducts (*FD*) slightly less than the length of spermatheca, directed laterally.

**Distribution.** Known only from the type locality in Tibet, China (Fig. 10).

## Genus *Stephanopsis* O. Pickard-Cambridge, 1869

**Comments.** This genus includes 24 species mainly distributed in Australasia, South America, and Asian mainland (WSC 2022). Nearly half of them (11 species) are described based either on single females or males (WSC 2022). Only one species was recorded from China on the Asian mainland, *S. xiangzhouica* Liu, 2022 (Liu et al. 2022c). Unfortunately, it is known only from the female in Jiangxi Province, China.

***Stephanopsis qiong* Liu & Yao, sp. nov.**

<https://zoobank.org/3DC97292-727A-461B-84DA-AEB83E2AB902>

Figs 5, 6

**Type material.** *Holotype* ♀: CHINA, Hainan, Ledong County, Jianfengling National Natural Reserve, Mingfenggu Scenic Spot, 18°44'25.87"N, 108°50'47.83"E, 4 April 2021, Yunhu Mo leg. (Tho-292, ASM-JGSU).

**Etymology.** The specific name refers to the Chinese abbreviation for Hainan Province; noun in apposition.

**Diagnosis.** The female of this new species resembles *Stephanopsis xiangzhouica* Liu, 2022 (see Liu et al. 2022c: 64, fig. A, B) in having the copulatory openings hidden by a transverse ridge, but can be distinguished by the inverted heart-shaped atrium (vs. oval) and the tube-shaped spermathecae separated by nearly as long as their width (vs. the oval spermathecae separated by their half width) (Fig. 5G, H).

**Description. Female** (holotype). *Habitus* as in Figs 5A, B, 6C, D. Total length 5.46, prosoma (Fig. 5A, B) length 2.32, width 2.86, anteriorly narrowed to 0.43× its maximum width, covered with numerous strong, short, radially distributed peg-like setae and dense short plumose setae, with three rows of short, strong setae along the midline. Eye diameters (Fig. 5C): AME 0.05, ALE 0.11, PME 0.08, PLE 0.09; inter-distances: AME-AME, 0.10, AME-ALE, 0.12, PME-PME, 0.25, PME-PL, 0.14, AME-PME, 0.36, AME-PL, 0.39, ALE-ALE, 0.37, PL-PL 0.67, ALE-PL, 0.16. MOA 0.44 long, front width 0.19, back width 0.41. Chelicerae (Fig. 5D, E) with three promarginal and two retromarginal teeth, and a small denticle in-between. Endites (Fig. 5B) nearly quadrilateral, longer than wide. Labium (Fig. 5B) rectangular, wider than long, anteriorly with strong setae. Sternum oval, anteriorly flattened, as long as wide, covered by very dense setae. Legs measurements (Fig. 5A, B, F): I 9.17 (3.09, 1.53, 2.22, 1.55, 0.78); II 6.86 (1.97, 1.14, 2.03, 1.28, 0.44); III 4.67 (1.39, 0.75, 1.31, 0.67, 0.55); IV 5.85 (1.69, 0.73, 1.21, 1.73, 0.49); spination (Fig. 5A, B, F): I Ti: d1, v8; Mt: d1, r1, v8; II Ti: d2, v8; Mt: d2, v8; III Pa: d1; cusps: I Fe: 5; Pa: 2; Ti: 3; II Fe: 9; Pa: 3; Ti: 3; IV Fe: 2. Opisthosoma (Fig. 5A, B) length 3.14, width 3.87, pentagonal with a notch posteromedially; dorsum covered with sparse peg-like setae; venter with numerous plumose setae medially.

**Colouration** (Fig. 5A, B). Prosoma reddish brown, with radial, irregular, dark brown mottled markings in the surface. Chelicerae, endites, labium, and sternum yellow-brown. Legs yellow to yellow-brown. Opisthosoma white to yellow, with numerous irregular guanine spots; venter yellow, with a few guanine spots on lateral parts.

**Epigyne** (Fig. 5G, H). Epigyne oval, wider than long. Atrium (*At*) large, inverted heart-shaped, covering 2/3 of epigynal field. Copulatory openings (*CO*) invisible, hidden by a transverse ridge (*TR*). Copulatory ducts very short, touching. Membranous sacs (*MS*) transparent, located anteriorly, covering 2/3 of epigynal plate, slightly separated. Glandular appendages (*GA*) nearly spherical, almost as long as 1/2 width of spermatheca. Spermathecae (*Sp*) tube-shaped, slightly separated by less

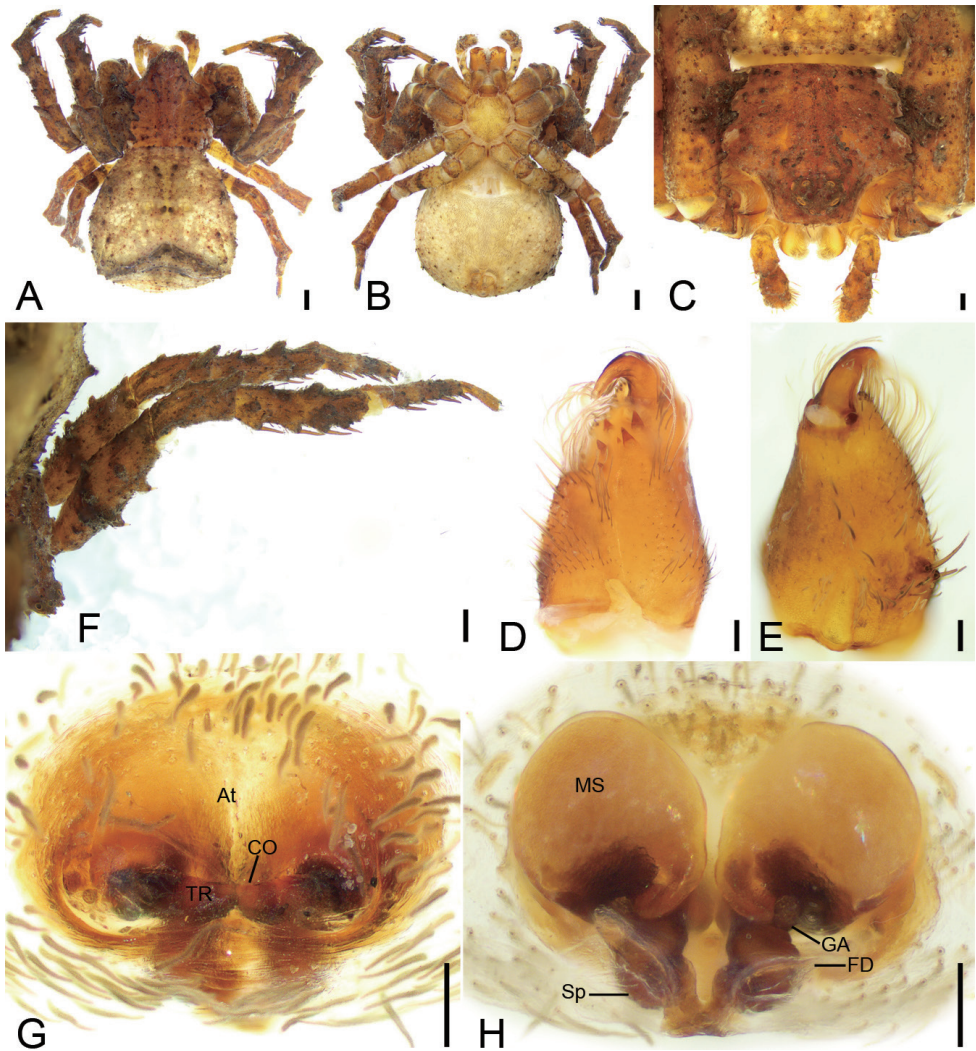


**Figure 5.** *Stephanopsis qiong* sp. nov., female holotype, preserved **A** habitus, dorsal view **B** same, ventral view **C** eyes, dorsal view **D** chelicera, ventrolateral view **E** same, dorsolateral view **F** leg I, dorso-prolateral view **G** epigyne, dorsal view **H** same, ventral view. Abbreviations: At – atrium, CO – copulatory opening, FD – fertilisation duct, GA – glandular appendage, MS – membranous sac, Sp – spermatheca, TR – transverse ridge of copulatory openings. Scale bars: 0.5 mm (**A, B**); 0.2 mm (**C**); 0.1 mm (**D–H**).

spermathecal width. Fertilisation ducts (*FD*) slightly less than the length of spermatheca, directed anterolaterally.

**Male.** Unknown.

**Distribution.** Known only from the type locality in Hainan Province, China (Fig. 10).

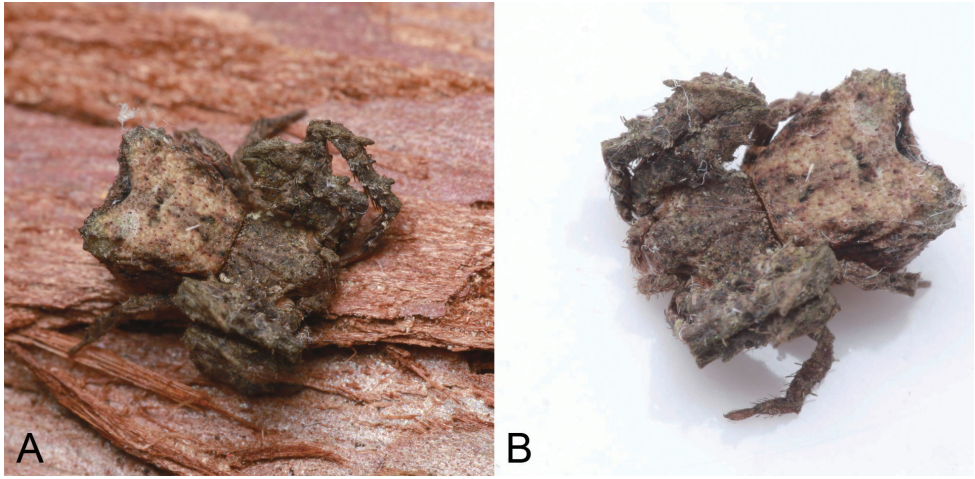


**Figure 6.** Photographs of living specimens from China **A, B** *Stephanopsis qiong* sp. nov., female.

***Stephanopsis xiangzhouica* Liu, 2022**

Figs 7–9

*Stephanopsis xiangzhouica* Liu, in Liu et al. 2022c: 64, figs 12A–I, 13A, B (holotype ♀ from Jinggang National Nature Reserve, Jiangxi Province, deposited in ASM-JGSU, No. Tho-17, examined).

**Material examined.** 1 ♂, 1 ♀, CHINA, Guangdong, Ruyuan County, Nanling National Natural Reserve, Waterfalls Scenic Spot, 24°54'52.11"N, 113°2'28.67"E, 779 m, 6 September 2020, Qingbo Huo leg. (Tho-295, ASM-JGSU).

**Diagnosis.** The male of this species resembles *S. nigra* O. Pickard-Cambridge, 1869 (see Machado et al. 2019: fig. 38C, D) in having a forked retrolateral tibial apophysis, but it can be distinguished by the retrolateral tibial apophysis being longer than tibia (vs. less than tibial length) and the embolus with a hook-shaped apex (vs. flagelliform) (Figs 7F–I, 8). The male of this species also resembles *S. altifrons* O. Pickard-Cambridge, 1869 (see Machado et al. 2019: 224, fig. 3C–F), *S. carcinoides* Machado, 2019 (see Machado et al. 2019: 243, fig. 20C, D), and *S. lata* O. Pickard-Cambridge, 1869 (see Machado et al. 2019: 253, fig. 29C, D), but it can be easily distinguished from them by the embolus having a hook-shaped apex (vs. flagelliform in all three species) and the retrolateral tibial apophysis with two morphologically different branches (dorsal branch much longer and thicker than the ventral) (vs. ventral branch much longer and thicker than the dorsal in *S. altifrons* and *S. carcinoides*; ventral branch indistinct in *S. lata*) (Figs 7F–I, 8). Female diagnosis as in Liu et al. (2022c).

**Description. Male. Habitus** as in Fig. 7A, B. Total length 4.77, prosoma length 2.17, width 2.29, anteriorly narrowed to 0.37× its maximum width, covered with

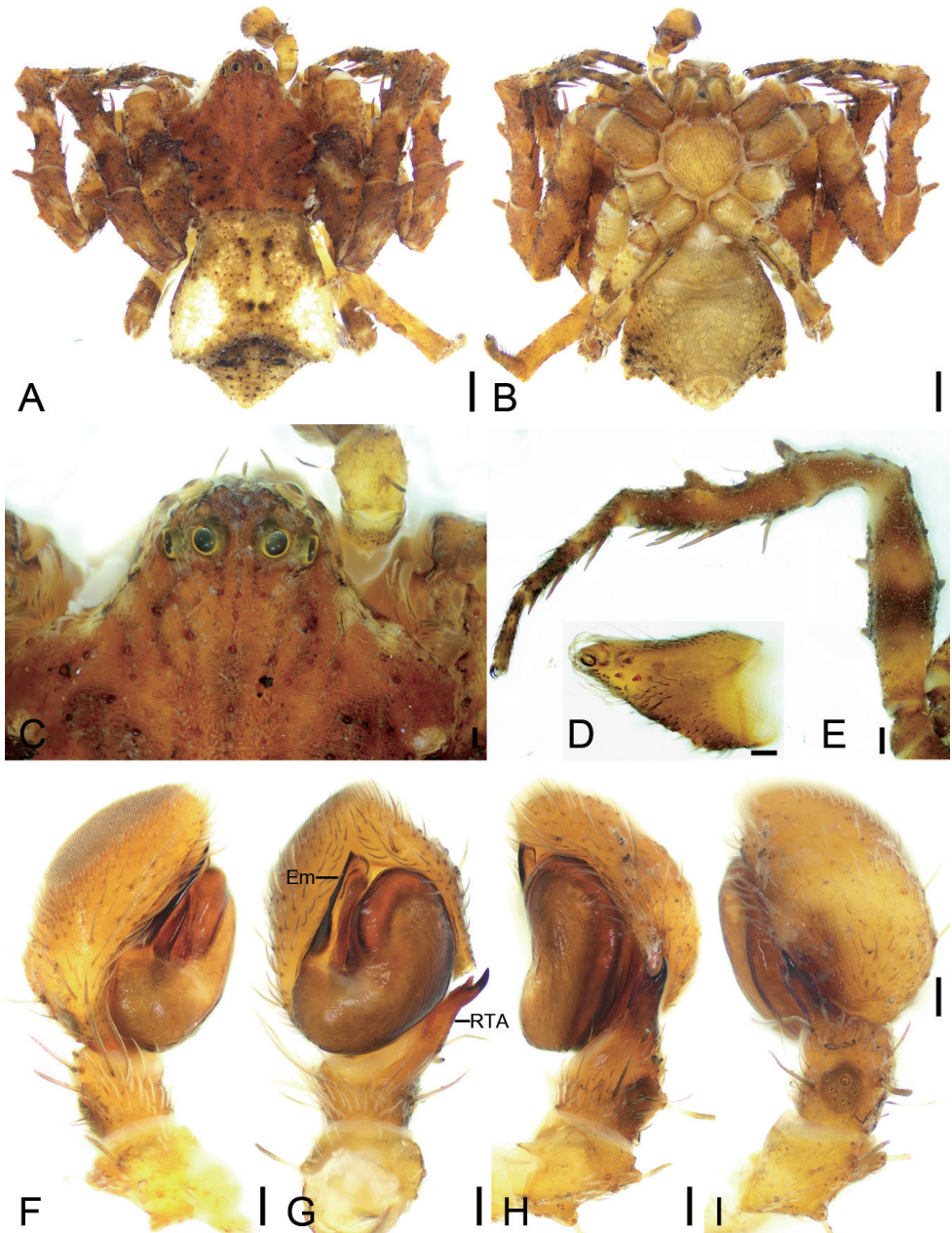


**Figure 7.** *Stephanopis xiangzhouica* Liu, 2022, male, preserved **A** habitus, dorsal view **B** same, ventral view **C** eyes, dorsal view **D** chelicera, ventral view **E** leg I, retrolateral view **F** palp, pro-lateral view **G** same, ventral view **H** same, ventro-retrolateral view **I** same, retro-dorsal view. Abbreviations: Em – embolus, RTA – retrolateral tibial apophysis. Scale bars: 0.5 mm (**A, B**); 0.2 mm (**C**); 0.1 mm (**D–I**).

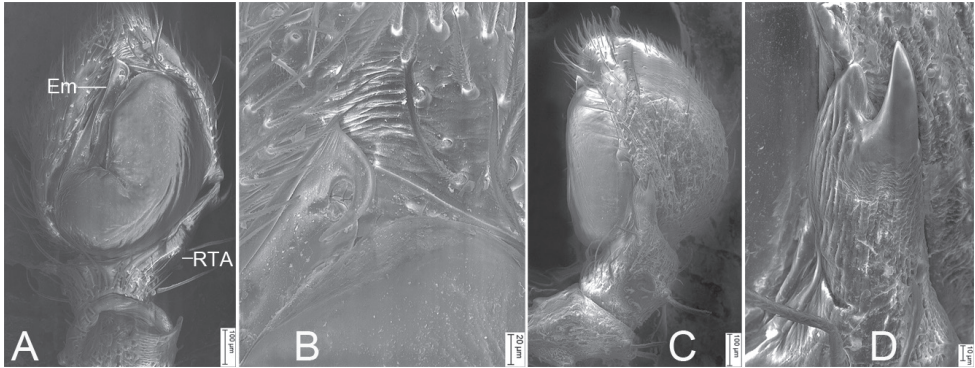


**Figure 8.** SEM micrographs of *Stephanopsis xiangzhouica* Liu, 2022, male palp **A** ventral view **B** same, details of embolus **C** retrolateral view **D** same, detail of retrolateral tibial apophysis. Abbreviations: Em – embolus, RTA – retrolateral tibial apophysis.

numerous strong, short, radially peg-like setae and dense short plumose setae, with three rows of short strong setae along midline. Eye diameters (Fig. 7C): AME 0.06, ALE 0.13, PME 0.10, PLE 0.10; interdistances: AME–AME 0.09, AME–ALE 0.05, PME–PME 0.21, PME–PLE 0.09, AME–PME 0.28, AME–PLE 0.34, ALE–ALE 0.13, PLE–PLE 0.60, ALE–PLE 0.13. MOA 0.42 long, front width 0.22, back width 0.41. Chelicerae (Fig. 7D) three promarginal teeth and one retromarginal tooth. Endites (Fig. 7B) nearly quadrilateral, longer than wide, laterally with long setae. Labium (Fig. 7B) rectangular, wider than long, anteriorly with strong setae. Sternum round, nearly as long as wide, covered by dense setae. Legs measurements (Fig. 7A, B, E): I 4.49 (1.62, 0.73, 1.12, 0.67, 0.35); II 4 (1.35, 0.73, 0.98, 0.6, 0.34); III 4.4 (1.37, 0.71, 1.08, 0.67, 0.57); IV 4.6 (1.63, 0.65, 1.06, 0.68, 0.58); spination (Fig. 7A, B, E): I Fe: v2; Ti: d2, v8; Mt: v8; II Fe: v4; Ti: v8; Mt: d3, v8; III Ti: p1; cusps: I Fe: 11; Pa: 4; Ti: 5; Mt: 2; II Fe: 11; Pa: 4; Ti: 4. Opisthosoma (Fig. 7A, B) length 2.58, width 2.11, pentagonal with pair of latero-posterior horns; dorsum covered with sparse brown peg-like and small, dense, plumose setae; venter with numerous plumose setae.

**Colouration** (Fig. 7A, B). Prosoma reddish brown. Chelicerae, endites, and labium yellow-brown. Sternum yellow, with yellow-brown margin. Legs mottled, I and II yellow to reddish brown, III and IV grey to yellow. Opisthosoma grey to yellow-brown, laterally with numerous irregular guanine spots; venter yellow.

**Palp** (Figs 7F–I, 8). Palp with a long retrolateral tibial apophysis (*RTA*), pincer-like in retrolateral view, longer than tibia; embolus (*Em*) flattened-shaped, with broad base, less than tegular length, originating at approximately the 8 o'clock position of the tegulum, with a distinct constriction in the subapical part, and a hook-shaped apex.

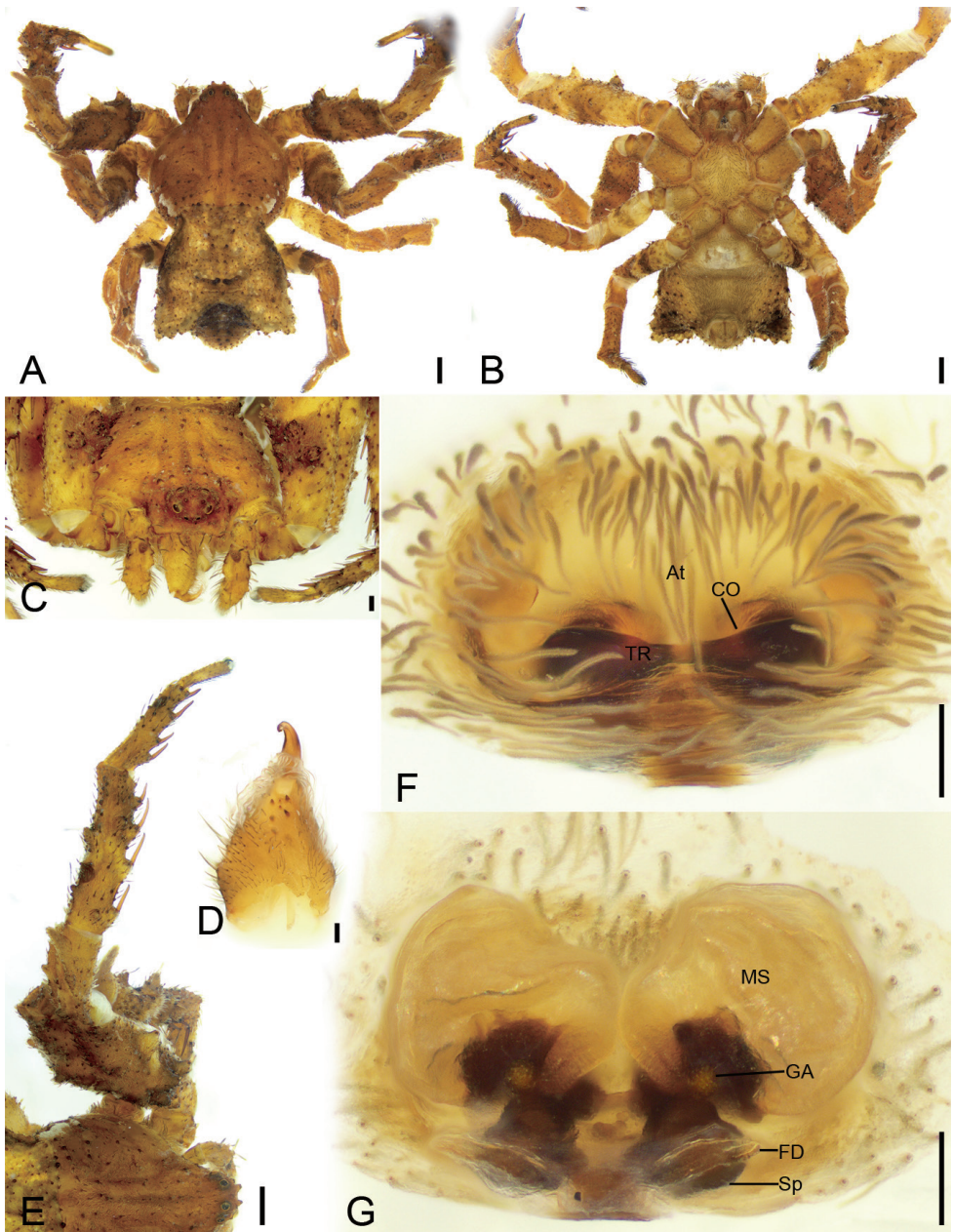


**Figure 9.** *Stephanopsis xiangzhouica* Liu, 2022, female, preserved **A** habitus, dorsal view **B** same, ventral view **C** eyes, dorsal view **D** chelicera, ventral view **E** leg I, prolateral view **F** epigyne, dorsal view **G** same, ventral view. Abbreviations: At – atrium, CO – copulatory opening, FD – fertilisation duct, GA – glandular appendage, MS – membranous sac, Sp – spermatheca, TR – transverse ridge of copulatory openings. Scale bars: 0.5 mm (**A, B**); 0.2 mm (**C**); 0.1 mm (**D–G**).

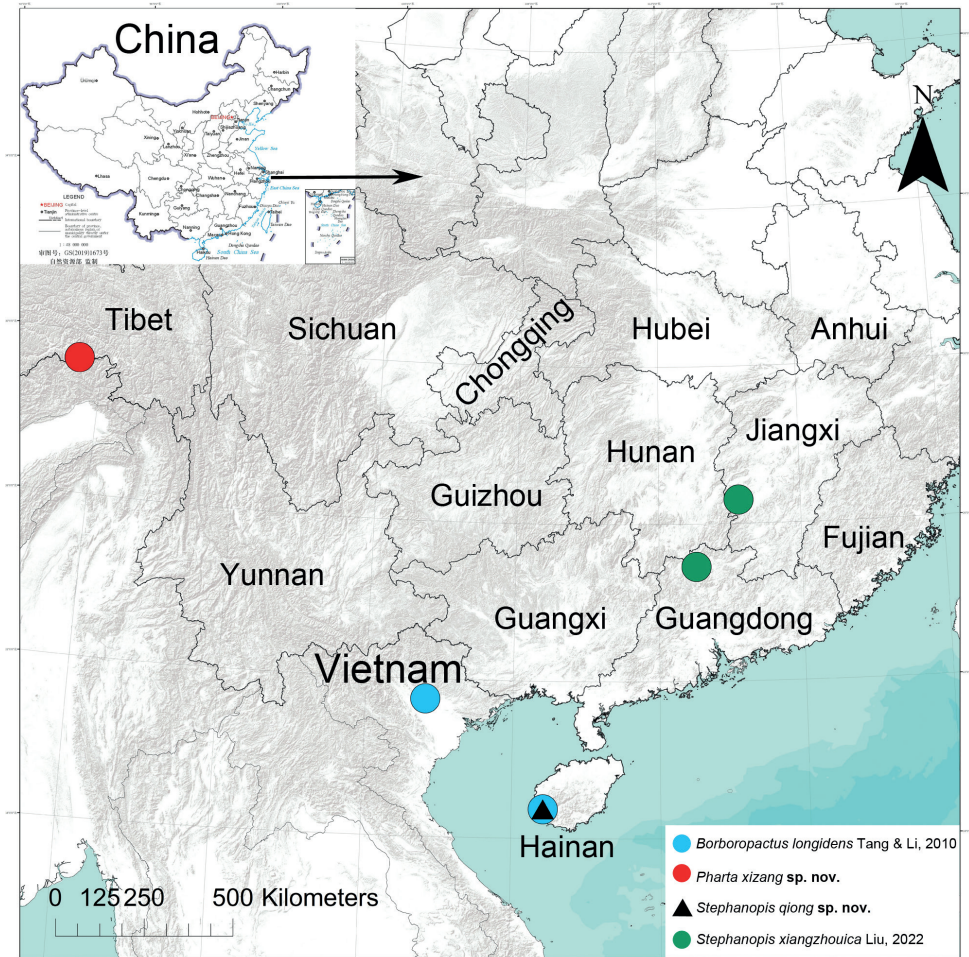


**Figure 10.** Records of *Borboropactus longidens* Tang & Li, 2010, *Pharta xizang* sp. nov., *Stephanopsis qiong* sp. nov. and *S. xiangzhouica* Liu, 2022 from Asia.

**Female.** Description in Liu et al. (2022c) for female sex. Female habitus shown in Fig. 9A, B; eyes, chelicerae, and leg I in Fig. 9C–E; and epigyne in Fig. 9F, G.

**Distribution.** Known from Jiangxi and Guangdong provinces, China (Fig. 10).

## Acknowledgements

We thank Yunhu Mo, Pham Dinh Sac, Qingbo Huo, Jian Chen, Jie Liu, Man Fang, Zengtao Zhang and Fengxiang Liu for their assistance in collecting the specimens.

We also thank Yejie Lin for reviewing the *Borboropactus* specimens collected from Vietnam which are deposited in Institute of Zoology, Chinese Academy of Sciences, Beijing, China, and Qianle Lu for providing exquisite photographs of living specimens. We are also grateful to Dr Suresh Benjamin, Dr Miguel Machado and subject editor Miquel A. Arnedo for their helpful suggestions and comments on the manuscript, and Dr Nathalie Yonow for improving the English of the manuscript. This research was sponsored by the Natural Science Foundation of China (32000301/32160243) and the Science and Technology Innovation Project for College Students.

## References

- Álvarez-Padilla F, Hormiga G (2007) A protocol for digesting internal soft tissues and mounting spiders for scanning electron microscopy. *The Journal of Arachnology* 35(3): 538–542. <https://doi.org/10.1636/Sh06-55.1>
- Benjamin SP (2011) Phylogenetics and comparative morphology of crab spiders (Araneae: Dionycha, Thomisidae). *Zootaxa* 3080(1): 1–108. <https://doi.org/10.11646/zootaxa.3080.1.1>
- Benjamin SP (2014) Two new species of *Pharta* Thorell, 1891 with the description of *Ibana senagang* gen. et sp. nov. (Araneae: Thomisidae). *Zootaxa* 3894(1): 177–182. <https://doi.org/10.11646/zootaxa.3894.1.15>
- Huang GQ, Lin YJ (2020) A new species of *Stiphropus* (Aranei: Thomisidae) from China and first documentation of myrmecophily in this genus. *Arthropoda Selecta* 29(2): 257–261. <https://doi.org/10.15298/arthsel.29.2.12>
- Li S (2020) Spider taxonomy for an advanced China. *Zoological Systematics* 45(2): 73–77.
- Li SQ, Lin YC (2016) Species Catalogue of China (Vol. 2). Animals. Invertebrates (1). Arachnida: Araneae. Science Press, Beijing, 549 pp.
- Lin YJ, Koh JKH, Shao L, Li SQ (2019) Description on two species of genus *Platythomisus* (Araneae, Thomisidae) from China and Singapore. *ZooKeys* 852: 73–84. <https://doi.org/10.3897/zookeys.852.34436>
- Lin YJ, Long Y, Koomen P, Yan XY, Li SQ (2022) Taxonomic notes on the genus *Phrynarachne* from China (Araneae, Thomisidae). *ZooKeys* 1085: 69–99. <https://doi.org/10.3897/zookeys.1085.77966>
- Liu KK, Liu JH, Xu X (2017) Two new species of the genus *Oxytate* from China (Araneae: Thomisidae). *Zootaxa* 4320(1): 193–200. <https://doi.org/10.11646/zootaxa.4320.1.12>
- Liu L, Zhang JC, Chen J (2021) [A new *Diaea* species (Araneae, Thomisidae) from China, with the transfer of *Loxobates spiniformis* Yang et al., 2006]. *Acta Arachnologica Sinica* 30(1): 20–25. <https://dx.doi.org/10.3969/j.issn.1005-9628.2021.01.003>
- Liu K, Li S, Zhang X, Ying Y, Meng Z, Fei M, Li W, Xiao Y, Xu X (2022a) Unknown species from China: the case of phrurolithid spiders (Araneae, Phrurolithidae). *Zoological Research* 43(3): 352–355. [Suppl. I: 1–5, Suppl. II: 1–223] <https://doi.org/10.11646/zootaxa.4613.2.4>

- Liu KK, Li WH, Yao YB, Li CZ, Li SQ (2022b) The first record of the thomisid genus *Ibana* Benjamin, 2014 (Araneae, Thomisidae) from China, with the description of a new species. *Biodiversity Data Journal* 10: e93637. <https://doi.org/10.3897/BDJ.10.e93637>
- Liu KK, Ying YH, Fomichev AA, Zhao DC, Li WH, Xiao YH, Xu X (2022c) Crab spiders (Araneae, Thomisidae) of Jinggang Mountain National Nature Reserve, Jiangxi Province, China. *ZooKeys* 1095: 43–74. <https://doi.org/10.3897/zookeys.1095.72829>
- Machado M, Teixeira RA, Milledge GA (2019) On the Australian bark crab spider genus *Stephanopsis*: taxonomic review and description of seven new species (Araneae: Thomisidae: Stephanopinae). *Records of the Australian Museum* 71(6): 217–276. <https://doi.org/10.3853/j.2201-4349.71.2019.1698>
- Meng ZY, Luo HP, Xiao YH, Xu X, Liu KK (2019) Redescription of *Borboropactus jiangyong* Yin, Peng, Yan & Kim, 2004 (Araneae, Thomisidae), with the first description of the male. *ZooKeys* 870: 137–148. <https://doi.org/10.3897/zookeys.870.35230>
- Tang G, Li SQ (2010) Crab spiders from Hainan Island, China (Araneae, Thomisidae). *Zootaxa* 2369(1): 1–68. <https://doi.org/10.11646/zootaxa.2369.1.1>
- Tang G, Yin CM, Peng XJ, Griswold C (2009) Six crab spiders of the family *Stephanopinae* from Southeast Asia (Araneae: Thomisidae). *The Raffles Bulletin of Zoology* 57: 39–50.
- Tian T, Zhou GC, Peng XJ (2018) A new species of *Pistius* Simon, 1875 (Araneae: Thomisidae) from Wuling Mountains, China. *Acta Arachnologica Sinica* 27(1): 7–11. <https://doi.org/10.3969/j.issn.1005-9628.2018.01.02>
- Wang C, Mi XQ, Peng XJ (2016) A new species of *Pharta* Thorell, 1891 (Araneae: Thomisidae) from China. *Oriental Insects* 50(3): 129–134. <https://doi.org/10.1080/00305316.2016.1197163>
- Wang C, Gan JH, Mi XQ (2020) A new species of the genus *Lysiteles*, with the first male description of *L. nudus* from Guizhou, China (Araneae: Thomisidae). *Sichuan Journal of Zoology* 39(3): 309–315. <https://doi.org/10.11984/j.issn.1000-7083.20200009>
- World Spider Catalog (2022) World Spider Catalog. Natural History Museum Bern. Version 23.5. <http://wsc.nmbe.ch> [Accessed 20 November 2022]
- Yin CM, Peng XJ, Yan HM, Bao YH, Xu X, Tang G, Zhou QS, Liu P (2012) Fauna Hunan: Araneae in Hunan, China. Hunan Science and Technology Press, Changsha, 1590 pp.
- Yu H, Zhang JS (2017) Two *Lysiteles* species from Leigong Mountains in Guizhou Province, China (Araneae: Thomisidae). *Acta Arachnologica Sinica* 26(2): 71–75. <https://doi.org/10.3969/j.issn.1005-9628.2017.02.02>
- Yu H, Li FM, Jin ZY (2017) Description of a new species of *Lysiteles* Simon from Guizhou Province, China (Araneae: Thomisidae). *Turkish Journal of Zoology* 41(6): 1076–1082. <https://doi.org/10.3906/zoo-1705-3>
- Zhang JS, Zhang WL, Deng LJ, Lu QL, Yu H (2022) *Synema guiyang* sp. nov., the fourth endemic species of *Synema* Simon, 1864 (Araneae, Thomisidae) from China. *Biodiversity Data Journal* 10: e85072. <https://doi.org/10.3897/BDJ.10.e85072>



# A new species of *Pseudopoda* (Araneae, Sparassidae) from China, with the description of different and distinctive internal ducts of the female vulva

Li-jun Gong<sup>1,2</sup>, Meng-yun Zeng<sup>1</sup>, Yang Zhong<sup>1,2,3</sup>, Hui-liang Yu<sup>4,5</sup>

**1** School of Nuclear Technology and Chemistry & Biology, Hubei University of Science and Technology, Xianning 437100, Hubei, China **2** Hubei Key Laboratory of Radiation Chemistry and Functional Materials, Hubei University of Science and Technology, Xianning 437100, Hubei, China **3** Administrative Commission of Jiugongshan National Nature Reserve of Hubei Xianning, Xianning, 437100, Hubei, China **4** Shennongjia National Park Administration, Shennongjia 442421, Hubei, China **5** Hubei Province Key Laboratory of Conservation Biology for Shennongjia Golden Monkey, Shennongjia 442421, Hubei, China

Corresponding authors: Yang Zhong ([hubeispider@aliyun.com](mailto:hubeispider@aliyun.com)); Hui-liang Yu ([64625235@qq.com](mailto:64625235@qq.com))

Academic editor: Dimitar Dimitrov | Received 11 November 2022 | Accepted 10 April 2023 | Published 2 May 2023

<https://zoobank.org/8070673D-B3F3-4686-88F3-EA264DA18F48>

**Citation:** Gong L-j, Zeng M-y, Zhong Y, Yu H-l (2023) A new species of *Pseudopoda* (Araneae, Sparassidae) from China, with the description of different and distinctive internal ducts of the female vulva. ZooKeys 1159: 189–199. <https://doi.org/10.3897/zookeys.1159.97463>

## Abstract

One new species of the genus *Pseudopoda* Jäger, 2000, *Pseudopoda deformis* Gong & Zhong, **sp. nov.** (♂, ♀), is described and documented with digital images from Shennongjia Forestry District, Hubei Province, China, based on morphology and DNA barcodes. This new species is separated from other *Pseudopoda* species by the unique type of internal ducts of the female vulva that are curved longitudinally, forming a narrow triangle or trapezoidal shape. In addition, DNA barcodes for this species are provided.

## Keywords

DNA barcoding, Hubei, huntsman spiders, morphology, taxonomy

## Introduction

*Pseudopoda* Jäger, 2000 is currently the largest genus in the family Sparassidae Bertkau, 1872. It comprises 251 species, of which 152 are recorded from China, representing 60.6% of the global species (WSC 2023). The genus has been recorded in areas from

South Asia (49 species in Nepal, India, Bhutan, and Pakistan), East Asia (154 species in China and Japan) and Southeast Asia (50 species in Myanmar, Thailand, Laos, and Vietnam) (WSC 2023).

While examining specimens recently collected from Shennongjia Forestry District of Hubei Province, central China, we found some huntsman spiders. The spiders described in this paper were identified as a new species based on comparison with other *Pseudopoda* species. The male palp of this new species has a slender embolus, and the female vulva has unique internal ducts. We used DNA barcodes of the species to match the sexes and for future use in identification.

## Material and methods

Specimens were examined and measured with an Olympus SZX7 stereomicroscope. Positions of tegular appendages are given according to clock positions, based on the left palp in ventral view. Male and female copulatory organs were examined and illustrated after dissection from the spider bodies; vulvae were cleared in a warm 10% potassium hydroxide (KOH) solution. All photographs were captured with a KUY NICE industrial digital camera (20.0 megapixels) mounted on an Olympus CX43 dissecting microscope and assembled using Helicon Focus 3.10.3 image stacking software. Photographic images were then edited using Adobe Photoshop CC 2018. All measurements were obtained using an Olympus SZX7 stereomicroscope and are given in millimetres (mm).

Leg measurements are shown as: total length (femur, patella, tibia, metatarsus, tarsus). Number of macrosetae is listed for each segment in the following order: pro-lateral, dorsal, retrolateral, ventral; in femora and patellae ventral spines are absent and thus the fourth article is omitted in the setation formula (Gong and Zhong 2020).

Abbreviations used in the text and figures are given below: **ALE** = anterior lateral eye, **AME** = anterior median eye, **AW** = anterior width of carapace, **C** = conductor, **CO** = copulatory opening, **CH** = clypeus height, **dRTA** = dorsal branch of RTA, **E** = embolus, **FD** = fertilisation duct, **Fe** = femur, **LL** = lateral lobes, **Mt** = metatarsus, **OL** = opisthosoma length, **OW** = opisthosoma width, **Pa** = patella, **PI** = posterior incision of LL, **PL** = carapace length, **PLE** = posterior lateral eyes, **PME** = posterior median eyes, **Pp** = palp or palpus, **PW** = carapace width, **RTA** = retrolateral tibial apophysis, **Sp** = spermophor, **T** = tegulum, **Ta** = tarsus, **Ti** = tibia. I, II, III, IV—legs I to IV, **vRTA** = ventral branch of RTA, **HUST** = School of Nuclear Technology and Chemistry and Biology, Hubei University of Science and Technology, Xianning, Hubei, China.

To obtain DNA barcodes, one mitochondrial gene (mitochondrial cytochrome oxidase subunit I [COI]) and one nuclear gene (Internal Transcribed Spacer 2 [ITS2]) were amplified and sequenced for four specimens. Primers (Folmer et al. 1994), PCR conditions and other information (e.g., extraction, amplification and sequencing procedures) are the same as in Zhang et al. (2021). The accession numbers are provided in Table 1. For phylogenetic inference, we used the dataset (COI + ITS2) from Cao

et al. (2016) and added the new sequences of *Pseudopoda deformis* Gong & Zhong, sp. nov. Phylogenetic analyses are the same as in Cao et al. (2016) and Zhang et al. (2017). Bayesian inference strongly supported the monophyly of the *P. deformis* Gong & Zhong, sp. nov. (Fig. 5).

**Table 1.** Information on newly sequenced *Pseudopoda deformis* Gong & Zhong, sp. nov. with GenBank accession numbers.

Voucher code	Sex	COI	ITS2
HUST-SPA-22-001	♂	OQ788976	OQ797662
HUST-SPA-22-002	♀	OQ788977	OQ797663
HUST-SPA-22-003	♀	OQ788978	OQ797664
HUST-SPA-22-004	♀	OQ788979	OQ797665

## Taxonomy

Family Sparassidae Bertkau, 1872

Subfamily Heteropodinae Thorell, 1873

Genus *Pseudopoda* Jäger, 2000

**Type species.** *Sarotes promptus* O. Pickard-Cambridge, 1885.

**Diagnosis (updated).** *Pseudopoda* was defined by Jäger (2000) according to the following combination of characters: male palp (Fig. 1A–C) with membranous conductor or absent, embolus arising on the left side of the tegulum and generally curved, RTA arising from tibia, basally or mesially and furcate or not; epigyne (Fig. 2A–C) with lateral lobes extending beyond epigastric furrow, and generally covering median septum (modified from Jäger 2000; Zhang et al. 2013; Jiang et al. 2018).

**Distribution.** Bhutan, China, Nepal, India, Japan, Laos, Myanmar, Pakistan, Thailand and Vietnam.

***Pseudopoda deformis* Gong & Zhong, sp. nov.**

<https://zoobank.org/1F62E2C1-3556-4B86-AE30-D907B4F204CB>

(变形拟遁蛛)

Figs 1–5

**Type material.** *Holotype* #m: CHINA: Hubei Province: Shennongjia Forestry District, Muyu Town, Guanmenshan Scenic Area (31.45°N, 110.40°E, 1200 m a.s.l.), 10.XII.2021, leg. Y. Zhong (HUST-SPA-22-001). *Paratypes*: CHINA: Hubei Province: Same locality, 1#f (HUST-SPA-22-002), 1#f (HUST-SPA-22-003), 1#f (HUST-SPA-22-004), 3#m, 4#f.

**Etymology.** The specific name is derived from the Latin word *deformis*, *-a*, *-um*, meaning distorted, referring to the shape of the internal ducts of the female vulva.

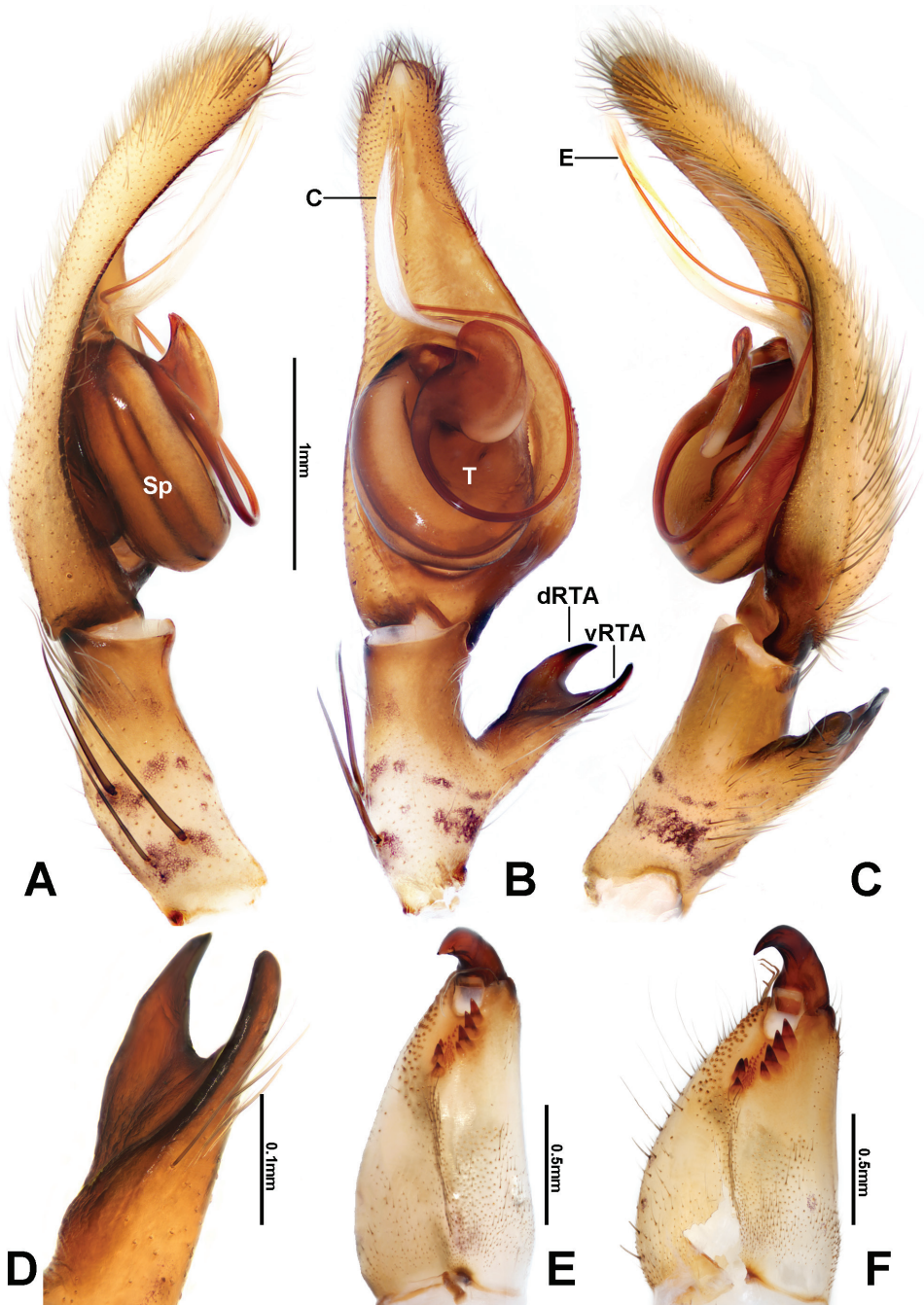


**Figure 1.** *Pseudopoda deformis* Gong & Zhong, sp. nov., male holotype (HUST-SPA-22-001), left palp (A–C), left male palpal tibia (D), and cheliceral dentition (E, F). **A** prolateral view **B** ventral view **C, D** retrolateral view **E** male, ventral view **F** female, ventral view. Abbreviations: C = conductor; dRTA = dorsal branch of RTA; vRTA = ventral branch of RTA; E = embolus; Sp = spermophore; T = tegulum. Scale bars: 1 mm (A–C); 0.1 mm (D); 0.5 mm (E, F).

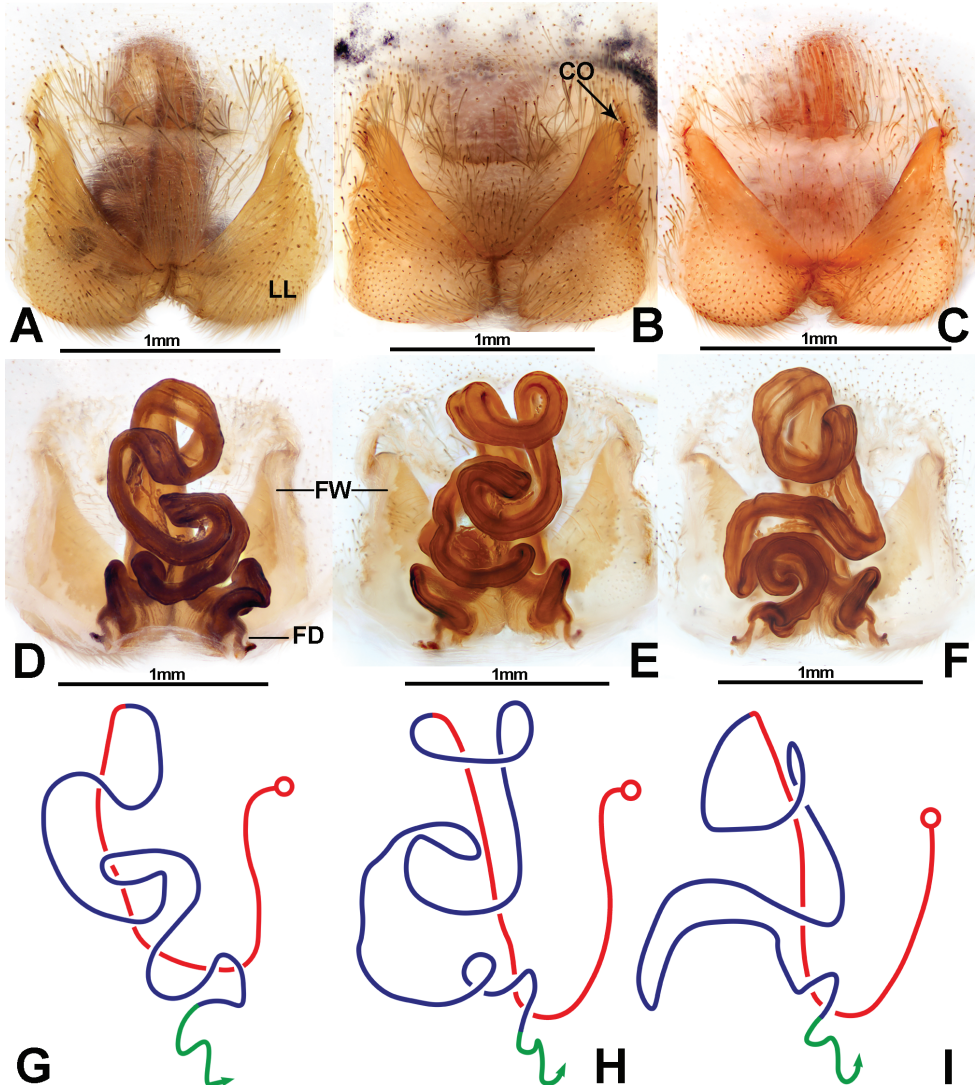


**Figure 2.** *Pseudopoda deformis* Gong & Zhong, sp. nov., female paratype (**A, D** HUST-SPA-22-002; **B, E** HUST-SPA-22-003; **C, F** HUST-SPA-22-004), epigyne (**A–C**), vulva (**D–F**), and schematic course of internal duct system (**G–I**). **A–C** ventral view **D–F** dorsal view. Abbreviations: CO = copulatory opening; FD = fertilisation duct; FW = first winding; LL = lateral lobes. Scale bars: 1 mm (**A–F**).

**Diagnosis.** Males of *Pseudopoda deformis* Gong & Zhong, sp. nov. are similar to those of *P. jiangi* Zhang, Jäger & Liu, 2023 (Zhang et al. 2023: figs 130, 131), *P. lushanensis* (Wang, 1990) (Quan et al. 2014: figs 4A–C, 5A–C) and *P. shuqiangi* Jäger & Vedel, 2007 (Jäger and Vedel 2007: figs 73–75) in having a long, filiform embolus. They can be distinguished from the two congeners by the following combination of characters: (1) Embolus arising from tegulum at 1:00-o’clock position, then curving

downward (8:30-o'clock position, upward in *P. lushanensis* and *P. shuqiangi*); (2) The basal part of embolus is oval (circular in *P. jiangi*); (3) The tip of the conductor is straight and extends to approximately the tip of the cymbium in ventral view (not in *P. lushanensis* and *P. shuqiangi*); and (4) RTA arising medially from tibia (subdistally in *P. lushanensis*; basally in *P. shuqiangi*) (Fig. 1A–C). The females of this species

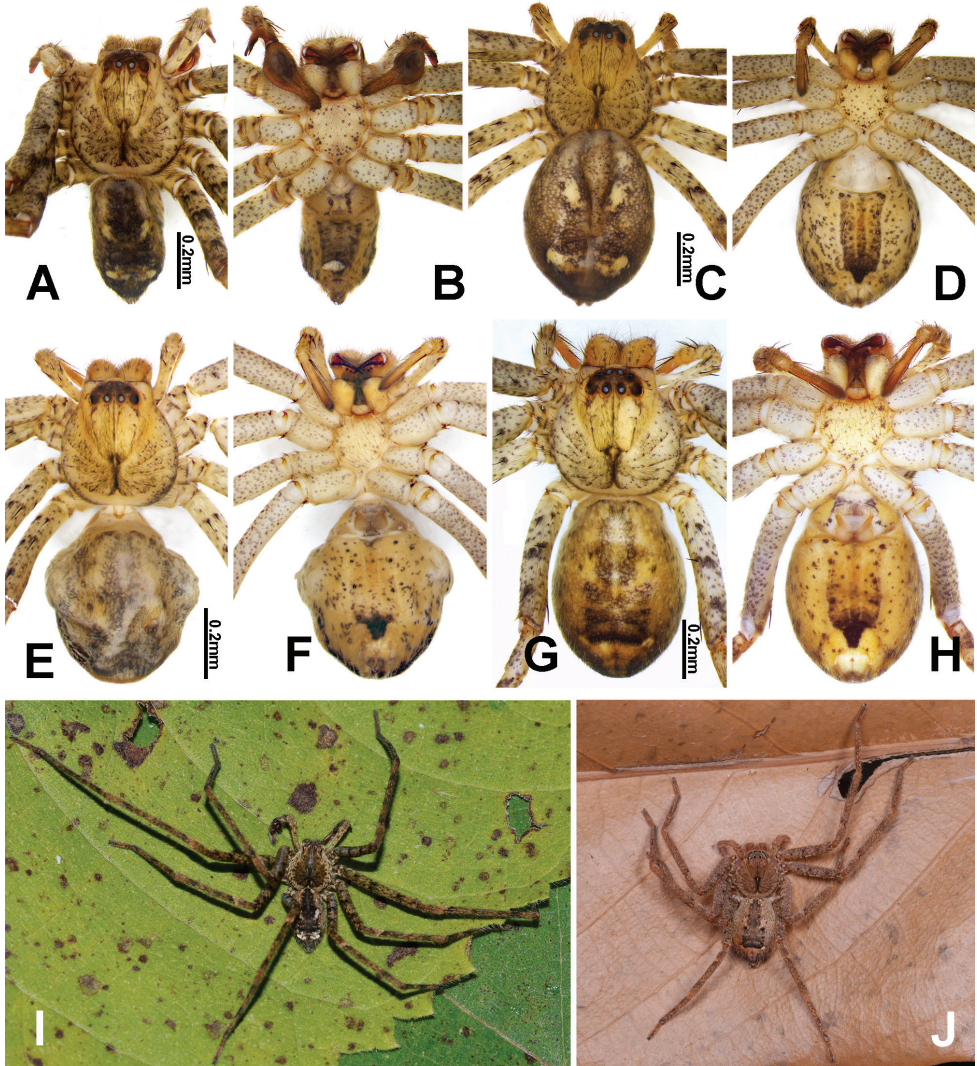


**Figure 3.** *Pseudopoda deformis* Gong & Zhong, sp. nov., habitus (A–H), and live specimens (I, J) A, I (HUST-SPA-22-001), holotype male, dorsal view B (HUST-SPA-22-001), holotype male, ventral view C, J (HUST-SPA-22-002), paratype female, dorsal view D (HUST-SPA-22-002), paratype female, ventral view E (HUST-SPA-22-003), paratype female, dorsal view F (HUST-SPA-22-003), paratype female, ventral view G (HUST-SPA-22-004), paratype female, dorsal view, H (HUST-SPA-22-004), paratype female, ventral view. Scale bars: 0.2 mm (A–H).

can be separated from other *Pseudopoda* species by their unique internal ducts of the vulva, which are curved longitudinally, forming a narrow triangle or trapezoidal shape (Fig. 2D–I).

**Description. Male.** PL 4.9, PW 3.4, AW 2.3, OL 4.6, OW 3.4. Eyes: AME 0.24, ALE 0.26, PME 0.27, PLE 0.33, AME–AME 0.21, AME–ALE 0.12, PME–PME 0.23, PME–PLE 0.16, AME–PME 0.29, ALE–PLE 0.18, CH AME 0.27, CH ALE 0.33. Setation: Palp: 131, 101, 2101; Fe: I–III 323, IV 321; Pa: I–IV 101; Ti: I–II 2228, III–IV 2126; Mt: I–II 2024, III 2026, IV 3036. Measurements of palp and legs: Palp 7.4 (2.1, 0.9, 1.3, –, 3.1), I 27.0 (7.1, 1.5, 8.2, 7.8, 2.4), II 29.6 (7.8, 1.5, 8.8, 8.9, 2.6), III 21.6 (6.0, 1.3, 6.1, 6.3, 1.9), IV 24.5 (6.5, 1.3, 6.9, 7.6, 2.2). Leg formula: II-I-IV-III. Chelicerae with three promarginal and four retromarginal teeth, and with ~51 denticles (Fig. 1E). Carapace yellowish brown dorsally, margin with black patches, with shallow fovea and radial furrows. Chelicerae deep reddish brown. Sternum yellow with lots of random black spots. Endites and labium pale yellowish brown. Legs brown, with dark dots randomly distributed and covered by short spines and seta. Opisthosoma black-brown dorsally, without spots. Opisthosoma uniformly yellowish brown with some black patches ventrally (Fig. 3A, B).

Cymbium approximately 2 times longer than tibia (Fig. 1A–C). The basal part of conductor is obscured in ventral view (Fig. 1B) by embolus base. Basal part of conductor slightly sclerotized (Fig. 1C). Embolus slender, encircling the tegulum counter-clockwise, ventrally pointed (Fig. 1B). RTA distally bifurcate, pincer-shaped in ventral view, dRTA moderately pointed at tip (Fig. 1B, D).

**Female.** PL 5.0, PW 4.8, AW 2.8, OL 6.7, OW 4.7. Eyes: AME 0.25, ALE 0.34, PME 0.26, PLE 0.38, AME–AME 0.18, AME–ALE 0.08, PME–PME 0.24, PME–PLE 0.18, AME–PME 0.29, ALE–PLE 0.17, CH AME 0.35, CH ALE 0.45. Setation: Palp: 131, 101, 2121, 1014; Fe: I–III 323, IV 321; Pa: I–IV 000; Ti: I–II 222(10), III–IV 2126; Mt: I–II 2024, III–IV 2026. Measurements of palp and legs: Palp 6.4 (2.1, 0.7, 1.0, –, 2.6), I 19.3 (5.5, 1.3, 5.6, 5.1, 1.8), II 20.5 (5.9, 1.3, 6.1, 5.4, 1.8), III 15.4 (4.6, 1.1, 4.5, 3.7, 1.5), IV 17.0 (5.0, 1.1, 4.5, 4.6, 1.8). Leg formula: II-I-IV-III. Chelicerae with three promarginal and four retromarginal teeth, and with ~46 denticles (Fig. 1F).

Epigynal field almost as wide as long, the anterior margins of lateral lobes forming a V-shape, median margin of lateral lobes united, internal duct systems not visible through cuticle, fertilisation ducts arising postero-laterally. In the dorsal view, internal duct systems differ extremely, and there is no regularity in the direction and structure of internal pipeline (Fig. 2).

Colouration as in males, opisthosoma brown dorsally (Fig. 3C–H).

**Habitat.** The specimens were collected on leaves at night with bare hands (Fig. 4A, B).

**Distribution.** Known only from Hubei Province, China (Fig. 4C).

**Remarks.** The monophyly of *Pseudopoda deformis* Gong & Zhong, sp. nov. is highly supported by molecular phylogenetic results based mainly on Chinese *Pseudopoda* species (Fig. 5).

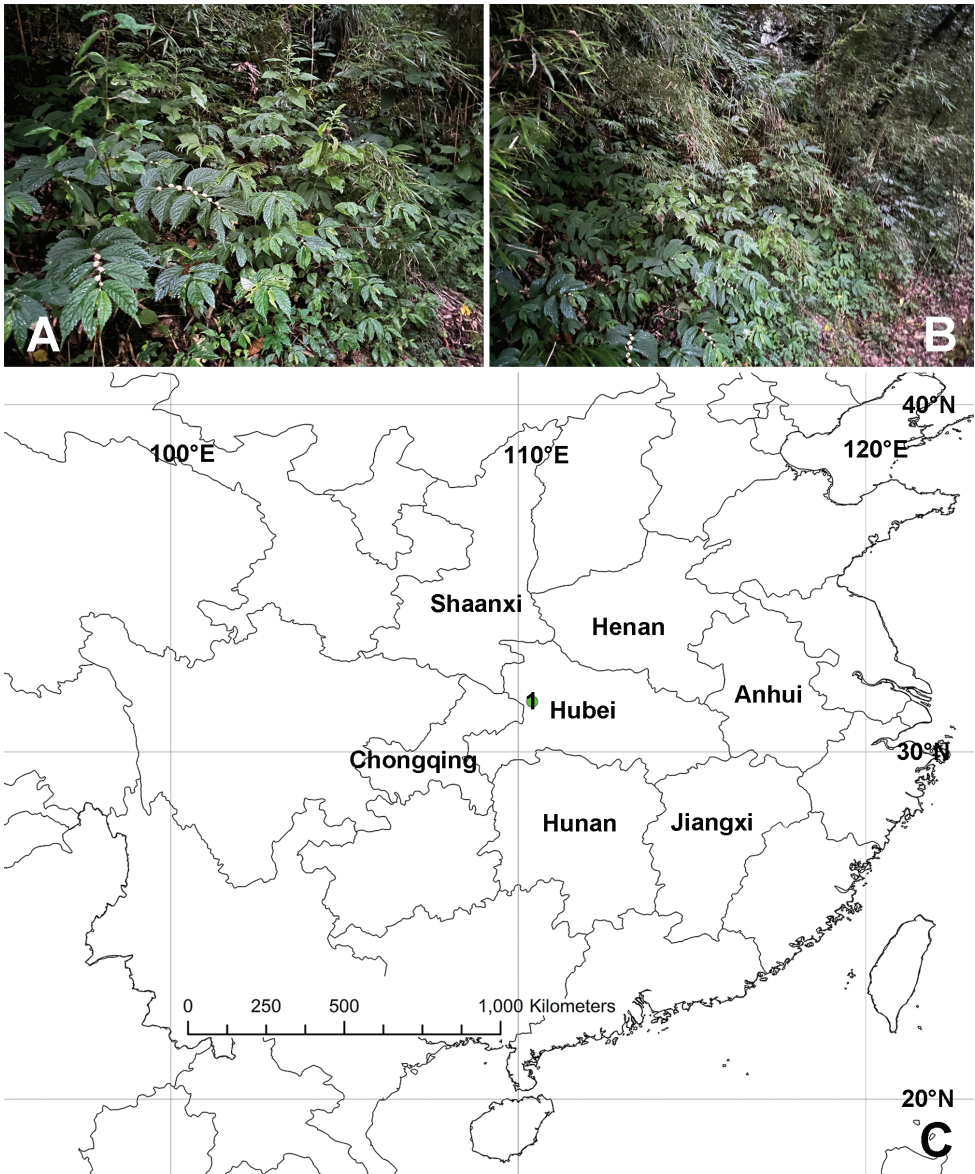


**Figure 4.** Photograph of the habitat (**A**, **B**) and collection locality of *Pseudopoda deformis* Gong & Zhong, sp. nov. (**C**).

## Discussion

We examined all specimens from Shennongjia (4 males, 7 females) and found no variation in the male palp. However, the females had different internal ducts in their vulva, which is not known to occur in other *Pseudopoda* spiders. In this paper, matching of the sexes of *Pseudopoda deformis* Gong & Zhong, sp. nov. was done using morphological and molecular data (Figs 3, 5). Females of this species resemble most *Pseudopoda*



species having the median margin of the lateral lobes converged medially with the anterior part V-shaped, but they can be distinguished from these species by the longitudinally bent internal duct system of the vulva (Fig. 2A–F). As shown in Fig. 2G–I, the female vulva is divided into three parts schematically to show the course of the internal duct system, leading to an interesting discovery. The first part is represented by a red line and is U-shaped in all three females examined. The third part is represented by a green line and is an inverted S-shaped. Variability occurs in the second part which is shown by the blue line, and there are irregularities to this variation.

## Acknowledgements

We thank Guofei Ma (Shennongjia National Park Administration) for assistance in collecting specimens. The English was checked by Sarah Crews (San Francisco, USA). This study was financially supported by the National Natural Sciences Foundation of China (32000303), the Technology Innovation Project of Hubei Province (2019AC161): Biodiversity research, monitoring and demonstration in Shennongjia National Park, Hubei Province Key Laboratory of Conservation Biology for Shennongjia Golden Monkey Foundation (No. SNJKL2021003), the Scientific Research Project of Education Department of Hubei Province (Q20222806), the Natural Sciences Foundation of Xianning City (2022ZRKX063), the Special Fund Projects of Hubei Key Laboratory of Radiation Chemistry and Functional Materials (2021ZX12), and a PhD grant from Hubei University of Science and Technology (BK202114).

## References

- Bertkau P (1872) Über die Respirationsorgane der Araneen. *Archiv für Naturgeschichte* 38: 208–233.
- Cao XW, Liu J, Chen J, Zheng G, Kuntner M, Agnarsson I (2016) Rapid dissemination of taxonomic discoveries based on DNA barcoding and morphology. *Scientific Reports* 6(1): 37066. <https://doi.org/10.1038/srep37066>
- Folmer M, Black W, Lutz R, Vrijenhoek R (1994) DNA primers for amplification of mitochondrial cytochrome c oxidase subunit I from diverse metazoan invertebrates. *Molecular Marine Biology and Biotechnology* 3: 294–299.
- Gong LJ, Zhong Y (2020) Redescription of *Pseudopoda taibaischana* (Araneae, Sparassidae), with the first description of the female. *ZooKeys* 991: 111–119. <https://doi.org/10.3897/zookeys.991.56969>
- Jäger P (2000) Two new heteropodine genera from southern continental Asia (Araneae: Sparassidae). *Acta Arachnologica* 49(1): 61–71. <https://doi.org/10.2476/asjaa.49.61>
- Jäger P, Vedel V (2007) Sparassidae of China 4. The genus *Pseudopoda* (Araneae: Sparassidae) in Yunnan Province. *Zootaxa* 1623(1): 1–38. <https://doi.org/10.11646/zootaxa.1623.1.1>

- Jiang TY, Zhao QY, Li SQ (2018) Sixteen new species of the genus *Pseudopoda* Jäger, 2000 from China, Myanmar, and Thailand (Sparassidae, Heteropodinae). *ZooKeys* 791: 107–161. <https://doi.org/10.3897/zookeys.791.28137>
- Quan D, Zhong Y, Liu J (2014) Four *Pseudopoda* species (Araneae: Sparassidae) from southern China. *Zootaxa* 3754(5): 555–571. <https://doi.org/10.11646/zootaxa.3754.5.2>
- Thorell T (1873) Remarks on synonyms of European spiders. Part IV. C. J. Lundström, Uppsala, 375–645.
- WSC (2023) World Spider Catalog, version 24. Natural History Museum, Bern. <https://doi.org/10.24436/2> [Accessed 10.04.2023]
- Zhang F, Zhang BS, Zhang ZS (2013) New species of *Pseudopoda* Jäger, 2000 from southern China (Araneae, Sparassidae). *ZooKeys* 361: 37–60. <https://doi.org/10.3897/zookeys.361.6089>
- Zhang H, Jäger P, Liu J (2017) One new *Pseudopoda* species group (Araneae: Sparassidae) from Yunnan Province, China, with description of three new species. *Zootaxa* 4318(2): 271–294. <https://doi.org/10.11646/zootaxa.4318.2.3>
- Zhang H, Zhong Y, Zhu Y, Agnarsson I, Liu J (2021) A molecular phylogeny of the Chinese *Sinopoda* spiders (Sparassidae, Heteropodinae): implications for taxonomy. *PeerJ* 9: e11775. [26 pp] <https://doi.org/10.7717/peerj.11775>
- Zhang H, Zhu Y, Zhong Y, Jäger P, Liu J (2023) A taxonomic revision of the spider genus *Pseudopoda* Jäger, 2000 (Araneae: Sparassidae) from East, South and Southeast Asia. *Megataxa* 9(1): 1–304. <https://doi.org/10.11646/megataxa.9.1.1>

